Laboratoire des Biomatériaux et Polymères de Spécialité, CSPBAT UMR 7244
Institut Galilée, Université Paris XIII

PhD THESIS

Presented by
Helena FELGUEIRAS

To obtain the degree of
DOCTEUR DE L'UNIVERSITÉ PARIS XIII
Discipline: Science de l'Ingénieur
Spécialité: Génie Biologique et Médical

Synthesis and Grafting of Bioactive Polymers to Create Biomimetic Surfaces Capable of Controlling the Host Response

Study of the Biological Mechanisms from the Origin of the Observed Activity

Defended on October 2nd of 2014, before the examination committee:

Reviewers Mrs. Margaret Evans, Professor at CSIRO, Sydney, Australia
Mrs. Brigitte Grosgogeat, Professor (PUPH) at Université Claude Bernard Lyon 1

Examiners Mrs. Véronique Migonney, Professor at Université Paris 13 and Thesis Director
Mrs. Nadine Varin-Blanc, Professor at Université Paris 13, INSERM
Mrs. Muriel Vayssade, Doctor at Université de Technologie de Compiègne

ACKNOWLEDGMENTS

This research project was conducted at the Laboratory of Biomaterials and Specialty Polymers (LBPS-CSPBAT UMR 7244, CNRS), Institut Galilée, from Université Paris 13.

First of all, I would like to express my sincere gratitude to my supervisor Professor Véronique Migonney, director in functions of the LBPS/CSPBAT laboratory, for taking the risk and accepting me as her PhD student. Her help, support, patience and friendship were very encouraging during the development of this research. It was a privilege to work with and be guided by her. I will always cherish these three years that I spent in the LBPS team.

I thank Professor Margaret Evans (CSIRO, Australia) for the insightful observations, work suggestions and availability to discuss this research along the years but most importantly for agreeing to be one of the juries of this thesis. I am truly honored by her presence.

To Professor Brigitte Grosgogeat (Université Claude Bernard Lyon 1) I extend my gratitude for her prompt acceptance to become a jury of this thesis and for the attention and time given to this work.

I thank Professor Nadine Varin-Blank (Université Paris 13) and Doctor Muriel Vayssade (Université de Technologie de Compiègne) for their valuable insights and constant availability. I am very grateful for their participation as members of the jury.

I would like to give a special word of recognition and gratitude to Professor Joachim Kohn from the New Jersey Center for Biomaterials (NJCBM), Rutgers University (USA), for allowing my participation in two Summer International Programs at his lab. His kindness and warm welcome were very reassuring during the entire time in the USA.

I am very grateful to Professor Sanjeeva Murthy from the NJCBM group for his guidance during the Summer International Programs. His pertinent suggestions, availability and continuous discussions helped me greatly during this investigation.

I would like to acknowledge Dr. Gerard Hélary, Dr. Géraldine Rohman, Dr. Danielle Geldwerth, Dr. Sylvie Changotade and Dr. Didier Lutomski, all from the LBPS team, for their encouragement, prompt advices, patience and above all friendship. I would like to extend this thank you note to all the former and current students and researchers at the LBPS, namely Ines Ben Aissa, Stephane Huot, Jean Sebastien Baumann, Céline Daudre, Amélie Auge, Gabriella Bostan, Miriam Machado e Joana Gomes for their constant support and great work atmosphere.

To Professor David G. Castner (University of Washington, USA) and Professor Robert Latour (Clemson University, USA) I extend my gratitude for the pertinent questions and advices during discussion meetings.

To Sven Sommerfeld, PhD student at the NJCBM team, I express my gratitude for the patience, help and enriching suggestions on the QCM-D work. I am thankful as well to the exchange students with whom I shared the six months I spent in the NJCBM group and to the various NJCBM researches that kindly offered their time and help in many occasions. Their support and enthusiasm resulted in wonderful memories. To all of them I wish the best of luck.

I also thank the CERAVER society for their collaboration and material production and to the ANR TECSAN, program ACTISURF, and the École Doctorale Galilée for the financial support provided along my studies.

Finally, I thank my family and friends for their support and constant motivation, especially in the most difficult times, and for being always unconditionally present in my life.

CONTENTS

LIST OF FIGURES

LIST OF TABLES

LIST OF ABBREVIATIONS/ NOMENCLATURE

Poly(NaSS) – Poly(sodium styrene sulfonate)
Ti6Al4V – Titanium alloy with aluminum and vanadium
ECM – Extracellular matrix
Col I – Collagen type I
OCN – Osteocalcin
HAP - Hydroxyapatite
RANKL – Receptor activator of NK-κB ligand
M-CSF – Macrophage colony-stimulating factor
OPN – Osteopontin
BSP – Bone sialoprotein
BMPs – Bone morphogenetic proteins
FGF – Fibroblast growth factor
ALP – Alkaline phosphatase
BMU – Basic multicellular unit
RGD – Arginine-glycine-aspartate motif/peptide
Fn – Fibronectin
Vn – Vitronectin
cDNA – complementary DNA
PAI-1 – Plasminogen activator inhibitor-1
BSA – Bovine serum albumin
FAK – Focal adhesion kinase
PKC – Protein kinase C
MAPK – Mitogen-activated protein kinase
ISO – International Organization for Standardization
ASTM – American Society for Testing Materials
PMMA – Poly(methyl methacrylate)
CP Ti – Commercially pure titanium
Ra – Average roughness
RUNX2 – Runt-related transcription factor 2
mRNA – Messenger RNA
PGE_2 – Prostaglandin E_2
TGF-β1 – Transforming growth factor-β1
TNF-α – Tumor necrosis factor-α
VCAN-1 – Vascular adhesion molecule-1
OMD – Osteomodulin
SULF1 – Sulfatase-1
QCM-D – Quartz crystal microbalance
Poly(DTEc) – Poly(desamino tyrosyl-tyrosine ethyl ester carbonate)
PS - Polystyrene
RT – Room temperature

Rz – Average maximum height roughness

Rp – Maximum profile peak height

Rq – Quadratic mean roughness

XPS – X-ray Photoelectron Spectroscopy

EDS – Energy Dispersive x-ray Spectroscopy

TB – Toluidine blue

FTIR – Fourier transformed InfraRed

ATR – Attenuated total reflection

XRD – X-ray Diffraction

PBS – phosphate buffered saline solution

SDS – Sodium dodecyl sulfate

DMEM – Dulbecco's modified eagle medium

FBS – Fetal bovine serum

HB – Heparin binding domain

ATCC – American type culture collection

SFM – Serum free medium

DD – Double depleted medium

TCPS – Tissue culture polystyrene

TBS-Triton X100 – Tris buffered saline-triton X100

VEGF-A – Vascular endothelial growth factor

TCA – Trichloroacetic acid

SD – Standard deviation

I. General Introduction

GENERAL INTRODUCTION

The continuing aging of the population has brought with it an ever-increasing need for materials specifically suited for biomedical applications. The fact that this need is increasing is no surprise if we compare the life expectancy of a hip implant, for instance, with the ever-increasing life expectancy of a patient. With normal implant longevity of 12 to 15 years, it is expected a patient that receives a hip implant at the age of 65 to endure at least one more surgical intervention, before the end of his life. Nowadays, this is one of the biggest concerns of biomedical researchers.

In the orthopedic domain, the search for specialized materials that respond both to the mechanical and chemical solicitations of the human body but assure a proper host response have lead to outstanding and revolutionary breakthroughs over the years. It is now clear that titanium and in particular the titanium alloy Ti6Al4V are the most favorable choices for bone substitution. They possess excellent corrosion resistance due to their ability to interact with water and air to form a spontaneous oxide layer, which also protects against ion release; great mechanical properties which approximate the material to the human bone (i.e. young modulus); and are compatible with the living tissue. Despite being continuously used in the medical field, titanium may present some challenges to a long-term implantation. Possible aseptic loosening due to inadequate tissue response (i.e. fibrous tissue formation and/or infection) may occur. Therefore, it is imperative to find solutions that, on one side, maintain the mechanical and chemical resistance and properties of the materials and, on the other side, improve the biological response. This is the “heart” of the present research work.

Based on previous investigations conducted by the Laboratory of Biomaterials and Specialty Polymers (LBPS-CSPBAT) team, we now know that the long-term response of polymeric and metallic implants can be improved by grafting bioactive polymers bearing anionic groups onto their surfaces. The interactions between the bioactive materials and the living tissue have been followed *in vivo* and *in vitro* and their potential to modulate the attachment, adhesion, spreading and differentiation of various cell types has been demonstrated. The mechanism by which the cells respond to the bioactive model surfaces has been investigated, as well. The results

point to a selective protein adsorption (i.e. fibronectin and vitronectin) with favorable affinity and conformations that allow to control the host response. By following this line of investigation, the LBPS developed a strategy that consists in the grafting of bioactive macromolecular chains from the poly(sodium styrene sulfonate) or poly(NaSS) polymer. It has been seen that this polymer aside from enhancing the cells activity also decreases bacterial adhesion. Data from *in vivo* testing has confirmed the stability of this bioactive polymer in physiological environments and the needless of protection against enzymatic degradation, overcoming limitations of pre-existing strategies of incorporation or release of bone-promoting proteins (BMPs, collagen…) and antibiotic drugs (gentamycin). Preliminary results on titanium have shown that this polymer induces the creation of new active sites along the surface for protein adsorption from the extracellular matrix aside from enhancing the osteoblastic differentiation, both alkaline phosphatase activity and mineralization. Nevertheless, much needs to be understood about the role of the surface chemistry on the cells development and its interaction with important proteins from the blood plasma and the extracellular matrix.

In this investigation, the authors:

(1) studied the impact of poly(NaSS) grafted onto Ti6Al4V substrates on the general osteoblastic cell behavior (from attachment to mineralization);

(2) followed the cells development on grafted Ti6Al4V materials pre-adsorbed with three important and well characterized proteins, albumin, fibronectin and collagen type I, both adsorbed individually and from a mixture, and we inferred about the effect poly(NaSS) exerts on cells when exposed by itself (without a protein interface);

(3) demonstrated the influence of two adhesive proteins, fibronectin and vitronectin, on the cells early adhesion on regular and double depleted media;

(4) put in evidence the importance of integrin-mediated cell attachment on fibronectin, vitronectin and collagen type I pre-adsorbed surfaces

(5) characterized the proteins conformation by assessing the amount of their active binding sites and the variations in cell morphology;

(6) and finally, determined the competitive character of albumin, fibronectin and collagen type I.

The totality of the experiments was conducted *in vitro*.

This thesis was subdivided in five chapters:

I) General Introduction: in this section a brief introduction to the main subjects of investigation was made and the objectives of the research were established.

II) Literature Review: this chapter includes a complete analysis of all topics related to the main subject of investigation. It followed a hierarchical orientation starting from the simplest and general aspects and continuously evolving to more complex and detailed information.

III) Materials and Methods: here a description of the techniques and materials employed in the project was provided. This included characterization sections, only related to the materials, and biological sections, composed of all necessary tests to understand the initial cellular behavior on treated Ti6Al4V materials.

IV) Results and Discussion: this section deals with the results from the entire experiments, with each one being exposed in the company of insightful observations and fundamented discussions.

V) Conclusions and Future Perspectives: as the title suggests, the main conclusions retrieved from the experimental data were provided and topics for future work were suggested.

II. Literature Review

1. BONE TISSUE

The bone tissue is a specialized form of connective tissue composed of mineral and organic phases that provide a great rigidity and hardness to the bone. Despite its inert appearance and high resistance, bone tissue is in fact a very dynamic structure. For the entire organism life, bone is in constant remodeling so its mechanical properties and metabolic functions remain viable.

Different cell types are involved in the bone tissue formation, namely osteoclasts, bone lining cells, osteocytes and osteoblasts. These cells are embedded within the mineralized extracellular matrix (ECM), formed primarily by fibrils of collagen type I (Col I), glycoproteins and proteoglycans, which allow the bone to maintain its functions of support and protection of the organism. Besides those, bone tissue is also involved in the skeletal muscles and tendon connections needed for the body movement; works as a lever system amplifying the strength generated during muscle contraction; and possesses a storage for calcium, phosphate and other ions, so important for several metabolic functions. More than 90% of the calcium in the human body is present in bones to guaranty the stiffness of the skeleton, supply the organism with the mineral, and preserve vital functions through bone resorption [1-3]. Recent reports have shown the remodeling process of bone to be an important regulator of glucose levels in blood, since the osteocalcin (OCN) hormone liberated by bone favors the synthesis and secretion of insulin [1].

1.1 Composition

Biochemically, the bone tissue is divided in two phases, organic (≈ 20% w/w) and inorganic (≈ 60% w/w). It is also composed of water (≈ 10% w/w) and several other organic molecules such as glycosaminoglycans, glycoproteins, lipids, peptides, enzymes and different ions.

Col I (86%) is the predominant constituent of the organic phase of bone. It provides elastic and viscoelastic capacities to the bone, enabling its resistance to tension stress. Small amounts of collagen types III, V and X can also be found in this phase, aside from various glycoproteins, one of which, the OCN, believed to play an important role during mineralization [3].

The collagen molecules are organized in parallel fibers, forming interfibrillar cross-links at the extremities of bone that provide stability to the matrix (three

dimensional structures). Their orientation goes towards the primary lines of stress by which the bone structure is regularly submitted. In certain stages of the bone matrix formation, the small amounts of other collagen types can be involved in the collagen fibrils size regulation (diameter). There are several gap regions or “holes” in between those collagen formations that work as initial deposits for hydroxyapatite (HAP) crystals, during mineralization. This way, the organic matrix will work as a molecular and structure basis for the initial deposition of the inorganic components, defining its efficiency [4].

The inorganic phase of bone is highly resistant to compression stress due to its main composition in calcium and phosphate ions. These are usually organized as HAP crystals.

The HAP present in the human bone is a ceramic of following composition $Ca_{10}(PO_4)_6(OH)_2$, with a hexagonal crystalline structure. In its natural form, HAP crystals display different impurities, typically as a way to overcome possible deficiencies in calcium and phosphate. Potassium, magnesium, strontium and/or sodium are usually found in the place of calcium ions; carbonate can be found substituting phosphate ions; whereas chloride and fluoride can be found replacing hydroxyl ions. These elements are very soluble and, as consequence, the bone is able to resolubilise and release its ions into the extracellular fluids as needed.

The incorporation of other elements in the crystalline structure of the HAP slows down during the organism life, becoming more and more crystalline. This phenomena explains the slower remodeling process of bone tissue correlated with aging [3,5,6].

1.2 Structure and Organization

The bone tissue can be classified according to its porosity and structural organization into cortical, also known as compact bone, and trabecular bone, also known as cancellous or spongy bone (Figure 1) [3,5].

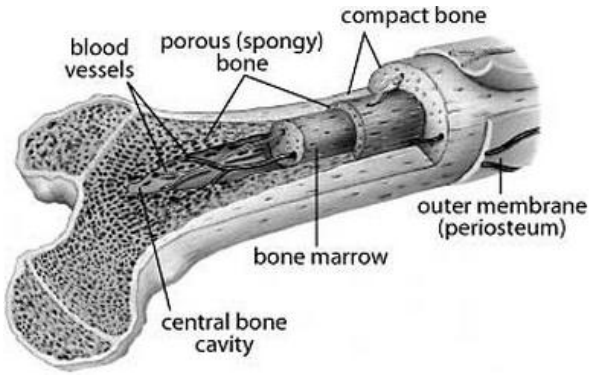

Figure 1. Bone tissue macroscopic organization [7].

The dense outer cortical bone encloses an irregular medullary space containing the cancellous bone, which is composed of branching networks of interconnecting bony trabecular elements. Both cortical and trabecular bone are composed of osteons (Figure 2).

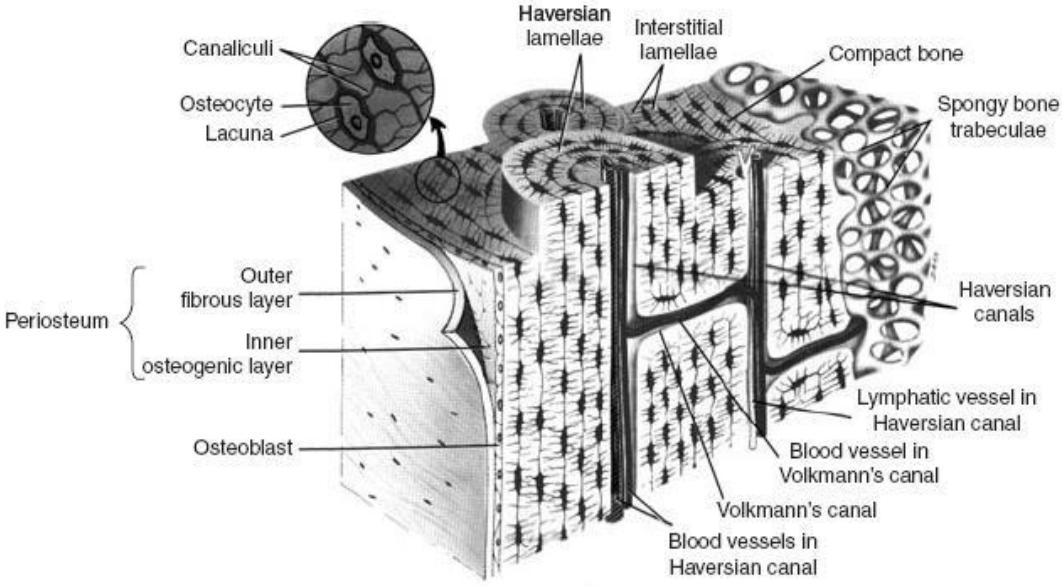

Figure 2. Bone tissue microscopic organization [3].

The adult human skeleton is composed of ≈ 80% cortical bone and ≈ 20% trabecular bone. However, different bones possess different ratios of cortical and trabecular bone. For instance, the vertebra has a ratio of 25/75 cortical to trabecular bone, while the femoral head has a 50/50 ratio. Despite the very distinct structural and functional tasks, their cellular elements are equal [3,5,7,8].

1.2.1 Cortical Bone

The cortical bone is a dense and solid hierarchical organization of osteons, also known as Haversian systems, that surrounds the marrow space. The Haversian systems are cylindrical in shape. They are composed of 6 to 8 concentric lamellae sheets of approximately 400 mm long and 200 mm wide that follow a parallel orientation according to the longitudinal axis of bone, creating a branching network within the cortical bone. In between the various lamellae there are gaps named lacunas where the osteoblasts differentiated into osteocytes are located. There are approximately $2.1x10^7$ cortical osteons in a healthy human adult and its porosity ranges between 5 and 10%. Cortical bone facilitates bone's main functions, support and protection, as well as system of levers of movement and chemical elements storage. It forms the cortex, or outer shell, of most bones and possesses a complex vascular system of blood vessels and nerves, which provide high sensitivity and regenerative capacities to the bone [3,5,7,8].

The cortical bone possesses an outer periosteal surface or periosteum and an inner endosteal surface or endosteum.

1.2.2 Periosteum and Endosteum

The periosteum is a fibrous connective tissue, highly vascularized, that covers the outer surface of all bones, with the exception of joints where bone is covered by joint cartilage. It attaches to the bone by means of strong collagenous fibers also named Shapey's fibers and provides an attachment site for muscles, ligaments and tendons. It is divided in an outer fibrous layer (containing fibroblasts) and an inner osteogenic layer (containing osteoprogenitor cells). In adults, it is responsible for bone remodeling (new bone formed after injuries), while in children is critical for bone formation and development.

The endosteum is a soft, thin, membranous layer of non-mineralized connective tissue that surrounds the inner cavity of cortical bone, trabecular bones and blood vessels (Volkman's canals) present in bone. It contacts directly with the bone marrow space and contains blood vessels, osteoblasts and osteoclasts. As the periosteum, the endosteum is also involved in the bone remodeling process by immobilizing osteoclasts during bone growth, preventing the formation of unnecessarily thick bones [2,3,9].

1.2.3 Trabecular bone

The trabecular or cancellous bone has a higher surface area to mass ratio than the cortical bone. Consequently, exhibits more flexible, light, softer and weaker characteristics. It is composed of osteons, also known as packets (semilunar shape), plates, and rods averaging from 50 to 400 mm in thickness that are organized as honeycomb-like networks. Bone marrow (major producer of blood cells) can be found in between these spaces. Due to its organization and greater surface area, trabecular bone is preferable for metabolic functions. There are approximately $1.4x10^7$ trabecular osteons in a healthy human adult. The trabecular bone is commonly found in the end of long bones, joints or within vertebrae, and contributes with 20% to the total skeletal mass [2,3,5].

1.3 Cell Types

From a histological point of view, the human bone is composed of several distinct cell types (Figure 3). Considering their impact in bone formation, special attention is provided to the osteoclasts, bone-lining cells, osteocytes and osteoblasts [1].

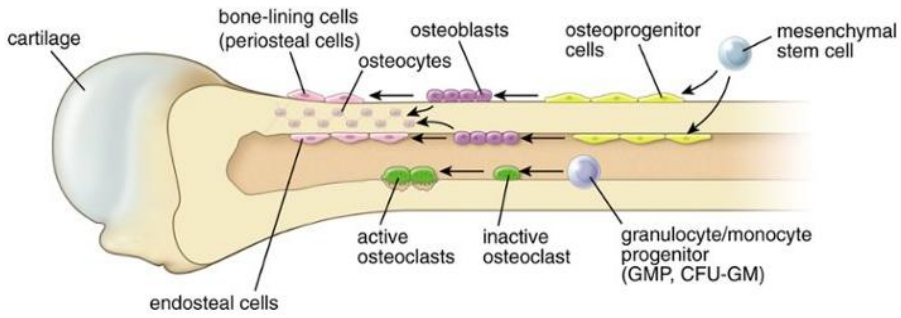

Figure 3. Bone cells [1].

1.3.1 Osteoclasts

Osteoclasts are large multinucleated cells with diameters ranging from 20 to 100 μm, only responsible for bone resorption (Figure 4). They possess an acidophilic cytoplasm including various vesicles and vacuoles. Osteoclasts derive from the fusion of mononuclear monocyte-macrophage precursor cells, a hematopoietic type of cells. Its formation occurs in association with the stromal cells in the bone marrow that secrete essential cytokines, the RANKL (receptor activator of NF-κB ligand) and the M-CSF (macrophage CSF), which trigger the differentiation of the hematopoietic

cells into osteoclasts. While RANKL is crucial for the osteoclast formation, the M-CSF is responsible for their survival and for cytoskeleton rearrangement required for bone resorption [1,3,10].

The newly formed osteoclasts must be activated to set the bone-resorbing cells activity. During that process, they become highly polarized cells since bone resorption depends on the osteoclasts ability to secret hydrogen ions (H^+) and the cathepsin K enzyme. The H^+ ions are used to dissolve the mineralized matrix of bone, whereas the cathepsin K digests the organic phase of bone (mainly Col I).

The osteoclasts bind to bone matrix via the integrin receptors, in particular the $\alpha_v\beta_3$ integrin that interacts with osteopontin (OPN) and bone sialoprotein (BSP). Upon contact with the bone matrix, the osteoclasts actin cytoskeleton is rearranged so the acidified resorption (secretion of hydrochloric acid and acidic proteases aside from the H^+ and the cathepsin K that favors the hydroxyapatite crystals dissolution) is sealed to the surrounding bone tissue. After their task is complete, the osteoclasts migrate into the adjacent marrow space, where they undergo apoptosis (they can live up to seven weeks), and the calcium and phosphate ions are liberated to the extracellular fluids [1, 10-13].

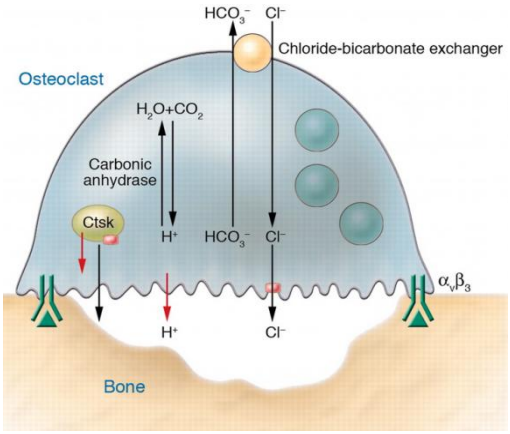

Figure 4. Mechanism of osteoclastic bone resorption [13]

The equilibrium between the osteoclasts and osteoblasts activity defines the velocity in which bone regeneration occurs.

1.3.2 Bone-lining Cells

Bone-lining cells are flat and highly interconnect with each other, possess an attenuated cytoplasm and a reduced metabolic activity (small number of organelles).

They derive from inactive osteoblasts, which are no longer involved in the remodeling process, and, as the name suggest, form a cellular layer on the surface of bone, protecting it and controlling ions exchange aside from assuring the nutritional support of osteocytes embedded in the underlying bone matrix. In addition, these cells are of importance in the bone remodeling process, since they possess various hormones and growth factors essential to its initiation [1,3,14].

1.3.3 Osteocytes

Osteocytes are star-shaped cells, derived from osteoblasts that become completely surrounded by osteoid. They are usually smaller than their precursors (loss of organelles) and occupy spaces named lacuna, which define the cells shape. They are able to extend their cytoplasm along the canaliculi (small channels) and communicate with neighboring osteocytes and bone-lining cells by means of gap junctions. Osteocytes can also communicate with distant cells through signaling molecules such as nitric oxides and glutamate transporters. These cells are the most abundant in the bone tissue (represent 95% of the total cells in a mature bone) with a life expectancy of approximately 25 years [1-3,15].

Osteocytes are the cells responsible for maintaining the bone matrix, since they can both synthesize new matrix and participate in its degradation. This function is also responsible for their longevity. In case of death, the resorption of bone matrix is assured by the osteoclasts while the remodeling is dependent on the osteoblasts activity. The osteocytes are also involved in the response to mechanical stimulation of bone, translating the stress signals from bending or stretching into biological activity, which can change gene expression and the cells apoptotic mechanism [15,16].

1.3.4 Osteoblasts

Osteoblasts are bone-forming cells responsible for the secretion of the bone matrix and the major cellular component of bone. They exhibit a cuboidal or polygonal shape (15-30 μm), possess a large nucleus and a cytoplasm rich in organelles with strong activity (granular endoplasmic reticulum, rounded mitochondria and well-developed Golgi apparatus). These cells are commonly found in the inner or outer surfaces of forming bone sites, typically as covering monolayers [1-3].

Osteoblasts arise from osteoprogenitor cells, self-renewing pluoripotent stem cells as mesenchymal stem cells, located in the bone marrow that induced by different local and systemic factors (bone morphogenetic proteins (BMPs), fibroblast growth factor (FGF) and others) differentiate into non-functional pre-osteoblastic cells and then into mature osteoblasts. Depending on the stimulant factor, stem cells can differentiate into several other types of cells (Figure 5) [17,18].

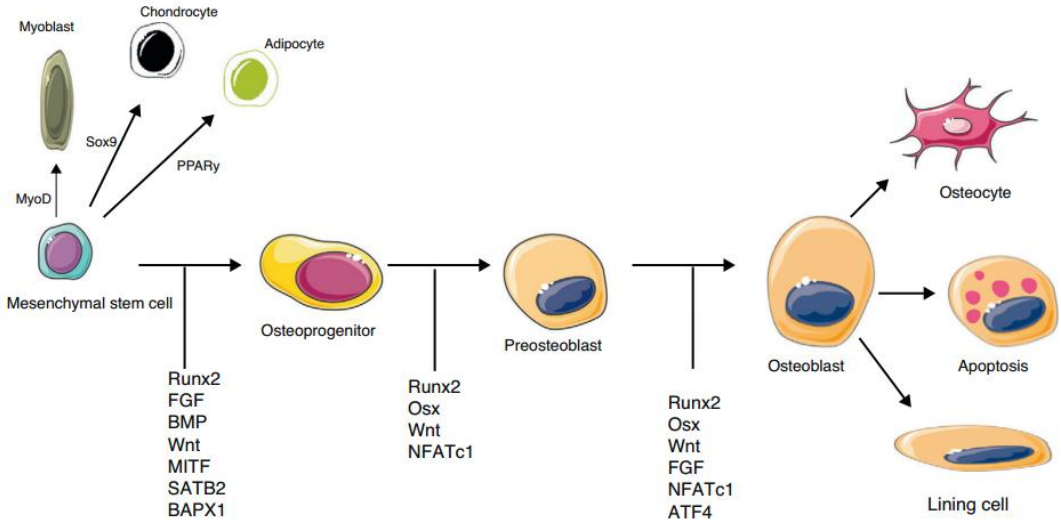

Figure 5. Different stages of osteoblasts formation and differentiation, and respective molecular signals [18].

Active osteoblasts are very versatile and the responsible for the mineralization of the bone matrix. They secret Col I, the main component, exhibit an intense alkaline phosphatase (ALP) activity that intensifies the concentration of calcium and phosphate ions aside from the hydroxyapatite formations, and are capable of synthesizing various specialized proteins such as OCN, BSP, OPN and BMPs that work as biomarkers of osteoblastic function and development. The osteoblasts are involved in the bone remodeling process, supervising the resorption and promoting the osteoclasts contact with the mineralized bone surface. In fact, they synthesize the cytokine RANKL to induce their differentiation into osteoclasts [3,17,19,20].

In the end of the bone remodeling process, most of the osteoblastic cells undergo apoptosis. Still, there is part that take new functions, differentiating into osteocytes or bone-lining cells.

1.4 Bone Dynamics

1.4.1 Formation and Growth

Bone formation (or ossification) is initiated during the first weeks after conception and its development is traditionally classified as endochondral (cartilage intervenes as bone precursor) or intramembranous (without cartilage intervention).

The endochondral ossification involves the formation of bone by means of hyaline cartilage models that are, with time, progressively substitute by bony tissue (Figure 6). After the third month of gestation, the cartilage models become highly vascularized and the osteoblasts start the formation of a collar of compact bone around the cartilage, leading it to disintegrate. At this point, osteoblasts can penetrate into the cartilage model and initiate its replacement with trabecular bone. The ossification process continues from the center to the extremities of the bone, until only cartilage remains at articular joints and growth regions. Most bones are formed this way [1-3,21].

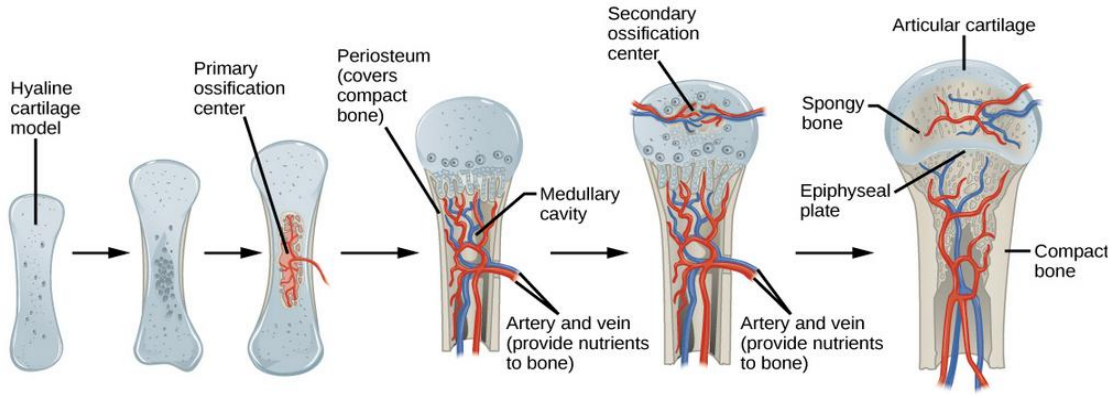

Figure 6. Endochondral ossification process [22].

The intramembranous ossification consists in the substitution of connective tissue membranes with bony tissue, in other words, bone is formed by differentiation of mesenchymal stem cells into osteoblasts. Here, bone formation starts at the eight week of gestation. Mesenchymal stem cells migrate and aggregate at specific areas, and start differentiating into osteoprogenitor cells. The region becomes highly vascularized and the aggregate enlarges. The cytoplasm of the osteoprogenitor cells changes, resulting in a more evident and complex structure, which induces the differentiation of the cells into osteoblasts. These, on its turn, synthesize collagen and other components of the bone matrix, expanding it. With time, the matrix calcifies and organizes as described in *section 1.2*. Most of the flat bones from skull and face are generated by intramembranous ossification.

As formation, bone growth starts during gestation but only ends in the early adulthood. Two stages of bone growth can be identified, the longitudinal and the radial. The longitudinal growth is mainly responsible for increasing bone length, while the radial is in charge of the bone cross-sectional area enlargement.

Important hormones are involved in the rapid formation and growth of bone. In females the estrogen is the predominant, whereas in males testosterone plays a major role. Several other growth hormones are implicated as well. Environmental factors such as physical activity and good nutrition can also be of influence during bone formation and growth [3,21,22].

1.4.2 Modeling

Bone modeling governs the enlargement, shape and size of individual bones during growth. This process allows bones to shape in response to inner or outer physiologic influences or mechanical forces, leading to the gradual adjustment of the skeleton. Here, bone formation, instigated by osteoblasts, and resorption, activated by osteoclasts, may occur in combination. Despite the antagonism of the two mechanisms, during bone modeling, they can work together to guarantee the appropriate shape and size of each individual bone (by adding or removing bone), allowing them to fit in harmony in one big and cohesive structure. While in childhood bone modeling is very frequent, in adults the remodeling process overlaps the modeling. Still, under certain circumstances such as renal osteodystrophy or hypoparathyroidism, the opposite can happen and the modeling stage may increase [3,21].

1.4.3 Remodeling

Bone remodeling is the process by which bone is renewed to maintain strength and mineral homeostasis. It involves continuous removal of old bone and its replacement by newly synthesized protein based matrix that later undergoes mineralization to form new bone. Bone remodeling occurs during the entire human life and, as in the modeling process, osteoblasts and osteoclasts work in close collaboration adding and removing bone, respectively. The balance of bone resorption and bone deposition is controlled/regulated by the activity of these two cell types.

During childhood, immature bone is replaced by bio-mechanically and metabolically competent bone through this process, whereas in adulthood bone remodeling is responsible for the replacement of aged, damage and/or mechanically unfit bone, preventing accumulation of microdamaged bone (from normal activity). In one year of an adult's life between 5 and 10% of total bone is renewed. Remodeling responds also to functional demands of mechanical loading by adding bone where needed and removing it where it is not necessary. Aside from maintaining the structural integrity of the skeleton and adapting its architecture to the environment demands, the remodeling is also required to supervise its metabolic functions by means of calcium and phosphorus storage. This constant resorption and formation of new bone makes bone a very dynamic tissue with a highly plasticity level.

The remodeling cycle in adults lasts approximately four months and takes place in the "basic multicellular unit" or BMU – small packets of cells located in the cortical or trabecular surface. It comprises five stages, activation, resorption, reversal, formation and mineralization (Figure 7), and involves three types of bone cells, the osteoblasts, osteoclasts and the osteocytes [3,21,23-25].

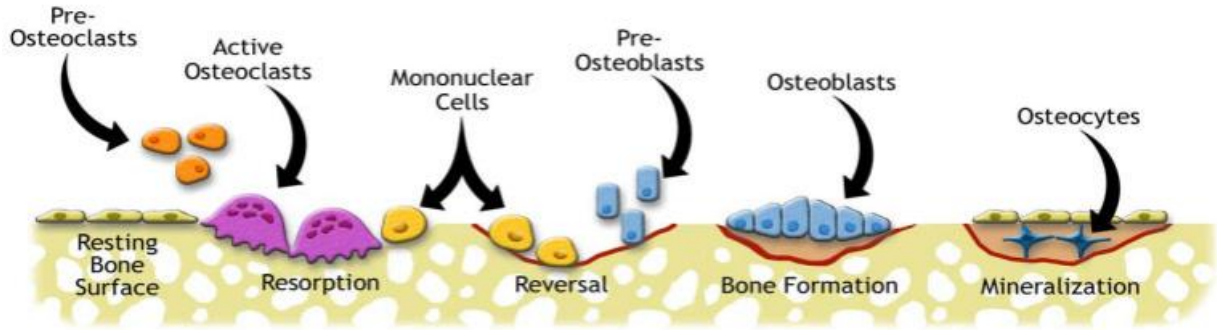

Figure 7. Bone remodeling cycle [26].

1. Activation or Quiescence: the resting bone surface is activated by the retraction of bone lining cells and digestion of the endosteal membrane by collagenase action. This phase lasts two to three days and is instigated by different mechanical and environmental stimuli. Precursors of osteoclasts are recruited and activated, differentiating into multinucleated osteoclasts (mature), which will then attach to the mineralized bone and initiate its resorption.

2. Resorption: the osteoclasts attached to the bone initiate the erosion of the surface, leading to the digestion of the mineral and osteoid matrix. This task is completed by the macrophages and allows the release of various important growth factors contained within the matrix, for instance the BMPs fundamental for the bone forming cells activation. This phase lasts between 2 to 4 weeks. Since the life expectancy of osteoclasts is limited to approximately 12 days, the progression of bone remodeling requires the continual addition of these cells.

3. Reversal: this is the intermediary phase between resorption and bone formation and the responsible for the transmission of bone inducing signals to various cells found in bone resorption cavities, including monocytes, osteocytes and pre-osteobasts. These signals are not yet known, however there are some who assume BMPs, bone matrix-derived factors or FGFs as prospective candidates. During this phase, the osteoclasts disappear and macrophage-like cells are seen at the bone surface area. These cells aside from inhibiting the osteoclasts resorption action can also stimulate the osteoblasts activity.

4. Formation: bone formation results from a complex cascade of phenomena. At first, osteoclasts are inactivated and detach from the bone surface, being afterwards replaced by osteoprogenitor cells or pre-osteoblasts. These cells are attracted to the surface by means of various cell signals during reversal phase, which simultaneously stimulate their proliferation. The BMPs induce cell differentiation onto osteoblasts that start the synthesis of the osteoid matrix, filling the pre-existent resorption cavities. This matrix is mainly composed of Col I and non-collagenous proteins (i.e. growth factors). Eventually, the remaining osteoblasts in function stop their activity and give rise to lining cells that completely cover the newly formed bone.

5. Mineralization: this phase is characterized by the secretion of ALP, an enzyme associated with the early ECM maturation, which increases the calcium and phosphate ions concentration and allows their deposition as hydroxyapatite crystals over the osteoid matrix. This stage begins 30 days after deposition of the osteoid and takes almost 90 days in the trabecular bone and 130 days in the cortical bone. At the end, the new bone returns to a resting state, until new remodeling is initiated [23-25].

1.5 Bone formation at the interface: Biological Mechanisms

1.5.1 Osteoinduction

As the name suggests, osteoinduction is the process by which osteogenesis is induced. Primitive osteoprogenitor cells, undifferentiated and pluripotent, such as mesenchymal stem cells differentiate into osteoblasts and new bone is generated. This phenomenon requires appropriated stimuli. High molecular weight glycoproteins as BMPs (abundant in the cortical bone) are the most common osteoinductive cell mediator. Osteoinduction is a basic biological mechanism that occurs frequently in fracture healing and implant incorporation. In bone grafts, the recreation of this process is of particular interest for a faster integration as it triggers the formation of new osteoblasts and, this way, new bone tissue at the site. Despite the osteoblasts presence before implantation/injury, their intervention during bone formation tends to be minor, being the newly osteoinduced osteoblasts the main executors [27-29].

The most common osteoinductive biomaterials are the natural HAPs and the bioceramics.

1.5.2 Osteoconduction

In layman terms, osteoconduction can be defined as the process by which bone cells are directed towards a material's surface and are allowed to grow on it. This is a three-dimensional phenomena characterized by the ability of growing bone in apposition or above pre-existing bone.

Osteoconduction occurs frequently in implantable materials. The biomaterial works as a passive physical support/structure, waiting for the cells to act without stimulating the formation of bone tissue. Bone is allowed to growth freely on the surface or down in pores, channels or pipes through cellular and vascular local invasion. However, and despite continuous debate, many believe osteoconduction cannot occur by itself and to be dependent on the osteoinduction process. The differentiation of osteoprogenitor cells into osteoblasts is indeed required for bone formation. Still, in practice, an injury is sufficient to recruit undifferentiated and pluripotent bone cells to the site. This raises the debate on whether or not a biomaterial acts as an osteoinductor [29,30].

Titanium and its alloys, in particular the Ti6Al4V, as well as stainless steel are favored as osteconductors. To the contrary, bone conduction cannot take place at copper and silver substrates [29].

1.5.3 Osteointegration

The term osteointegration was introduced for the first time by Branemark (1969) which described this phenomenon as the "*direct structural and functional connection between the living bone and the surface of a load-carrying implant*", after observing a total and permanent integration of titanium screws on a rabbit femur [31]. Later, Donald's Illustrated Medical Dictionary defined osteointegration from a histological perspective as "*the anchorage of an implant by the formation of bony tissue around the implant without the growth of fibrous tissue at the bone-implant interface*" [32]. The Williams Dictionary of Biomaterials offered another description of osteointegration as "*the concept of a clinically asymptomatic attachment of a biomaterial to bone, under conditions of functional load*" [33]. Over the years, this terminology has changed and adapt. Despite their continuous application nowadays, limitations to those definitions have been detected. Neither took into consideration that, in particular situations, osteointegration happens despite the absence of a direct or chemical bond between the implant and bone, and just a physical contact is observed. For that reason, generally an implant is accepted as osteointegrable when its anchorage to the bone is such that no relative movements are detected at the interface and the bond generated endures under normal load conditions (Figure 8) [29,31,34,35].

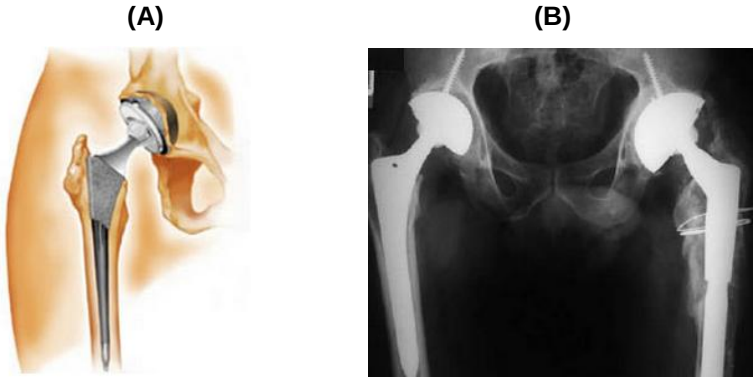

Figure 8. (A) Schematic representation of an osteointegrated hip implant [36] and (B) real life radiography of a similar outcome [37].

Osteointegration is not an isolated phenomenon and is dependent on both osteoconduction and osteoinduction. For instance, toxic materials that do not allow osteoconduction will not osteointegrate. Osteointegration implies that bone anchorage is maintained over time, through the consolidation of bone at the implant

site in normal and healthy conditions and without intermediate fibrous tissue or fibrocartilage formation [29,31,34,35].

These are the foundations for a successful osteointegration:

1. Viable and healthy bone, highly vascularized for a good ossification process (must not cause necrosis or inflammation);
2. Small space, without fibrous tissue, between bone and implant to keep the stability of the implant without micromovements (it should be less than 150 µm);
3. Implant biointegrable and compatible with the living tissue with mechanical stability and resistance similar to the natural bone, as well as appropriate design/conception, surface chemical composition, topography and morphology [38].

After implantation, the injured area should be allowed to heal without load for a considerable time, which can go up to several months depending on its location and dimension [34,35].

2. INTERFACE BONE – BIOMATERIAL

The interaction of an implant with the living tissue is a very sensitive phenomenon, which in a short period of time triggers a cascade of events (determine the biocompatibility of the material) that culminate with the cells attaching to the surface of the material (Figure 9).

An interface that is formed between two different phases, solid (biomaterial), and liquid (the surrounding biological environment, i.e. blood), usually exhibits high energy that can only be stabilized by the adsorption of substances from the medium, such as proteins. Water molecules bond to the biomaterial, originating an ionic layer that allow the proteins to adsorb, modifying their structure and functions according to the materials' outermost layer properties, coat the substrate and establish a reliable connection with cells. This might appear a simple mechanism but many are the implications to the cells response these events may represent. In consequence, a complete analysis of each one of those phenomena is required [39-42].

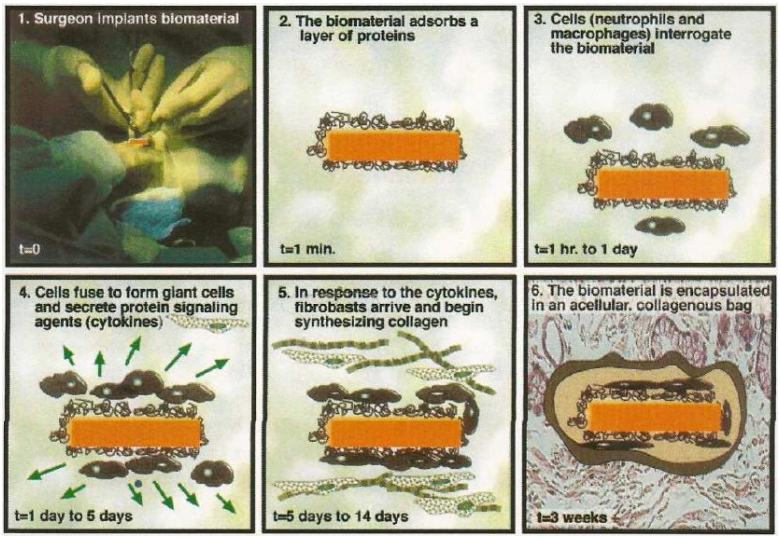

Figure 9. Biomaterial interaction with the living system and correspondent intermediary biochemical and biophysical phenomena [39].

2.1 Protein Adsorption

It is commonly state the first event taking place at the interface bone-biomaterial is protein or macromolecule adsorption from the biological fluids. Evidently this phenomenon is not the first, since water adsorption, ion bonding and adsorption of low molecular weight solutes, such as amino acids, occurs prior to it.

Still, protein adsorption remains the most important. Due to its rich, competitive and complex nature, these biological structures have the ability to disrupt the entire system at the interface changing the host response. The tendency of proteins to accumulate in between phases has led scientists to argue that the comprehension of the proteins behavior at interfaces is in fact a big step towards the comprehension of their normal and natural behavior [43-45].

Proteins are large complex amphipathic molecules composed of amino acids that contain combinations of ionic, polar and apolar regions exposed to the environment by a three dimensional arrangement. These regions grant the protein a "surface active" character allowing it to interact with various materials, both *in vitro* and *in vivo*. The biomaterials surface properties induce changes in the proteins behavior during adsorption, particularly in their conformation, by means of intermolecular forces. Van der Waals forces, Lewis acid-base forces and hydrophobic interactions are some of the many intermolecular events that affect the intrinsic structural stability of the proteins. In consequence, those alterations are reflected by the biological responses that follow, i.e. cell attachment. As proteins are the primary elements to be recognized by cells, their reaction towards the implantable material is believe to be a consequence of the interfacial protein layer [44,45].

2.1.1 Function and Structure

The treatment and understanding of protein adsorption requires familiarity with the concepts of protein function and structure, at least its basis.

Proteins are high molecular weight macromolecules resultant from the co-polymerization of up to 20 different amino acids (8 have apolar side chains, 7 have polar and 5 have charged polar). As general rule, a chain of amino acids is only named protein if superior to 40 units; otherwise it is identified as a peptide. In the human body there are near 10^5 different proteins, each one with a specific role. Proteins are involved in nearly all biological processes, managing the transport and storage of vital substances, providing mechanical support and protection, acting as catalysts of biochemical reactions, and others. Thus, in order to accommodate their functions, proteins fold into one or more spatial conformations driven by different non-covalent interactions. Their specificity is therefore determined by the acquired structure and chemical composition [44-46].

There are four levels of protein structure, the primary, the secondary, the tertiary and the quaternary (Figure 10). The primary structure refers to the amino acid organization as a linear sequence. The unique and specific amino acid organization is particular to each protein and it is hold together by way of covalent bonds (peptide bonds). Hydrogen interactions are then created between amino acids from different positions along the protein chain, causing it to bend and fold resulting in various secondary structures (i.e. α-helix or β-pleated sheet). A three dimensional conformation is here created but only reaches full potential by means of intramolecular associations [42,44,47]. Hydrophobic/hydrophilic interactions, ionic interactions, hydrogen bonding, salt bridges and covalent disulfide bonds are the most common associations – tertiary structures. On its turn, the quaternary structure refers to the regular association of two or more polypeptide chains, at different structure levels, to form a complex. A multi-subunit protein is generated that tends to be stabilized mainly by weak interactions between residues exposed by polypeptides within the complex [46-48].

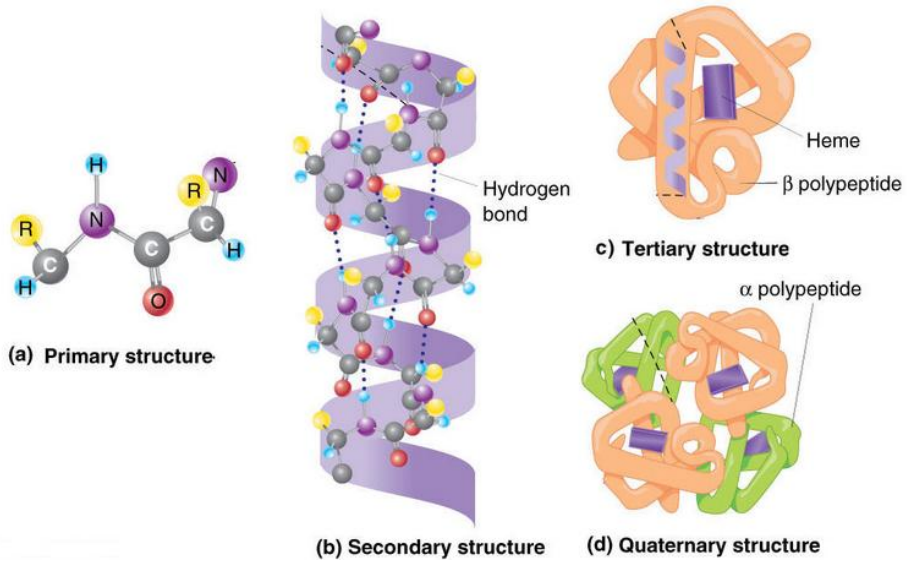

Figure 10. Four levels of protein structure [48]

2.1.1.1 Structure and Orientation of the Adsorbed Protein Layer

The structure of proteins adsorbed on a biomedical substrate is hard to identify and even harder to predict. The majority of proteins adsorb as monolayers generating close-packed formations of mass density between 1 to 5 mg/m^2. However, this range cannot be assumed as absolute. It all depends on the protein molecular orientation, conformation state and, as expected, the properties of the

outermost layer of the substrate. Multilayer adsorption is not as common but can also occur, particularly in high concentrated protein solutions [46,49,50].

Norde [46] by studying the adsorption of different types of proteins at solid-liquid interfaces stated that we cannot assume a definitive structure of a protein on a substrate but only infer about its most likely adsorption orientation. Since proteins are typically asymmetric and only in exceptional cases they exhibit a spherical shape (generally proteins present elliptical, rod-like or heart-like shapes), when on a surface they adopt a certain orientation that determines which side of the molecule interacts with the material and which side stays in contact with the solution. The local amino acid composition of specific regions of a protein determines its affinity to the surface. Usually, the proteins' structure is subdivided into four domains, hydrophobic, hydrophilic, positively and negatively charged, that are exposed to the surface accordingly to the exhibited character (Figure 11) [49-51].

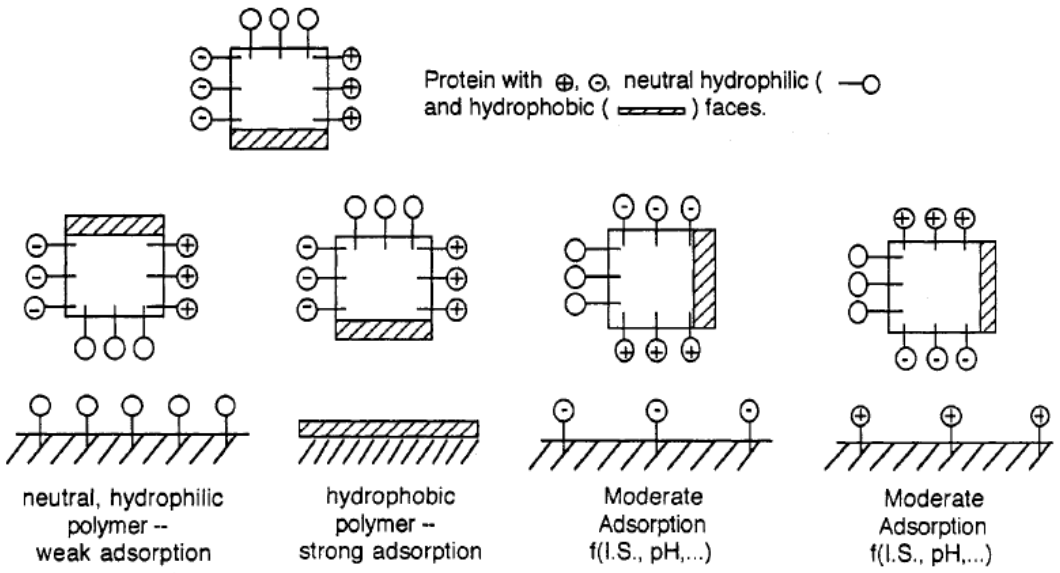

Figure 11. Schematic representation of proteins' domains and respective interactions with substrates of different nature, hydrophilic, hydrophobic, positively charged and negatively charged [51].

Structurally stable proteins can admit two types of orientation, the "side-on", with the short axis of an elliptically shaped molecule being perpendicular to the surface, or the "end-on", where the long axis is the perpendicular one. Inevitably, the "end-on" results in a more saturated monolayer than the "side-on" orientation [52].

As a rule, bigger proteins possess more binding sites. In consequence, their potential to adsorption is increased and its orientation is even harder to predict. Here, the unfolding properties of the proteins as well as its stability play a major role on the

adsorption process. Regardless the protein original structural rearrangement, its unfolding can lead to increased active site exposure for protein surface contacts, which will follow the predicted interaction paths described on Figure 11 [50,51,53].

2.1.2 Interactions with the Surface

Proteins adsorb onto solid surfaces through various interactions. Hydrophobic and electrostatic are the most common.

2.1.2.1 Hydrophobic

Hydrophobic bonds between proteins and surfaces are very common. In water, protein molecules tend to fold to minimize the exposure of their intrinsic hydrophobic groups. Thus, in order to establish a connection with the substrate both protein and substrate need to dehydrate. Hydrophobic dehydration results from the bonding of protein's hydrophobic domains with the hydrophobic regions on the substrate, and these phenomena are mainly driven by entropy positive changes (gain). Here, protein conformational changes may occur, which contributes to the irreversible adsorption character of these connections. Though these changes in conformation driven by the hydrophobic character of the interactions may also be associated with protein denaturation or loss of function activity, they can also be beneficial, for instance, by enhancing the proteins activity or their stability.

It has been established that interactions between a protein and a surface augment with increasing hydrophobicity of the surface and protein.

Hydrophobic dehydration is relatively unimportant for hydrophilic surfaces and/or rigid-like hydrophilic proteins, which explains the frequent superiority of hydrophobic substrates in regard to the amount of adsorbed proteins [46,51,52,54,55].

2.1.2.2 Electrostatic

Overall electrostatic interactions depend on the surface and protein charges, both of which are usually function of pH and solution ionic content. For instance, at low pH proteins are positively charged, whereas at high pH conditions proteins are negatively charged. Only when the isoelectric point equals the physiological pH, the positive and negative charges of a protein are in balance and, at this point, a molecule is neutral. Adsorption rates will be accelerated if proteins and substrates

share opposite charges. However, the mass load is generally maximized at the isoelectric point (pH at which the net charge is minimized).

Ion incorporation can influence protein interaction with surface via transport of ions from solution to the protein layer or charge redistribution. The presence of counter-ions is implied in the adsorption of proteins to like-charged surfaces, which may explain the participation of calcium ions in some adsorption processes.

Electrostatic interactions are considered a more decisive parameter for protein adsorption of rigid-like proteins and tend to occur more frequently in adsorption processes to hydrophilic surfaces. In this case, proteins are less susceptible to structural changes and as consequence are allowed to keep their original conformation (interior hydrophobic groups) [46,51,52,56].

2.1.3 Kinetics of Protein Adsorption

The kinetics of single protein has been discussed by many groups and different models have been proposed to explain it. Still, there are some steps on which all agree: transport of proteins towards the interface, its adsorption, and the subsequent structural rearrangement. By combining these steps the overall rate of the adsorption process can be estimated [46].

In the majority (or totality) of the systems, the transport towards the surface is controlled by diffusion. This step is majorly influence by the stability of the environment. For instance, elevated temperatures can accelerate the diffusion rate of proteins and by consequence the amount adsorbed. In low protein concentration systems, the rate of diffusion is expected to be slower than the actual adsorption, while in higher, the diffusion rate is expected to determine the rate of adsorption. Protein-surface interactions are intimate dependent on the concentration of the protein solution and by extent so are their structural rearrangements. A protein that adsorbs at a slower rate from a low concentrated environment has more time to unfold and spread over the surface than if the rate of arriving molecules was superior. In these cases, a more favorable conformation may be achieved. On the other hand, in high concentrated environments the amount of proteins attracted to the surface increases, which reduces the available spaces for connection and leaves the final extent of the structural rearrangements as function of relative rates of arrival. In this case, the affluence of protein molecules at the surface induces changes in the

conformation, most likely as result of intermolecular interactions rather than protein-surface interactions [46,47,49-51,57].

2.1.4 Conformational Changes and Stability

It is well accepted that many proteins undergo conformational changes after adsorption. Despite their complex nature, proteins cannot be understood as rigid structures but more as flexible chains. By interacting with the surface, proteins gain energy which impels them to maximize their contact through conformational rearrangements. Initially, proteins interact with the substrates through surface domains exposed in their native condition. Driven by the need of more favorable conformational states, rearrangements of the proteins structure take place resulting in the loss of the proteins' original secondary level and in gain of energy. In particular cases, reorganization of the protein structure does not occur immediately, being the protein layer still in risk of elution. However, after achieving conformational stability, which may take between few minutes to several hours depending on the size and structural "rigidity" of the protein, some proteins can even be found irreversibly attached to the material surface [46,47,49-52,58].

Changes in the environment (pH, temperature…) and in the material surface (free energy, wettability, charge…) can alter the protein conformation. It is therefore conceivable that these changes will affect the protein's biological functions. There have been reports on protein functions being activated only after adsorption. The opposite has also been seen through the inactivation or reduction of certain enzymes activity as consequence of adsorption [50,52].

2.1.5 Reversibility and Irreversibility

During adsorption, the protein rearranges its structure to an optimal one, which increases the molar free energy of adsorption, in other words the energy necessary to break the connection protein-surface. Besides, by changing its orientation in order to fit the requirements of specific regions of the substrate, the protein develops multipoints of attachment. In consequence, the protein desorption process as inverse of the protein adsorption process is no longer appropriate. The only possible alternative to break the connection is to overcome the sum of free energy gain during protein adsorption and rearrangement. Still, even if possible, since the activation energy for adsorption is much smaller than the necessary to initiate desorption, the

later process would be much slower and last much longer. For these reasons, none or very little proteins desorb by itself and many consider the protein adsorption process as irreversible [46,47,49-52,57,58].

According to previous research, the adsorption process can only be reversed biologically through the exchange of protein molecules, with the pre-existent proteins being displaced by others of different molecular weight and affinity to the surface [58]. Though proteins may be detached from the surface, those which have rearranged their structure to fit the demands of the substrate may never recover their natural conformation.

2.1.6 Competitive behavior

The competitive adsorption behavior of proteins is important to many interfacial phenomena, particularly to the biocompatibility of biomaterials to blood and tissue. Body fluids are composed by different kinds of proteins that mutually compete to any exposed surface. Adsorption from these fluids may be a very complex process but has many advantages; enriching the surface with proteins that possess the highest affinity to it is one of those [59-61].

The most common phenomenon known from competitive protein exchanges on surfaces is the Vroman effect (Figure 12). Molecules in a protein mixture diffuse to a surface at different rates. Thus, a protein that arrives first can be displaced from a surface by subsequently arriving proteins. These proteins that are capable of displacing early adsorbed proteins are considered to have higher affinity to the surface and are typically larger and conformational flexible, which enables them to adhere strongly to the material (development of more contact points) [59,62]. By the end of the adsorption process, the initial population of proteins at the surface is no longer the same and neither are the proteins in solution. The final composition of the adsorbed layer is therefore a result of the type, amount and relative affinity of proteins recruited from and available in the solution, as well as their reversible adsorption character [42].

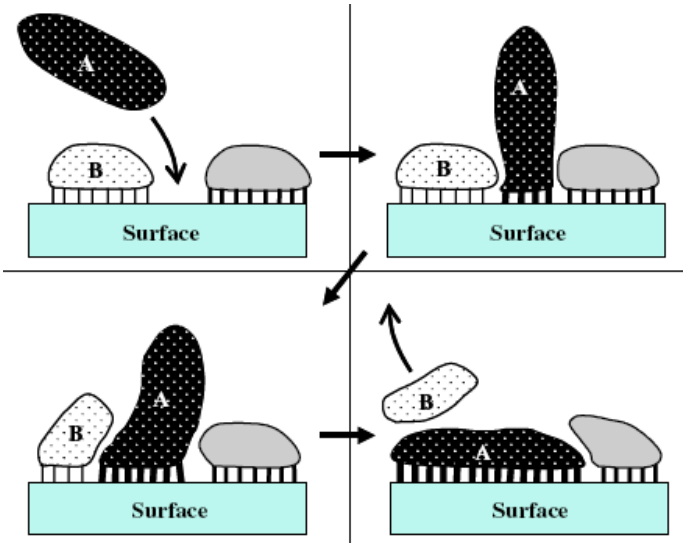

Figure 12. Schematic representation of the Vroman effect, with protein B that arrives first to the surface being displaced by protein A which creates more stable bonds with the available binding sites of the surface [42].

The irreversibility of protein adsorption results in fundamental differences between competitive adsorption processes. While the adsorption behavior of low molecular weight proteins in mixtures can be predicted from the analysis of their individual behavior, which develops towards an equilibrium state, the same may not happen between proteins of different molecular weights. Aside from the proteins affinity referred above, the time elapsed between the arrival of the first proteins and the next may be of particular importance for the reversibility of the interactions. Since proteins undergo molecular relaxation and spreading over the surface some time after arrival, in case of two proteins with similar affinity to the surface competing from the same location the first will be in advantage over the other [42,46,50,52].

Another major factor determining the outcome of any competitive system is the relative concentrations of the species or molecules in competition. Generally increasing concentrations of a given protein in solution result in roughly proportional increasing amounts of that protein adsorbed onto the surface. However, here, a complete molecular evaluation of the system must be performed to confirm this statement as valid. Since the rate of transport and adsorption as well as the rate of conversion to an irreversible state and the affinity towards the surface limit the amount and type of proteins adhering to it, nothing guaranties that high concentrate proteins will adhere preferentially [46,50-52,60-62].

2.2 Dynamics of Cell Adhesion

The term “adhesion” in biomaterials is commonly associated with different phenomena. In short term events, it is related to the cell attachment to biomaterials by means of ionic forces, Van der Walls forces, etc., while in long term events other biological molecules, ECM proteins, cell membrane proteins or cytoskeleton proteins, are involved in the adhesion process.

The adsorption of proteins onto a biomaterial surface is a complex process but can occur in a small time frame of minutes or even seconds. Thus, by the time cells reach the surface, they no longer recognize the material but rather the adsorbed protein layer. Through their membrane-bound receptors or ligands, cells identify bioactive binding sites on the protein layer, mainly integrins (ECM proteins), connecting and behaving accordingly to the information received by signal pathways (Figure 13). This association allows the cell cytoskeleton organization, by means of focal adhesions that spread along the surface, and impel the cell normal development on the biomaterial [63-65].

As stated in previous sections, the type, amount, orientation, conformation and packing density of proteins, as function of surface and environment conditions, determine whether the available bioactive sites from the biomaterial surface may be recognized by the cell membrane receptors [42,46]. Therefore, to understand the observed host response is essential to understand the way cells interact with the exposed surface and the role of the particular molecules involved.

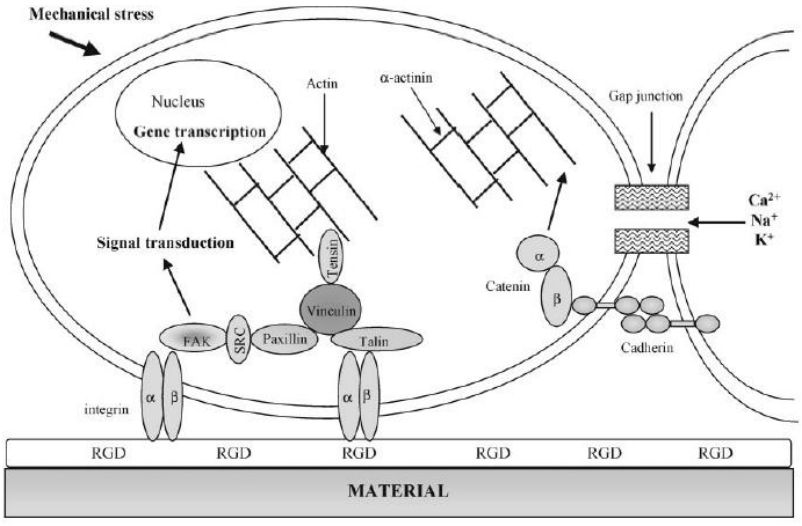

Figure 13. Schematic representation of the long-term cell adhesion to biomaterials process and respective proteins and molecular events associated [63].

2.2.1 Focal Adhesions

Focal adhesions, also known as focal contacts or adhesion plaques, are sites where integrin mediated adhesion (receptor of cell membrane and major components of focal adhesions) links to the cell actin cytoskeleton. These cell-matrix adhesions play essential roles in various cell biological processes namely cell motility, proliferation, differentiation, cell survival and even in the control of gene expression. They are found at the cell periphery or more centrally, usually associated with the ends of stress fibers of cells cultured on two dimensional rigid substrates.

Focal adhesions are specialized regions of the plasma membrane where bundles of actin filaments are anchored to transmembrane receptors through a multi-molecular complex of junctional proteins (Figure 14). These close junctions are normally at 10 to 15 nm from the substrate surface and are very difficult to identify *in vivo*. They participate in the structural link between the receptors and the actin cytoskeleton but as well as in the transmission of signal pathways involving signaling molecules that include kinases and phosphatases [63,66,67].

Focal adhesions are highly dynamic structures that grow and shrink due to the turnover of their junctional proteins, in response to external and mechanical stress forces exerted by or through the surrounding matrix, as they life cycle progresses so their components evolve. For example, mature adhesions develop increased stability, with integrin receptors well defined (external faces) and internal faces formed of proteins like talin, vinculin or tensin mediating the interactions between the actin filaments and the membrane receptors [66-68].

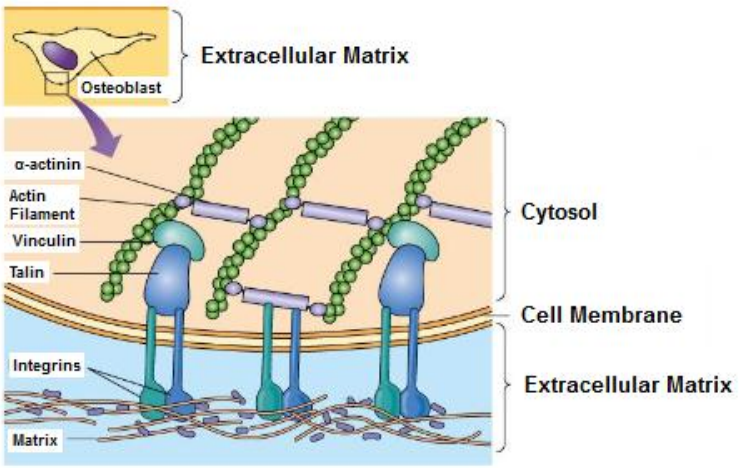

Figure 14. Molecules involved in the formation of focal adhesions [69].

It has been shown that for osteogenesis to occur, the formation of large focal adhesions must take place, since osteoblasts express a more contractile phenotype with increased intracellular tension that must be supported [70].

The formation of focal adhesions occurs essentially in cells with low motility and is promoted *in vitro* by extracellular proteins such as fibronectin and vitronectin, which ensure the maintenance of the cells shape and cytoskeleton organization [63,71].

2.2.2 Adhesion Molecules

Adhesion molecules are characterized by their ability to interact with specific ligands from the cellular membrane or from other ECM proteins. They can be subdivided into four categories, the selectins, the immunoglobulin superfamily, the integrins and the cadherins. Up to this moment, only the last two classes, integrin and cadherins, have been identified as part of the osteoblastic cells adhesion process [63].

2.2.2.1 Integrins

Integrins are critically important for the cell adhesion to the biomaterial, since they are the main and best characterized protein receptor that cells use to both bind and respond to the ECM stimuli. They are a large family of transmembrane heterodimeric glycoproteins that connect the intracellular and extracellular environments. Integrins are composed of 24 heterodimers of two noncovalently associated transmembrane glycoproteins subunits the α and β. There are 16 different α subunits and 8 β. Due to their diversity of structures, the same integrin molecule can bind to various ligand-binding domains. Its binding specificity is determined by the ECM domain of integrins that recognizes diverse matrix ligands. Controversially, different integrins may bind to the same extracellular ligands. For instance, 9 different integrins can bind to fibronectin. Its recognition is usually done through the central cell-binding sequence, the arginine-glycine-aspartate peptide or RGD motif.

Integrins possess a large extracellular domain that bind to the ECM, a single-membrane-spanning transmembrane domain, and a short cytoplasmic domain that links to the cell cytoskeleton (Figure 15). They are responsible for mediating the interactions between the ECM and the cytoskeleton. Most integrins are connected to bundles of actin filaments, which given the right conditions, may lead to the formation

of focal adhesions. They play key roles in the assembly of the actin cytoskeleton and modulate signal transduction pathways that control biological and cellular functions, including cell adhesion, migration, proliferation, differentiation and apoptosis [72-75].

Currently, it has been described that bone cells express preferentially the α_1 and α_5 subunits, with some sub-populations expressing α_2 and α_v as well. On its turn, the β_1 appears to be the predominant receptor forming dimmers with 12 distinct α subunits. The most common dimmers expressed by human osteoblasts are $\alpha_1\beta_1$, $\alpha_3\beta_1$, $\alpha_5\beta_1$, $\alpha_v\beta_5$, $\alpha_2\beta_1$, $\alpha_4\beta_1$, $\alpha_v\beta_1$ and $\alpha_v\beta_3$ [63].

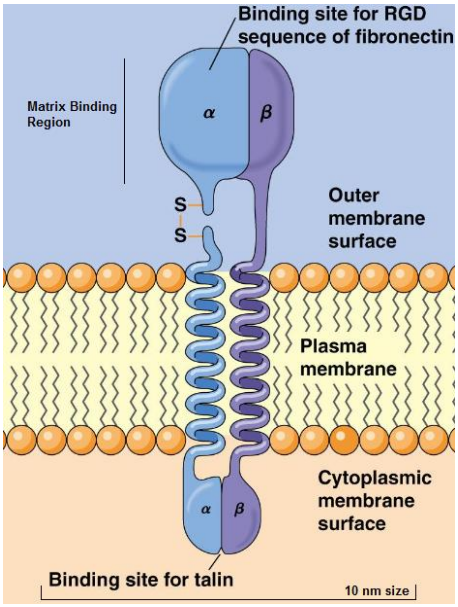

Figure 15. Sbunit structure of an integrin cell-surface matrix receptor, with a large extracellular domain with specificity to fibronectin RGD motifs and a short cytoplasmic domain with specificity to talin proteins [69].

The understanding of the integrin subunits involvement in the cell adhesion process provides essential information to the biomaterial improvement, as well as for the definition of the role of different proteins during implantation. There are many ECM proteins involved in cell adhesion. Here, special attention will be given to the fibronectin, vitronectin and collagen type I proteins.

1. Fibronectin (Fn) is a large multidomain glycoprotein and one of the most abundant ECM proteins that intervene in the cell adhesion to biomaterials. In its soluble form, Fn is very common in blood and other interstitial fluids. It exhibits a very stable compact conformation that hinders the interactions to other ECM proteins and restricts self-assembly. In this state, Fn is of major importance to the activation of

scar and blood coagulation events. On the other hand, when insoluble, Fn presents a very fibrous structure and is mainly found in the ECM usually associated with connective tissue and basement membranes [76,77].

Fn is composed of two homologous subunits, each with a molecular weight of ≈ 250 kDa each, covalently linked near their carboxy termini (or C-terminal domain) by a pair of disulfide bonds (Figure 16). Fn is remarkably organized. Each monomer is subdivided into modules with repeating amino acid motifs that are classified as Fn-I, Fn-II and Fn-III. The Fn-I is essentially present at the extremities and is composed of 12 sequences, each with 45 amino acids; the Fn-II is formed by two sequences of 60 amino acids; and the Fn-III is located in the center of the molecule and possesses 16 sequences of 90 amino acids. The modules are grouped as functional domains for cell binding and are separated by short hinge regions, which allow the molecule to adopt different configurations according to its state: globular in soluble Fn, and elongated in insoluble. This protein is known as multifunctional since it possesses, from a subunit point of view, various binding sites for biological structures including collagen, heparin, fibrin and various membrane receptors [78-81].

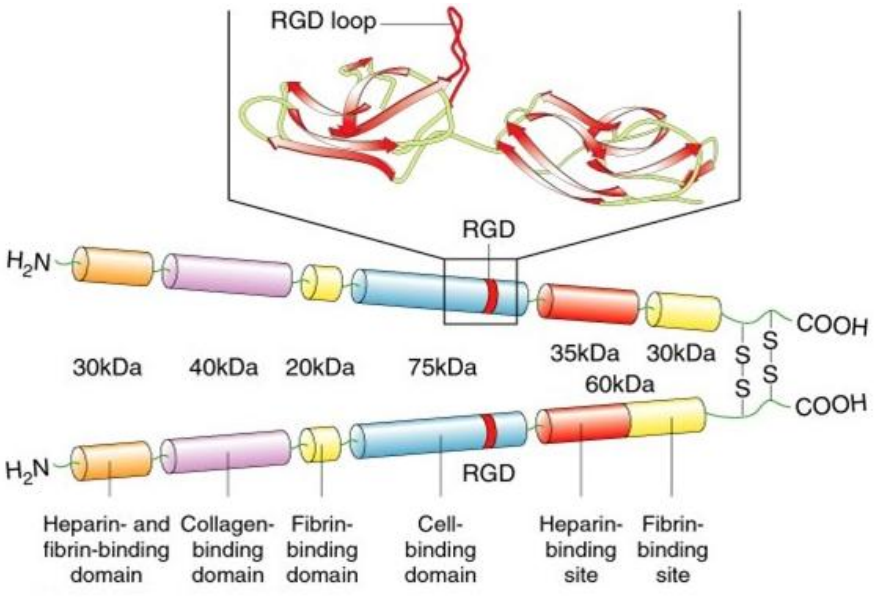

Figure 16. Representation of the fibronectin protein molecular organization and respective binding sites [81]

The most important Fn cell binding sites are located in the $III_{9\text{-}10}$ modules. At this region Fn binds to integrins, preferentially through the $\alpha_5\beta_1$ subunits (others: $\alpha_{IIb}\beta_3$, $\alpha_v\beta_3$, $\alpha_3\beta_1$ and $\alpha_v\beta_1$). Here, the most critical site for osteoblastic cell attachment

is the RGD peptide (75 kDa), a widely occurring arginine-glycine-aspartate amino acid sequence. The recognition of this simple tripeptide located in the III_{10} module of Fn is very complex and depends on flanking residues, the protein three dimensional structure and individual features of the integrin-binding pockets. For instance, by bonding with integrins, the RGD sequence allows the protein to assemble into fibrils constituting the primitive structure of the ECM. However, at this point, other Fn regions intervene to guarantee the integrity of the molecule while stretching, one in particular the N-terminal domain. Besides, the amino acid sequence PHSRN located near the RGD domain in the III_9 module, acts in synergy with the RGD site maintaining its stability and specificity and supporting its interactions with other integrins. These interactions trigger different signal pathways that will then influence the cell response [77,78,82].

Fn has been widely studied due to its impact on the cell behavior around biomedical implants. *In vitro* studies have shown that the cell function in cultures can be changed according to the amount of Fn adsorbed or the substrate used. It has also been hypothesized that conformational changes of Fn, as a result of surface properties, affect the presentation of integrin binding sites and therefore the cells development [79]. Garcia et al. [83] even showed that integrin-Fn interactions increase with the amount of ligands available, allowing the transmission of desirable signal pathways, which instigate the activation of intracellular genes and phenotypes responsible for inducing migration, proliferation and differentiation.

2. Vitronectin (Vn) is a multifunctional glycoprotein present in blood and in the ECM. Its complete amino acid structure of 459 units was initially deduced from a human liver cDNA. Vn promotes cell adhesion and spreading, inhibits the membrane-damaging effect of the terminal cytolytic complement pathway, and binds to several serine protease inhibitors. It has been also speculated that Vn may be involved in hemostasis and metastasis processes.

Vn is composed of one only peptide of 75 kDa of molecular weight, present in the human plasma at a concentration of 200 to 400 µg/mL. Vn can also be found, but in smaller concentrations, in the elastine fibers of skin or in the stroma of injured tissue. 30% of its molecular mass is composed of carbohydrates. Vn is predominantly found in the plasma as a folded monomer stabilized (presumably) by ionic interactions between its polyanionic and polycationic segments. In human blood two

distinct molecular forms can be identified: a single chain (75 kDa) and a clipped form of two chains (65 and 10 kDa) held together by way of a disulfide bond [84,85].

Its structure is thought to be divided in three major domains with binding regions for target ligands (Figure 17). The first is the N-terminal somatomedin B domain that consists of 44 amino acids and is assumed to be a key binding site for several integrins, including the plasminogen activator inhibitor-1 (PAI-1). This domain is followed by a specific binding sequence, the RGD site, through which Vn mediates the cell attachment and spreading. The second and central domain of Vn is thought to mediate binding to some bacteria and is located between the 131 and the 342 amino acids. At last, the C-terminal domain that accommodates the Vn plasminogen binding site also contains another important specific binding region, the heparin-binding sequence [84].

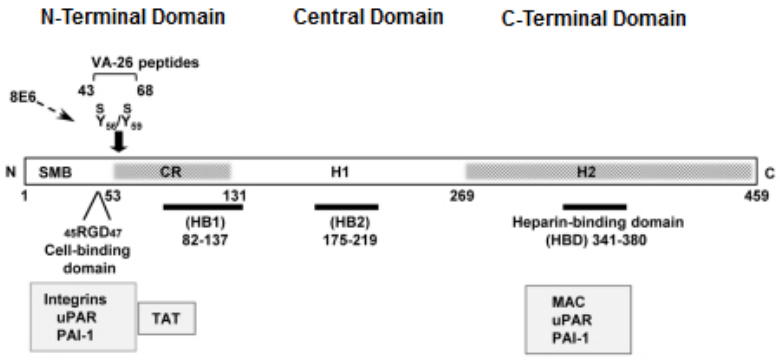

Figure 17. Vitronectin domains, N-terminal, Central and C- terminal [86].

The Vn molecule is recognized by five particular integrin combinations, the $\alpha_v\beta_1$, $\alpha_v\beta_3$, $\alpha_v\beta_5$ and $\alpha_{IIb}\beta_3$. The $\alpha_v\beta_3$ is probably the most well known receptor for Vn and recognizes the RGD sequence near the N-terminal domain. The RGD peptide is identified as well by the $\alpha_{IIb}\beta_3$ but only when this sequence is activated on platelets surface. The sequence of amino acids that compose the heparin binding site is mainly recognized by the $\alpha_v\beta_5$ integrins [63,84].

3. Collagen Type I (Col I) is an extremely important ECM protein, majorly present in the connective tissues (tendons, bone, skin, cornea and many interstitial connective tissues). 25-35% of the total amount of proteins in the human body are collagen and, from the 16 existing types, Col I is the most common, representing near 90% of the organic mass of bone. Col I is part of the fibrous proteins family with

a structural role in the pluricellular organisms and is one of the longest proteins known to man [87].

Col I is usually recognized by its hierarchical fibril structure (Figure 18), on which the smallest structure is a triple helix composed of three polypeptide α-chains of high concentrations in glycine, proline and hydroxyproline amino acids. The three chains, staggered by one residue relative to each other, are supercoiled around a central axis in a right-handed manner to form a triple helix. Here, the glycine residue plays a major role since it is present in every third position of the polypeptide chains leading to an assembled structure of repetitive units $(Gly\text{-}X\text{-}Y)_n$. Glycine is usually found in the center of the triple helix, with the outer positions being available for more bulky side chain amino acids. In Col I those amino acids are regularly the proline and the hydroxyproline. The Col I triple helix is usually formed as a heterotrimer by two identical α_1(I)-chains and one α_2(I)-chain. In fibril collagens, the three chains come together in a right-handed helix with approximately 300 nm in length and 1.5 nm wide, which corresponds to approximately 1000 amino acids [88,89].

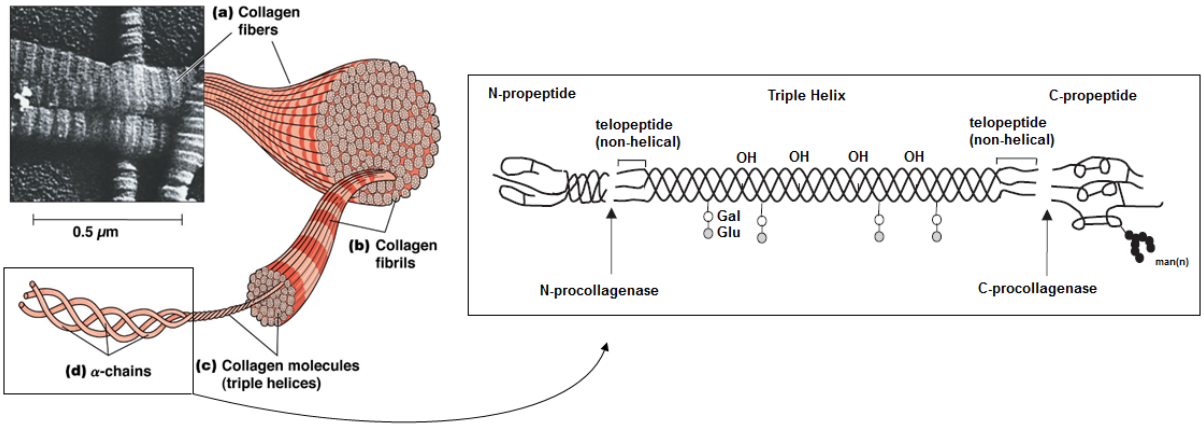

Figure 18. Collagen type I hierarchical organization [69] and molecular structure of the triple helix of α-chains [89].

In most organs and notably in tendons, Col I provides tensile stiffness. In bone, Col I defines considerable biomechanical properties concerning load bearing, tensile strength and torsional stiffness, in particular after mineralization. In addition to its structural and mechanical properties, Col I can also interact with other ECM molecules, adhesion proteins and growth factors. Fn, for instance, is one of the many proteins that possesses a binding site for collagen [89].

Col I is known to establish important interactions with receptors from the cellular membrane of osteoblastic cells, being recognized by the $\alpha_1\beta_1$, the $\alpha_2\beta_1$ (the most important and common) and the $\alpha_3\beta_1$ integrins [63].

2.2.2.2 Cadherins

Cadherins are transmembrane glycoproteins that mediate cell-to-cell adhesion. These molecules localized in adherence junctions, sites specialized of cell-to-cell adhesion, can establish linkages with the actin-containing cytoskeleton of various cell types. Their typical structure consists of an N-terminal external domain, where the binding functions are located; a single transmembrane segment; and a cytoplasmic C-terminal domain of approximately 150 amino acids.

Cadherins act by means of intracellular partners the catenins, which interact with intracellular proteins. These proteins are essential for the cadherin functions. Catenins were initially described as a set of three proteins α-, β- and γ-. The β-catenins bind directly to the cadherin cytoplasmic domain, whereas the α- catenin bind to the β-catenin and links the complex to the actin cytoskeleton by direct interaction with the cell actin fibers (Figure 19). In some cases the γ-catenin replaces the β-catenin in mediating cadherin-cytoskeletal complexes.

Osteoblasts have been shown to express E-cadherins, N-cadherin, cadherin-11 and low levels of cadherin-4. The expression of cadherin-4 is modulated by the bone morphogenetic protein-2 (BMP-2) [63,90].

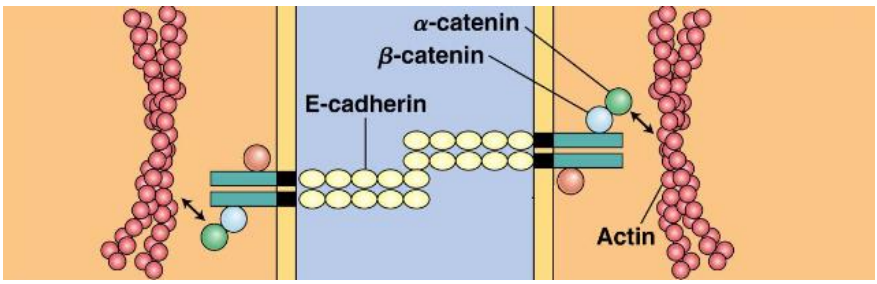

Figure 19. Cell-to-cell adhesion mediated by cadherins, with α- and β-catenin intracellular partners [69].

2.2.3 Non-Adhesion Molecules

The role of non-adhesion or non-specific molecules on the cell-biomaterial interface is not yet completely clear. However, it is believe that non-specific proteins such as albumin or osteonectin may activate other proteins during cell adhesion,

influencing their adsorption. For instance, there have been reports exposing the effect of bovine serum albumin (BSA) on the binding of Fn to tissue culture plates. They demonstrated an increased binding and biological activity of Fn as a result of the BSA presence [91]. On its turn, osteonectin has been shown to activate matrix molecules such as Fn, Vn and Col I by inducing different protein conformations that led to higher exposure of integrin-binding sites [92].

In this section we will give special attention to albumin and its role on osteoblast-biomaterial interactions.

1. Albumin is a small globular serum protein (66 kDa), predominantly found in blood plasma (60-70%) in a concentration of 40 mg/mL (adults). It is considered a non-adhesive or non-specific molecule with a main function of controlling the colloidal osmotic pressure of blood. Albumin is also involved in transport of low water soluble molecules such as lipids, salts, ions and even drugs.

Albumin comprises three homologous domains that assemble to form a heart-shaped molecule, each of which containing two subdomains, IA, IB, IIA, IIB, IIIA and IIIB. These are stabilized by 17 dissulfide bonds providing a relative flexibility to the molecule. Due to its small size, low molecular weight and high concentration in the human plasma, albumin is regularly the first protein arriving to the surface of a biomaterial [93,94].

Its conformation and orientation has been found to be affected by the surface properties. For example, studies have shown that the albumin amino acids exposure is enhanced on titanium surfaces but decreases on gold substrates. It has also been shown that its hydrophobic amino acid residues are preferentially oriented to hydrophobic surfaces such as polystyrene.

The most common binding receptor to albumin in cell membranes is the albondin. Albumin can also bind to a range of hydrophobic ligands including fatty acids, steroids, various cations and anesthetics [94].

2.2.4 Cell Signaling

Integrins are used both as mechanical anchors and signal transducers. It is based on the information received through these signals that cells regulated their activity, including migration, survival, differentiation and motility, and respond to inputs transmitted by grow factors, for instance. These signals correspond to external

stimuli arriving at the cell surface and are the major category of intracellular signal pathways. The other category is composed by the pathways activated by signals from within the cells. Both categories are relevant to the transmission of internal messages that activate the effectors of the cell response [95]. Nonetheless, special attention will be given to the first and biggest category of signals.

The signaling pathways activated by integrins have been identified through the analysis of biochemical events that trigger the integrins engagement and by the identification of focal adhesion complexes. Protein phosphorylation is one of the earliest events detected in response to integrin stimulation and has provided evidence of the integrins ability to regulate tyrosine phosphorylation. Here, the molecules involved in the signal transmission are the focal adhesion kinases (FAK), whose oligomerization is mediated by the protein talin. FAK appears to play a central role in integrin-mediated signal transduction since its activity and phosphorylation of paxilin and tesisn (for instance) is enhanced upon integrin engagement.

It has also been suggested that the protein kinase C (PKC) and the mitogen-activated protein kinases (MAPK) in signaling pathways are linked to integrin receptors. The PKC signaling is mainly associated to the cell attachment and spreading, while the multifunctional MAPK signaling system consists of separate pathways that function to control a number of different cellular processes that include gene transcription, metabolism, motility, cell proliferation, apoptosis, synaptic plasticity and long-term memory. Members of the Src family of tyrosine kinases, which are capable of phosphorylating FAK, have also been implicated in integrin signaling events, and so have been different phospholipid mediators and small molecular weight GTPases [73,75,95,96].

Aside from the previous, there are other signal pathways that transfer information across the cellular membrane: cyclic AMP signaling pathway, receptor-operated channels, voltage-operated channels, redox signaling, nitric/cyclic GMP signaling pathway, phospholipase D signaling pathway, janus kinase/signal transducer, activator of transcription signaling pathway, and others. In certain occasions these signal pathways may interact with each other for the intended cell response.

Due to the signaling system complexity, opportunities to subversion and aberrations may occur, leading to possible diseases (i.e. cancer, inflammatory diseases, angiogenesis…) [73,95].

2.2.3.1 *Growth Factors in the Osteoblasts Development*

Growth factors are very important to the osteoblastic cells development. In previous sections, it has been shown that BMPs can contribute to the cells differentiation and mineralization processes. Here, the participation of the BMPs in the osteoblasts development on implantable substrates is briefly characterized.

Many studies have shown that there is a close relationship between integrins and BMPs. BMPs are required for osteoblastic cells differentiation but they are only capable of inducing strong osteoblastic gene expression in the presence of ECM signals, for example the MAPK pathway, a transducer of integrin signals to the cell nucleus. It has also been seen, that the expression of human osteoblasts by means of integrins is enhanced in the presence of BMP-2 as well as their adhesion [20,97]. Lai et al. [98] by following the osteoinductive capacity of the BMP-2, as function of specific integrins activity, determined that by blocking the integrins' function the BMP-2 expression was harshly reduced. This was then reflected in a reduced ALP, calcium and phosphate production and diminished expression of OCN, OPN and BSP. It was also hypothesized that integrins may serve as anchors for BMP-2 receptors at focal adhesion sites. However, there is still much to understand in regard to these associations.

3. BIOMATERIALS

The idea of preserving the human body integrity for the longest time possible motivated the biomaterials development [99,100]. They became an essential tool in the medical field in the late 1800s, after the introduction of aseptic surgical techniques by Dr. Joseph Lister (1860s) [101].

By definition (and according to the Williams Dictionary of Biomaterials [33]), a biomaterial is "*a non viable material used in a medical device, intended to interact with biological systems (…) to evaluate, treat, augment or replace any tissue, organ or function of the body*". Ideally, it should not induce an abnormal host response when implanted and the preservation of human body integrity must be the main priority [99,100].

Biomaterials are primarily employed in medical applications usually integrated into devices or implants (rarely used as isolated materials) (Figure 20). They are also used in biological research or even in equipments for processing biomolecules for biotechnological applications. Either way, biomaterials must always be considered in the context of their final fabricated sterilized form [39;102].

As a science, the study of biomaterials is relatively young, about fifty years old. It deals with the physical and biological properties of the materials with a special attention to the interactions shared with the living tissue [39,100,103]. Biomaterials science has experienced a strong development over the history translated by a huge financial investment. In the year 2000, the global market of biomaterials was estimated at 18.4 billions of Euros (23 billions of US Dollars).

However, this market is still growing. It is expected for the year of 2015 an approximate investment of 51.8 billions of Euros (64.7 billions of US Dollars) [103,104]. Further investigation is required to deepen the knowledge on the complex biological responses stimulated by the materials after implantation [100].

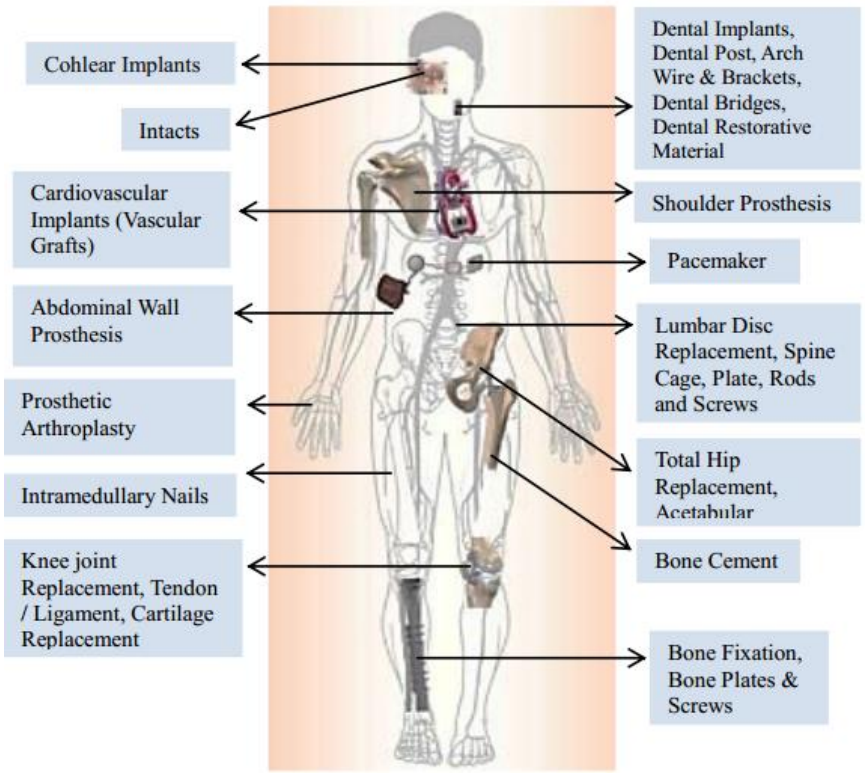

Figure 20. List of implants with human anatomy significance [103].

3.1 Recommended properties

The most important requirement that a material must fulfill to be consider a biomaterial is to be accepted by the human body without causing any adverse effect (inflammation, allergies and/or early rejection associated with toxicity), both during and pos surgery (recovering period). Good mechanical properties are another important requirement. The biomaterial should be capable of resisting high mechanical solicitation, which means its strength should be sufficient to sustain forces without breaking. Considerable fatigue strength and fracture toughness are also in the list of the demands. Nevertheless, excellent corrosion resistant continues to be the highest gold. The living system is a complex environment that changes and adapts accordingly with the human needs. Extreme corrosive conditions may happen sporadically but, when do, can affect and even damage the material. The resistance to constant use and varying loading may also be determinant for a long term success. The highest imposition to a biomaterial is that it should not fail as long as the host lives [105-107].

The schematic representation of Figure 21 lists all the demands a material must met for a successful implantation.

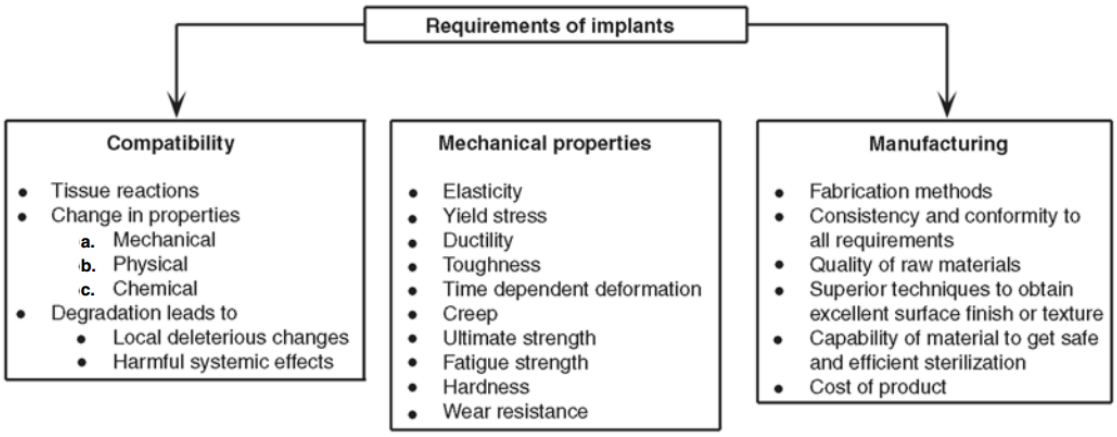

Figure 21. Implant material requirements in orthopedic applications [105].

Unfortunately, the materials currently available for orthopedic and dental implantations, despite being selected based on the criteria described above, still present some challenges. After 12 to 15 years they tend to fail and the patient must be submitted to a new surgery. To overcome this problem, researchers nowadays are dedicated in the creation of biomaterials capable of mimicking the physicochemical properties of tissues which they are meant to augment or replace. The improvement of the material's biocompatibility is one of the most important goals [39,105-107].

3.2 Biocompatibility

The concept of biocompatibility is unique to biomaterials science and common to all classes of biomaterials. It was firstly defined by the Williams Dictionary of Biomaterials (1987) as "*the ability of a material to perform with an appropriate host response in a specific application*" [33,39]. Later (2008), due to the improvement and development of the biomedical field, Williams Dictionary proposed a new definition, "*biocompatibility refers to the ability of a biomaterial to perform its desired functions with respect to a medical therapy, without eliciting any undesirable local or systemic effect in the recipient or beneficiary of the therapy, but generating the most appropriate beneficial cellular or tissue response in that specific situation, and optimizing the clinically relevance of the therapy*" [108]. In other words, the biomaterial must be accepted by the surrounding tissue and by the body as a whole without causing an abnormal inflammatory response, incite allergic or immunologic reaction or even cancer [39,108,109].

This is considered the most important property of a biomaterial and the one that defines its acceptance by the human body. Whether a biomaterial is biocompatible or not is strictly dependent on what physical function they are requested to and what biological response it is intended [39,109].

Before considering a material biocompatible, a thorough evaluation must be conducted. Precise cellular *in vitro* tests, defined by international standards and carefully controlled to allow reproducibility at different laboratories, must be done. Nowadays, the International Organization for Standardization (ISO) and the American Society for Testing Materials (ASTM) are the companies responsible for defining such evaluations [106].

3.3 Classes of Biomaterials

The science of biomedical materials involves a study of the composition and properties of the materials according to the function they will exercise and the environment they will be placed in. Since biomaterials can be selected from different classes between the natural (from human and animal origin) and synthetic derived, this section will be dedicated to the introduction of the biomaterials with the highest relevance to the present study, the synthetic. This is the most common category of materials used in the fabrication of implantable devices for the biomedical field. It is subdivided in four classes, composites, ceramics, polymers and metals that can be used either individually or in combination, depending on their specific application and the required properties [39,100,101].

3.3.1 Composites

The materials that contain two or more distinct constituents or phases, on a microscopic or macroscopic size scale, are named composites. The composite materials are divided in two phases, the matrix, which consists in the bulk continuous phase, and the reinforcement, which is the non-continuous phase and usually is formed by materials that possess superior mechanical or thermal properties, depending on the demands of the application.

Bone is a perfect example of a natural composite. Minerals are embedded as reinforcing elements while the collagen serves as matrix. In the biomedical field, the most successful applications of composites as biomaterials happen in the dentistry field, being extensively used as restorative materials or dental cements. They can

also be found in prosthetic limbs, where the combination of low density/weight and high strength materials make them ideal for such applications. However, due to the lack of consistency in the fabrication of composites, these materials still present some design and conception problems [39,100].

3.3.2 Ceramics

Ceramics are non-metallic inorganic materials with a limited range of formulations. Their microstructure is highly dependent on the applied manufacturing process and, consequently, their mechanical and biological properties. Despite have been used less extensively than metals or polymers, they possess remarkable properties: great strength and stiffness; high resistance to corrosion and wear; and low density and hardness. However, ceramic components tend to suffer from early failures due to their low fracture toughness and sensibility to the presence of cracks or other defects [39,110].

One of the first applications of ceramics as biomaterials consisted of replacing the traditional metallic femoral heads of hip prostheses by high-density and highly pure alumina (Boutin 1972). Since there, important efforts have been made to improve the material processing and design. Nowadays, ceramics can be found in several different biomedical fields such as dentistry, orthopedics and even general medicine, as medical sensors. The most popular ceramics are carbon, alumina and zirconia – bioinert (does not cause a reaction when placed in contact with the biological host) – and the bioactive glasses [111,112].

3.3.3 Polymers

Polymers form a versatile class of biomaterials due to their inherent flexibility to be synthesized or modified to match the physical and mechanical properties of various human tissues and organs.

The application of natural origin polymers in medicine date back thousands of years. In contrast, the use of synthetic is relatively recent. The first attempt was conducted in the 1940s, using a biostable synthetic polymer, the poly(methyl methacrylate) (PMMA), as an artificial corneal substitute. Ever since, polymers have occupied a prominent place between the biomaterials, becoming the most widely used materials in biomedical applications (Figure 22).

Polymers are macromolecules formed of large chains composed of many repeated units (monomers). Their main properties go from unique flexibility, lightweight and easy manufacture, to good resistance to biochemical attacks and good biocompatibility. They are mostly used when complex forms and high flexibility are needed [113].

Nowadays, a huge variety of polymers are available in the market: vinyl acrylics, polystyrene, epoxies, polycarbonates, silicones, polyethers, polysulfids and polyacrylic acids are between the many. These are used in the construction of prosthetic appliances, artificial teeth, temporary crowns, cements, and others [3].

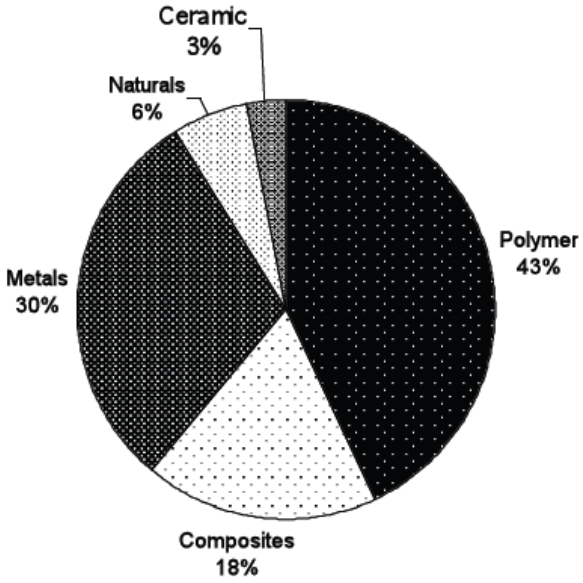

Figure 22. Global biomaterials market in 2002 [112].

3.3.4 Metals

Metals have been used as implants since more than 100 years ago, when Lane first introduced metal plate for bone fracture fixation in 1895 [114]. From that first experiment until now much as changed and evolved in their clinical use. Nevertheless, the reason that led to their initial selection for medical devices remains the same, high strength and resistance to fracture [3,114,115]. If properly processed, this class of materials provides reliable long term implant performance in major load-bearing situations. Metals can be used from simple wires and screws to fracture fixation plates, dental materials and total joint replacements for hip, knees, shoulders, and so on. In addition, the good electrical conductivity of metals favors their use for neuromuscular stimulation devices such as pacemakers.

The most popular metals for medical applications are: titanium, cobalt, stainless steel, nickel, chromium and the noble metals, like gold, tantalum, platinum, palladium, silver, iridium and niobium [39,115,116]. Since, the object of this study is the titanium material we will be focusing on that with a special attention to the titanium alloy, Ti6Al4V.

3.4 Titanium Metal and Alloys

The titanium (Ti) metal was discovered in 1790 and was firstly used as paint addictive to obtain the color white. It was only in 1940 that the American specialists in aeronautic started to focused their attention on the metal itself rather than on its derivatives.

After the second half of the twentieth century, Ti and its alloys started to be used widely in industry as well as in the biomedical field, particularly as hard tissue replacements. Due to their physical and chemical properties, their good corrosion resistance and biocompatibility, these materials have been, for decades, successfully employed in the orthopedic and dental fields. Their properties depend on their basic structure and manipulation during fabrication. In this last case, the importance of keeping a low iron content is fundamental to assure that no adverse interactions between implant and the human body will occur [114,115].

Ti is a nonmagnetic material, occupies the 22nd position of the periodic table, has an atomic mass of 47.9 g and is the fourth more abundant metal in the Earth crust. The melting point is approximately 1668ºC, whereas for its commercial alloys is around 538ºC. At less than 882.5ºC exhibits a hexagonal close-packed alpha crystalline structure and if the temperature is higher than that a body-centered cubic beta arrangement takes place.

According to the ASTM, Ti is classified in two categories: commercially pure and alloys. The first one is subdivided in four grades depending on the percentage of oxygen, iron, nitrogen, carbon and hydrogen. Regarding the alloys, the most common in the biomedical field is the Ti6Al4V composed of aluminum (≈ 6%) and vanadium (≈ 4%) [39,116,117].

Regardless the category, the material should not induce a harmful biological response and not suffer degradation when in contact with tissue or body fluids. The properties listed in Table 1 favor greatly commercially pure (CP) Ti and Ti6Al4V as bone substitutes. Their ability to react with water and air (oxygen) to produce a stable

and continuous oxide layer (passive film of 2 to 10 nm of thickness) it is in the bases of their excellent corrosion resistance and exceptional biocompatibility. This passive film has the ability of repassivation in the presence of oxygen, allowing its regeneration even after mechanical damage or removal of the layer [118].

Table 1. Mechanical properties of CP Ti, Ti6Al4V and cortical bone [39,116-118].

Metal	Tensile Strength (MPa)	Yield Strength (MPa)	Elongation (%)	Elastic Modulus (GPa)	Density (g/cm^3)	Reduction of Area (%)	Type of Alloy
CP Ti Grade 1	240	170	24	102.7	4.5	30	A
CP Ti Grade 2	345	275	20	102.7	4.5	30	A
CP Ti Grade 3	450	380	18	103.4	4.5	30	A
CP Ti Grade 4	550	485	15	104.1	4.5	25	A
Ti6Al4V	895-930	825-869	6-10	110-114	4.5	20-25	α+β
Cortical Bone	140	-	1	18	0.7	-	-

Once the material enters in contact with the biological medium, chemical and biochemical interactions take place: first hydroxylation and hydration of the oxide occurs; then adsorption of calcium and phosphate ions, for instance; followed by the adsorption of macromolecules such as proteins. This last step induces a biofilm formation that promotes the osteoblastic cells attraction and consequently leads to the tissue formation.

From a biological point of view, Ti possesses an important characteristic for implantation which is the ability to osteointegrate. Due to the high dielectric constant (from 50 to 170 depending on crystal structure) that characterizes these materials, a strong interaction (strong Van der Waals bonds) with the living tissue is formed without the need of extra adhesives. Consequently, the forces required to break the bond are proportionally high [114,115,118,119].

3.4.1 Titanium Alloy, Ti6Al4V

Pure Ti and Ti alloys are now the most attractive metallic materials for biomedical applications.

The alloys are classified as alpha (which contain neutral alloying elements or alpha stabilizers, such as Al or O), alpha+beta (which generally contain a combination of alpha and beta stabilizers) and beta (which are metastable and contain sufficient beta stabilizers such as Mo or V), depending on the microstructure

presented while at room temperature. Ti6Al4V, a grade 5 and alpha-beta alloy (Table 2), is the most widely used of the high strength Ti alloys. The combination of this property with its light weight, formability and excellent corrosion resistance, have made the Ti6Al4V a world standard for orthopedic and dental implantations. It is significantly stronger than CP Ti while having similar stiffness and thermal properties. Besides, this alloy possesses excellent fatigue strength which is of great advantage for lifetime implantations [114,118].

Table 2. Ti6Al4V chemical composition [114,118].

Element	Percentage (%)
Carbon – C	0.100
Titanium – Ti	Balance
Aluminum – Al	5.500 to 6.750
Vanadium – V	3.500 to 4.500
Nitrogen – N	0.050
Iron (Maximum) – Fe	0.400
Oxygen (Maximum) – O	0.020
Hydrogen (Maximum) – H	0.015
Other, Total (Maximum)	0.400

3.4.2 Problematic with titanium and its alloys

In order to achieve an implant system that responds completely to the human body demands, the physical and chemical properties of the materials' outermost layer must be controlled.

As was pointed earlier, the Ti based materials are capable of creating a protective oxide layer when in contact with oxygen. Unfortunately, that passive film spontaneously formed is not completely ideal for biomedical uses. It has a heterogeneous formation and is very thin, tending to disappear when rubbed. If so, it causes the diffusion of the Ti oxide to the biological surroundings, which will then act as abrasive elements. All these phenomena incapacitate the implant chemical adhesion to the biological material [32,39], which can even occur years after implantation (implant loosening).

Concerning the Ti6Al4V alloy, the issue of toxicity raised by the presence of vanadium is one of the biggest concerns. After implantation, this problem may appear due to the dissolution of ions. Indeed, if the oxide layer is not reformed before exposure to the biological environment, vanadium can be release and, consequently, a negative host response may take place.

To overcome these limitations, over the years, several surface treatments have been proposed. From simple modifications in the physical or chemical properties of the surface [120,121] to the immobilization of bioactive molecules, both from inorganic and organic origins (i.e. HAP [122] – precipitation of calcium and phosphate groups – or adhesion sequences such as RGD [123]), the options are many.

4. CURRENT SURFACE TREATMENTS OF TITANIUM

4.1 Role of Surface Properties on the Cellular Behavior

Ti and its alloys are favored as implant materials for orthopedic applications with direct contact to bone. These materials possess excellent corrosion resistance, low toxicity, “acceptable” compatibility with the living tissue and good mechanical properties, namely high tensile strength and durability, high ductility and low density [115,124,125]. Despite their continuous use in the medical field, aseptic loosening due to unsatisfactory response of the tissue surrounding and possible infection still occurs [126]. This challenge has motivated research from various perspectives, mechanical, physical and chemical, giving rise to different alternatives to improve the surface properties. However, this was only accomplished once understood the impact of each one of the Ti surface characteristics on the cells behavior.

A substantial number of studies have been conducted to examine the osteobastic cells behavior on Ti treated with different surface techniques. *In vitro* and *in vivo* researches have demonstrated that surface topography, wettability and chemical composition can significantly affect the cells development from early attachment to late differentiation (mineralization).

4.1.1 Topography

Cell adhesion, proliferation, differentiation, metabolic activity and the synthesis of ECM proteins are very sensitive to surface properties. There are numerous reports that show that surface roughness or topography affects the rate of bone tissue integration and biomechanical fixation of titanium implants, both *in vivo* and *in vitro*. This property has been pointed by many as a stimulant factor in the creation of a microenvironment favorable for cell adhesion, migration and differentiation [127,128].

The most common mechanical methods of surface modification applied to Ti based materials are the machining, grinding, polishing and blasting, which usually associate other physical treatments such as shaping or removal of surface materials. These are frequently applied with the aim of modifying the surface to obtain specific surface topographies and morphologies to improve cells development [121].

Linez-Battailon et al. [129] by studying the role of surface roughness of Ti6Al4V materials on the MC3T3-E1 cells proliferation, morphology and expression of different adhesion cells has shown exactly this. They used five surface treatments, sandblasting, 80, 1200 and 4000 grade polishing and mirror polishing, to induce different roughness levels, and followed the MC3T3-E1 cells initial behavior on those. The results revealed the cells preference for smoother surfaces with increased proliferation rates and different spreading patterns. To the contrary, the diminished cell growth on these materials indicated a lower adhesion performance and decreased cell activity, which included differentiation and mineralization. In this study, it was also seen that the expression of actin, vinculin, Fn and Col I varies with respect to the surface roughness. While on rougher substrates the actin cytoskeleton appears disorganized, the amount of vinculin contact points and Col I was increased. Fn expression did not change with the Ti6Al4V roughness.

Anselme et al. [130] conducting a similar experiment, evaluated the long term adhesion of osteoblastic cells on CP Ti substrates with different morphologies and concluded that human osteoblasts spread more intimately on surfaces with lower roughness amplitude. Cells behavior was tested on seven morphologies created by five surfaces treatments, electron-erosion, sandblasting, polishing, acid-etching and machine-tooling. As in [129], it was again seen that cells adhesion is intensified on rougher materials. By observing the osteoblasts adhesion power, they reached an interesting conclusion that points that human osteoblasts are more sensitive to the roughness organization and morphology of the surfaces than actually to its amplitude.

Simon et al. [131] investigated the biocompatibility and corrosion resistance of CP Ti submitted to five different surface treatments, namely sintered microspheres porous Ti, plasma spray, sandblasted and acid etched combination, and sandblasted with HAP, and demonstrated that MG63 osteoblast-like cells behavior is influenced by the surface treatment. Porous Ti increased significantly the cell attachment, morphology, proliferation and ALP production, suggesting a better biocompatibility compared to the rest of the substrates, aside from putting in evidence an excellent electrochemical performance.

During an *in vivo* study, Gabbi et al. [132] was able to prove that micro-roughness can considerably affect osteointegration. The aim of the study was to perform an analogy between bone tissue responses to differently treated Ti implants: chemically-treated rough Ti achieved by double acid etching process, bioactive Ti obtained by Bio-Spark, and untreated machined Ti (control). By following the body local reaction to the implantable materials, they confirmed that all treatments can improve and accelerate osteointegration in relation to the control, in particular the double acid etching process which stimulated considerably more the early cells development. Gabbi et al. consider surface roughness as a key factor for osteoblasts adhesion and colonization during neo-deposition around Ti implants.

Hayakawa et al. [133] conducted an *in vitro* study where they followed the viability and total protein contents of MC3T3-E1 osteoblast-like cells cultured on Ti with different surface mechanical treatments, nanometer smoothing (average roughness, Ra ≈ 2.0 nm) and sandblasting (Ra ≈ 1.0 μm), and biochemical treatments, namely, with and without Fn immobilization. They demonstrated that the combination of sandblasting and Fn provided better cell viability, while Fn on its own motivated a better arrangement of the attached cells. The smooth surfaces were responsible for higher cell attachment with more spread cells. In the end, no significant differences were found on the total protein contents between the four surfaces.

Since different roughness usually leads to different morphologies, Teixeira et al. [134] decided to investigate the effect of pore size on osteoblastic phenotype development. Porous Ti disks with three pores sizes, 312 μm, 130 μm and 62 μm, were cultured with osteoblastic cells from human alveolar bone up to 14 days. It was seen that bigger porous size regulated the cell growth by stimulating the osteoblast proliferation. On the other hand, bone markers gene expression, namely the runt-related transcription factor 2 (RUNX2, a master transcriptional factor that initiates bone formation), ALP, Col I, BSP and OPN, was enhanced in the presence of smaller porous size substrates (62 μm). These results suggested that the size of porous together with the thickness of the porous coating, also considered to influence the cells phenotype expression, on Ti materials could contribute to the development of Ti

implants with ideal surface morphology that yield osteointegration in challenging bone sites.

Despite the continuous research for surface treatments that will allow a perfect topography and morphology, until this day there is no absolute values or ideal characteristics defined for the titanium material. As well, the cell response may not yet be totally clear. There are some authors that admit a negative effect induced in the cells activity, cell adhesion [135] and phenotype expression [136], by rougher surfaces. Others point that different cell types or cells at different maturation stages may display opposite behaviors when cultured on rougher materials [137,138].

4.1.2 Wettability and Surface Energy

The surfaces wettability and energy are normally a result of differences in surface composition and/or topography. Despite this interdependence, many studies have shown that protein adsorption is directly affected by these two important properties and, in consequence, so is the cells attachment. Kasemo et al. [139] has even pointed that surface wettability may be the real instigator of osteointegration, since water molecules are the first to associate with the biomaterial in a living organism. This argument was supported by Hallab et al. [140] that demonstrated the surface energy to be more important than the surface roughness for cell adhesion strength and proliferation. The same was detected by Schakenraad et al. [141]. They even pointed that surface energy may be the dominant factor for cell attachment even after the solid surface has been covered by a protein layer. Based on these revelations, many investigators have dedicated their attention to these important aspects of Ti implants to better predict the cells response.

Ponsonnet et al. [142] followed the cell attachment and spreading on various Ti materials, CP Ti, Ti6Al4V and NiTi (titanium nickel alloy), and based their conclusions on the surfaces hydrophilicity, free energy, interfacial energy and roughness. They were capable of establishing a relationship between the surfaces wettability and roughness and it was concluded that on rougher surfaces the water contact angles tend to increase. However, surface energy could only be determined when separated from the surface roughness, as the contact angles and the shape of the drops change on the material with time. Therefore, the materials were polished,

becoming smother (Ra < 0.015 μm). It was established that all materials were hydrophilic and that having a low polar component (or low fractional polarity) influenced positively the cells proliferation. The interfacial free energy values were low for all investigated surfaces indicating good biocompatibility. Taking into account roughness, it was demonstrated that after a certain value (between 0.08 and 1 Am) cell proliferation becomes difficult, showing that the higher the roughness the lower the cell proliferation rates. In conclusion, surface energy was found as the dominant factor to determine cell adhesion. Nevertheless, data showed that roughness can strongly disturb the relationships between surface free energy and cell proliferation.

Rupp et al. [143] showed that the surface wettability and its energy can play a major role on the protein adsorption and on the osteoblasts adhesion. By evaluating the materials wettability as a result of different surface topographies (sandblasting and acid-etiching treatments) and Fn immobilization, they were capable of establishing a correlation between surface properties, showing that average micro-structured surfaces possess superior wettability and surface energy. This combination of properties led to an improved initial biological response at the interface through the attraction of more ECM proteins. It was seen that the micro-structured surfaces, once in the complete wettable configuration, may improve the initial contact with host tissue after implantation, due to the drastically increased hydrophilicity. They also demonstrated that osteointegration is accelerated in the presence of Fn and that to be a result of the successful collaboration between roughness and wettability.

Zhao et al. [144] studied the MG63 cells growth and differentiation on sandblasting and acid etching modified Ti and demonstrated that the surface energy and the hydrophilicity of the materials can affect more significantly the cells behavior than roughness by itself. They created microscaled and submicroscaled structures of enhanced surface energy, similar to the osteoclasts resorption pits on bone wafers, and detected an intense osteoblastic differentiation. The hydrophilic nature of the substrates increased the OC and the ALP activity of the cellular layer and created a favorable osteogenic environment by enhancing local factors as prostaglandin E_2 (PGE_2) and transforming growth factor-β1 (TGF-β1).

Despite the clear benefits of wettable surfaces, sometimes they may not be necessary to improve the host response. Kubies et al. [145] by developing a comparative study between different commercially available implantable materials and the normal human osteoblasts reaction to it and capacity of blood coagulation showed exactly this. The osteoblasts proliferation and the expression of bone tissue mediators, such as TGF-β, ALP, tumor necrosis factor-α (TNF-α), interleukin-8 (IL-8) and vascular adhesion molecule-1 (VCAN-1), were monitored on Ti, Ti6AL4V, CrCoMo alloy, zirconium oxide ceramics, polyethylene and carbon/carbon composite. The results revealed the Ti acid etched materials to be the most suitable for bone tissue substitutions due to its high osteoblasts proliferation and osteogenesis markers expression, low inflammatory cytokines production and intensive blood clot formation. These outcomes were promoted by a higher polar surface energy, which exhibited the highest effect on all materials, and a superior surface roughness (Ra>3.5 μm). Here, it was seen that the wettability of the surface was irrelevant to the cells behavior.

4.1.3 Chemical Composition

The modification of the Ti chemical composition is a very common process in the biomedical field. Ti is usually characterized as a biopassive material, since the healing process induced by it is slower than on materials with bioactive properties, such as HAP. However, due to its physiological fragility, calcium and phosphate based ceramics cannot be used by itself as bone substitutes. Therefore, the use of Ti as bulk material is recommended. Bioactive coatings are usually used on Ti materials to improve and fasten their integration in the human body [146,147]. Different techniques may be applied to this task, grafting, anodization, chemical and physical vapor deposition, sol-gel technique, plasma spray and sputtering are some of the many [121].

Olivia et al. [148] tested two new formulations of bioactive glass coated on Ti6Al4V substrates on primary cultures of human osteoblasts and confirmed their bioactive and osteoconductive properties. A non-bioactive glass, uncoated Ti6Al4V and polystyrene were used as control against the bioactive glasses. It was seen that the last induced a rapid and strong osteoblastic proliferation with the cells spreading along the surface, creating a close and compact layer, and expressing high levels of

OC. This was not seen on the rest of the substrates which exhibited a minor proliferation and cytoplasmic extension. Aside from stimulating the osteoblasts proliferation and colonization, these glasses allowed in a successive differentiative step the expression of important osteoblasts biochemical markers. Olivia et al. study provided evidences of the bioactive glasses coated on Ti based materials potential for prosthetic application and as bone substitutes.

Feng et al. [149] incorporating calcium, phosphate ions and the carbonate apatite onto Ti followed the effect of the surface chemistry on the initial rabbit osteoblast response. They observed that the number of adhering cells as well as the ALP activity was superior for the apatite coated substrates and that to be closely followed by the calcium coated Ti. The phosphate coated surfaces registered lower amounts of cells and ALP which were only surpassed by the untreated Ti (control), the lowest from the group. They observed that calcium ions favor protein adsorption, such as Fn and Vn as ligands of osteoblasts, due to positive electricity and chemical and biological functions, becoming more relevant than the phosphate ions to the initial interactions between culture medium, osteoblasts and Ti surfaces. Calcium ions also played an important role on the apatite coated materials, since they represented the active sites for osteoblast adhesion and promoted it in the phosphate ion sites.

Park et al. [150] by studying the *in vitro* bioactivity of magnesium and magnesium/HAP coated Ti determined that these two surface coatings had the potential to accelerate the implant osteointegration and stimulate the osteoblastic differentiation. The magnesium and the magnesium/HAP were successfully coated on Ti substrates using radio frequency and direct current magnetron sputtering and their performance was compared to non-coated smooth Ti (surface roughness was similar for all materials). The ALP activity of the MC3T3-E1 cells was followed and the expression of important bone markers including BSP and OCN was evaluated. The results showed an improved cellular response with regard to proliferation, ALP and bone markers activity, on both magnesium and the magnesium/HAP coated Ti. No significant differences were detected between these two coatings, despite from a small increase on the ALP and BSP levels induced by the HAP.

Uezono et al. [151] proposed an innovative approach for quick implant osteointegration that consisted in the coating of Ti materials with a HAP/Col I nanocomposite. Here, three substrates were tested, machined Ti rods (control), HAP coated Ti and HAP/Col I coated Ti. *In vivo* bone formation was investigated on male Sprague-Dawley rat calvarium specimens via histomorphometrical analyses and bonding strength tests. It was seen that all the control substrates and half of the HAP Ti triggered an inflammatory response by fibrous encapsulation. To the contrary, the nanocomposite coated materials were almost totally surrounded by new bone tissue without encapsulation. HAP/Col I coating stimulated bone contact ratio, the greatest between all surfaces, and led to a superior bonding strength to bone.

Using the same combination Col I and HAP, Cecconi et al. [152] confirmed the previous argument. They inserted coated and uncoated Ti implants on New Zealand white rabbits and followed the bone formation at the site. After 45 and 90 days, the animals were sacrificed and the bone implant contact, the trabecular thickness and the calcium-phosphate ratio were measured. It was seen that all implants healed without fibrous encapsulation and that the coated materials significantly improved bone formation. The data demonstrated that Ti integration can be enhanced by this coating combination, accelerating stable implant fixation and the early loading of the device.

For many years, the use of HAP coatings on Ti materials was the most common and viable alternative in orthopedics. However, due to the instability of HAP in physiological environments (degradation), nowadays, other options are being searched. Biochemical modifications of Ti materials with the immobilization of ECM proteins or other peptides are attracting more and more attention [121]. In contrast to calcium and phosphate coatings, biochemical surface modification utilizes critical organic components of bone to affect tissue response [153].

4.2 Biochemical Modification of Ti Surfaces

The main goal of biochemical modifications of biomaterials is to immobilize proteins, peptides, or grow factors onto the surface in order to induce a specific cell/tissue response, in other words to control the tissue implant interface. A variety of techniques can be applied to this function; however an extensive literature review

shows that Ti materials usually bond with these biological molecules by means of physical bonding, for instance electrostatic, hydrophobic and Van der Waals interactions, or chemical bonding, such as covalent interactions [121,153].

For the purpose of this research, special attention will be given to the adsorption of ECM molecules (Fn and Col I, for instance), and to the peptides immobilization in particular the RGD sequence.

4.2.1 ECM Molecules Immobilization

The ECM components are very importance to the osteoblastic cells development, since they modulate their behavior during implantation. Adsorption and immobilization of these elements, particularly proteins, on the implantable surfaces can induce the recruitment of more osteogenic cells precursors, provide a more favorable environment for osteogenic cells differentiation, enhance cell attachment and increase the bond strength between cells and biomaterial. Since the 80's, different proteins have been tested on Ti based materials. Col I is probably one of the most common proteins used, due to its abundance in the ECM and capacity to modulate cell growth and differentiation [154].

Morra et al. [155] study was one of first that used Col I in association to Ti surfaces to modulate the osteoblast response. They covalently linked the protein to the material using hydrocarbon plasma followed by acrylic acid grafting, creating a complete and homogeneous adlayer. The surfaces cytotoxicity was investigated *in vitro* using SaOS-2 osteoblastic cells, while the osteointegration rate was followed *in vivo* in rabbits. The results from the *in vitro* studies confirmed these altered surfaces to be safe, despite no implications to the ALP and cells growth rate were detected between these and unmodified materials. To the contrary, *in vivo* studies revealed a significant increase on bone growth and bone-to-implant contact in the presence of Col I modified surfaces, which validates the ability of these biochemical modifications to enhance the bone healing rate. These observations were late confirmed by Van den Dolder et al. [156]. They observed that initially fewer cells were attracted to the covalently linked Col I compared to the Ti control, decreasing their proliferation rates. More importantly, they established this combination stimulates osteoblastic cells differentiation, improving and accelerating the osteointegration process.

Aside from Col I, Fn attracted much attention as well. This is a major adhesive glycoprotein that binds to other ECM components and facilitates the interaction of

different molecules in a stable interconnected network. Due to its central binding domain, the RGD peptide, Fn is capable of promoting osteoblastic cells adhesion and proliferation [77,78]. Pugdee et al. [157] using a simple tresyl chloride activation technique immobilized Fn on Ti surfaces and examined the MC3T3-E1 osteoblastic cells attachment and gene expression. They observed a higher cell attachment rate and enhanced expression of BSP and osteomodulin (OMD) on the Fn coated surfaces but reduced sulfatase-1 (SULF1) and mRNA levels, which implies a decrease in the glycosaminoglycan degradation and, consequently, an early promotion of matrix mineralization. In this study, Fn's impact on bone formation was attested. Yoshida et al. [158] conducted a similar experiment where aside from testing the implications of Fn (immobilized with the previous method) on the MC3T3-E1 cells behavior, they also tested the influence of surface topography. Here, smooth (Ra≈2.0 nm) and sandblasted (Ra≈1.0 μm) Ti surfaces were used to monitor the cells proliferation rates, ALP activity, OCN production and mineralization. In the end, the nanometer-smooth surfaces were seen to display higher ALP activity, OCN production and mineralization. In this case, the immobilization of Fn decreased the ALP production but increased it for the sandblasted materials. On the other hand, the presence of Fn led to a beneficial rearrangement of the cells cytoplasm, promoting their spreading, particularly on the smooth material. The MC3T3-E1 cells expression of various bone tissue markers was also followed by Rapuano et al. [159] on Fn immobilized Ti materials. As before, Fn enhanced the ALP, OCN, BSP, OPN, Col I and RUNX2 expression and even accelerated their production and activity, with their peaks being revealed earlier than on unmodified Ti conditions. Once again, Fn immobilization assured its value during osteoblasts differentiation and consequent osteointegration.

4.2.2 Peptides Immobilization

The ability of cells to adhere to a biomaterial, proliferate and organize their ECM into a functional tissue depends on the molecules involved during cell attachment, in particular the integrins. Integrins interact with short amino acid sequences of several proteins to create strong bonds to support their maturation along time. The most common sequence is the RGD which has been identified in plasma and ECM proteins, including Fn, Vn, Col I, OPN and BSP. This peptide is recognized by the majority of the cell membrane receptors and is an essential

mediator of osteoblasts attachment. Since peptides exhibit superior physiological stability than proteins, its application and immobilization by covalent bonding on Ti surfaces has become more and more recurrent. Nowadays, it has been shown that synthetic peptides that contain the RGD amino acid can essentially mimic cell attachment activity as if they were the original molecule [154]. One of the first *in vivo* investigations with RGD-containing peptides immobilized on Ti substrates was conducted by Ferris et al. [160]. Their study was designed to evaluate the quality and quantity of new bone formed on Ti rods coated with RGDC (Arg-Gly-Asp-Cys) peptides implanted in rat femurs. After 2 and 4 weeks of implantation, a significant thicker shell of new bone was observed around the RGDC treated implants compared to the plain ones. Mechanical pull-out testing were conducted after 4 weeks, as well, and revealed a superior (38% more) interfacial shear strength for the peptide modified Ti rods, suggesting this coating may enhance osteointegration at the site. In another *in vivo* study, Kroese-Deutamn et al. [161] evaluated the formation of new bone in a porous Ti fiber mesh implant coated with cyclic RGD peptide, containing a phosphonate anchor. They inserted the treated and untreated Ti implants into the cranium of a rabbit and followed the bone development up to 8 weeks. As before, the presence of RGD peptides increased the bone formation and ingrowth in relation to the uncoated Ti materials. Secchi et al. [162] confirmed the previous observations and the importance of RGD and RGD-containing sequences on the cell attachment regulation by covalently grafting RGDS and RGES (control) peptides onto Ti using an APTS linker. The peptides increased the surfaces roughness and hydrophilicity. The MC3T3-E1 cells were cultured afterwards and their behavior followed. Significantly more cells were found attached to the RGDS coated Ti than on the RGES, with the first contributing favorably to the osteoblasts phenotype expression and inhibition of apoptosis. During this investigation, it was seen that RGD-containing peptides enhanced osteoblasts attachment and their survival rates, putting in evidence their potential to promote osteointegration *in vivo*.

Biochemical methods of surface modification are promising approaches to modify and induce a specific cell response on Ti, at least at a laboratory level. Difficulties, however, may be found when it comes to the stability of the immobilized proteins/peptides on the surface and their accessibility to active sites of cells. Besides, physical adsorption of the molecules may not be successful for long-term

implantation due to possible desorption. On the other hand, the covalent binding may require the use of different chemical reactions, which can be aggressive towards the molecules reducing their bioactive potential. On top of everything, the cost of these processes and proteins/peptides synthesis may not be viable at an industrial level. Still, this continues to be a very acceptable and potentially capable surface modification method for Ti based implants [121,163].

4.3 Grafting of Bioactive Polymers

The grafting of bioactive polymers bearing appropriate chemical functions on implantable materials can modulate the cells entire activity, including attachment and spreading. This is an original and innovative approach based on old and well founded knowledge. Over the years, the notion of bio-specificity or specific recognition between two biomolecules has been applied to improve the host response at the interface cell-biomaterial. It became even more relevant with the introduction of biochemical surface modification methods in tissue engineering and biomaterials science.

The distribution of appropriate chemical groups along the polymeric macromolecular chains allows polymers to impart specific biological properties to the materials surface, such as modulation of the cellular or bacterial behaviors. Regarding the cells activity, these groups can intervene in the creation of new active sites capable of interacting with ECM proteins, implicated in the cell response [164]. These sites have been shown to possess specificity to adhesive proteins such as Fn or Vn and to be capable of modulating their affinity and conformation towards the implantable device, in order to maximize the exposure of their intrinsic binding domains to cells [164,165].

This concept of grafting bioactive polymers onto implantable surfaces has been the main research subject of the Laboratory of Biomaterials and Specialty Polymers (LBPS-CSPBAT UMR CNRS 7244) for over 20 years. Their efforts allowed, in an initial phase, the synthesis and grafting of anionic functionalized “model polymers”. These were synthesized from PMMA materials (methyl methacrylate, methacrylic acid and sodium styrene sulfonate or NaSS) with carboxylate and sulfonate functions through radical copolymerization. Different copolymers were prepared varying the molar proportions of two monomers but maintaining their insoluble character in physiological medium. After stabilized, the cells, proteins and

bacterial behavior were followed *in vitro* and *in vivo* on these materials. It was seen that by varying the ratio between carboxylate and sulfonate groups they were capable of inhibiting the bacterial adhesion and induce osteoblastic maturation, particularly by enhancing the ALP and calcium production at the ECM [166,167]. Later, they observed that bioactive coatings could be created using only one monomer carrying sulfonate functions [164]. To the purpose of this study, the next section will be dedicated to the direct grafting of the anionic polymer poly(sodium styrene sulfonate) (poly(NaSS)) onto Ti based substrates.

4.3.1 Grafting of Poly(sodium styrene sulfonate)

The concept of grafting a bioactive polymer through radical polymerization on metallic surfaces is relatively new. This method is based on the creation of free radicals at the surface that under specific environmental conditions interact with the monomers in solution, inducing their polymerization [164].

The activation of Ti surfaces by chemical oxidation in a mixture of pure sulfuric acid (H_2SO_4) and hydrogen peroxide (H_2O_2) leads to the production of Ti hydroxides and peroxides. The existence of these elements has been confirmed previously and its value attested. For instance, Tengvall et al. [168] demonstrated that in physiological medium Ti can react with H_2O_2 and create a thick protective oxide layer. On its turn, Takemoto et al. [16,170] in two different investigations reported that Ti substrates treated with H_2O_2 and subsequently heated achieved higher blood compatibility than untreated Ti. They showed that by heating the Ti material after oxidation it was possible to induce the decomposition of Ti peroxides into free radicals. This same ideology has been followed by the LBPS investigators. After chemical oxidation, the metallic substrates are immersed in a monomeric solution and heated at 70°C to induce the formation of free radicals but, most importantly, the covalent linkage between these and the monomers – radical polymerization.

Noirclere et al. [171] in a preliminary study reported the poly(NaSS) effect on osteoblast-like cells grafted onto Ti surfaces. Here, Ti was functionalized by chemical grafting with a bioactive polymer bearing anionic sulfonate groups. A thoroughly characterization of the grafted substrate put in evidence the hydrophilic character of the treated material and confirmed the presence of sulfur and sodium. After successful radical polymerization, the MG63 cells were cultured on the materials and the biological response was followed. Significant improvement of cells adhesion

strength to these altered surfaces was detected and so was an increase of the calcium production during mineralization. The surface modification with anionic sulfonate groups was proved to be effective and to contribute to bone regeneration *in vitro*. These results were corroborated by Mayingi et al. [172] research. Later, Hélary et al. [164] in a similar investigation proved the ability of poly(NaSS) grafted onto Ti to improve MG63 cells ALP activity aside from the adhesion strength and calcium production. More recently, Michiardi et al. [173] conducting *in vitro* and *in vivo* preliminary tests on Ti6Al4V surfaces grafted with sulfonate (poly(NaSS)) and carboxylate groups (methylacrylic acid) implanted on rabbit femoral bones, confirmed the previous observations. *In vitro*, poly(NaSS) induced the highest cell adhesion levels, while *in vivo*, it was responsible for a superior percentage of mineralized bone around the implant.

These results provide evidence of the poly(NaSS) ability to improve and promote osteointegration both *in vitro* and *in vivo*. Nonetheless, much needs to be understood in regard to the effect of poly(NaSS) grafted onto Ti6Al4V on the osteoblastic cells general and molecular behavior and on important biological molecules. The objective of the present research is exactly this; to provide evidences that sustain these observations and uncover new information that support our previous premise: “poly(NaSS) grafted on Ti6Al4V improves and promotes osteointegration”.

III. MATERIALS & METHODS

– 1st Part. Substrates –

1. MATERIALS

1.1 Disks

1.1.1 Substrates Preparation

Ti6Al4V disks (1.3 mm of diameter) furnished by the CERAVER company (France) were used as substrates. Before use, the material was polished with a series of SiC papers from 500 grit up to 1200 grit and cleaned in Kroll's reagent (2% HF, Sigma, and 10% HNO_3, Acros, in 88% H_2O) for 30 s. Afterwards, the substrates were submitted to several washes in distilled water (dH_2O) and dried under vacuum at 60°C.

1.1.2 Surface Modification

For the grafting process, the monomer NaSS (Sigma) was selected (Figure 23). It was purified by recrystallization in a mixture of water/ethanol (10/90 v/v) at 70°C. Once the monomer was completely dissolved, the solution was filtered and placed at 4°C for crystal formation. Afterwards, the crystals were recovered, dried under vacuum at 60ºC, and store at 4ºC before use.

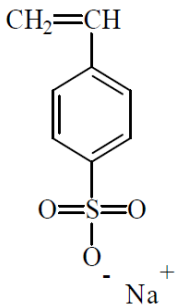

Figure 23. Chemical structure of the sodium styrene sulfonate monomer.

Chemical grafting (Figure 24A) was performed in an atmosphere poor in oxygen (≈ 99% argon). Ti6Al4V disks were immersed in H_2SO_4/dH_2O (50/50 v/v, Sigma) for 1 min, to eliminate possible contaminants and start the oxidation reaction. The same volume of H_2O_2 (Sigma) was added and left for 3 min in contact with the surfaces (agitation). This process is named chemical oxidation and is accompanied by gas release (Figure 24B) and alterations in color of the solution (Figure 24C). After

several washes with dH_2O, the oxidized Ti6Al4V were submerged in a 0.7 mol/L NaSS in dH_2O solution, previously degassed. The round bottom beakers hermetically closed were then left for 15 h at 70ºC. The elevated temperature allows the peroxide bond to break, leading to the radical polymerization of the NaSS monomers. All surfaces were, in the end, thoroughly washed in dH_2O, under agitation, to eliminate the homopolymer formed.

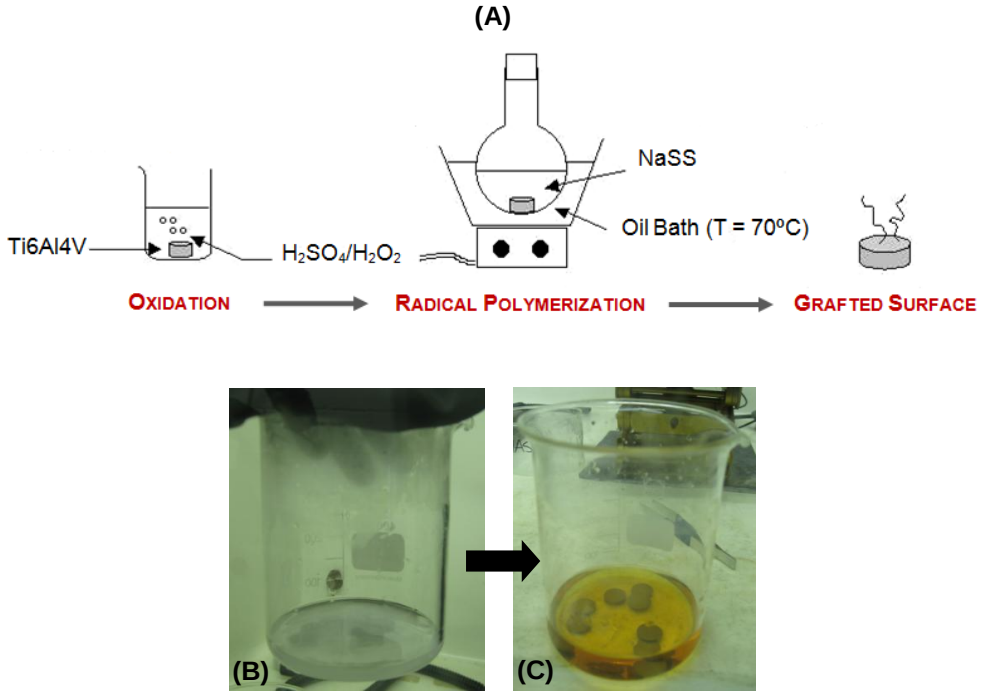

Figure 24. (A) Schematic representation of the chemical grafting process. Chemical oxidation of Ti6Al4V substrates: (B) sulfuric acid/dH_2O action and (C) addition of hydrogen peroxide.

1.2 Quartz Crystals

1.2.1 Substrates preparation

Tests conducted using quartz crystals were preformed in real time using a quartz crystal microbalance with dissipation (QCM-D, QSense, Sweden). Gold-coated QCM-D sensors with and without a 50 nm thick vapor deposited Ti6Al4V layer (Figure 25) were purchased from QSense (Sweden). The fundamental resonance frequency of the crystals was 5 MHz. Data from the 3rd to the 11th overtones was recorded and used.

Before any QSense measurement, the sensors were sonicated in 99% ethanol (10 min, Sigma) and twice in MilliQ® ultrapure water (10 min each, Millipore), followed by drying in N_2 and UV ozone sterilization (10 min).

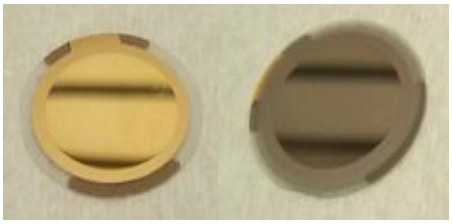

Figure 25. Gold and Ti6Al4V sensors.

1.2.2 Surface Modification

Ti6Al4V sensors were physisorbed with 15% (w/v) poly(NaSS) in pure water (Sigma) for 15 h at room temperature (RT) and under agitation. This is a simple process in which the electronic structure of the atom or molecule is barely perturbed upon adsorption (absence of chemical bonds). The binding energy depends on the polarization and on the number of atoms involved. Van der Waals forces are the fundamental interactions.

In this case, the grafting process could not be applied to the sensors due to their weak structure (very thin) and fragility of the Ti6Al4V film (easily removed with weak acids). Other methods were tested to graft or coat the poly(NaSS) polymer onto the Ti6Al4V surfaces. Physisorption was identified as the best alternative to the surface functionalization of the Ti6Al4V sensors.

Some gold coated sensors were spin coated with 1% (w/v) poly(desamino tyrosyl-tyrosine ethyl ester carbonate) (poly(DTEc)) in tetrahydrofuran (THF, OmniSolv), others were spin coated with 10% (w/v) polystyrene (PS) in toluene (Sigma) and the rest was used as uncoated gold substrates. The spin coating was conducted at 3000 rpm for 30 s, and 50 µL of each solution were used per sensor. The coated crystals were dried under vacuum overnight.

Poly(DTEc) (Figure 26) has been in many occasions indicated as one of the most suitable polymers to construct scaffolds for bone regeneration [174]. The use of poly(DTEc) in anterior crucial ligament reconstruction [175] and cancellous bone fracture fixation [176] has been previously reported in rabbits. Moreover, its unique osteocompatibility has been confirmed in canine models [177], foreseeing many applications in the orthopedic field.

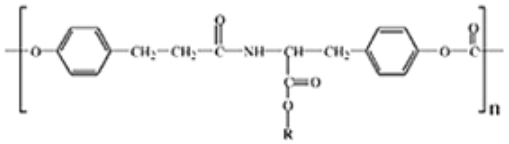

Figure 26. Poly(DTEc) chemical structure.

PS (Figure 27), on its turn, is a common synthetic polymer used in the medical field. It has high transparency and processability, with low production cost associated, but most importantly is a non-toxic material. PS is used in a wide range of disposable biomedical devices, including tissue culture plates, test tubes and diagnostic components. In *in vitro* investigations, disposable PS culture dishes are widely used as blanc tests for cell attachment [178,179].

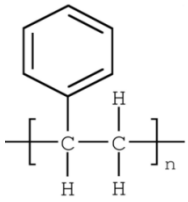

Figure 27. Polystyrene chemical structure.

1.2.3 Data Treatment

QCM measurements were carried out in a Q-Sense E4 instrument (Q-Sense AB). A peristaltic pump (Ismatec, IDEX Health & Science GmbH, Wertheim, Germany) at constant flow rate of 25 µl/min (nominal) was used during protein tests.

In analyzing QCM-D data, when the surface coatings and adsorbed protein are rigid and laterally homogeneous, the dissipation change is negligible compared to the frequency change, the hydrated surface mass can be calculated using the Sauerbrey equation [180]:

$$\Delta f = -C.\Delta m,$$

with the mass sensitivity of the crystal, C, equal to 17.7 ng/cm^2.s. The increase in dissipation was less than 1x10^{-6} per 20 Hz drop in frequency for BSA and Fn, and hence the Sauerbrey equation was used to estimate the adsorbed protein mass with hydration. Data from the 3rd to the 11th overtones were used. Although the dissipation was larger with Col I, to keep the analysis consistent, we used Sauerbrey even in this instance, thus underestimating its adsorbed mass

2. SURFACE CHARACTERIZATION

2.1 Morphology

The morphology of the ungrafted and grafted Ti6Al4V surfaces was observed by scanning electron microscopy (SEM, Hitachi TM3000, Germany). This equipment generates 3D images, allowing the observation of the materials macro and submicron features. It uses a high energy beam of electrons in a raster scan pattern that interacts with the atoms at or near the samples' surface, under vacuum conditions. The materials in study must be electrically conductive, at least the outermost layer, and electrically grounded to prevent accumulation of electrostatic charge [181,182,183]. The Ti6Al4V substrates tested required little preparation since they were already conductive. Ungrafted and grafted surfaces, previously cleaned and dried, were observed using the Shadow 2 mode with electron beam intensity of 15 kV and magnification ranging from 100x to 2000x.

2.2 Topography

The surfaces topography was investigated using a microtopographer (Micromesure STIL, model CHR 150-N, France) that does both profile delineation (2D evaluation - 2D graphics) and analyses of surface area (3D evaluation – 3D models). This is a non-contact optical profiling system that measures step heights (up to 0.1 nm) and surface roughness. It uses a confocal chromatic technology system with a set of chromatic lens that detect reflected white light and specific wave lengths emitted by the surface. Here, only light travels above the material so damages or surface modifications can be avoided [184,185,186].

This equipment uses a probe that possesses an amplitude of measurement of 310 µm, an axial resolution of 10 nm, a spot diameter of 4 µm and a lateral resolution of 2 µm. 3 equally separated areas of 0.5 mm^2 per sample were examined and treated with a microroughness filter with a cut-off of 0.08 mm. Data recovered was examined using the software Mountains Map (DigitalSurf). The average results were reported as average roughness (Ra), average maximum height roughness (Rz), maximum profile peak height (Rp) and quadratic mean roughness (Rq) for 2D (Figure 28), and the corresponding values Sa, Sz, Sp and Sq for 3D.

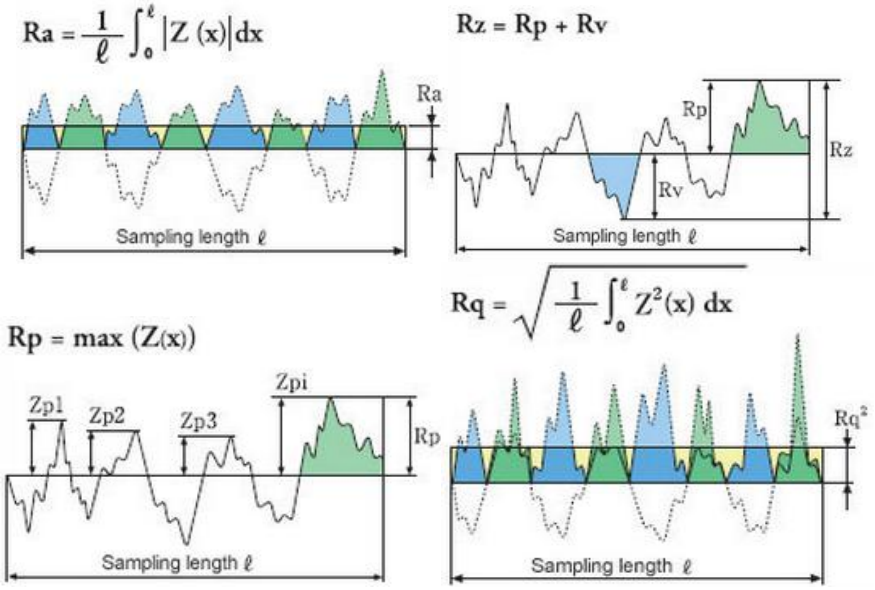

Figure 28. Schematic representation of Ra, Rz, Rp and Rq, four roughness (2D) parameters [187].

2.3 Chemical Composition

X-ray photoelectron spectroscopy (XPS) and energy dispersive X-ray spectroscopy (EDS) were the two techniques used in the analyses of the ungrafted and grafted surfaces chemical composition.

In the XPS method, the sample is irradiated with mono-energetic x-rays causing photoelectrons to be emitted from the material surface. The energy and intensity of a photoelectron peak provides information about the identity, chemical state and quantity of each element detected. Here, only the composition of the outermost layer (first atomic layer) is evaluated (Figure 29A) [188,189]. A K-Alpha XPS Instrument (Thermo Scientific) was used in this investigation. 50,000 eV x-ray was applied in the identification of individual elements, while 200,000 eV was used for the entire survey. Their concentration was determined by detailed scans of each one of the elements. The x-ray spot size used was 400 μm. High resolution spectra were profile fitted (Thermo Avantage 4.51 software), and the resulting peaks areas were used to calculate the elemental composition.

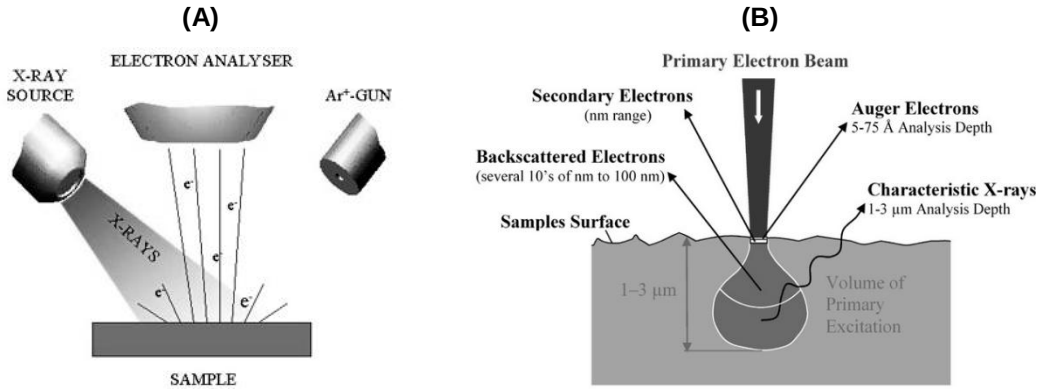

Figure 29. Representation of the (A) XPS [190] and (B) EDS principles [191].

The EDS system (usually associated to the SEM equipment) measures the number of emitted electrons by the sample, in response to an electron beam bombardment, versus their energy. Its principle is based on the unique atomic structure of each element and, in consequence, a unique identification. Therefore, electrons can be excited from different energy levels (outer positions equals to higher energy levels while inner positions to lower), allowing the elemental identification to be done not only at the surface but at the bulk of the material as well (Figure 29B) [182,183]. Identification of the chemical composition of the ungrafted and grafted Ti6Al4V was conducted on 3 areas of 0.1 mm^2 randomly selected on each sample.

2.4 Toluidine Blue Colorimetric Method

Toluidine blue (TB, Figure 30) is an acidophilic metachromatic dye that selectively stains acidic tissue components (sulfonic, carboxylic and phosphatic chains), through the complexation of the $N^+(CH_3)_2$ with anionic groups such as the $-SO_3^-$ [192,193]. This way, the TB allows the quantification of grafted polymers, as poly(NaSS), on different materials.

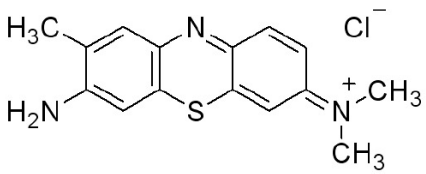

Figure 30. Toluidine Blue molecule.

Ti6Al4V disks were individually immersed in a TB (Acros) aqueous solution ($5x10^{-4}$ M, pH≈10) at 30ºC for 6h. This step allows the complexation of the TB with

the grafted sulfonate groups. The samples were then rinsed with a $5x10^{-3}$ M sodium hydroxide aqueous solution to remove the non-complexed dye. This step continues until the solution becomes colorless. Afterwards, the disks were immersed in a mixture of acetic acid/dH_2O (50/50 v/v, Sigma) for 24 h, inducing TB decomplexation. The concentrations of decomplexed TB were measured by visible spectroscopy at 633 nm using a Perkin-Elmer spectrometer lambda 25.

To determine the quantity of grafted molecules on the Ti6Al4V surfaces several steps must be taken. The first consisted in the determination of the molar extinction coefficient ε of TB. A calibration curve (Figure 31) was created with concentrations from $4x10^{-6}$ to $5x10^{-5}$ M (initial solution $1x10^{-3}$ M diluted 20x, 25x, 50x, 100x, 200x, 250x) of TB in acetic acid using the formula OD = f(C), with OD = absorbance at 633 nm.

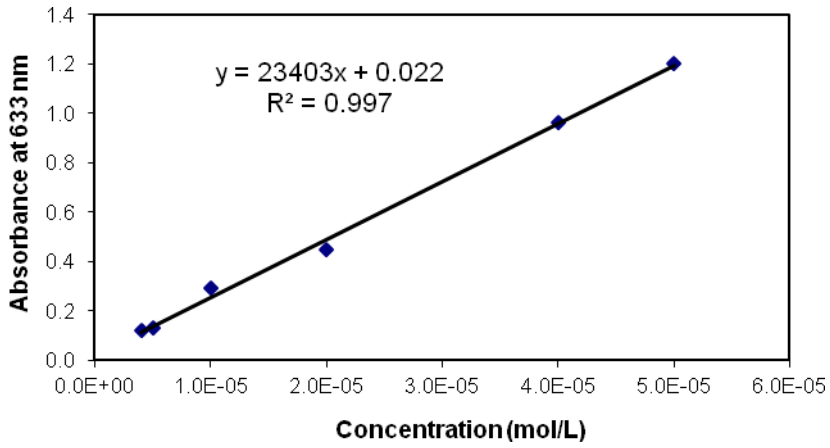

Figure 31. Toluidine blue calibration curve, with ε equals to 23403 $L.mol^{-1}.cm^{-1}$.

Using the Beer-Lambert law:

$$A = \varepsilon.l.c,$$

with *A* = absorbance at 633 nm, ε = molar extinction coefficient of TB, *l* = length of the optical trajectory (in this case 1 cm), and *c* = concentration, the concentration of the molecule that adsorbs could be determined (NaSS).

Finally, the amount of sulfonate grafted molecules on the Ti6Al4V surfaces was calculated using the following relationship:

$$m = [NaSS].V.M_{NaSS} \text{ (in g)},$$

with V = solution volume (5.10^{-3} L) and M_{NaSS} = NaSS molecular mass (206.2 $g.mol^{-1}$). The quantity of grafted material is expressed in function of the surface area in g/cm^2.

2.5 Surface Energy and Wettability

Contact angle evaluations are specific for any given system and are determined by the interactions across three interfaces, solid-liquid (γ_{sl}), liquid-vapor (γ_{lv}), and solid-vapor (γ_{sv}).

The most common way to determine the wettability of a surface consists in measuring the angle (θ) between a small liquid drop (stable) and a solid surface (Figure 32).

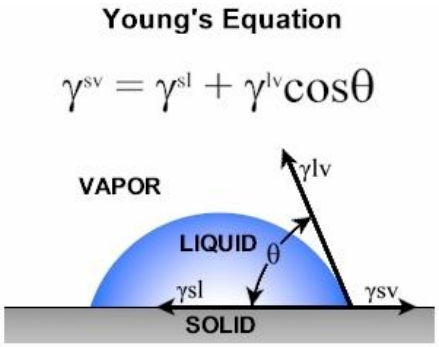

Figure 32. Schematic representation of a contact angle measurement [194].

The wettability of the poly(NaSS) grafted and ungrafted surfaces to pure water (polar liquid); formamide (polar liquid, Sigma); ethylene glycol (polar liquid, SDS) and diiodomethane (apolar liquid, Reagent Plus®) was assessed using a dynamic contact angle apparatus (DSA 10 Kruss Instrument), following the sessile drop method. The volume of the liquid droplets was 2 µL and the angles' values were recovered 8 s after the drop entered in contact with the surface.

The surface energy was calculated by applying a set of mathematical equations, previously described by [195]. The Young's equation on Figure 32 projects the relationship between the three interfaces, with a liquid droplet in equilibrium ($\gamma_{sv} = \gamma_{sl} + \gamma_{lv}cos\theta$).

By combining the Young's equation with the Dupré's equation that expresses the adhesion work, Wa, between a solid and a liquid (1), the Young-Dupré formulation (2) is generated,

$$Wa = \gamma_{lv} + \gamma_s - \gamma_{sl} \quad (1)$$

$$Wa = \gamma_{lv}(cos\theta + 1) \quad (2).$$

This relates the contact angle (θ) and the energy of the liquid vapor interface (γ^{lv}).

Fowkes suggested the total surface energy to be a result of different molecular forces

$$\gamma = \gamma^d + \gamma^p \quad (3),$$

with γ^d = dispersive forces, and γ^p = polar interactions. He considered the γ^d to be the most important for the system, proposing

$$Wa = 2(\gamma_s^d \gamma_{lv}^d)^{\frac{1}{2}} \quad (4).$$

The Young-Dupré formulation was then re-written as

$$\gamma_{lv}(1 + cos\theta) = 2(\gamma_s^d \gamma_{lv}^d)^{\frac{1}{2}} \quad (5).$$

Later Owens, Wendt and Kaelble adjusted the Fowkes equation to a more general form that had into consideration both dispersive and polar components

$$Wa = 2(\gamma_s^d \gamma_{lv}^d)^{\frac{1}{2}} + 2(\gamma_s^p \gamma_{lv}^p)^{\frac{1}{2}} \quad (6).$$

By combining it with the Young Dupré formulation (5) a new equation to determine the surface energy of a solid was generated

$$\gamma_{lv}(1 + cos\theta) = 2(\gamma_s^d \gamma_{lv}^d)^{\frac{1}{2}} + 2(\gamma_s^p \gamma_{lv}^p)^{\frac{1}{2}} \quad (7).$$

This equation requires the use of liquids with dispersive and polar components known and contact angle measurements. All these formulations were taken into consideration to determine the surface energy of the ungrafted and grafted Ti6Al4V materials.

2.6 Fourier-transformed infrared spectroscopy

Fourier-transformed infrared (FTIR) spectra, recorded in an attenuated total reflection (ATR), were obtained using a Nicolet Avatar 370 Spectrometer. This technique analyzes the vibrations characteristics of the chemical interactions present on the surface and consequently the grafting homogeneity.

FTIR is most useful for identifying chemicals that are either organic or inorganic and perhaps the most important tool to identify types of chemical bonds (functional groups) [196,197].

The Ti6Al4V spectra were obtained with a 4 cm^{-1} resolution using a 45º Ge crytals (4000 cm^{-1} – 600 cm^{-1}). The disks were pressed uniformly against the crystal, in order to get a good contact, using a smart Omni sampler. To reduce the background noise, 128 acquisitions were built-up per surface point. 3 points randomly selected on each substrate were tested.

2.7 Crystalline Structure

X-ray diffraction (XRD) is one of the most important non-destructive tools to determine the atomic and molecular structure of a crystal. The beam of x-rays that enters in contact with the crystalline atoms diffracts into many directions, with specific angles and intensities. By measuring those specificities, a three dimensional picture of the density of the electrons within the crystal can be generated and, as consequence, the atoms position, structure, size, chemical bonds, etc. can be determined. This technique can be used in many different materials with the ability to form crystals [198,199]. Here, the data was obtained on a Philips X'pert Theta/Two-theta diffractometer using copper Kα radiation (wavelength = 1.542 Å) from a tube operated at 45 kV and 40 mA. The scans were conducted between 10° and 90° degree 2θ counting for 2 s at every 0.02° interval.

– 2nd Part. Biological Testing –

After the substrates being prepared and thoroughly characterized, the sterilization process took place and the biological tests were initiated. The following *in vitro* experiments were conducted so the influence of the sulfonate groups on the osteoblast-like cells behavior could be established and the mechanisms involved during cell attachment identified.

1. SURFACES CONDITIONING AND STERILIZATION

1.1 Disks

Prior to cell culture, all Ti6Al4V disks were conditioned in a set of aquous solutions: 1.5 M sodium chloride (NaCl, Fisher), 0.15 M NaCl, pure water and phosphate buffered saline solution (PBS, Gibco), 3 h each and repeated 3 times (under agitation). These washes were done so all impurities or residues present on the substrates during processing were eliminate and, therefore, unable to interfere with the biological tests (cell culture is extremely sensitive to contaminations). They also had an important impact on the pH of the surface, approaching it to the physiologic pH (pH = 7.4). After, each side of the Ti6Al4V substrates was sterilized with ultraviolet light (UV, 30 W) for 15 min.

If the material was not used immediately it could be stored at 4°C in a PBS and 1% antibiotics (penicillin-streptomycin, Gibco) solution.

1.2 Quartz Crystals

Before contact with the biological material all QCM-D sensors were sonicated in 99% ethanol and twice in MilliQ® ultrapure water, followed by drying in N_2 and UV ozone sterilization, each for 10 min. Once placed in the QCM chambers, PBS was flowed through their surfaces to obtain the correct pH. The equipment was set up for a temperature equal to 37ºC and only after stability of the PBS frequency the biological solutions were introduced.

After each experiment with proteins, the crystals were washed. The gold, the Ti6Al4V and the physisorbed sensors were sonicated with 2% sodium dodecyl sulfate (SDS, Sigma) solution in pure water for 30 min, then 15 min with dH_2O and

another 15 min with MilliQ® ultrapure water. This was followed by drying in N_2 and UV ozone sterilization, for 10 min. The poly(NaSS) physisorbed sensors were then submitted to a new physisorption process for 15 h. In the end, several washes with different solutions were conducted: 1.5 M NaCl, 0.15 M NaCl, pure water and PBS, 3 h each. The poly(DTEc) spin coated crystals required a different cleaning process that consisted in the total elimination of the poly(DTEc) layer. The substrates were sonicated for 10 min with 2% SDS, then for 15 min in 95% ethanol and another 15 min with THF. In between, 10 min dH_2O washes were conducted. Finally, MilliQ® ultrapure water was used for 15 min and the sterilization process completed as before. A new spin coating of poly(DTEc) on the gold coated sensors was preformed. The same cleaning process was applied to the PS sensors with the exception of THF which was substituted by toluene. In the end, here too, a new spin coating was conducted.

On the cell culture experiments, to eliminate the attached biological material, all sensors were washed with PBS (10 min), dH_2O (10 min), ethanol 95% (10 min), guanidine hydrochloric acid 4M (HCl, 20 min), guanidine HCl 8M (20 min), sodium hydroxide 1M (NaOH, 20 min), HCl 1M (20 min), ethanol 95% (10 min), dH_2O (10 min), and finally twice with MilliQ® ultrapure water (15 min each). N_2 was then applied to dry the crystals and the UV ozone to sterilize them. New spin coating and physisorption processes were carried out in the respective crystals.

2. INTERFACE PROTEIN – SURFACE

After conditioning and before cell work, the substrates were left in a non-complete medium solution of Dulbeco's Modified Eagle Medium (DMEM, Gibco) and 1% penicillin-streptomycin, fungizone and L-glutamin, all from Gibco, for 24 h at 37°C and 5% CO_2 (antibiotic protection).

2.1 Absence of proteins

To determine the importance of proteins and the poly(NaSS) on the cellular response, tests were conducted in the absence of proteins. After conditioning, disks were immersed in a non-complete medium solution and left until the cell tests were

initiated. This way, only antibiotics and chemical elements were adsorbed onto the surfaces.

2.2 Fetal Bovine Serum Adsorption

After the 24 h in a non-complete medium solution, the materials were transferred to a complete medium environment (equal composition of the non-complete medium plus 10% fetal bovine serum (FBS, Gibco)), and left undisturbed overnight for protein adsorption. Cell seeding was then initiated.

2.3 Single Protein Adsorption

2.3.1 Disks

BSA (Sigma), human Fn (Sigma) and Col I (Sigma) were adsorbed onto the substrates at 37°C at a concentration of 4000 µg/mL in PBS, 20 µg/mL in PBS and 10 µg/mL in acetate buffer (0.1 M, pH 5.6), respectively. These three proteins were selected to this study for their importance to bone regeneration processes (Fn and Col I) or abundance in biological fluids (BSA). In a selective group of experiments, Vn (Sigma) was also studied. This was used at 20 µg/mL in PBS.

After conditioning, as happened for the FBS proteins' adsorption, the substrates were left in a non-complete medium solution for 24 h (antibiotic protection). Only then, each protein was placed in contact with the surfaces. Protein adsorption lasted 1 h. To block non-specific binding regions, the materials were immersed in a 1% BSA solution in non-complete medium, for 30 min. PBS was used between solutions to remove unattached biological material. These steps preceded the cellular experiments.

2.3.2 Quartz Crystals

The procedure and solutions described above were also applied to the QCM-D sensors. However, differences must be pointed. While for the disks, all materials were submerged or immersed in the protein solutions, for the quartz sensors the solutions were flowed through the surfaces (25 µL/min) or directly injected (0 µL/min), depending on the evaluation in progress. For instance, to evaluate the kinetics of each protein on the different crystals or its competition, a continuous flow was maintained until saturation was reached. On the other hand, when cellular tests were conducted, each protein was injected for 1 h and then blocked for 30 min with

1% BSA. PBS was both used between solutions to remove unattached material and as baseline. The protein concentrations remained unchanged. The influence of the acetate buffer solution (Col I) was less than 5 Hz and was, therefore, small enough to be neglected during the analysis.

2.4 Proteins' Conformation

The conformation of Fn (most important during initial cell attachment) adsorbed onto the Ti6Al4V/poly(NaSS) sensors was examined through the amount detected of heparin (HB) and RGD binding sites. This was determined by monitoring the amount of antibodies bound to each of these sites using QCM-D. Three different antibodies against each of the following, N-terminal (MAB1936) and C-terminal (MAB1935) HB domains, and the RGD peptide (MAB1934) were used. The binding of antibodies to these and all the other active binding sites on Fn was assessed using a polyclonal antibody (AB1945) (Millipore, all reactive with human Fn and used at 100 µg/mL). For the totality of the experiments, antibodies were left in contact with Fn-adsorbed substrates until saturation was reached (25 µL/min). Protein conformation was also followed on disks, this time by assessing the cells morphology and attachment ability. The details of those experiments will be described in a next section.

2.5 Protein Competition

2.5.1 Sequentially

The goal of these experiments was to understand the effect of one protein on the other when adsorbed onto the same substrate.

The sequential adsorption of the proteins BSA, Fn and Col I was conducted on QCM-D crystals at 37 ºC and contact flow of 25 µL/min. Each surface was exposed to a pair of proteins at a time for a total of six combinations: BSA + Fn, Fn + BSA, Col I + BSA, BSA + Col I, Col I + Fn and Fn + Col I. The concentration of each protein was kept the same. PBS was again used to establish the baseline. The adsorption of the first protein was followed until a plateau was reached. Then, a protein solution was introduced into the same substrate and left until a "new adlayer" reached saturation. Between injections, PBS was used to clean the system and remove unattached fractions of the proteins.

2.5.2 Mixture

As in the sequential adsorption, the objective of these experiments was to determine the competitive character of the three proteins, but this time when together in a mixture. The tests were conducted at 37ºC and constant flow of 25 µL/min (QCM-D analysis). Two proteins were used for each test in three combinations (BSA & Fn, Col I & Fn and Col I & BSA, in a ratio of 50/50 v/v for each protein) on each substrate. The proteins' concentration was kept the same. PBS was again used to obtain the baseline. The proteins' mixture was kept in contact with each sensor until the frequency and dissipation shift reached a plateau (saturation).

3. OSTEOBLAST-LIKE CELLS CULTURE

3.1 Cell Line

MC3T3-E1 cells, mouse calvaria-derived osteoblast-like cells line, from American Type Culture Collection (ATCC), CRL 2593, subclone 4, were selected to this study. This cell line is a well established model to study the influence of the surface properties on the general cell behavior as well as *in vitro* osteoblastic differentiation. This cell line is capable of preserving its own cellular profile for longer without risking the loss of phenotype expression.

3.2 Cellular Expansion

Osteoblastic cells were cultured in complete medium of DMEM at 37ºC and 5% CO_2 in air. Criovials with cellular content were unfreezed in a 37ºC water bath. The cellular suspension was mixed with culture medium, centrifuged for 3 min at 3000 rpm and finally resuspended in 10 mL of complete medium. Cells were seeded in a T_{75} (75 cm^2 of area, Sarstedt) polystyrene culture flask and monitored every 24 h. Medium was changed twice a week.

3.3 Cell – Material Interactions

Different experiments were conducted to evaluate the relationship established between cells and material at the interface: viability, morphology, attachment, early differentiation and mineralization are some of the many.

The individual impact of the poly(NaSS) on osteoblast-like cells was determined by conducting experiments in the absence of proteins. Here, the intention was to see the contribution of the poly(NaSS) to the cellular development without the participation of other nutrients or biological molecules. Simultaneously, the importance of the proteins to the cell survival was also confirmed. In a second group of experiments, the combined effect of the bioactive polymer and several proteins, both individually (BSA, Fn, Col I and Vn) and in mixture (FBS, BSA & Fn, Fn & Col I and Col I & BSA), was assessed. Molecular events taking place at the interface were followed and identified using antibodies against both specific protein binding domains (heparin domains and RGD sequence) and important integrins from the cellular membrane (Fn-$\alpha_5\beta_1$, Col I-$\alpha_2\beta_1$, and Vn-$\alpha_v\beta_1$, from Millipore, all at 100 µg/mL). The RGD peptide was also used (Sigma, 1000 µg/mL) to test the cell behavior in the presence of this Fn binding sequence. The significance of each one of these elements to the initial and posterior osteoblastic development was determined.

For the totality of the experiments, $5x10^4$ cells/mL was the cellular concentration used, while the culture medium was defined according to the type of culture conditions, absence of proteins (non-complete medium or serum free medium, SFM), absence of adhesive proteins (double depleted medium, DD) and presence of proteins (complete medium). Experiments using DD were divided into 3 categories: DD, 20 µg/mL in of Fn in DD and 20 µg/mL in of Vn in DD, so the absence and presence of specific adhesive proteins in the medium could be tested. Experiments with disks were conducted on 24-well tissue culture polystyrene plates (TCPS).

Each test described below is followed by a list of experiments conducted and the respective conditions applied.

3.3.1 Viability

3.3.1.1 Alamar Blue

Cells viability was followed from 30 min to 14 days of culture. After the specific incubation periods, the medium was removed, the samples washed with PBS and transferred to new wells. A mixture of fresh medium with alamar blue (0.1 mg/mL of rezazurine in 1 M ammonium hydroxide, Sigma) in a proportion of 10/1 v/v, respectively, was added to each sample and control. This evaluation requires a positive and a negative control. The positive control corresponded to cells cultured

directly on TCPS wells, for the same time periods as the tested samples, while the negative corresponded only to culture medium. Everything was then incubated at 37 ºC for 1 day. The content of each well was transferred for a 96 well plate and read in a spectrometer at 560 and 590 nm. The difference between the two readings gives the reduced alamar blue levels (or the cells metabolic activity). Details of the method can be found in the *Invitrogen* platform or [200].

This procedure was applied to the following set of experiments:

1. Disks + SFM + Cells (Maximum 3 days of culture)
2. Disks + FBS + Cells
3. Disks + Single Proteins + Cells
4. Disks + Mix Proteins + Cells

3.3.1.2 Calcein and Propidium Iodide Staining

The morphology and spreading of the dead and live MC3T3-E1 cells on the different surfaces was studied by fluorescent microscopy (ZEISS Axiolab, Germany) using calcein (reacts with live cells, Molecular Probes) and propidium iodide (reacts with dead cells, Sigma) as staining reagents. The MC3T3-E1 cells were observed from 30 min to 3 days. After each period, the medium was removed and the surfaces washed twice with PBS. 500 µL of calcein in PBS (1/1000 v/v) were added to each sample and left for 30 min at RT, under agitation. The latter was then replaced with 500 µL of propidium iodide in PBS (1/1000 v/v), which were left in contact with the substrates for 5 min at RT. In the end, the surfaces were again washed with PBS. The entire procedure was conducted protected from light. Pictures were taken using a digital camera Olympus Camedia C-5050.

This procedure was applied to the following set of experiments:

1. Disks + SFM + Cells
2. Disks + FBS + Cells

3.3.2 Morphology

4 h after incubation (or 2 h for the integrins-blocking evaluations on crystals and 30 min for specific single protein analyses), the MC3T3-E1 organization, shape and size on the substrates were studied. The cells morphology was evaluated by fluorescent microscopy (ZEISS Axiolab, Germany).

The medium was initially removed, the materials rinsed with PBS and fixated with 4% formaldehyde (Sigma) in PBS for 30 min at 4 ºC. Then, they were washed twice in a 4% of PBS/BSA (v/w) solution, permiabilized with 0.1% of Triton x100 (Sigma) in PBS (v/v) and immersed for 30 min in a 3% PBS/BSA (v/w) solution, under agitation. Anti-vinculin (Sigma) diluted in 1% PBS/BSA (1/200 v/v) was added to each sample and incubated for 1 h at 37 ºC. Before each dye/staining reagent addition, the surfaces were washed two times with 0.05% Tween 20 (Sigma) in PBS (v/v). The IgG antibody (rabbit anti-mouse, Molecular Probes) diluted in 1% PBS/BSA (1/200 v/v) was left in contact with the surfaces for 30 min at RT, protected from light (all the steps from this point were conducted protected from light). The alexa fluor 488 phalloidin (FluoProbes^{TM}) in 1% PBS/BSA (1/40 v/v) was added and kept for 1 h at RT. Finally, 2% of DAPI (Sigma) dissolved in water (w/v) were added and left for 10 min at RT. In the end, the samples were washed twice with dH_2O and stored, protected from light, at 4ºC. Pictures were taken using a digital camera (Olympus Camedia C-5050). Area evaluations were conducted using the Image Pro Plus 5.0 software.

This procedure was applied to the following set of experiments, which include the DD tests:

1. Disks + SFM + Cells
2. Disks + FBS + Cells
3. Disks + Single Proteins + Cells
4. Disks + RGD + Cells
5. Disks + Single Proteins + Anti-binding domains + Cells
6. Disks + Single Proteins + Anti-integrins with Cells
7. QCM-D Crystals + Single Proteins + Anti-integrins with Cells
8. Disks + Mix proteins + Cells

3.3.3 Attachment and Proliferation

The number of cells was determined using a cell counter (Multisizer III – Coulter Counter Z2 Beckman). After 5, 10, 15, 30 min (initial attachment), 4 h and 1, 3, 7, 10, 14 (proliferation) days of incubation, the cells were detached from the surfaces using trypsin-EDTA and re-suspended in *Beckman Coulter*® isoton in a 0.005% v/v ratio, before analysis.

This procedure was applied to the following set of experiments, which include the DD tests:

1. Disks + SFM + Cells
2. Disks + FBS + Cells
3. Disks + Single Proteins + Cells
4. Disks + RGD + Cells
5. Disks + Single Proteins + Anti-binding domains + Cells
6. Disks + Single Proteins + Anti-integrins with Cells
7. Disks + Mix Proteins + Cells

Concerning the evaluations of cell attachment conducted on the QCM-D equipment, the amount of cells was determined by following the frequency changes and by translating those values into mass density (Sauerbrey equation). Here cells were left to attach onto the different sensors for only 2 h (static conditions, 0 µL/min) so information about the initial cell attachment (influence of receptors from the cell membrane, integrins) and passage to proliferation stages could be taken. These experiments were always conducted in the presence of proteins, pre-adsorbed for 1 h.

This procedure was applied to the following set of experiments:

1. QCM-D Crystals + FBS + Cells
2. QCM-D Crystals + Single proteins + Cells
3. QCM-D Crystals + Single Proteins + Anti-integrins with Cells

3.3.4 Attachment Strength

The attachment strength of the MC3T3-E1 cells was studied from 5 min to 3 days of culture. The cellular suspension with the non-adhered cells was removed; the disks were washed twice with PBS and then split in two groups. In the first group, the adhered cells were detached using trypsin and the number determined using the Multisizer III equipment (see *section 3.3*). The determined value corresponds to the number of cells before the application of the shear stress, N_1. In the second group, the Ti6Al4V disks were exposed to a shear stress using a rotary stirring device for 15 min. Garcia et al. [201] proposed an equation that allowed the determination of a shear stress τ of 10 dyn/cm^2,

$$\tau = 0.8r\sqrt{\rho\mu\omega^3},$$

where r is the radial distance from the center of the disk, ρ is the fluid density (approximately 1g/cm^3), μ is the fluid viscosity (0.85 cP or 0.85 x 10^3 Pa.s) and ω is the angular velocity of the disk ($\omega = \frac{2\pi.rpm}{60}$ in s^{-1}).

The materials were washed with PBS and the remaining cells on the surfaces detached using trypsin. The cells were then counted (N_2). The percentage of adhered cells after the application of the shear stress was determined by dividing N_2 per N_1 and multiplying by 100 % (percentage correspondent to the totality of cells attached to the surface before stress).

This procedure was applied to the following set of experiments, which include the DD tests:

1. Disks + SFM + Cells
2. Disks + FBS + Cells
3. Disks + Single Proteins + Cells (30 min)
4. Disks + RGD + Cells (30 min)
5. Disks + Single Proteins + Anti-binding domains + Cells (30 min)
6. Disks + Single Proteins + Anti-integrins with Cells (30 min)
7. Disks + Mix Proteins + Cells (30 min)

3.3.5 Differentiation

The enzyme ALP is responsible for the liberation of phosphate into the ECM during the transformation of the p-nitrophenylphosphate substrate into p-nitrophenol. It is an indicative of osteoblastic functional evolution, more precisely the beginning of bone formation. Its activity was followed from 7 to 28 days.

In *in vitro* cultures, osteoblast-like cells do not possess the ability to produce calcium and phosphate by themselves. In consequence, the medium composition was changed. Ascorbic acid (Sigma) and β-glicerophosphate (Sigma) were included in a reason of 0.00805 g and 1.08 g in 500 ml of DMEM, respectively, to promote the cells maturation.

The culture medium was initially removed; the samples were washed 3 times with PBS and placed in a new plate. 1 ml of Tris Buffered Saline (TBS)-Triton X100 solution (0.4844 g Trizma Base (Sigma), 1.6 g NaCl, 2 ml Triton and 198 ml dH_2O), at 37°C, were added to each well and the plates left under agitation for 1 h, to separate the ALP from the cellular membrane. The resultant suspension was

removed to tubes and strongly mixed for 5 min. This was followed by three cycles of freezing at -80°C and unfreezing at 37°C.

The resultant enzymatic activity was measured with a spectrometer (Perkin-Elmer). 500 µl of suspension from each tube were mixed with 500 µl of p-nitrophenylphosphate substrate (Acros) in a concentration of 20 mM (AMP buffer solution, pH = 10.2, with 0.742 g p-nitrophenylphosphate (20 mM), 0.0407 g MgCl2 (2 mM, Merck), 0.0891 g 2-amino-2-methyl-propanol (10 mM, Acros) and 100 ml of dH_2O) and left in the incubator for 30 min at 37°C. The quantity of p-nitrophenol produced was determined by optic density at 405 nm of absorbance against a p-nitrophenol (Acros) range of concentrations (Table 3) in the AMP buffer.

Table 3. P-Nitrophenol (p-NP) range of concentration in AMP.

[p-NP] (µmol/mL)	**0**	**0.05**	**0.1**	**0.15**	**0.2**	**0.25**	**0.3**	**0.4**
Solution p-NP (µL)	0	5	10	15	20	25	30	40
AMP Buffer (µL)	1000	995	990	985	980	975	970	960

The ALP activity was normalized in relation to the total amount of proteins contained in suspension, which was detected with the commercial kit, BioRad (Bio-Rad Laboratories). 25 µl of suspension were combined with 125 µl of a reactive A' (reactive A' = 10 µl of reactive S + 500 µl of reactive A) and 1 ml of reactive B. 15 min later, the solution was measured by optic density at 750 nm (Table 4).

Table 4. BSA range of concentrations in TBS-Triton.

BSA (µg/mL)	**0**	**0.05**	**0.1**	**0.2**	**0.3**	**0.4**	**0.6**	**0.8**
BSA 1 mg/mL (µL)	0	5	10	20	30	40	60	80
Tampon TBS-Triton (µL)	100	95	90	80	70	60	40	20

This procedure was applied to the following set of experiments:

1. Disks + FBS + Cells
2. Disks + Single Proteins + Cells
3. Disks + Mix Proteins + Cells

3.3.5.1 BMP-2

The BMP-2 is commonly known for its role as a stimulant of bone production. In osteoblastic cells, BMP-2 stimulates angiogenesis by inducing the production of

VEGF-A (vascular endothelial growth factor). In order to attest this phenomena and the role of BMP-2 in the differentiation of osteoblast-like cells, Ti based substrates were pre-adsorbed with this protein for 1 h (Sigma, 10 µg/mL). Cells seeded onto these treated substrates were incubated for 14 days. The level of differentiation was assessed by following the cells ALP activity as described previously.

This procedure was applied to the following set of experiments:

1. Disks + BMP-2 + Cells

3.3.6 Mineralization

Calcium and phosphate precipitation are two indicators of mineralization. As before, in *in vitro* cultures, medium supplements are needed to induce osteoblastic maturation. Thus, ascorbic acid and β-glicerophosphate were added in equal amounts. Tests were conducted until 28 days of culture.

The medium was initially removed, the samples washed twice with PBS and transferred to a new plate. 1 mL of 15% trichloroacetic acid (TCA, Sigma) in ultra pure water (w/v) was added and left for 1 h in contact with the surfaces, under agitation and RT. This experiment was divided in two stages, first the calcium detection and second the phosphate. 10 µL of solution were then combined with 1 mL of Arsenazo III (Sigma) at 0.2 mM in PBS. After 15 min undisturbed, the quantity of calcium produced was measured by optic density at 650 nm of adsorbance against a calcium chloride ($CaCl_2$) and TCA range of concentrations in Arsenazo III (Table 5).

Table 5. Calcium range of concentrations in TCA.

Ca^{2+} (µg/mL)	**0**	**50**	**100**	**200**	**500**	**600**	**800**	**1000**
$CaCl_2$ 10 mg/mL TCA (µL)	0	5	10	20	40	60	80	100
TCA 15% (µL)	1000	995	990	980	960	940	920	900

The remaining solution in contact with the materials was left for another 48 h under agitation and at RT for posterior phosphate detection. 100 µL of the resultant suspension were then combined with 800 µL of AAM (2v acetone, 1v 2.5 mol/L sulphuric acid in dH_2O and 1v 10 mM ammonium molybdate in dH_2O, all from Sigma) and 80 µl of citric acid (Sigma) at 1 mol/l in dH_2O. After well mixed the solution was left to rest for 30 min. The phosphate concentration was measured by optic density at

355 nm of adsorbance and compared to a (di)sodium hydrogenophosphate (Na_2HPO_4) and TCA range of concentrations in AAM (Table 6).

Table 6. Phosphate range of concentrations in TCA.

PO_4^{2-} (µg/mL)	**0**	**10**	**20**	**40**	**100**	**120**	**160**	**200**
Na_2HPO_4 0.2 mg/mL TCA (µL)	0	50	100	200	500	600	800	1000
TCA 15% (µL)	1000	950	900	800	500	400	200	0

This procedure was applied to the following set of experiments:

1. Disks + FBS + Cells
2. Disks + Single proteins + Cells
3. Disks + Mix proteins + Cells

4. STATISTICAL ANALYSES

Surface characterization evaluations were conducted on 12 samples (each technique) while for the cellular tests 6 were used.

Numerical data were reported as mean ± standard deviation (SD). Statistical significance was determined by on-way analysis of variance (ANOVA) followed by the pos-hoc Bonferroni test, using the GraphPad Prism 5.0 software. Significance was defined as having $p < 0.05$.

IV. Results and Discussion

– 1st Part. Surface Characterization –

The first part of this investigation consisted in the chemical grafting of poly(sodium styrene sulfonate), a bioactive and very promising polymer for orthopedic and dental applications, onto the surface of the titanium alloy Ti6Al4V. Here, a complete analysis of the surfaces was conducted, which included morphology, topography, chemical composition, grafting density, surface energy, wettability and crystalline structure. Some of these techniques were also applied to characterize the quartz crystals used during the QCM-D experiments. In this set of tests, however, instead of chemically grafting the poly(NaSS), the polymer was physically adsorbed (physisorption). Since the Ti6Al4V layer on the quartz crystals was too thin and fragile, the oxidation step that precedes radical polymerization during grafting could not be applied without damaging the crystal or removing the Ti layer.

The totality of the surfaces evaluations was performed prior to cell culture in a non sterile environment.

1. DISKS

Prior to any test, including characterization, the Ti6Al4V disks were polished in a series of SiC papers and cleaned in Kroll's reagent. The grafting process was conducted afterwards. Both ungrafted and grafted Ti6Al4V surfaces were characterized and their differences highlighted.

1.1 Surface Morphology

The ungrafted and grafted surfaces morphology was observed by SEM. Micrographies were obtained using the Shadow 2 mode with electron beam intensity of 15 kV and 100x resolution (larger surface area). The results are given by Figure 33.

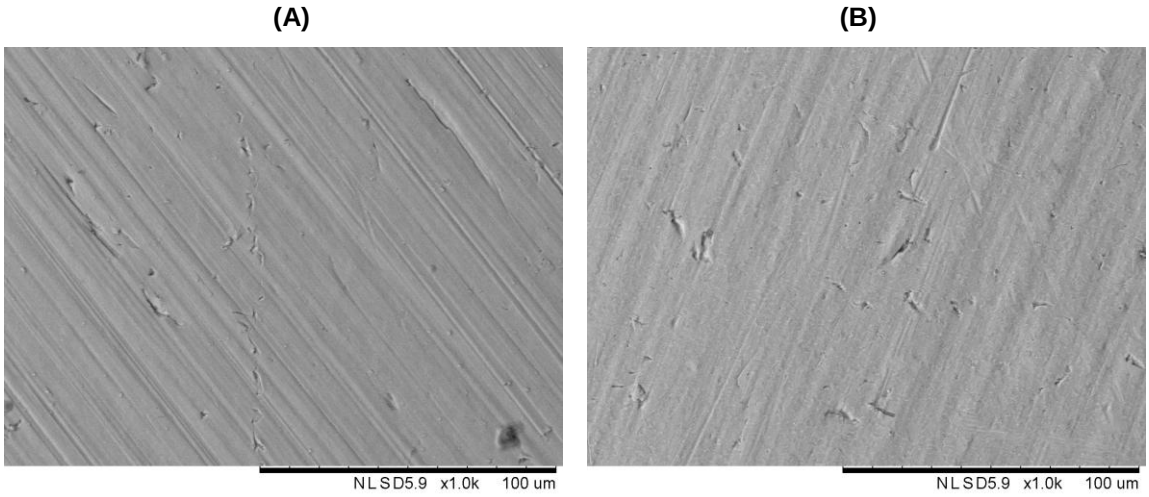

Figure 33. SEM micrographies of the (A) ungrafted and (B) grafted Ti6Al4V surfaces.

Both ungrafted and grafted disks exhibit a very regular and standardized morphology with the surfaces topography following the polishing pattern (equal direction). Still, by looking attentively to the surfaces roughness a small difference can be detected. It appears the scratches resultant from the polishing process on the grafted Ti6Al4V (Figure 33B) are not as deep as the ones registered by the ungrafted disks (Figure 33A). It is important to notice that the conditions of the polishing process were kept constant for the totality of the experiments. Therefore, the addition of poly(NaSS) during chemical grafting resulted in a more homogenous/uniform morphology.

The Kroll's reagent was successfully applied in the removal of visual impurities from the surfaces.

1.2 Topography

Although SEM evaluations offer the opportunity to study the surfaces morphology, it is not yet possible to quantify certain topography aspects. Only detailed topographic analysis by means of surface roughness measurements can provide such information. In the previous section, the grafting process was assumed to influence the roughness and topography of the surfaces. Here, we test that theory.

The surfaces roughness was measured using a microtopographer. The results from the surfaces profile delineation (2D) are shown on Table 7 (average Ra, Rz, Rq and Rp) and Figure 34 (graphical profile), while the surface area evaluations (3D) are given by Table 8 (average Sa, Sz, Sq and Sp) and Figure 35 (3D surface area model).

Table 7. Profile delineation (2D) of the ungrafted and grafted Ti6Al4V disks roughness.

Profile 2D	Ungrafted	Grafted	Difference
Ra ± SD	0.256 ± 0.062	0.212 ± 0.034	0.044
Rz ± SD	1.782 ± 0.443	1.532 ± 0.244	0.250
Rq ± SD	0.333 ± 0.081	0.277 ± 0.043	0.056
Rp ± SD	0.927 ± 0.223	0.766 ± 0.122	0.161

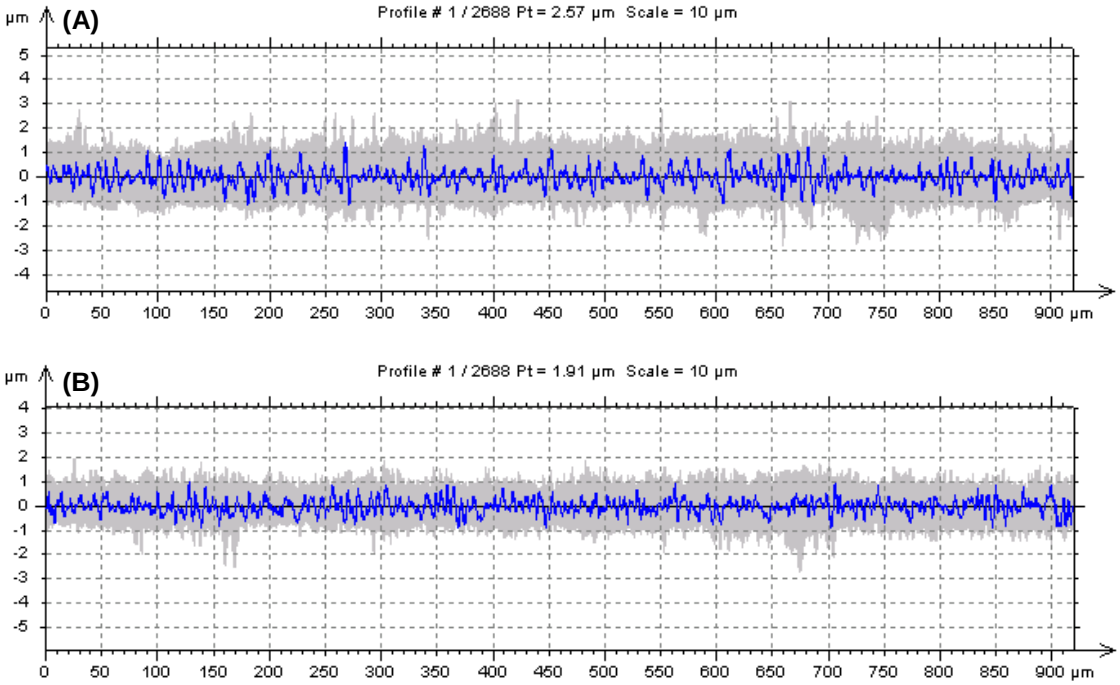

Figure 34. 2D profile delineation of (A) ungrafted and (B) grafted Ti6Al4V surfaces.

2D delineation or profilometry is considered the standard method to measure topographical properties, due to its extensive use in mechanical engineering and detailed analysis of single profiles. However, this evaluation is only local and limited to length dependent profiles of a certain region of the surface. It does not follow the evolution of the roughness parameters along the entire extension of the material. 3D surface evaluations, on the other hand, are more general since they measure average roughness parameters of entire areas. From a topographical perspective, they are assumed as more realistic by considering a larger amount of data. Nevertheless, both evaluations are fundamental to proper characterize a biomaterial.

Table 8. Surface area (3D) evaluation of the ungrafted and grafted Ti6Al4V disks roughness.

Surface 3D	Ungrafted	Grafted	Difference
Sa ± SD	0.289 ± 0.093	0.228 ± 0.031	0.061
Sz ± SD	7.307 ± 3.989	5.495 ± 0.814	1.812
Sq ± SD	0.397 ± 0.150	3.082 ± 0.040	0.093
Sp ± SD	3.798 ± 2.194	3.082 ± 0.673	0.717

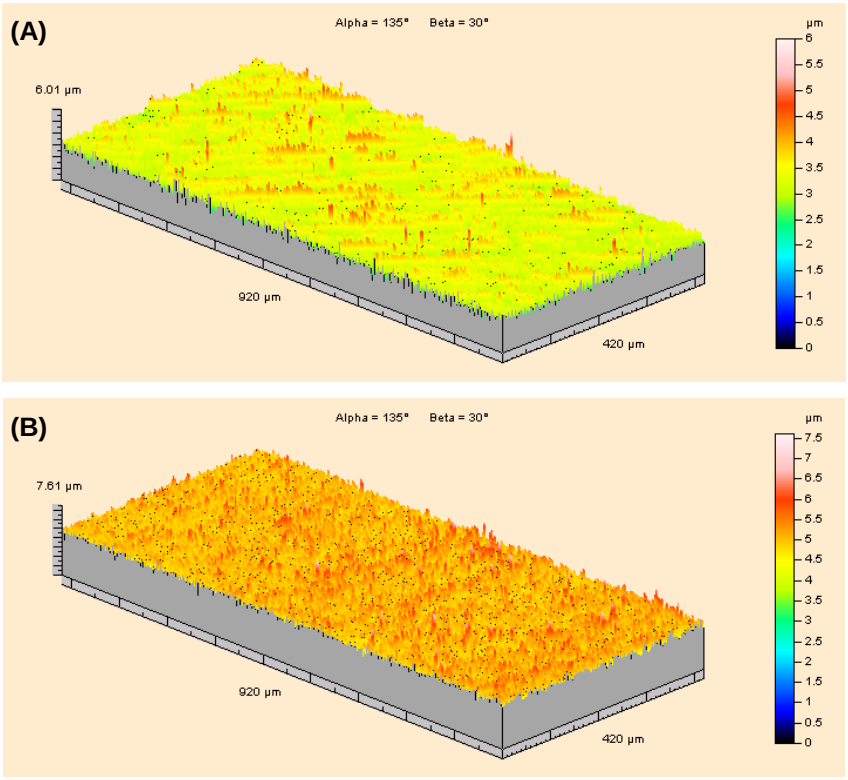

Figure 35. 3D model area of (A) ungrafted and (B) grafted Ti6Al4V surfaces.

The surfaces topography measurements provided by Table 7 and 8 confirm our morphological observations. In fact, the grafting process reduces the roughness of the surfaces, decreasing the Ra, Rz, Rp and Rq, both in 2D and 3D. A minor difference is detected between the roughness parameters measured on the ungrafted and on the grafted surfaces. During polymerization, the poly(NaSS) fills the surface existing valleys leading to a more regular and homogeneous topography. Similar observations were made in [172]. However, this topographical uniformity introduced by the bioactive polymer was not statistically significant ($p<0.05$).

In the literature there is no predefined or standardized average roughness for Ti based materials from which an optimal cell response can be acquired. There are some authors that admit rougher surfaces may induce a negative effect on the cell

adhesion [135] and phenotype expression [136]. However, there are others that point different cell types or cells at different maturation stages may display improved host response when cultured on rougher materials [137,138]. From the results, no predictions about the ungrafted and grafted surfaces influence on the cells response can be raised. Nonetheless, it can be established that possible differences in cell behavior between the two types of surfaces will not be an effect of their morphology or topography.

Despite the similarity between the 2D and 3D evaluations, the roughness parameters appear to be more affected by the 3D surface readings, in particular the Sz and Sp. By observing the Figures 34 and 35 we can conclude that by analyzing a larger surface area the 3D model acquires additional data and by consequence considers the surface in its full extension. Furthermore, these results reveal that to have a real perception of the vertical distance between the highest peak and deepest valley and their average size, a 3D analysis should be preformed.

1.3 Chemical Composition

The surfaces chemical composition was determined using the XPS and EDS techniques. XPS provides the atomic percentage of the chemical elements present on the Ti6Al4V surfaces, while EDS aside from analyzing the elements at the materials surface goes further and tests the chemical composition of the consecutive layers of material that follow the outermost (1^{st} atomic layer). By combining the information from the XPS and the EDS analyses a more precise atomic composition can be established. Table 9 gives the elemental composition of the ungrafted and grafted Ti6Al4V surfaces.

Table 9. XPS elemental composition of ungrafted and grafted Ti6Al4V surfaces.

	XPS Atomic Composition (%)							
Surface	**C**	**O**	**Ti**	**Al**	**V**	**Na**	**S**	**Imp.**
Ungrafted	6.8 ± 3.3	21.5 ± 2.6	52.3 ± 4.8	15.4 ± 1.8	3.4 ± 0.7	-	-	0.6 ± 0.5
Grafted	64.5 ± 1.4	12.7 ± 3.3	2.1 ± 1.1	0.0 ± 0.0	0.4 ± 0.0	7.7 ± 1.4	12.0 ± 1.9	0.5 ± 0.5

The atomic composition of the ungrafted materials (control) was found as expected [170-172]. Substantial amounts of Ti, aluminum (Al) and vanadium (V), the

original chemical elements of the alloy, were detected as well as oxygen (O), product from the material spontaneous oxidation, and small levels of carbon (C), a very common contaminant found on metallic surfaces.

After grafting, the quantity of C increased almost 10 times, a result of the hydrocarbon layer introduced by the poly(NaSS) coating, while the O levels decreased almost 40%. Ti experienced a significant reduction (≈ 96%) caused both by the oxidation reactions that took place during the grafting process and by the formation of the polymeric layer. The same happened to the remaining alloy elements, Al (≈ 99%) and V (≈ 88%). Grafting is a very efficient surface treatment by hiding the original surface elements and by exposing new important ones, such as sodium (Na) and sulfur (S).

The fact that the Ti6Al4V elements disappear almost completely during polymerization allow us to infer about the thickness of the poly(NaSS) layer. According to the XPS parameters, the x-ray beam scans the chemical composition of a surface until 5 nm in depth. Hence, it is conceivable the layer of poly(NaSS) to be superior than that. Furthermore, during XPS analysis experiments were made after removal of several atomic layers of the grafted surfaces. The idea was to eliminate possible contaminations on the surface and simultaneously test the chemical grafting resilience. A sputtering process with argon of ion energy of 3000 eV was repeated 3 times (120 s each), removing each time 40 nm of grafted material. In the end, the chemical composition of the surfaces was assessed and declared unchanged. The efficiency of the grafting process was, this way, evidenced and the grafting layer assumed as superior to 125 nm in thickness.

These evaluations were found similar for all tested samples confirming the grafting process as a reproducible surface treatment [173].

Despite all precautions during manipulation and the removal of contaminants during Kroll's reagent action, small impurities majorly in the form of nitrogen were detected by the XPS, before and after sputtering.

The XPS measurements aside from providing quantitative elemental analysis of a given surface can as well be used for qualitative information. By identifying the binding energy associated with each element that composes a surface, it is possible to determine its specificity but more importantly its ionic character. Ramirez et al.

[202] by studying the composition of the Ti alloy Ti6Al4V established this relationship. Table 10 shows their findings.

Table 10. Binding energies and composition of the high energy spectra of each chemical element, Ti2p, Al2p, V2p, O1s and C1s, present on Ti6Al4V surfaces [adapted from 202].

Element	Binding Energy (eV)	Ionic Character & Chemical Interaction
Ti 2p	453.3	Ti^{0}: Ti metal
	455.1	Ti^{II}: TiO
	456.8	Ti^{III}: Ti_2O_3
	458.4	Ti^{IV}: TiO_2
Al 2p	71.5	Al^{0}: Al metal
	74.0	Al_2O_3
V 2p	512.1	V^{0}: V metal
	515.1	V_2O_3
O 1s	529.9	TiO_2, V_2O_3
	531.5	Al_2O_3, C=O
	533.1	SiO, C-O
	534.8	-OH
C 1s	284.8	C-C, C-H
	286.2	C-O
	287.5	C=O
	288.8	O-C=O

The ionic character and chemical interactions established by Ramirez team were determined for a specific binding energy. However, ito accommodate changes in the elemental binding energy from one tested surface to another a standard deviation of ± 0.5 eV was established. This same variation will be applied in this study.

The following survey spectra are representative of the ungrafted (Figure 36A) and grafted (Figure 36B) Ti6Al4V XPS chemical composition.

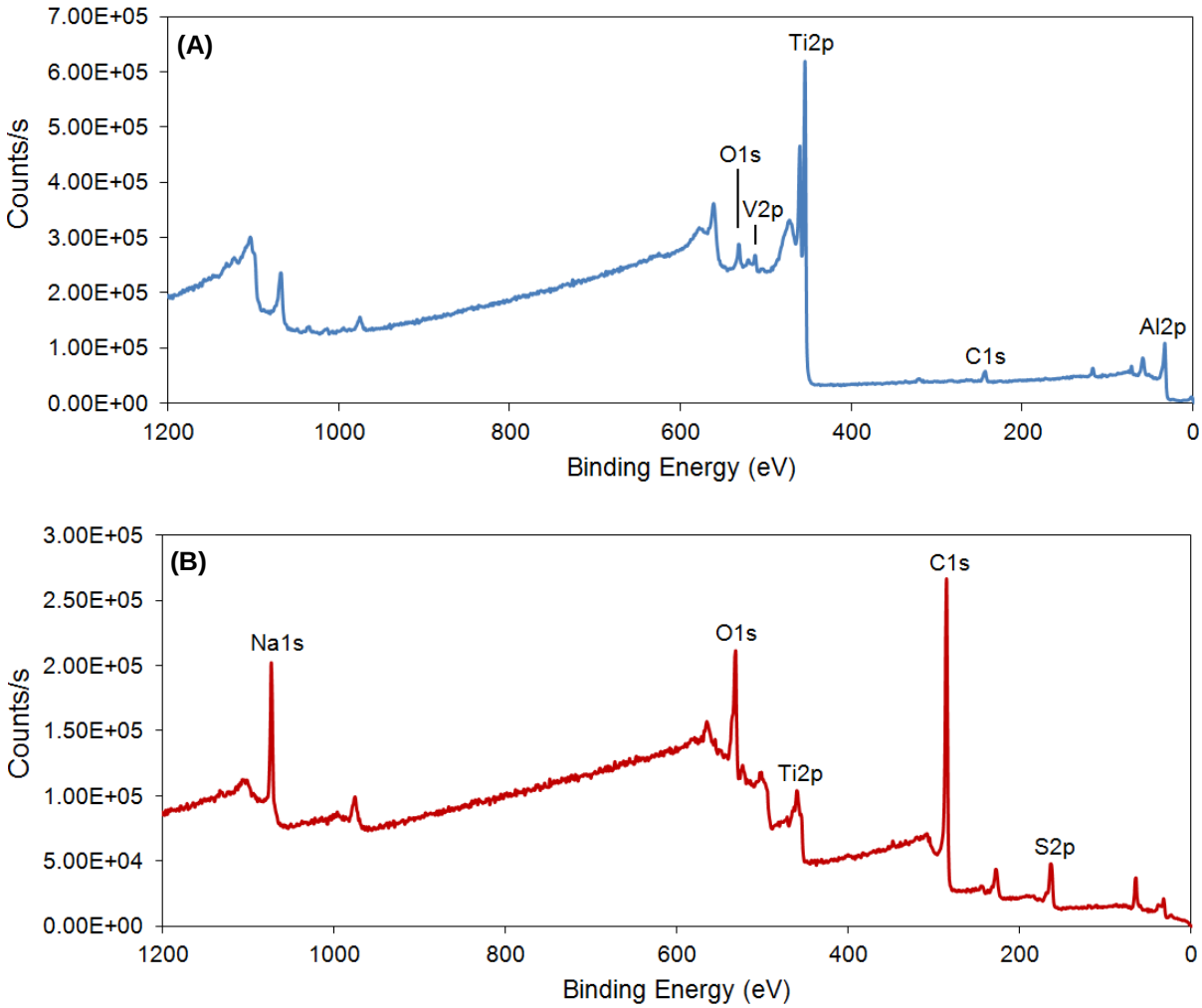

Figure 36. XPS survey spectra of (A) ungrafted and (B) grafted Ti6Al4V surfaces and respective elemental identification.

The spectra above are in agreement with the results from Table 9. The elements from the ungrafted surfaces are well defined and were easily identified, while some components of the grafted could not, namely the Al (inexistent) and the V (only identified through high resolution spectra). Each element is associated with one or consecutive binding energies according to the peaks detected. For instance, during C detection on the ungrafted surfaces (Figure 37) three peaks were identified. Hence, three binding energies were recovered and each one related to the respective ionic character/chemical interaction.

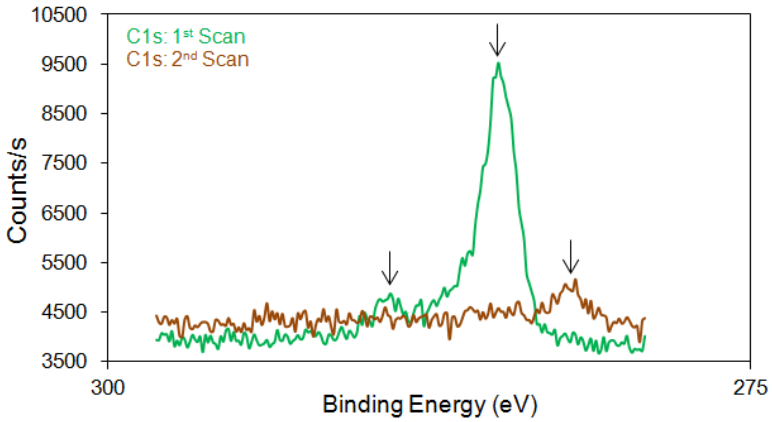

Figure 37. High resolution XPS spectra of carbon on ungrafted materials and respective peak identification (arrows).

High resolution spectra were acquired for each element and their binding energies identified according to Ramirez et al. [202]. The results are given by Table 11 and 12, respectively ungrafted and grafted surfaces. As the ionic character or chemical interaction of the S and Na high resolution spectra from the grafted surfaces are not available for correlation in Ramirez et al. work, their binding energies were not considered in Table 12.

Table 11. Binding energies and composition of the high energy spectra of each chemical element, Ti2p, Al2p, V2p, O1s and C1s, found on the ungrafted Ti6Al4V surfaces.

Element	Binding Energy (eV)	Ionic Character & Chemical Interaction
Ti 2p	454.7	Ti^{II}: TiO
	459.0	≈ Ti^{IV}: TiO_2
Al 2p	72.6	≈ Al^0: Al metal
	74.0	Al_2O_3
V 2p	513.2	≈ V^0: V metal
	515.3	V_2O_3
O 1s	531.1	Al_2O_3, C=O
	533.0	SiO, C-O
C 1s	284.5	C-C, C-H
	287.5	C=O
	289.0	O-C=O

Table 12. Binding energies and composition of the high energy spectra of each chemical element, Ti2p, V2p, O1s and C1s, found on the grafted Ti6Al4V surfaces.

Element	Binding Energy (eV)	Ionic Character & Chemical Interaction
Ti 2p	458.6	Ti^{IV}: TiO_2
V 2p	514.5	≈ V_2O_3
O 1s	533.2	SiO, C-O
C 1s	284.7	C-C, C-H
	287.3	C=O
	288.9	O-C=O

From these results it is possible to corroborate our initial premises on the efficiency of the grafting process. The poly(NaSS) coating masks the surface original elements and, in consequence, less chemical interactions are established between them. Their ionic state is affect as well. On both ungrafted and grafted substrates, the oxides of the chemical elements were found in abundance as expected (spontaneous oxidation). Nevertheless, binding energies in between the metal and oxide states were detected for Al and V. In this case, two explanations may be raised. The first relates to a possible ionic state in between the Al^0/V^0 and the Al_2O_3/V_2O_3 states not identified by Ramirez et al. The second consists in the assumption that a larger range, more than ± 0.5 eV, of Al and V binding energies may occur for their oxide in response to their stability. Since none of these explanations can be confirmed and the energy values in question were not found in the literature, we will assume those as correspondent to the Al and V metal states.

To confirm the previous observations EDS evaluations of the surface composition, and some atomic layers afterwards, were conducted. The results are shown on Table 13.

Table 13. EDS elemental composition of ungrafted and grafted Ti6Al4V surfaces.

Ti6Al4V	EDS Atomic Composition (%)						
	C	Ti	Al	V	O	S	Na
Ungrafted	20.5 ± 5.6	69.0 ± 4.7	7.5 ± 1.5	3.1 ± 0.7	-	-	-
Grafted	36.3 ± 2.3	30.7 ± 1.2	3.4 ± 0.2	1.6 ± 0.2	27.3 ± 2.6	0.6 ± 0.1	0.2 ± 0.1

As before, reductions in the Ti, Al and V levels were detected as well as the increased in C after radical polymerization. Interestingly, S and Na were not the only

elements to be found exclusively on the grafted substrates, O was also detected only on these surfaces. As the oxygen reactions and oxides only occur at a material's surface and since the EDS analysis is "an invasive" technique that considers more bulk than surface, the inexistent of O on the ungrafted materials is expected. On the other hand, during chemical grafting, oxidation and reduction reactions involving the sulfonate groups (SO_3^-) from the poly(NaSS) take place. O is liberated to the environment but may occur as well associated with the other chemical elements and incorporated onto the grafted coating. As a result, EDS, by being capable of identifying the elements from the bulk, allows the detection of the O elements from within the sulfonate coating.

With the exception of O, the EDS elemental composition of the ungrafted and grafted substrates follows the same proportional pattern observed on Table 9 (XPS). Some elements, namely S and Na, however, are not as important as the XPS analysis highlighted. The differences between the EDS and XPS evaluation processes explain the disparities.

In order to have a clear view of the distribution of the elements on the Ti alloy and to confirm the homogeneity of the poly(NaSS) coating, elemental mapping was carried out using the EDS system on grafted samples. Figure 38 shows the results.

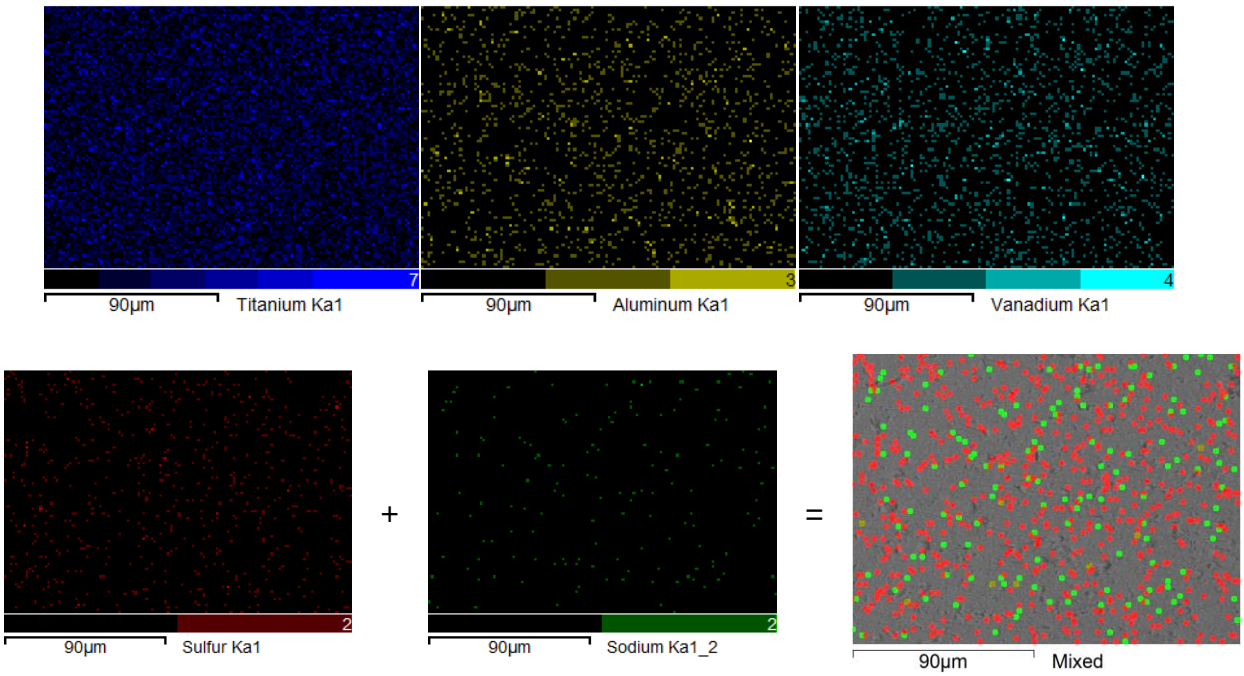

Figure 38. Elemental mapping/distribution on a grafted Ti6Al4V surface.

The chemical elements distribution was found random on both ungrafted and grafted substrates. Figure 37 only provides the results from the grafted surfaces, since the distribution of the Ti, Al and V elements on the ungrafted did not reveal any particular difference from the previous.

Interestingly, by combining the Na and S we confirmed these elements to be randomly disperse on the surface but uniformly distributed, without saturated areas. Even if this evaluation does not translate the real amount of Na and S to be found on the outermost atomic layer (XPS gives a more precise evaluation of the surface composition), it confirms the grafting process to be a homogeneous surface treatment.

1.4 Toluidine Blue Colorimetric Method

The amount of poly(NaSS) on the grafted surfaces was determined using the toluidine blue (TB) colorimetric method.

After the 15 h polymerization and all the washes in between, it was noticed that the samples passed from a grey to a yellow/blue coloration, an indicative of the polymer presence (Figure 39).

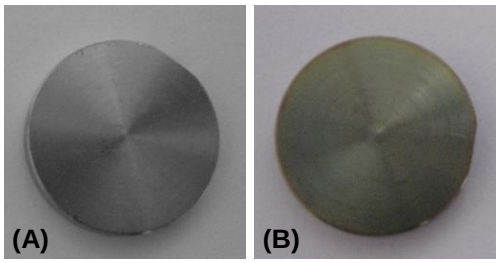

Figure 39. (A) Ungrafted and (B) grafted Ti6Al4V surfaces.

By allowing the grafted disks to contact for 6 h with the TB, the complexation of the dye with the SO_3^- groups occurred. The TB colorimetric method allowed, this way, the quantification of the poly(NaSS). The amount of polymer found was determined as 1.63×10^{-5} g/cm^2 ± 2.56×10^{-6} g/cm^2, proving once again the success of the grafting process. Ungrafted samples did not react with TB. These results show that the grafting conditions are in fact optimized, something that has been the research goal of many PhD students along the years. The amount of poly(NaSS) coated is substantially superior than that registered in previous investigations [171,203].

In the literature although, smaller amounts of polymer have been identified after grafting, ranging from $1.00x10^{-7}$ to $1.00x10^{-6}$ g/cm^2 [204,205]. They explain these quantities by the presence of non-grafted polymer chains, formed by free radicals in solution, which are entangled and retained in the inner graft polymer network generating a thick coating with a multilayer structure. Hence, when dye conjugates enter in contact with the polymeric layer they do not distinguish these inner chains and only report the polymer present on the outer coating. The same event may be taking place during poly(NaSS) grafting onto Ti6Al4V. Despite the substantial improvement of the poly(NaSS) density over previous work, during TB complexation its totality may not be taking into consideration. As seen by the EDS and XPS results, the polymeric layer generated during grafting is more than 100 nm thick, which accounts for multiple monomer associations and creation of long chains. Therefore, when the surfaces are exposed to TB the polymer encased in the network may not be exposed.

1.5 Surface Energy and Wettability

The wettability of a biomaterial surface is of extreme importance to the cell development but most importantly to protein adsorption. The hydrophilicity or hydrophobicity of the ungrafted and grafted substrates was put to test by measuring the contact angles of water, formamide, ethylene glycol and diiodomethane, after 8 s of contact with the surface. The results are given by Table 14.

Table 14. Liquid contact angles of ungrafted and grafted Ti6Al4V surfaces.

Ti6Al4V	Water (º)	Formamide (º)	Ethylene Glycol (º)	Diiodomethane (º)
Ungrafted	61.9 ± 8.9	54.0 ± 6.4	45.2 ± 6.5	37.0 ± 6.6
Grafted	37.2 ± 9.2	20.0 ± 2.2	25.0 ± 5.8	45.2 ± 5.5

The polar liquids (water, formamide and ethylene glycol) contact angles decreased with the grafting process, while the inverse happened with the apolar liquid (diiodomethane), reflecting the hydrophilic nature of the surfaces. An important decrease in the water contact angles after grafting as been reported by Hélary et al. [164] and Mayingi et al. [203].

During radical polymerization, the poly(NaSS) chains on the Ti alloy are formed by molecular weight distribution. However, that distribution may not always be

homogeneous. Noirclere et al [171] study demonstrated the poly(NaSS) grafted on Ti materials to create a 16º contact angle in the presence of water, which is half of the obtained on Ti6Al4V. They observed that in some cases the angle could not be determined as the water was completely absorbed by the polymeric layer. This can be explained by the distribution of the polymeric chains on the Ti tested by Noirclere et al. As the poly(NaSS) chains are generated randomly along the surface, it allows for areas with chains large enough to result in the absorption of the liquid. This effect is not rejected by our results, as poly(NaSS) is water soluble and polymeric "swell" under the effect of water or culture medium may still occur [206,207]. Nevertheless, it should be highlighted that Ti6Al4V materials may be more suitable for poly(NaSS) grafting than pure Ti, since they allow for a more reliable and uniform coating to be generated.

By using the contact angle measurements it was possible to determine the surface free energy and by extension the respective dispersive and polar components. The results are shown on Table 15.

Table 15. Surface energy and quantification of dispersive and polar components of ungrafted and grafted Ti6Al4V surfaces.

Ti6Al4V	Total Surface Energy γ (mN/m)	Dispersive Comp. γ^d (mN/m)	Polar Comp. γ^p (mN/m)	γ^d/γ (%)	γ^p/γ (%)
Ungrafted	29.3	9.4	19.9	32.1	67.9
Grafted	57.3	13.1	44.2	22.9	77.1

As the contact angle measurements, the total surface energy shows an increase in the hydrophilic character of the Ti6Al4V disks by the addition of poly(NaSS). In total, the bioactive coating allowed for an energy increase of 28 mN/m. This augment in energy is in fact due to a ≈ 77% contribution of the polar component, which is associated to the polar nature of the NaSS molecule, more precisely the SO_3^- ionic groups. These observations are consistent with previous work [163,208].

From a biological perspective, the hydrophilic nature of the grafted surfaces may affect positively the cells behavior as they allow for proteins to interact more easily with the surface and to create an environment compatible with osteogenesis [209,210].

1.6 Fourier-Transformed Infrared Spectroscopy

To identify the chemical groups characteristics of the poly(NaSS) when grafted onto the Ti6Al4V metal, we used the ATR-FTIR technique. The spectrum from Figure 40 is representative of Ti6Al4V surfaces ungrafted and grafted with poly(NaSS), between 930 and 1830 cm^{-1}.

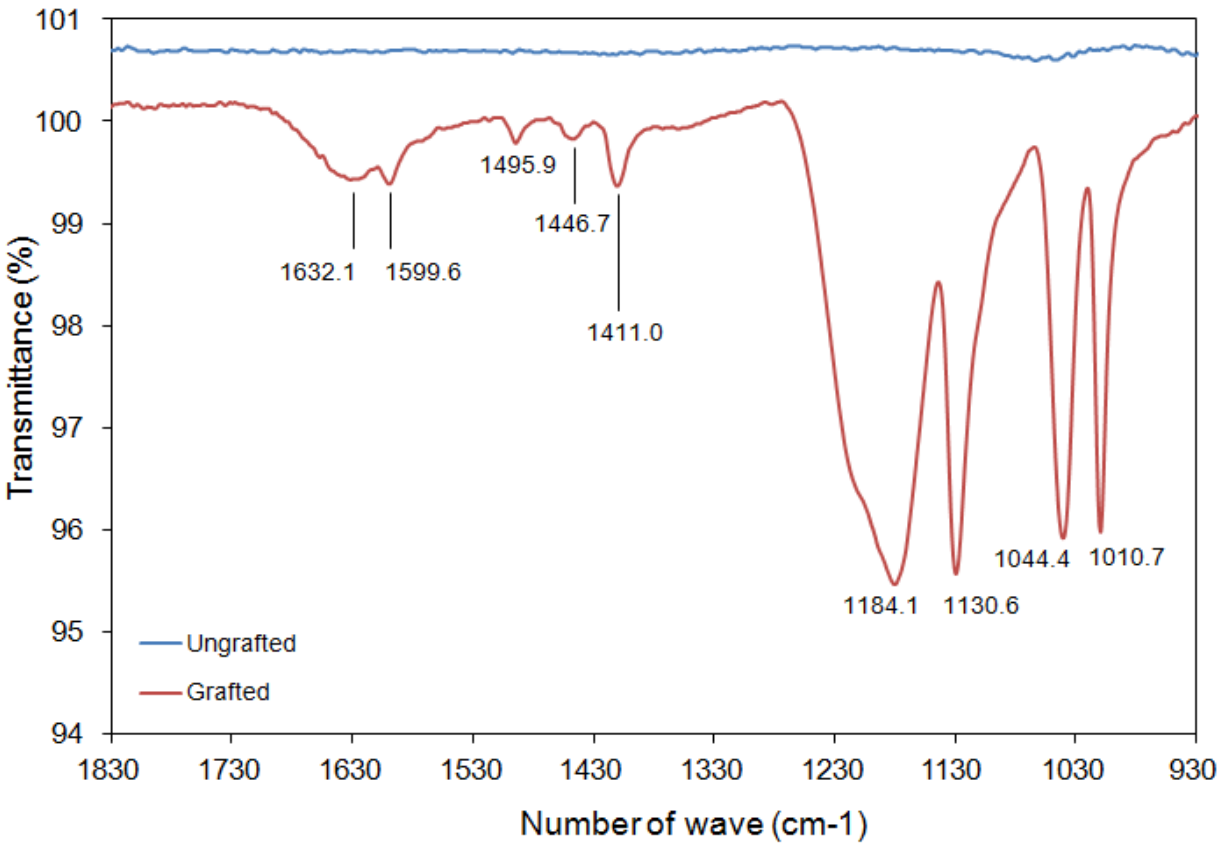

Figure 40. ATR-FTIR spectrum from Ti6Al4V surfaces, ungrafted and grafted with poly(NaSS).

As expected, no peaks were noticed on the ungrafted surfaces – absence of the bioactive polymer. On the other hand, several peaks were detected in the presence of poly(NaSS). Table 16 summarizes their intensity and classifies each peak according to their correspondent chemical groups and interactions established.

Table 16. Adsorption bands characteristics of poly(NaSS) [adapted from 170].

Number of Wave (cm^{-1})	Peak Intensity	Chemical Groups & Interactions
1635-1595 and 1496-1433	Weak	ν (C=C) from the Aromatic Ring
1411	Medium	ν (SO_2)
1185-1130	Strong	$SO_3^-Na^+$ (salt)
1044	Strong	ν (O=S=O)
1010	Strong	Aromatic Ring

The aromatic ring and the symmetric vibrations of the SO_3^- groups generated a NaSS doublet (O=S=O) located at 1010 and 1044 cm^{-1}. The absorption of the sulfonic acid salt was detected by the peaks between 1130 and 1185 cm^{-1}, which are also associated with asymmetric vibrations. Asymmetric valence vibrations were also found for the group SO_2 at 1411 cm^{-1}. Finally, the series of peaks between 1635 and 1433 cm^{-1} are attributed to stretching vibrations of bonds (C=C) of the benzene ring.

Similar observations were made in previous work [172], confirming the grafting process to be successful. In those cases, however, the peaks registered between 1635 and 1411 cm^{-1} were not distinguished due to background noise.

1.7 Crystalline Structure

The crystalline structure of the ungrafted and grafted Ti6Al4V substrates was determined by XRD. The spectra are given by Figure 30.

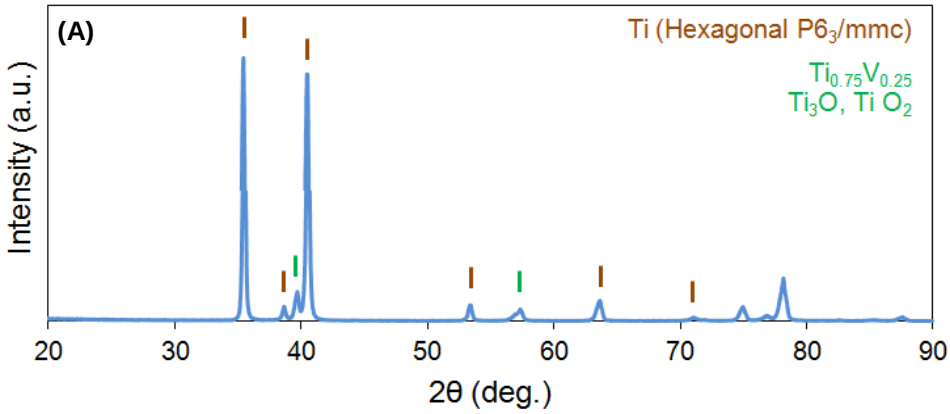

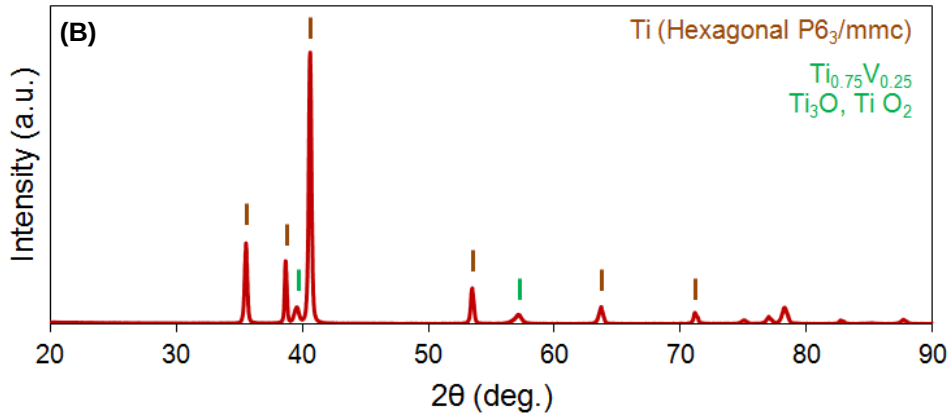

Figure 41. XRD spectra of (A) ungrafted and (B) grafted Ti6Al4V substrates.

Despite from a small difference in peaks intensity, which can be explained by naturally occurring structural variations between tested samples, both ungrafted and grafted surfaces exhibited equal crystalline structure. The material basic structure (RT) was confirmed with various peaks identifying the hexagonal closed packed rearrangement, the most typical and characteristic structure of Ti based materials. Oxide formations and conjugates of Ti and V were also detected, although in smaller amounts. As expected the grafting process and the presence of poly(NaSS) did not affect the Ti6Al4V crystalline structure.

2. CRYSTALS

Prior to any test, including characterization, the QCM-D crystal were sonicated in 99% ethanol and twice in MilliQ® ultrapure water, followed by drying in N_2 and UV ozone sterilization. The poly(NaSS) physisorption and poly(DTEc) or PS spin coating were applied afterwards. During characterization special attention will be given to the Ti6Al4V sensors, as the biological outcomes from the treated (physisorbed) and untreated (control) crystals will be correlated with the results obtained from the grafted and ungrafted disks, respectively.

2.1 Morphology

The sensors morphology was observed by SEM. Micrographies were obtained using an electron beam of 20 kV of intensity and 100x resolution (larger surface area). The results are given by Figure 42.

Figure 42. SEM micrography of a Ti6Al4V QCM-D crystal.

A very regular and smooth morphology is exhibited by the QCM-D sensors. This was observed for the totality of the studied surfaces. Due to the fragility of the crystals no topographical measurements were conducted. Therefore, we can only suppose about the smoothness transmitted by the SEM micrographies.

2.2 Chemical Composition

The sensors chemical composition was determined using the XPS technique. As the thickness of the Ti6Al4V deposited layer did not exceed 50 nm, EDS analyses were not conducted. The elemental composition of the 1st monoatomic layer of the Ti6Al4V and the poly(NaSS) physisorbed sensors is shown on Table 17.

Table 17. XPS elemental composition of Ti6Al4V and poly(NaSS) coated sensors.

	XPS Atomic Composition (%)							
Sensors	**C**	**O**	**Ti**	**Al**	**V**	**Na**	**S**	**Imp.**
Ti6Al4V	3.3 ± 1.0	18.8 ± 2.4	56.9 ± 3.3	17.2 ± 2.0	3.3 ± 0.1	-	-	0.6 ± 0.1
Poly(NaSS)	5.3 ± 3.3	15.4 ± 1.3	49.4 ± 2.7	16.1 ± 2.4	1.7 ± 0.3	10.8 ± 1.9	0.7 ± 0.1	0.7 ± 0.0

The presence of Na and S, slight increase in C, decrease in O, and a reduction of the original Ti6Al4V elements Ti, Al and V on the poly(NaSS) coated surfaces, confirmed the presence of this bioactive polymer on the sensors surface after physisorption. Equal observations were made on the grafted disks. The explanations used in the 1st Part, subsection 1.3 can be applied in this case. Still by comparing these results with previous studies [164,173,208] or even the results from

the subsection 1.3, it is shown that physisorption is not as efficient as chemical grafting with 10 times less polymer being detected. Nevertheless, between all techniques tested this was the most favorable and less aggressive towards the surface.

As expected, a superior amount of C was detected in the poly(DTEc) and PS coated sensors and of Au in the gold sensor. Therefore, their chemical composition analyses were not taken into consideration.

2.3 Toluidine Blue Clorimetric Method

The poly(NaSS) physisorbed onto the Ti6Al4V sensors was determined using the TB method and by measuring the drops in frequency caused by the addition of the poly(NaSS) coating through QCM-D.

After 15 h of physical contact between a solution at 0.7 M of poly(NaSS) and the sensors, the surfaces were washed and dried with N_2. Afterwards, they were divided in two groups. In the first, the sensors were complexated with TB, following the same procedure as the disks, and in the second their frequency was measured. Here, it is important to refer that the frequency of the sensors used in the last group was measured as well before physisorption so differences between before and after coating could be detected. The amount of poly(NaSS) was determined as 9.03×10^{-7} g/cm^2 ± 1.06×10^{-8} g/cm^2 using the TB and 1.06×10^{-6} g/cm^2 ± 1.11×10^{-7} g/cm^2 using the QCM-D system. In both cases, the values were approximated, confirming the validity of the characterization processes applied. Comparing these results with the TB values obtained with the grafted material, it is possible to conclude that the total amount of polymer coated onto the sensors is 10 times less than that registered by the grafted surfaces. This is to be expected, since the grafting process results from the chemical activation of the surface and consequent radical polymerization of the monomer NaSS, sharing covalent bonds with the material and developing long anionic chains; while physisorption, as the name suggests, results from the physical adsorption of the polymer onto the surface of the sensors, generating weak links and smaller chemical chains.

2.4 Wettability

Data from contact angle measurements of the four tested surfaces is given by Table 18. The results show the Ti6Al4V sensors to be the most hydrophilic from the

group, while the PS are the most hydrophobic. Contrary to previous investigations and the results from the subsection 1.3, in which poly(NaSS) coating made Ti based materials more hydrophilic [164,208], in our studies it made the surface more hydrophobic as indicated by an increase in the water contact angles.

Table 18. Water contact angles of Ti6Al4V, poly(NaSS) physisorbed, gold, poly(DTEc) and PS QCM-D sensors.

Sensors	Average ± SD (º)
Ti6Al4V	30.9 ± 2.7
Poly(NaSS)	44.9 ± 2.5
Gold	67.2 ± 4.8
Poly(DTEc)	77.3 ± 3.6
PS	84.0 ± 1.9

Poly(NaSS) is typically chemical grafted onto Ti6Al4V. However, because of the fragility of the Ti6Al4V layer deposited by PVD onto the gold surfaces (crystals), poly(NaSS) was deposited by physisorption. PVD, by its very nature does not produce continuous films as Ti disks. Thus, while physical adsorption of the poly(NaSS) on Ti based disks form a continuous layer of polymer, this may not be the case of PVD, and hence could influence its wettability. Furthermore, the amount of poly(NaSS) was smaller than that registered on the grafted disks. Despite this small contradiction to previous work, the poly(NaSS) coated sensors remain hydrophilic.

2.5 Crystalline Structure

The crystalline structure of the Ti6Al4V sensors was evaluated by XRD. As reported by the XPS results, the amount of poly(NaSS) physisorbed onto the crystals was 10 times less than that registered on grafted disks. Therefore, and since no indication of the grafted poly(NaSS) influence on the structure on the Ti alloy disks was detected, the crystalline structure of the poly(NaSS) physisorbed crystals was neglected from the study. Figure 43 shows the spectrum of the Ti6Al4V sensor.

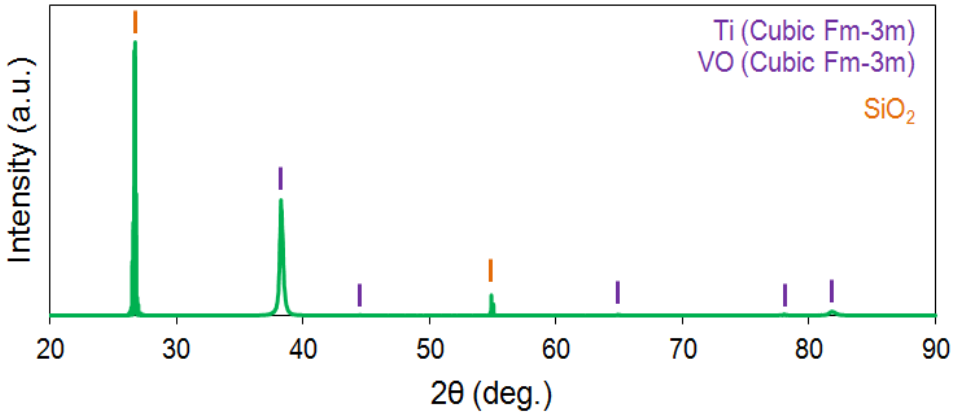

Figure 43. XRD spectra of a Ti6Al4V QCM-D sensor.

The spectrum suggests the crystalline structure of the Ti alloy deposited on the crystals to be predominantly a body-centered cubic rearrangement. Usually, the atomic structure of Ti based materials undergoes a transformation from a hexagonal close-packed arrangement to a body centered cubic arrangement when heated [211,212]. That phenomenon may occur during PVD deposition, which explains the differences between the crystalline structure of disks and crystals. SiO_2 predominantly found on quartz sensors was also detected, as expected.

– 2nd Part. Biological Testing –

In the second part of this study, the behavior of osteoblast-like cells in contact with ungrafted and grafted disks as well as differently treated quartz crystals was tested.

Different culture conditions were evaluated, including SFM and FBS supplemented medium, to understand the impact of proteins in the cell early attachment and the influence poly(NaSS) exerts by itself in the host response. The effect of adhesive proteins, i.e. Fn, in the cell attachment and progressive maturation was determined by adsorbing single and protein mixtures, and by testing the cell development in DD conditions. Moreover, the mechanisms by which cells establish reliable and strong interactions with protein treated substrates were characterized by means of integrin-mediated evaluations and protein binding domains restrictions. The conformation of specific proteins, as a result of the poly(NaSS) presence, was also considered and so was the impact of the RGD sequence in the early cell attachment. Finally, the competitive character of three important proteins, BSA, Fn and Col I I was assessed and categorized according to the substrate in test.

The totality of the biological experiments was preformed after thorough sterilization of the Ti disks and the QCM-D crystals.

1. FBS SUPPLEMENTED MEDIUM VS SERUM FREE MEDIUM

Ten years ago, researchers synthesized “bioactive model polymers” bearing SO_3^- groups and proposed a step by step mechanism with which they could modulate the cell response. By setting up the grafting of polymers bearing SO_3^- on Ti6Al4V surfaces by a grafting “from” technique they assured the creation of covalent bonds between the grafted polymer and the alloy. More recently, it has been confirmed the positive effect of grafted sulfonate groups on the osteoblastic cell response *in vivo* and *in vitro*, using different model surfaces as substrates. However, the mechanism by which that interaction, surface-protein-cell, is accomplished has not yet been exposed. In this section, we investigate the role of the SO_3^- groups on the early osteointegration of ungrafted and poly(NaSS) treated surfaces, in the presence and in the absence of FBS proteins, *in vitro.*

1.1 Viability – Alamar Blue Analysis

The first assessment to be made in a study that limits the basic elements needed for cell survival, more precisely the proteins and the nutrients from the FBS, is the cell viability.

The alamar blue viability tests were conducted from 30 min to 3 days (4320 min) of culture in the presence (CM) and absence (NCM) of FBS proteins. The results are shown in Figure 44.

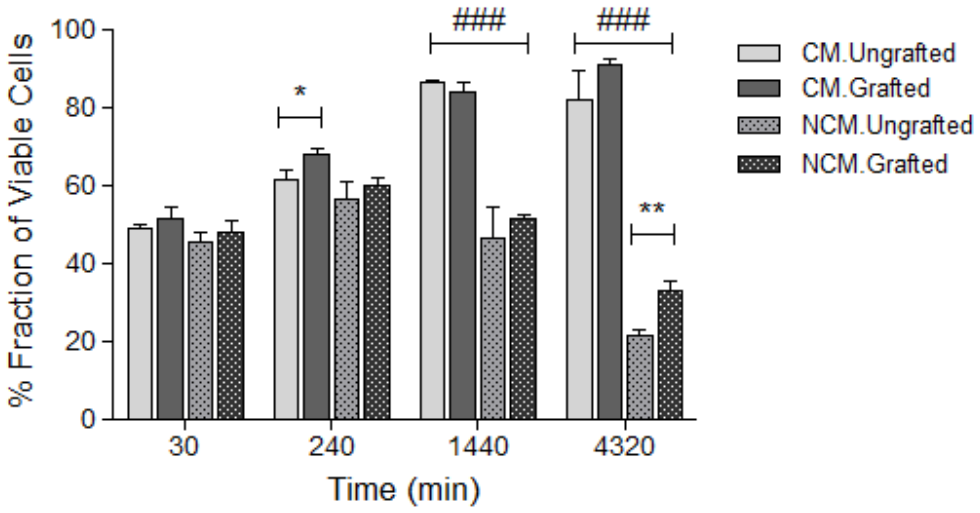

Figure 44. MC3T3-E1 cells viability on ungrafted and grafted Ti6Al4V dics cultured for 30, 240, 1440 and 4320 min in the presence of FBS proteins (CM) and in its absence (NCM). Significant differences between CM and NCM cultures are indicated by # while between ungrafted and grafted surfaces in equal conditions (CM or NCM) are indicated by * (#/* p<0.05; ##/** p<0.001; ###/*** p<0.0001).

In the first moments of cell contact (30 min) the viability pattern was similar whatever the tested surface. After 4 h (240 min), a small difference became perceptible between cells cultured on ungrafetd and poly(NaSS) grafted materials and between CM and NCM conditions. However, it was after 1 day (1440 min) of culture that the medium supplements started to play a major role. The presence of FBS proteins contributed to the survival and development of the osteoblastic cells. This phenomenon has been extensively study over the years [63,213]. In the absence of nutrients and proteins, it was expected the MC3T3-E1 cells to experience starvation and that to lead to a quick and extreme reduction on their life expectancy. That was confirmed with survival rates lower than 50% at day 1. Despite the continued viability decrease on the NCM cultures with time, the fraction of viable cells at day 3 (4320 min) was found higher on poly(NaSS) grafted surfaces when

compared to ungrafted. The SO_3^- groups from the poly(NaSS) macromolecular chains grafted onto Ti surfaces were shown to induce Fn and Col I secretions *in vitro* and *in vivo* [214,215]. Therefore, the fact that cells tend to respond more favorably even in the absence of proteins would suggest that the poly(NaSS) grafted exhibit biological properties, which play a crucial role in those particular conditions. The presence of SO_3^- groups could mitigate partially the defect of proteins by stimulating the secretion of these by the cells which in this particular case are in “direct” contact [164,173].

1.2 Viability – Calcein and Propidium Iodide Staining

To confirm the data from the alamar blue viability tests and to assess the osteoblastic cells spreading and morphology, fluorescent microscopy evaluations were conducted. Live and dead cells were stained in green and red, respectively, using calcein and propidium iodide dye reagents. Our findings are shown on Figure 45.

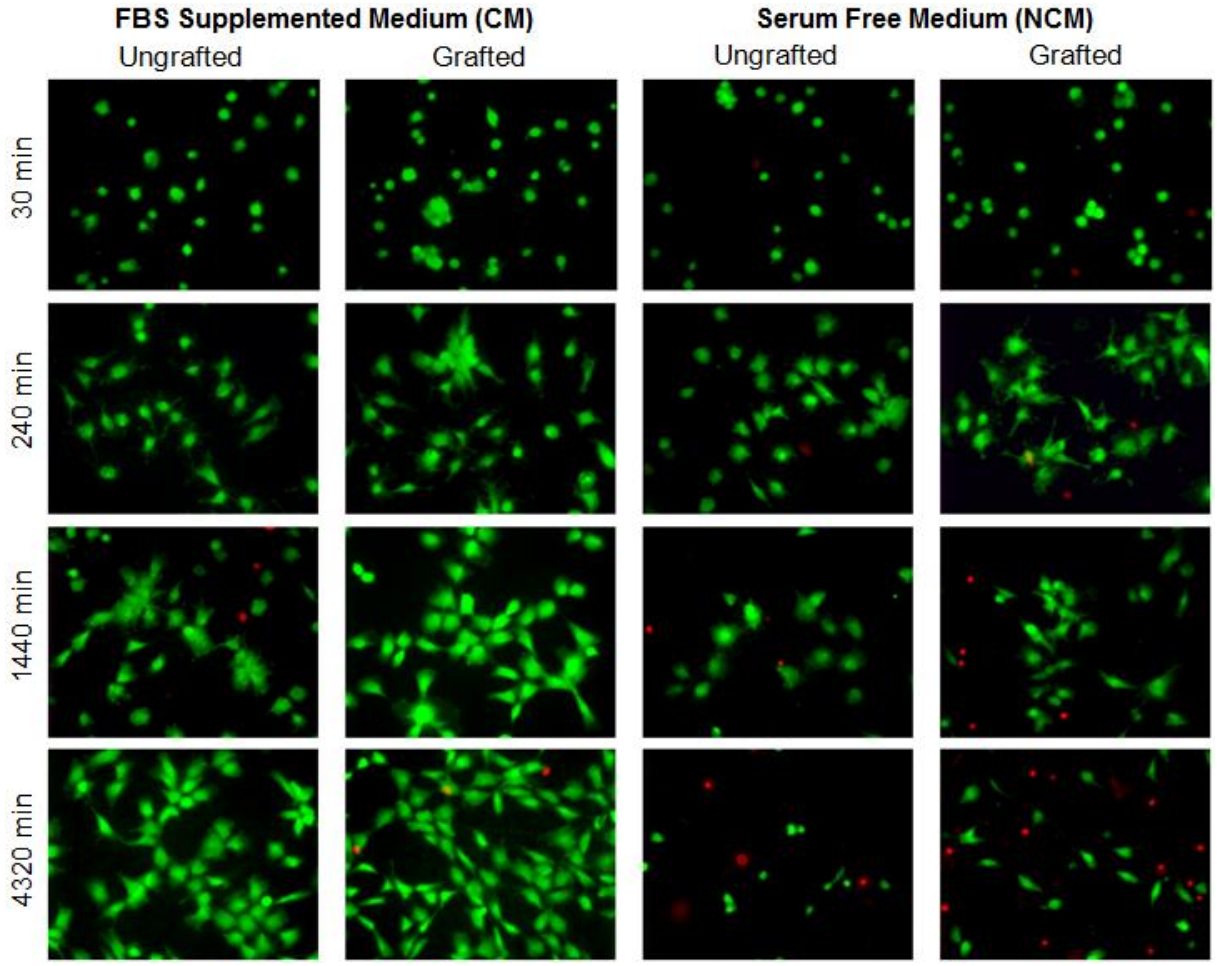

Figure 45. MC3T3-E1 cells morphology and spreading on ungrafted and grafted Ti6Al4V surfaces cultured from 30 to 4320 min in CM and NCM conditions (20x resolution).

The cells spreading and morphology was similar on all tested surfaces after 30 min of incubation. The osteoblastic cells still presented a round shape and the majority was stained in green (most of the red stained cells were located in the border of the Ti6Al4V samples). At 4 h, a more elongated shape was dominant between the MC3T3-E1 cell morphology. The cytoplasm started to expand and evidences of protrusions extending along the surface were found. As before, the majority of the cells were live. At day 1 the differences between the cells cultured in the presence and absence of the FBS elements intensified. In the NCM cultures, a decrease in number of cells was detected. A small part of the cells displayed an elongated shape (morphology expected in regular conditions), while the rest returned to a more round morphology. Despite being smaller than the living cells, the dead represented ≈ 50 % of the total amount. Regardless the culture conditions, CM or NCM, more cells (total amount) were visible on the poly(NaSS) grafted surfaces than on the ungrafted. Given the nutrients and the proteins from the FBS to be essential

for cell survival and particularly development/maturation [213], after 3 days of incubation only a minority of cells remained on the NCM cultures. At this point, the MC3T3-E1 cells on the ungrafted substrates were mainly round and most were dead.

Interestingly, the osteoblast-like cells attached to the grafted Ti6Al4V, despite being less and smaller than at previous time points, still displayed an extended cytoplasm with elongated protrusions. Previous investigations, have shown the ability of poly(NaSS) to create long lasting bonds with cells in the presence of proteins, allowing them to spread freely in the surface and to develop strong focal adhesions (Figure 46) [164,166,173,208]. The novelty introduced by this test was the capacity of the bioactive poly(NaSS) to prolong the interface created with the cells in the absence of proteins. We believe this to be a consequence of stronger physical bonds developed both through the SO_3^- groups' presence and the activation of specific cell functions, a phenomenon seen before [216]. Poly(NaSS) has been identified as a trigger of early signaling pathways (FAK phosphorylation and MAPK cascade) associated with important cell events, namely adhesion, migration and spreading. Knowing the ECM of osteoblastic cells to be a complex and diverse system with many different proteins and growth factors [20,217,218], it is expected, in SFM conditions, the surface properties and in particular the bioactive poly(NaSS) to stimulate the production of proteins of interest by the cells and, consequently, to activate the signal pathways necessary to extend the cells viability and their interaction with the biomaterial [216].

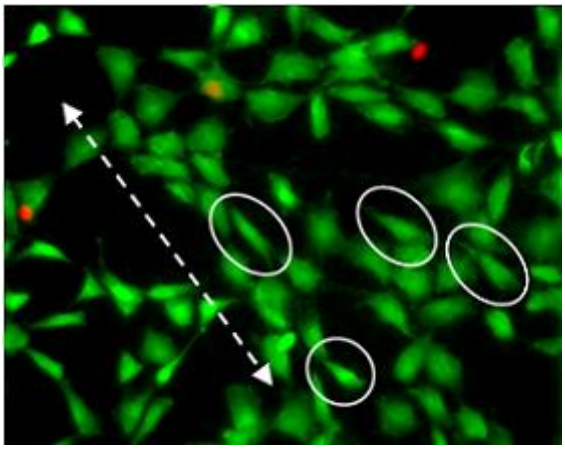

Figure 46. MC3T3-E1 cells spreading on grafted Ti6Al4V after 4320 min (3 days) in CM conditions. The ⟷ symbolizes the orientation preferably followed by the cells and the ▢ highlights particular cells with cytoplasm protrusions already extending in that direction.

All along the experiments, MC3T3-E1 cells exhibited a heterogeneous orientation on both grafted and ungrafted surfaces. Still, after 3 days on the CM grafted cultures, evidences of cytoplasmic rearrangement from some cells in one direction and following the surface topography could be seen (Figure 46). This is a necessary phenomenon in order to generate a complete and stable cell layer on the implantable material [63]. Once more, evidences of the poly(NaSS) impact on early cellular events were found.

1.3 Cell Attachment

The MC3T3-E1 cell numbers on each tested surface were registered from 5 min to 3 days. Figure 47 shows the results.

From 5 to 30 min no differences were detected between the two culture types. At 4 h, small differences in the cell numbers were evidenced between CM and NCM conditions. From 1 to 3 days, however, the influence of the FBS elements in the cell development became obvious. While nourished cells continued their progressive growth, cells cultured in SFM experienced a reduction in number. This happens because cells interact directly with the molecular structure of the adsorbed protein layer rather than with the molecular structure of the material surface. They bind to specific bioactive features exposed by the adsorbed proteins by way of membrane-bound receptors. That interface stimulates intracellular processes which determine the cellular response. These interactions are based on chemical bonds [63,213]. In CM conditions, the MC3T3-E1 cells were capable of generating such connections that supported their development with time [164,173]. To the contrary, NCM cultured cells were not. During the 3 days period, only physical bonds were established [208]. These interactions are not capable of supporting the cells development on their own for long periods of time. Ultimately the cells starve, rearrange their morphology (from elongated to round) and later die. Figure 45 supports this statement.

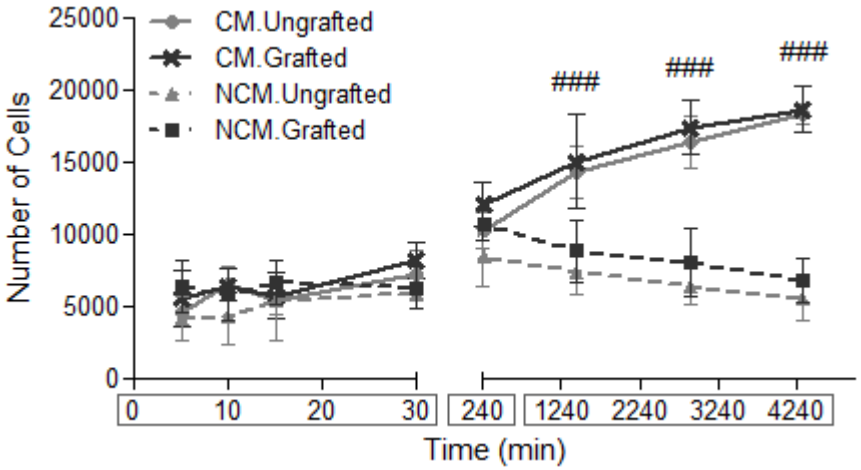

Figure 47. MC3T3-E1 cells attachment on ungrafted and grafted Ti6Al4V surfaces cultured in CM and NCM conditions, from 5 min to 3 days. Significant differences between CM and NCM cultures are indicated by # (### $p<0.0001$).

Despite the lack of significant distinctions, from 4 h to 3 days, the average number of cells on the grafted Ti6Al4V was always superior to the ungrafted, even in NCM conditions. We believe the physical bonds established between the MC3T3-E1 cells and the poly(NaSS) in the NCM cultures allowed the cells to sustain their structure longer and, consequently, led to the activation of specific functions. Zhou et al. [214] and Huot et al. [219] using RT-PCR to study the Fn and the Col I gene expression on different substrates reached conclusions that corroborate this discussion. Their studies suggest the ability of this bioactive polymer to stimulate the cellular secretion of these two proteins in quantities and speed that overcome the registered on ungrafted substrates (maximum levels were reached sooner by grafted materials). Fn and Col I play an important role in the cell initial attachment to a biomaterial and in intra- and extra-cell communications. The early signal pathways triggered by the poly(NaSS) enhanced the genetic expression revealed by these proteins and, consequently, led to stronger and more efficient interactions with the surface [216]. The number, spreading and morphology revealed by the MC3T3-E1 cells cultured on grafted Ti6Al4V and NCM conditions confirm these phenomena to be in progress during this experiment.

1.4 Attachment Strength

In order to test the cells adhesivity or attachment strength towards the ungrafted and grafted Ti alloy, a shear stress of 10 dyn/cm^2 was applied for 15 min to each substrate. The percentage of remaining attached cells is given by Figure 48.

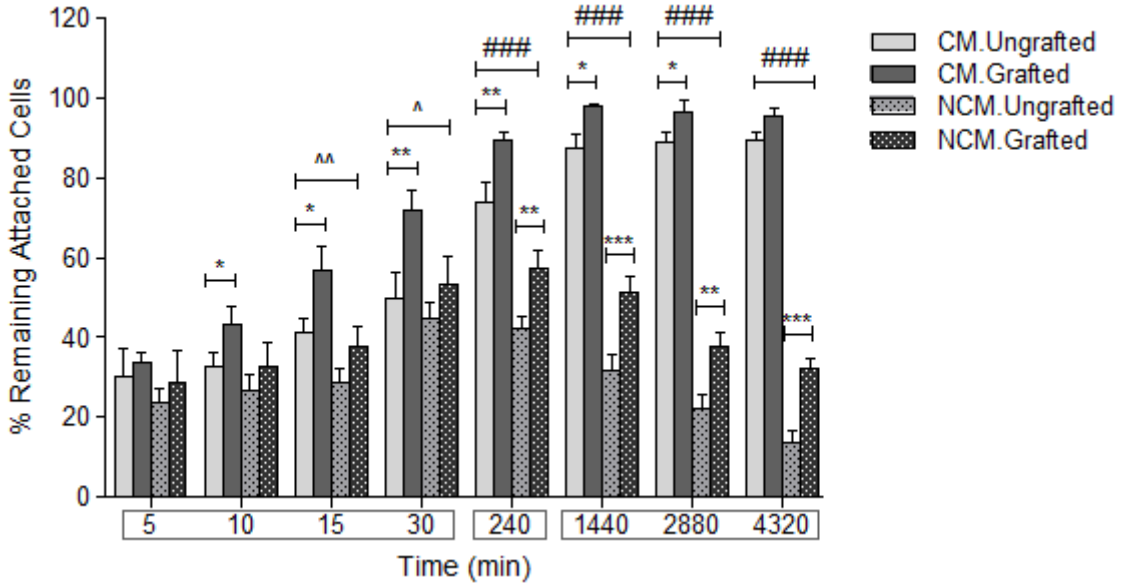

Figure 48. Percentage of remaining attached cells after the application of a shear stress of 10 dyn/cm^2 for 15 min. Significant differences between: CM and NCM cultures are indicated by #; ungrafted and grafted in the same culture conditions (CM or NCM) by *; ungrafted surfaces in different conditions (CM vs NCM) by +; and between grafted surfaces in different conditions (CM vs NCM) by ^ (#/*/+/^ $p<0.05$, ##/**/++/^^ $p<0.001$ and ###/***/+++/^^^ $p<0.0001$).

Differences between cells cultured on ungrafted and grafted surfaces, in CM and NCM conditions, were observed right from the initial moments of attachment. For the majority of the time points, the cells cultured in the presence of FBS and poly(NaSS) displayed the higher resistance to stress. Poly(NaSS) increases the interactions strength between the two systems, cell and biomaterial, by inducing the creation of more resistant and numbered adhesion points (focal adhesions) [164,173,208]. The chemistry of the grafted surfaces is assumed to have a major impact on protein adsorption and cell attachment [208]. Previous studies have shown the enhanced affinity of the bioactive polymer to adhesive proteins, such as Fn or Vn, over BSA [216,220,221]. This preference affects the interface, which is directly associated with the cells ability to spread and establish a reliable connection to the implantable material [83,222]. Even in low concentrations (such as in the FBS), Fn and Vn play a major role in the cells attachment strength. This way, the bond generated is more difficult to break and, therefore, more resistance to shear stress. After 4 h of culture, the bond strength increased in the presence of the FBS proteins, reducing the differences between ungrafted and grafted materials (development of strong chemical bonds representative of the cell maturation). The percentage of cells

still attached to the surface was enhanced, surpassing 80%. For the totality of the experiments, the bond strength was always superior in the presence of proteins.

In the NCM cultures, despite a small improvement introduced by the poly(NaSS) in the initial stages, it was only after 4 h that it had the biggest impact on the osteoblasts attachment strength. The ungrafted cultures experienced a loss in adhered cells almost 20 times higher than the grafted. Again, the poly(NaSS) chains were fundamental to the cells development and to the creation of better-quality physical bonds with the surfaces [208]. This experiment allows for a better appreciation of the polymer importance to the cells initial and continuing development on implantable surfaces.

The grafting of SO_3^- groups onto Ti6Al4V substrates favors the adhesion of cells that are capable of resisting detachment under stress circumstances.

Main Conclusions

The experiments carried out in this study have shown the benefit of poly(NaSS) grafted onto Ti6Al4V surfaces in the early stages of osteoblastic cultures, *in vitro*. Indeed, the results showed that (i) the fraction of viable cells was superior on grafted materials than on ungrafted and (ii) the poly(NaSS) is capable of supporting the cell structure and morphology for longer, all in NCM conditions. In addition, SO_3^- groups exhibited by the poly(NaSS) macromolecular chains allowed for stronger physical bonds to be developed between cell and biomaterial, conferring a superior resistance to stress of 10 dyn/cm^2.

2. SINGLE PROTEIN ADSORPTION AND CELL BEHAVIOR

Functionalization of surfaces with poly(NaSS) is a recent approach to Ti6Al4V materials. Previous work has shown the radical polymerization of poly(NaSS) to be successfully preformed on Ti based substrates with promising biological responses [223]. Poly(NaSS) is stable in physiological environments and is not susceptible to enzymatic degradation, overcoming the limitations of pre-existing strategies of incorporation and/or release of bone-promoting proteins (BMPs [224], collagen [225]) and antibacterial drugs (gentamycin…) [226]. Furthermore, bacteria experiments on these chemically altered materials demonstrated their higher resistance to bacteria

adhesion, particularly to the staphylococci family [227], which includes the *Staphylococcus aureus* a bacteria with high affinity to Ti [228,229]. The bacteria inhibition promoted by the SO_3^- groups was also confirmed in the presence of different adhesive (i.e. Fn) and non-adhesive (i.e. BSA) proteins, increasing the hopes for a better and more reliable implantation [230]. In this section, we explore a little further the impact of protein adsorption on poly(NaSS) grafted Ti6Al4V substrates but this time from a cell point of view.

Cell-surface interactions are dependent on the initial adsorption of proteins. Once an implantable material enters in contact with the living system, rapid adsorption of proteins occurs on the surface. These proteins provide an adhesion network for the attachment of cells both *in vivo* and *in vitro*, and mediate all the interactions that follow [231]. The cells that reach the protein coated substrate attach to the ECM of those highly complex particles. Since there is no actual contact between the implant and the cells, the resultant biological activity will depend on the recruited proteins [43,232] and, by consequence, so will the long-term compatibility of the biomaterial. As the influence of the SO_3^- groups on the early and late osteoblastic response and the associated molecular phenomena, in the presence of important ECM and plasma proteins, remains to be understood, cell and protein data was collected. Single protein tests with BSA, Fn, Col I and Vn were conducted in the form of cell attachment, including integrin-mediated and protein binding domains adhesion, morphology, differentiation and mineralization, as well as protein conformation tests.

As Ti6Al4V disks and QCM-D sensors were used to collect information about the protein and cell behaviors. Along this section and when necessary the experiments discussion will be divided in disks and sensors.

- General Cell Behavior -

2.1 Cells Viability

The MC3T3-E1 cells viability was tested in the presence of three independent proteins, BSA, Fn and Col I, and a common protein mixture, the FBS. The cell survival rates after 4 h of culture are shown on Figure 49.

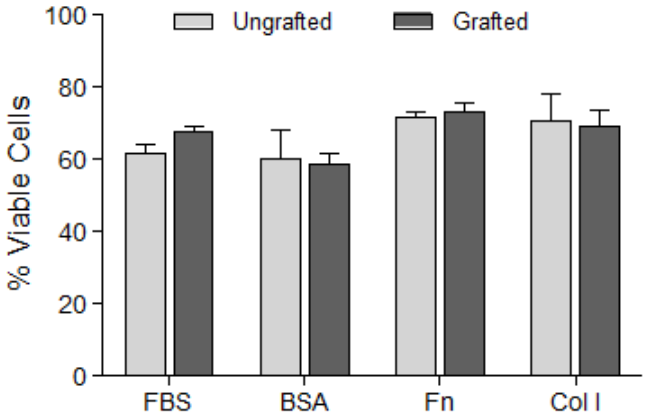

Figure 49. Percentage of viable cells attached to the ungrafted and grafted Ti6Al4V surfaces after 4 h of culture.

Data was found similar between proteins and between surface treatements (ungrafted vs grafted). The pre-adsorption of proteins had no effect on the MC3T3-E1 cells viability. Survival rates were found between 60% and 75% for the totality of the tests. The absence of superior survival rates may be an effect of the short incubation period and/or detachment of cells during processing. Equal observations were made earlier with FBS coated substrates (2nd Part, Section 1).

2.2 Spreading and Morphology

The early osteoblast-like cells spreading and morphology was acquired 30 min after incubation on ungrafted and grafted substrates, pre-adsorbed with FBS, BSA, Fn and Col I. The results are given by Figure 50. Due to the condensation of the cells biological material the intensity of the staining reagents could not be balanced and the quality of the fluorescent images was therefore limited.

As expected at this time point, round shaped cells were observed in the majority of the tested conditions. At 30 min of contact most of the cells are still initiating their interaction with the surface and therefore only small cytoplasm extensions/protrusions were detected. Interestingly, poly(NaSS) was seen to intensify cell spreading even at this time point, particularly on BSA and Fn pre-adsorbed grafted surfaces compared to ungrafted. Still, the lowest cell spreading was registered on the BSA treated substrates. Here, most of the cells cytoplasmic content was concentrated in a round formation and no focal adhesions were detected, pointing the absence of strong structural links with the surface [72,73]. To the contrary, Fn was seen to promote early cell expansion, even on ungrafted surfaces, with cells already in a more spread polygonal shape sharing many focal adhesion

points with the surfaces. These differences between cells cultured on BSA and Fn treated substrates can be explained by the specificity of the proteins. While BSA is a non-adhesive protein with little influence in the cell development, Fn is an adhesive protein known to promote osteoblastic cell attachment due to its many and important binding domains [63,233].

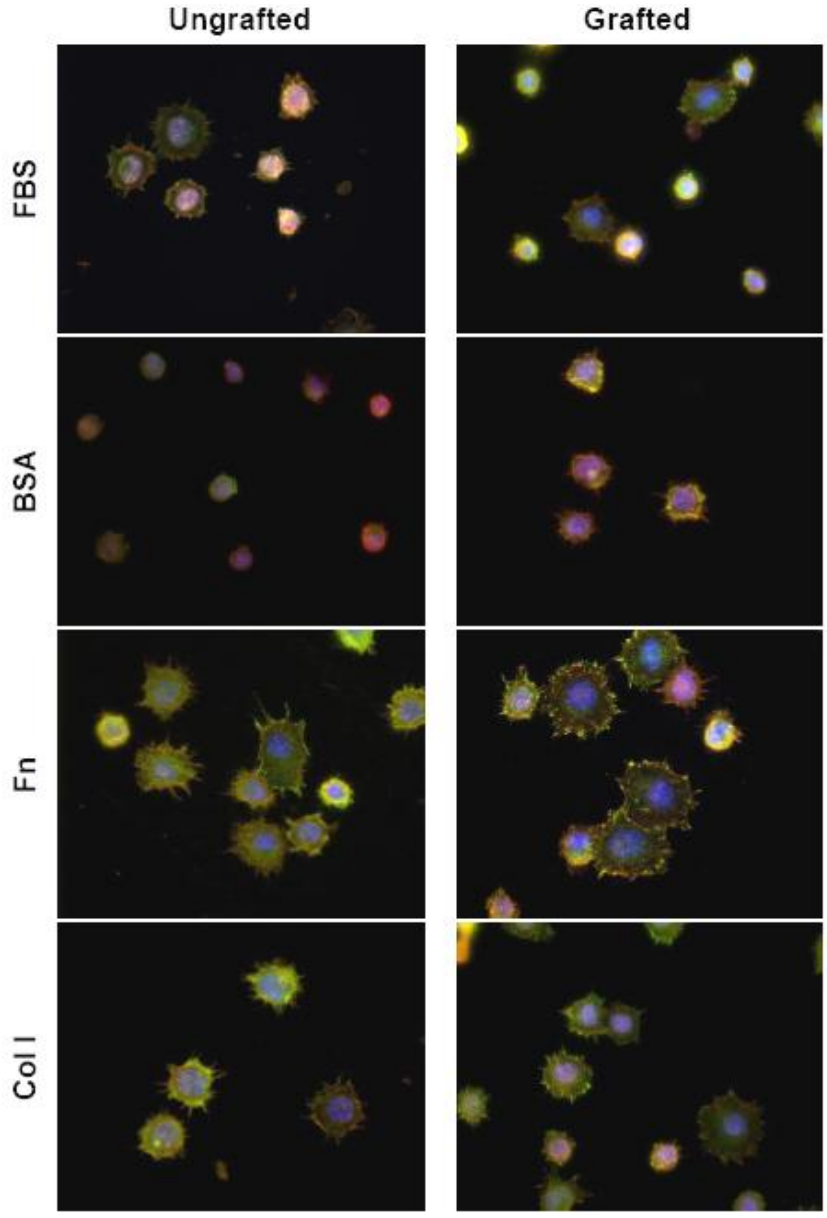

Figure 50. MC3T3-E1 cells morphology on ungrafted and grafted Ti6Al4V surfaces after 30 min of culture (50x magnification).

The MC3T3-E1 osteoblastic cells morphology was observed, as well, after 4 h of culture. This time point is referred by many as the period of maximum cell attachment [234]. Hence, in order to have a better perception of the cells

organization above the Ti alloy surfaces, the images acquired from the three staining reagents, anti-vinculin, phalloidin and DAPI (respectively focal adhesions, actin fibers and nucleus), were analyzed separately. The results are shown on Figure 51.

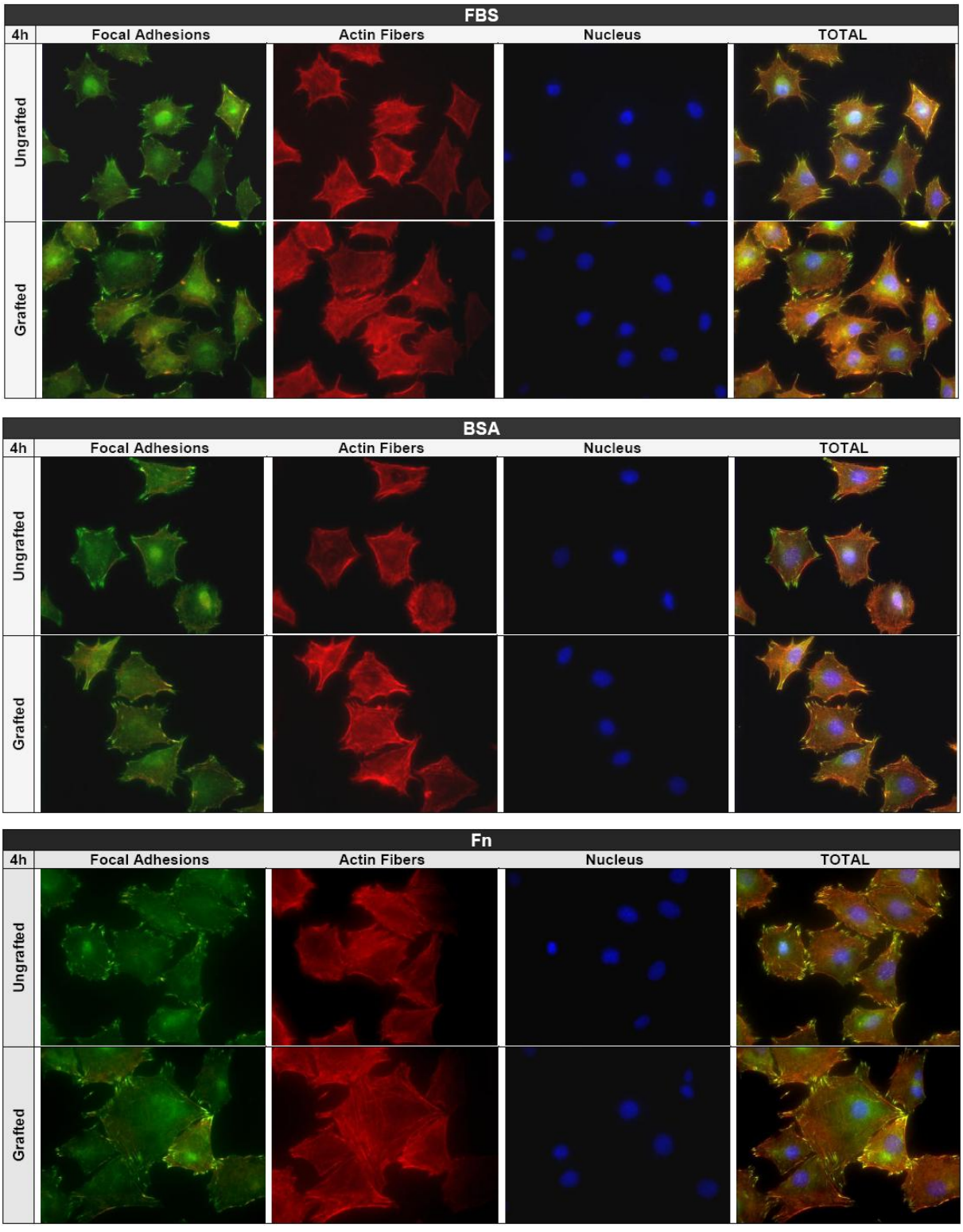

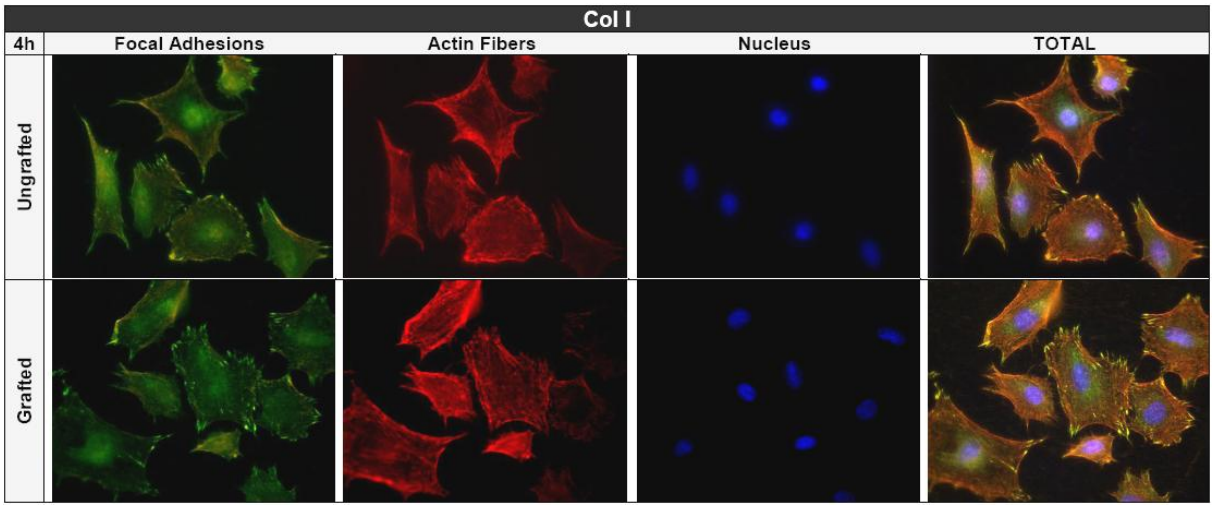

Figure 51. MC3T3-E1 cells morphology after 4h of culture on ungrafted and grafted Ti6Al4V substrates, pre-adsorbed with FBS, BSA, Fn and Col I. Focal adhesion points were stained with anti-vinculin, the actin fibers with phalloidin and the nucleus with DAPI (50x magnification).

After 4 h of culture, the MC3T3-E1 cells exhibited a well defined morphology, with an organized actin cytoskeleton, numerous focal adhesion points and a very clear nucleus, within which several organelles could be distinguished (bright blue dots). This morphology is categorized as the typical for osteoblasts [235] and was only observed in some cells cultured on Fn pre-coated substrates at 30 min of contact (Figure 50).

At 4 h, the majority of the cells were already well spread along the Ti alloy. The presence of poly(NaSS) increased the cells area and confluence, in particular when it was combined with Fn and Col I (Figure 52), representing an improvement of ≈ 19% and ≈ 15% respectively. The amount of focal adhesion points was as well influenced by the SO_3^- groups, augmenting in 1/3 its presence on Fn and Col I grafted substrates compared to ungrafted. The hydrophilic character of the surfaces is enhanced in the presence of the anionic groups of the poly(NaSS). It has been reported that biomaterials of hydrophilic nature incite more intensively cell spreading due to the increased development of focal contacts, which result from favorable protein binding [236,237]. Both Fn and Col I possess various binding regions for integrin association (main components of focal adhesions), including the RGD oligopeptide. This sequence supports integrin-mediated adhesion and by consequence regulates cell spreading and morphology [83,222]. The binding domains of the Fn molecule have been associated with osteoblastic cells attachment through various membrane receptors, $\alpha_5\beta_1$, $\alpha_2\beta_1$, $\alpha_3\beta_1$, $\alpha_4\beta_1$, $\alpha_v\beta_1$ and $\alpha_v\beta_3$. This accounts for the increasing number of focal adhesions observed [63,233].

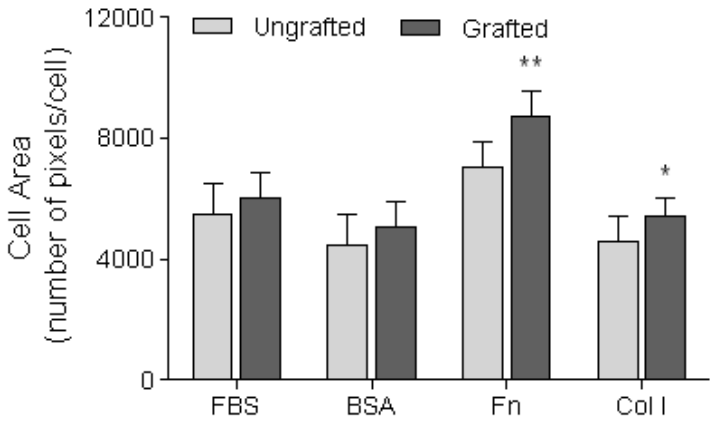

Figure 52. MC3T3-E1 cells area after 4 h of culture. Significant differences between ungrafted and grafted surfaces pre-adsorbed with the same proteins are indicated by * (*p<0.05 and ***p<0.0001).

Between all proteins BSA represented the smallest improvement in cell spreading and confluence. BSA is a non-adhesive or non-specific protein and for that reason has little influence on the cell behavior. Nevertheless, it has been shown that hydrophilic materials such as Ti can alter the conformation of BSA, increasing the exposure of its binding domains compared to hydrophobic materials such as polystyrene [93]. Here, that may be the case as the cells area is close to that registered on FBS culture conditions, where adhesive proteins like Fn or Vn can be found.

2.3 Attachment Strength

The percentage of cells that remained attached to the ungrafted and grafted surfaces pre-coated with BSA, Fn, Col I and FBS, after the application of a shear stress of 10 dyn/cm^2, is given by Figure 53. These experiments were conducted 30 min after cell seeding.

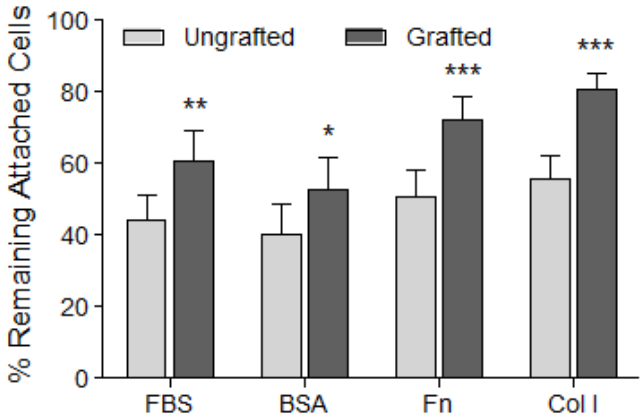

Figure 53. Percentage of cells that remained attached to the substrates after the application of a shear stress of 10 dyn/cm^2 for 15 min. MC3T3-E1 were cultured for 30 min. Significant differences between ungrafted and grafted surfaces pre-adsorbed with the same proteins are indicated by * (*p<0.05, **p<0.001 and ***p<0.0001).

The presence of poly(NaSS) on the grafted materials exerted a positive effect by increasing the resilience of the bond cell-biomaterial between 5 and 30% compared to the ungrafted, for the totality of the tested conditions. Once again, Fn and Col I displayed the highest cell numbers maintaining the cell-biomaterial bond of ≈ 75% and ≈ 81% of the attached cells, respectively. Similar percentages were obtained by Garcia et al. [238] when testing the adhesivity of osteoblast-like cells from the line ROS on bioactive glass surfaces pre-coated with Fn. In their experiments, equal culture conditions to the ones of this study were applied: 30 min incubation and 15 min shear stress of 10 dyn/cm^2. They observed that Fn adsorption increases cell adhesion strength and that BSA does not affect significantly the behavior of cells, pointing the differences in attachment to be independent from variations in non-specific interactions. The same analogies can be established with the results from Figure 53. Between all proteins, BSA registered the lowest bond strength, being only capable of sustaining the interaction of 50% of the cells, while Fn and Col I two specific and adhesive proteins impacted the most on the cells attachment strength.

As pointed earlier, the chemistry of the SO_3^- groups plays a major role on protein adsorption. It can affect the orientation, the conformation and the amount of the adsorbed protein but most importantly the type of protein that adsorbs. Previous studies have shown the enhanced affinity of the bioactive polymer to adhesive proteins, such as Fn, over BSA [216,220,221]. Moreover, it has been shown that detachment of cells on Fn pre-coated surfaces occurs at the cell-Fn junction and not

at the Fn-substrate interface, ruling out the possibility that differences in cell adhesion arose from differences in adsorption strength between Fn and the underlying substrate [238,239]. Therefore, the preference for these type of proteins at the interface conditions in an important way the cell behavior, explaining the results acquired.

Fn and Col I possess various binding sites for cell attachment, including the heparin binding domains and the RGD sequence [77,78,82]. These regions are known to offer strong adhesion points that support cell expansion above the surface, creating an environment compatible with osteointegration [83,222]. This way, the connection created is more difficult to break. These observations are consistent with the cell morphologies from Figure 51.

2.4 Proliferation

The cell proliferation curves on ungrafted and grafted Ti6Al4V materials were followed from 30 min to 14 days of incubation. The results are shown on Figure 54.

For the majority of the time points no statistical differences were detected between cell proliferation rates on ungrafted and grafted substrates, as expected [240]. However, it is noticeable that the number of cells increased substantially with time, especially on the Fn pre-coated surfaces. In these conditions, it was even detected a significant cell improvement over the ungrafted surfaces at day 14. The combined effect of the anionic groups from the poly(NaSS) with the Fn molecule has again proven its value. According to Garcia et al. [222] the presence of RGD motifs can greatly increase the integrin-mediated interactions which support adhesion, proliferation and differentiation *in vitro*.

These results confirm our morphology and attachment strength analyses and provide more information about the Fn influence on the initial cell development.

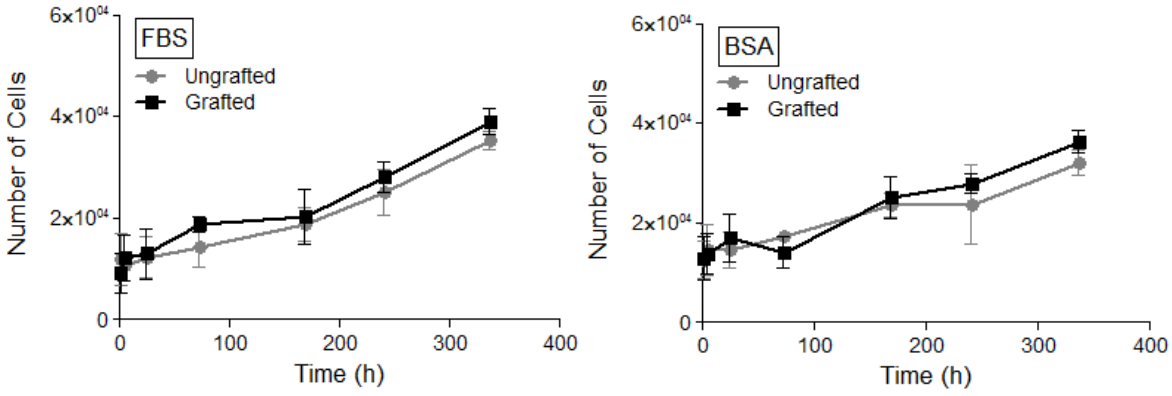

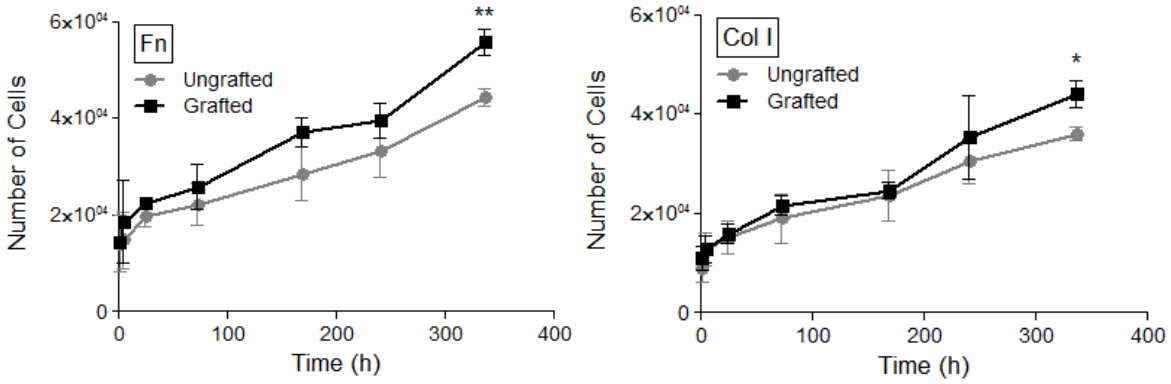

Figure 54. Evolution of the MC3T3-E1 osteoblastic cells number on ungrafted and grafted surfaces, pre-adsorbed with FBS, BSA, Fn and Col I, from 4 h to 14 days of culture. Significant differences between ungrafted and grafted surfaces pre-adsorbed with the same proteins are indicated by * (*p<0.05 and **p<0.001).

2.5 Differentiation and Mineralization

ALP is an early marker of the osteoblasts differentiation relating to the production of a mineralized matrix. It is an enzyme present in the cellular membrane capable of releasing phosphate ions to the ECM that interact with the pre-existing calcium ions, leading to the matrix mineralization (precipitation of calcium phosphate) [164]. In this experiment, the ALP activity was followed from 7 to 28 days of culture on ungrafted and grafted substrates pre-adsorbed with FBS, BSA, Fn, Col I and BMP-2. As the highest metabolic activity, consistent with the beginning of the ECM formation, was registered at day 14, only those values were statistically treated and shown on Figure 55.

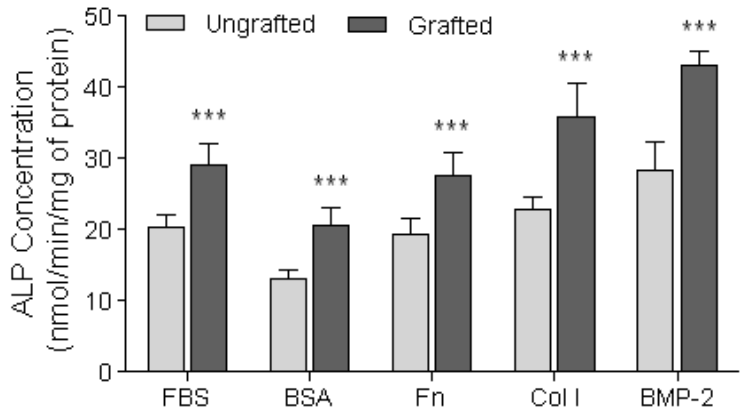

Figure 55. ALP concentration after 14 days of culture. Significant differences between ungrafted and grafted surfaces pre-adsorbed with the same proteins are indicated by * (***p<0.0001).

The ALP concentrations before and after day 14 were lower than those registered at that time point. This occurs because at the beginning of the MC3T3-E1

cells development, proliferation is the dominant phase, while after day 14 the ALP concentration decreases in response to the ECM mineralization [241].

The ALP production was significantly enhanced by the poly(NaSS) grafting, which suggests the SO_3^- groups to accelerate the osteoblastic cells differentiation sequence most likely through a surface-protein mediated mechanism [242]. In a previous research, Mayingi et al. [172] have shown that the poly(NaSS) grafted onto CP Ti substrates can improve the ALP production by 19%, in the presence of FBS proteins, compared to ungrafted. Here, in the same conditions, we experienced an improvement of ≈ 31%, thus confirming the validity of our results and the improvement of the grafting process.

El Khadali et al. [166] by following the response of fibroblastic cells on poly(NaSS) functionalized PMMA substrates determined that the ionic distribution of the SO_3^- groups above the surface was in a certain way random. It was seen that the arbitrary organization of the bioactive groups modulated the cell response, including differentiation, by means of specific protein adsorption. The same analogy can be applied here. In the presence of adhesive proteins, Fn and Col I, the ALP activity was significantly enhanced compared to BSA, a non-specific protein. As the polymer distribution is not entirely homogeneous, the grafted material generates an environment compatible with “specialized” protein adsorption, favoring Fn and Col I. The proteins are allowed to adsorb by adapting their conformation and, through that, increasing the exposure of their binding sites. The cells that reach the surface of the biomaterial interact directly with these sites responding accordingly to the signals received, in this case by boosting the cells differentiation. Besides, the cell spreading and adhesion strength has been shown to favor the MC3T3-E1 cells differentiation and mineralization [164].

The SO_3^- groups allowed for an improvement of ≈ 28% on the Fn and of ≈ 34% on the Col I pre-adsorbed surfaces. In regard to the BMP-2 growth factor, the functionalized surfaces improvement over the untreated Ti6Al4V was of ≈ 35%. Between all proteins, this was as well the one that stimulated the most ALP production. The BMP-2 is one of the most potent bone forming agents available. It can accelerate osteoblast differentiation and stimulate the expression of bone matrix proteins, such as Col I, BSP, OPN and even Fn [97,243]. Lai et al. [98] by following the influence of BMP-2 on human osteoblasts (HOBs), and inherent integrin functions, demonstrated that this growth factor increases the levels of $\alpha_v\beta$ and $\alpha\beta_1$

integrins on the cell surface. Moreover, they showed that the BMP-2 receptors overlap with these integrins in osteoblasts and that possible disturbs on their functions can retard significantly the matrix mineralization. Their research suggests that the $\alpha_v\beta$ and $\alpha\beta_1$ receptors modulate cell differentiation and mineralization by regulating the BMP-2 activity. Since poly(NaSS) increases the protein binding sites for integrin adhesion, it is conceivable the combination of the SO_3^- groups with the BMP-2 to provide a stimulant environment for cell differentiation and therefore explaining the increased production of ALP.

As the MC3T3-E1 cells differentiation is enhanced by the grafted material it is expected the mineralization to be favored as well. The calcium and phosphate productions were assessed after 28 days of culture. The results are shown in Figure 56 (in reason of the its cost the BMP-2 was not considered in the mineralization experiments).

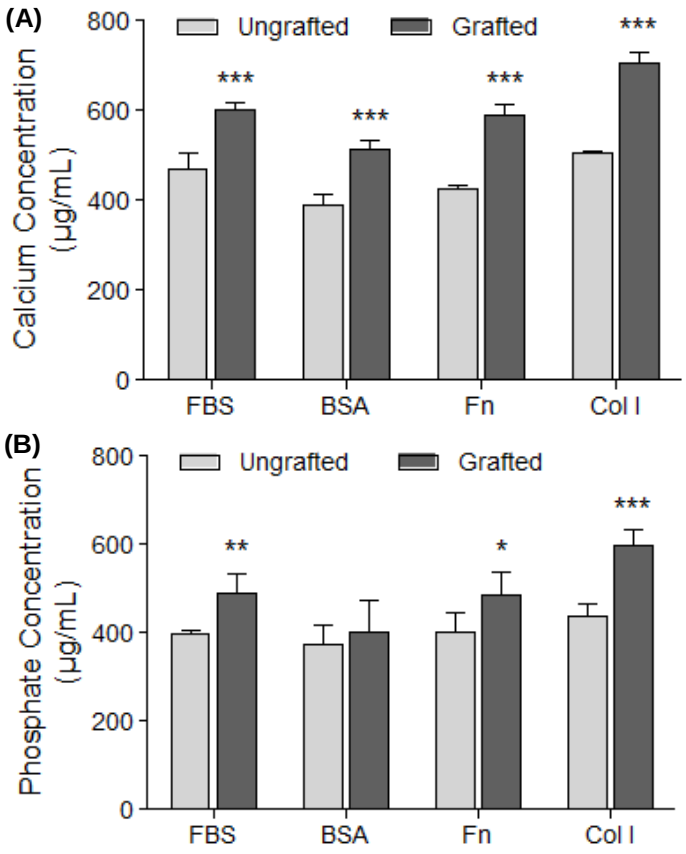

Figure 56. (A) Calcium and (B) phosphate production after 28 days of culture. Significant differences between ungrafted and grafted surfaces pre-adsorbed with the same proteins are indicated by * (*p<0.05, **p<0.001 and ***p<0.0001).

Calcium and phosphate are markers of the late differentiation of osteoblasts, more precisely the mineralization. As happened for the ALP, the amount of calcium and phosphate increased on all functionalized substrates compared to ungrafted Ti6Al4V. On calcium, the improvements were registered between 22%, with the exception of Col I that accounted for an improvement of ≈ 28%. This same protein was found to have an important influence over the phosphate production, increasing its levels above all the other tested proteins and by raising its production in ≈ 27% compared to untreated substrates. Such observations suggest that the mineralization was not only influenced by the poly(NaSS) but as well by the protein adsorbed.

Col I is known to activate specific signaling pathways that affect the expression of bone cell phenotypes associated to the ECM formation and maturation [244,245]. Furthermore, the supplemented medium (β-glycerophosphate and ascorbic acid addition) is considered an instigator of osteogenic markers expression, which includes Col I the main component (≈ 80%) of the organic cell matrix [246,247]. Rezania et al. [248] has even shown that the mineralization at the bone-substrate interface can be accelerated by the “attraction and immobilization” of amino acid sequences of important ECM proteins, like Col I, responsible for regulating adhesion and differentiation of bone-derived cells. Therefore, the exposure of the Col I binding domains as product of the poly(NaSS) grafting may be behind the results from Figure 56.

- Interface Cell-Biomaterial -

In this segment we discuss the interactions between cell and biomaterial by means of protein binding and integrin association. The information was recovered from disks and sensors and by that reason two subsections were defined.

2.6 Disks

At the interface, cells contact with the protein layer rather than with the surface of the substrate. Hence, to understand the impact these molecules have on the MC3T3-E1 cells development, cultures of 30 min and 4 h were prepared. Evaluations were conducted by blocking important binding domains of proteins and integrin receptors from the cellular membrane, and the osteoblast-like cells morphology (4 h), attachment (4 h) and attachment strength (30 min) were determined on:

1) Disks pre-coated with Fn:
    a) N-Terminal blocked;
    b) RGD Peptide blocked;
    c) C-Terminal blocked;
    d) Integrins $\alpha_5\beta_1$ blocked.
2) Disks pre-coated with Col I:
    a) Integrins $\alpha_2\beta_1$ blocked.
3) Disks pre-coated with Vn:
    a) Integrins $\alpha_v\beta_1$ blocked.
4) Disks pre-coated with the RGD peptide.

2.6.1 Spreading and Morphology

The processes by which cells become established upon a surface involve initial attachment and cellular spreading. The molecules involved in this task include the ECM proteins, transmembrane receptors from the cell membrane, and intracellular cytoskeleton components, like focal adhesions [249]. Thus, to better understand the interaction between surface-protein-cell and the effect each one of these components has in the cells initial spreading, MC3T3-E1 cells were cultured on ungrafted and grafted materials and their morphology analyzed.

Fn is one of the ECM proteins with the biggest impact in cell adhesion and for that reason its structure has been extensively studied [77,78,82]. The main binding regions responsible for cell attachment in Fn are the HB domains, the synergy peptide PHRSN, which stabilizes the RGD-integrin interactions and preserves its specificity, and the central adhesive peptide RGD [77,237]. Due to its importance to cell attachment, we decided to block the HB domains (N-Terminal and C-Terminal) and the RGD peptide on the Fn molecule with monoclonal antibodies and observe the changes they introduced in the cell morphology in comparison to unblocked Fn. The results are shown on Figure 57.

For the totality of the tested conditions, the amount of cells detected (visually) was reduced in comparison to the unblocked Fn. This is to be expected since these binding domains represent important areas for integrin association, the main and best characterized receptor that cells use to both bind and respond to the ECM stimuli. By blocking these regions, recognition of the integrins $\alpha_5\beta_1$, $\alpha_2\beta_1$, $\alpha_3\beta_1$, $\alpha_4\beta_1$, $\alpha_v\beta_1$ and $\alpha_v\beta_3$ (all viable alternatives known to support osteoblastic cells attachment)

is reduced [63] and therefore less cells are capable of attaching. Regarding its morphology, all cells exhibited a polygonal shape, some with more cytoplasm extensions than others, but all with abundant bundles of actin fibers within its structure.

Fn is also known to induce the reorganization of actin microfilaments to promote cell adhesion and spreading, which in turn affects cell morphology and migration [250,251]. According to Figure 57, cell organization, by means of cytoplasm expansion and amount of focal adhesions, is inhibited by the presence of the monoclonal antibodies. Table 19 provides evidences to this statement.

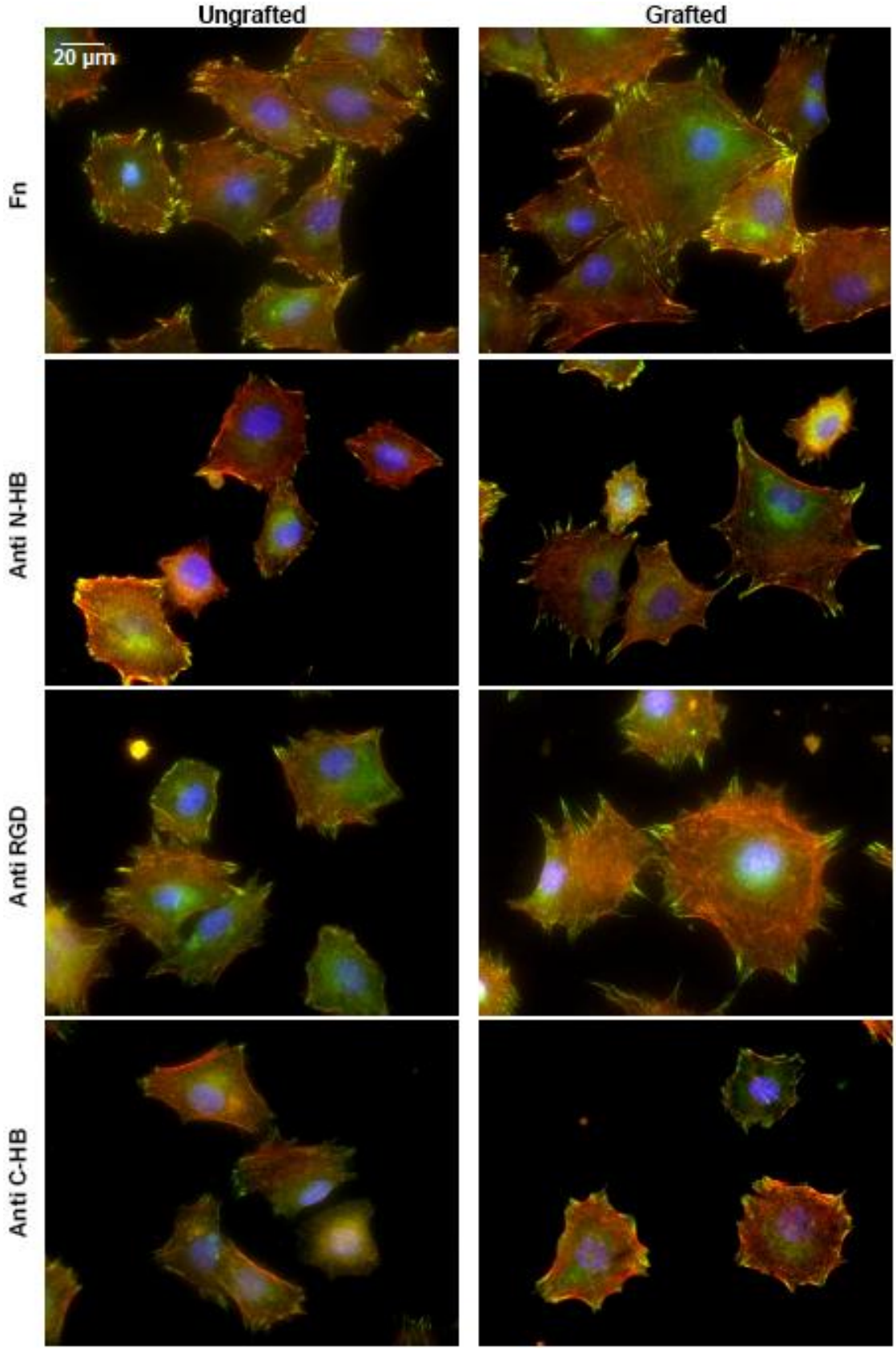

Figure 57. MC3T3-E1 cells morphology on ungrafted and grated surfaces pre-coated with Fn, after 4 h of culture. The N-Terminal and C-Terminal HB domains and the RGD peptide were blocked using monoclonal antibodies (50x magnification).

Table 19. Percentage of inhibition in cell spreading and focal adhesions by cells cultured on blocked Fn (N-HB, RGD and C-HB binding regions) relatively to unblocked Fn.

% to unblocked Fn	Spreading (%)		Focal Adhesions* (%)	
	Ungrafted	Grafted	Ungrafted	Grafted
Anti N-HB	11.2 ± 6.4	14.4 ± 8.7	36.8	25.2
Anti RGD	15.3 ± 5.0	10.9 ± 3.3	29.5	19.3
Anti C-HB	9.4 ± 2.1	20.4 ± 1.5	58.4	36.9

* These results should be perceived as approximations since only manual measurements, using 3 images per condition and equal amount of cells, were conducted. The cell analysis software used did not possess this tool.

The MC3T3-E1 cytoplasm expansion and amount of focal adhesions were considerably conditioned by the presence of the antibodies (Table 19). Interestingly, the cells cultured on poly(NaSS) grafted surfaces experienced a more intensive inhibition on cytoplasm expansion than the cells cultured on the ungrafted, when compared with the results from the surfaces pre-adsorbed with unblocked Fn. The opposite situation was detected in regard to the amount of focal adhesions. These observations suggest that the blocking of each one of the 3 selected binding regions on the Fn molecule slows down the cell migration and spreading above the grafted substrate, presumably as product of new chemical bonds being generated between other binding domains available and the cell receptors. Due to their diversity of structures, the same integrin molecule can bind to various ligand or binding sites. Its specificity is determined by the ECM domain of integrins that recognizes diverse matrix ligands [72,73]. For that reason, when the protein adapts a new conformation in response to the SO_3^- groups, less focal adhesions may be lost but more time may be required for the connections to be established, conditioning simultaneously cell expansion. Nevertheless, it is important to refer that for the majority of the cases the area of the osteoblast-like cells cultured on the grafted substrates was superior to that observed on the ungrafted (Figure 58).

Another interesting aspect to be pointed from these results is the importance of the C-HB to the cells early attachment. Yamada et al. [252] has shown that the C-HB exhibits higher affinity to cellular proteoglycans than the N-HB, therefore explaining the increased effect of this domain on the cells morphology, size and focal adhesions. The same was observed by Latz et al. [218] on poly(NaSS) functionalized PMMA surfaces.

Differences in cell morphology, namely formation of focal adhesions, between binding domains can result from the specificity of the mechanism of cell attachment.

On the RGD-motifs the cell attachment mechanism is integrin-mediated, whereas the attachment to HB domains can be both electrostatic or integrin-based [248].

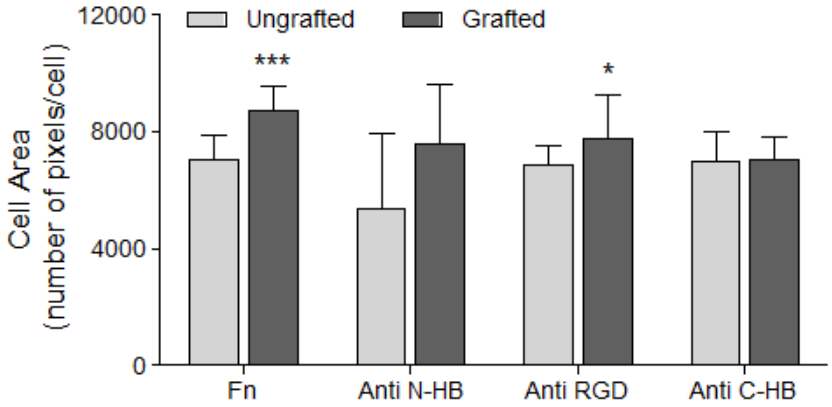

Figure 58. MC3T3-E1 cells area on surfaces pre-adsorbed with unblocked and blocked Fn (N-HB, RGD and C-HB), after 4 h of culture. Significant differences between ungrafted and grafted surfaces pre-adsorbed with the same proteins are indicated by * (*p<0.05 and ***p<0.0001).

The RGD peptide is a widely occurring arginine-glycine-aspartate amino acid sequence with an important effect on the osteoblast-like cells early attachment. Because of its superior physiological stability, its adsorption and immobilization onto Ti-based surfaces has become a recurrent technique to improve cell attachment [145]. In this experiment, we adsorbed the RGD peptide onto ungrafted and grafted Ti6Al4V and followed the osteoblastic cells morphology after 4 h of culture. The results are shown on Figure 59.

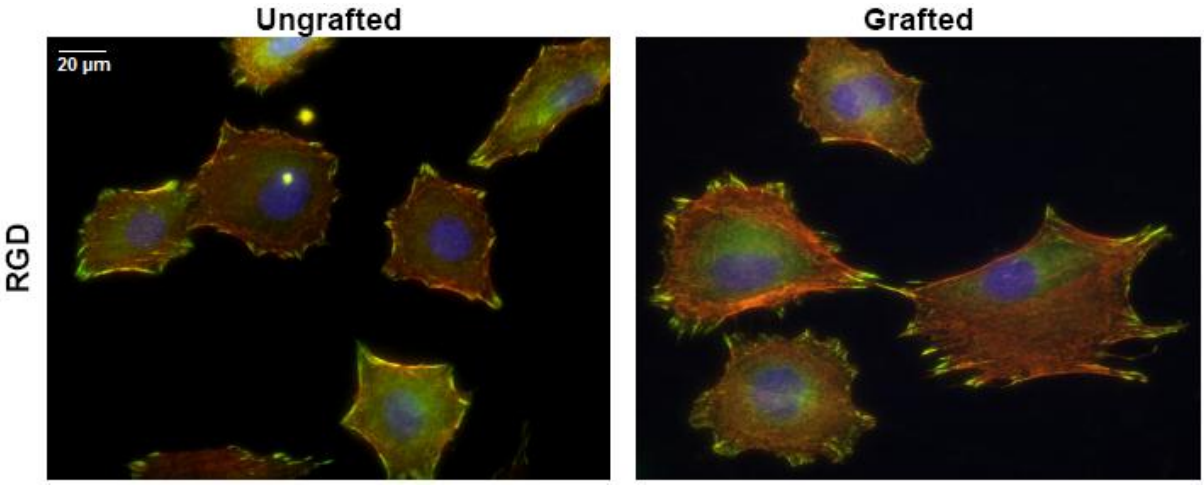

Figure 59. MC3T3-E1 cells morphology on ungrafted and grafted Ti6Al4V surfaces pre-coated with the RGD peptide, after 4 h of culture (50X magnification).

The RGD sequence is recognized by various integrin receptors from the osteoblastic cells. For instance, 9 different integrins can bind to Fn and its recognition is mainly done through the central cell-binding sequence, the RGD motif [74,75]. For that reason, many focal adhesion points were detected on both ungrafted and grafted surfaces. Though poly(NaSS) increased in ≈ 17% the amount of focal contacts, it was in the cell expansion that its influence was the most remarkable. Cells doubled in size and longer cytoplasmic extensions were observed.

In contrary to what was expected, a smaller amount of cells was observed (visual) on these treated surfaces compared to ungrafted and grafted Ti6Al4V pre-adsorbed with Fn. This could be explained by the fact that RGD is only a small peptide from the Fn molecule. It has been shown that the affinity of integrins to short RGD-containing peptides to vary significantly from integrin to integrin [253,254]. On the other hand, studies have demonstrated an increased affinity by all cell receptors to larger protein fragments or the intact protein (containing the RGD sequence), indicating that other domains closer to the RGD contribute significantly to the contact between ligands and integrins. The amino acid sequence PHSRN that works in synergy with the RGD motif has been identified as the main stabilizer of the integrin adhesion at the RGD site. This peptide has been recognized as the activator of the ECM domain of important integrins, such as the $\alpha_5\beta_1$ heterodimer, determining its specificity [255-257]. Thus, it is possible that the interactions established on the RGD pre-adsorbed surfaces are not as stable as the ones on the Fn coated substrates, hindering cell expansion.

The MC3T3-E1 cells morphology was also followed in the presence of antibodies against specific integrins, $\alpha_5\beta_1$, $\alpha_2\beta_1$ and $\alpha_v\beta_1$. Ungrafted and grafted surfaces pre-coated with Fn, Col I and Vn were tested. The results after 4 h of culture are given by Figure 60.

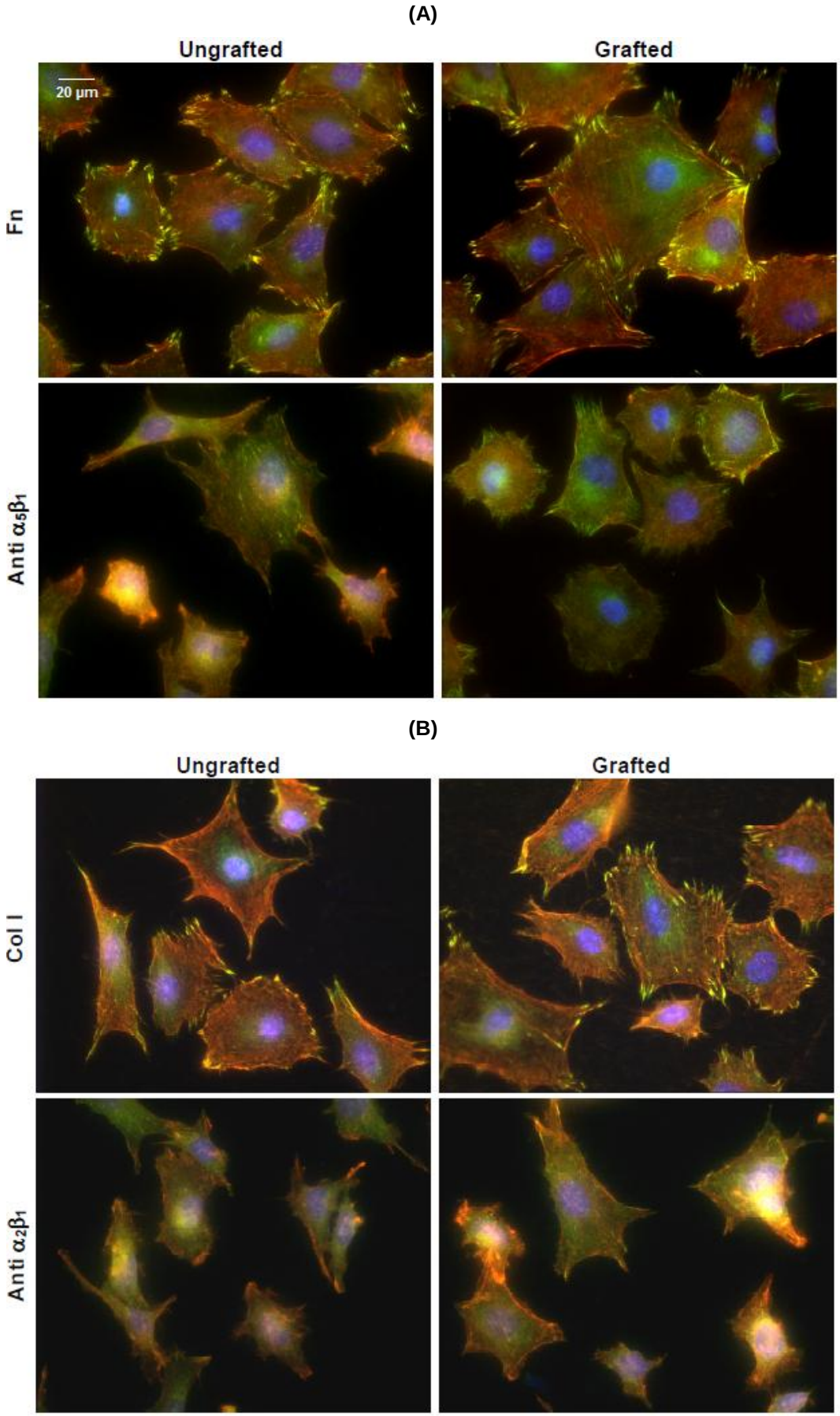
(A)
Ungrafted
Grafted
20 µm
Fn
Anti α5β1
(B)
Ungrafted
Grafted
Col I
Anti α2β1

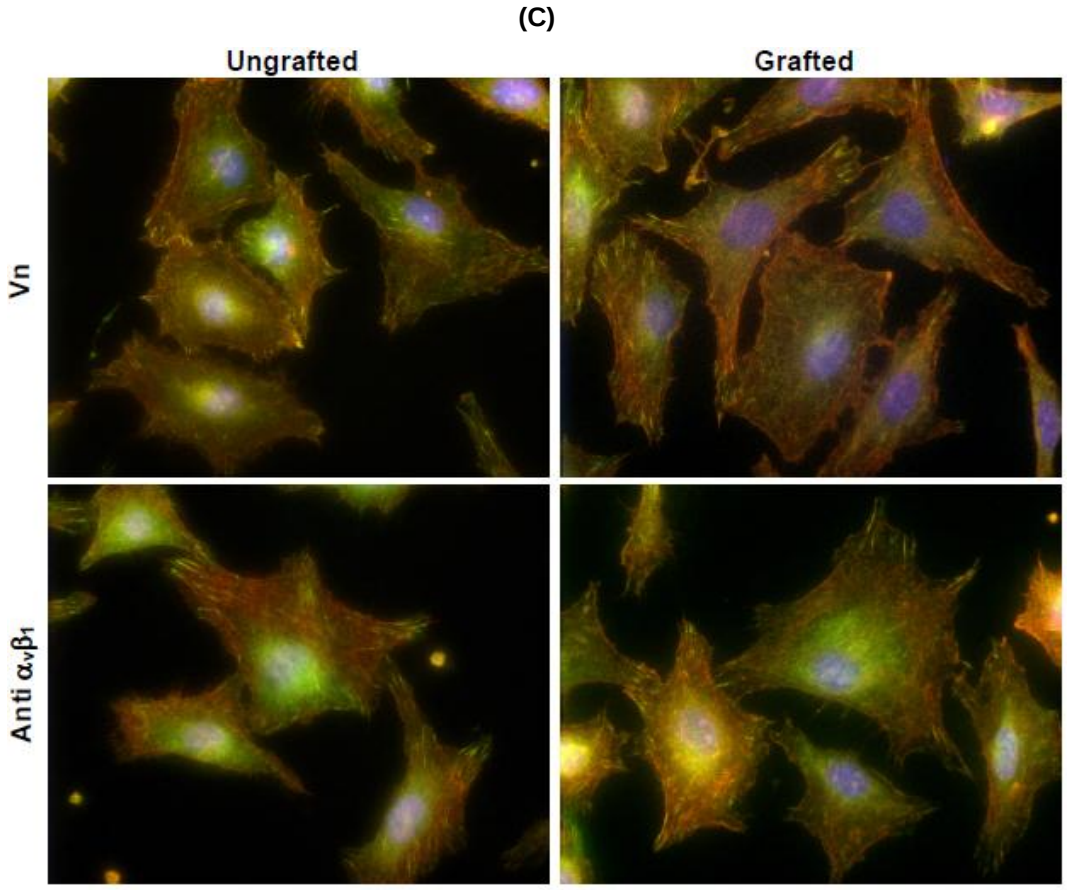

Figure 60. MC3T3-E1 cells morphology on ungrafted and grafted Ti6Al4V pre-adsorbed with (A) Fn, (B) Col I and (C) Vn. Antibodies against the integrins (A) $\alpha_5\beta_1$, (B) $\alpha_2\beta_1$ and (C) $\alpha_v\beta_1$ were applied (50X magnification).

The osteoblastic cells morphology was strongly influenced by the presence of the anti-integrins. In Figure 60A, cells experienced an important reduction in size and in actin bundle of fibers (cells with weak staining). By blocking the integrin $\alpha_5\beta_1$, some of the cells lost their identity as osteoblasts and became more elongated, the typical fibroblastic morphology. This was noticed preferentially on ungrafted substrates. On the grafted, the majority of the cells still exhibited a polygonal shape although cytoplasmic expansion was significantly reduced (Table 20). The amount of focal adhesions was as well diminished on these substrates. The same was seen for the Col I treated substrates (Figure 60B). The use of the anti-integrin $\alpha_2\beta_1$ induced a significant reduction in actin cytoskeleton but, most importantly, in focal adhesion points.

Cells cultured on grafted surfaces pre-coated with Fn and Col I were capable of sustaining better the cells cytoskeleton than the ungrafted. While on the grafted the antibodies caused a size reduction between 46% and 37%, respectively Fn and Col I, on the ungrafted it was near 51% for both. These results confirm the

importance of the heterodimers $\alpha_5\beta_1$ and $\alpha_2\beta_1$ for the integrin-mediated attachment of cells to Fn and Col I proteins. In many researches, these integrins have been indicated as the most important for cell binding to these proteins [235,236]. Interestingly, when it comes to the amount of focal adhesion points the ungrafted surfaces were found to sustain more of these connections than the grafted. On the grafted materials, the presence of the antibodies caused a reduction in ≈ 75% and ≈ 91%, respectively Fn and Col I. Once again, we perceive the impact of the poly(NaSS) on the cells behavior. The results state without doubt the cell adhesion to be mediated by integrin binding and that to be preferably made through the integrins $\alpha_5\beta_1$ and $\alpha_2\beta_1$ on Fn and Col I. These observations provide significant evidence of the protein conformational changes as product of the SO_3^- groups of the poly(NaSS).

On the Vn pre-coated surfaces (Figure 60C), cells were well spread and confluent. Many focal adhesion points were observed and the actin cytoskeleton was well organized. Here, the action of the anti-integrin $\alpha_v\beta_1$ was not as effective as the antibodies used on the Fn or Col I coated substrates. The morphology of the cells experienced little change (insignificant decrease in size), maintaining their polygonal and well spread structure. Regarding the development of focal adhesions, only a small decrease was perceived, less than 20% on both ungrafted and grafted materials. Interestingly, these integrins appear to have more impact on the ungrafted surfaces than on the grafted. This may be explained by the specificity and preferable recognition of other integrins by the Vn molecule when in contact with poly(NaSS). As pointed several times along this work, poly(NaSS) is capable of changing the proteins conformation favoring some protein binding sites over others. Perhaps here, like for Fn and Col I, poly(NaSS) allows more cells to bind to Vn using the integrin $\alpha_v\beta_3$, its most more common and important receptor [63].

Table 20. Percentage of inhibition in cell spreading and focal adhesions by cells cultured with anti-integrins ($\alpha_5\beta_1$, $\alpha_2\beta_1$ and $\alpha_v\beta_1$) relatively to cells cultured in unblocked conditions.

% to unblocked Fn, Col I and Vn (respectively)	Spreading (%)		Focal Adhesions* (%)	
	Ungrafted	Grafted	Ungrafted	Grafted
Anti $\alpha_5\beta_1$	52.2 ± 15.1	44.5 ± 4.6	65.4	74.7
Anti $\alpha_2\beta_1$	49.8 ± 10.3	36.9 ± 5.7	83.2	91.0
Anti $\alpha_v\beta_1$	0.4 ± 0.0	3.0 ± 0.3	18.3	15.6

* These results should be perceived as approximations since only manual measurements, using 3 images per condition and equal amount of cells, were conducted. The cell analysis software used did not possess this tool.

The enhanced formation of focal adhesions by osteoblasts plated on grafted surfaces pre-coated with Fn, Col I and Vn proteins suggest that the pre-coating of Ti6Al4V substrates with ECM molecules may be a good incentive to osteointegration, in particular when combined with the bioactive poly(NaSS).

2.6.2 Attachment

The attachment of cells on differently treated surfaces in the presence and absence of anti-binding domains and anti-integrins is shown on Figure 61.

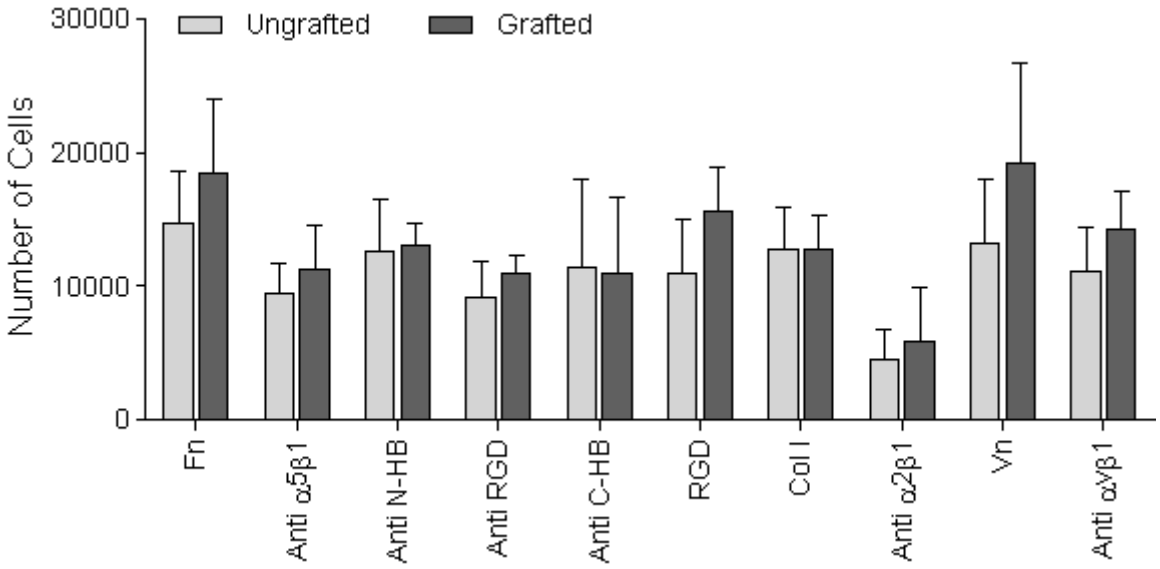

Figure 61. MC3T3-E1 cells attachment on ungrafted and grafted substrates pre-adsorbed with Fn, Col I and Vn, after 4 h of culture. Antibodies against binding domains of Fn (N-HB, RGD and C-HB) and integrins ($\alpha_5\beta_1$, $\alpha_2\beta_1$, $\alpha_v\beta_1$, respectively Fn, Col I and Vn) were used.

For the majority of the conditions, poly(NaSS) was found to induce a slight increase in the MC3T3-E1 numbers. However, it was not significant.

Fn and Vn stimulated significantly the osteoblastic attachment and proliferation, above Col I and the RGD site ($p<0.05$). These two ECM proteins are very adhesive, and have proven their impact in the early cell attachment in many occasions [249]. The amount of cells attached was reduced by the presence of the anti-binding regions and the anti-integrins, as expected. Their effect was the most significant on the Col I surfaces using the $\alpha_2\beta_1$ anti-integrin. These observations confirm the importance of the $\alpha_2\beta_1$ integrin for cell attachment to Col I surfaces. Our morphological examinations corroborate these results.

2.6.3 Attachment Strength

The adhesivity of the cell-biomaterial bond was put to test after 30 min of contact by applying a shear stress of 10 dyn/cm^2. MC3T3-E1 osteoblast-like cells were cultured on Fn, Col I and Vn adsorbed Ti6Al4V and their adhesivity was tested in the presence and absence of anti-binding domains and anti-integrins. The results on ungrafted and grafted surfaces are shown on Figure 62.

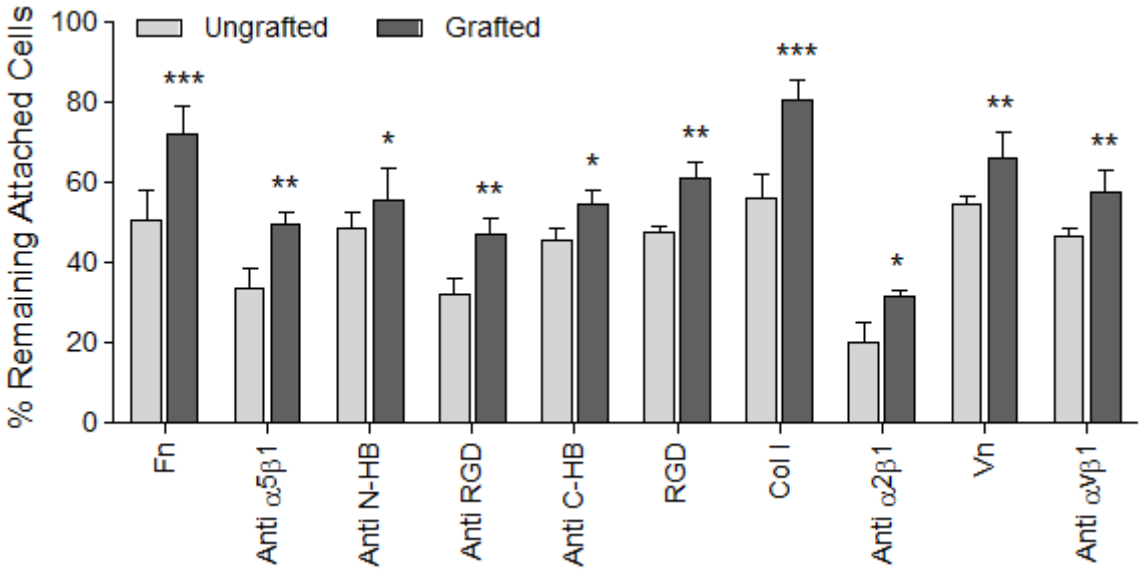

Figure 62. Percentage of cells that remained attached to the substrates after the application of a shear stress of 10 dyn/cm^2 for 15 min. MC3T3-E1 were cultured for 30 min. Significant differences between ungrafted and grafted surfaces pre-adsorbed with the same proteins are indicated by * (*p<0.05, **p<0.001 and ***p<0.0001).

The resilience of the bond cell-biomaterial was highly improved by the SO_3^- groups of the poly(NaSS), for the totality of the tested surfaces. Fn and Col I pre-coated on the grafted substrates promoted a bond so strong that only 20-25% of the cells were lost during stress.

The antibodies used against the HB domains and the RGD sequence reduced the adhesivity of cells in ≈ 55% and ≈ 47%, respectively, for the grafted material and ≈ 46% and ≈ 32%, respectively, for the ungrafted. It seems that by blocking the central adhesive site of Fn (RGD), the structural link that sustains the cells on the surface is highly challenged. Rezania et al. [248] has shown that cells attach preferentially through integrins onto the RGD sequence, while electrostatic interactions tend to take place on the HB domains. It may be possible that the connections made at the HB terminals are not as strong as the ones that take place at the RGD site.

Regarding the anti-integrin tests, the information acquired shows the importance of the $\alpha_5\beta_1$ integrin ($p<0.0001$) in the osteoblastic attachment to the Fn protein. It is also clear this integrin-mediated attached to be favored in the presence of poly(NaSS). The same is perceived with the anti-integrin $\alpha_2\beta_1$ on the Col I treated surfaces. This integrin enhances significantly ($p<0.0001$) the cells attachment strength to Col I, promoting it above all the other tested proteins. The chemistry of the SO_3^- groups plays a major role on protein adsorption. It can affect the orientation, the conformation and the amount of the adsorbed protein. In this particular case, poly(NaSS) stimulates the exposure of active binding sites in the Col I structure highly recognized by this integrin. Regarding the integrin $\alpha_v\beta_1$, its effect on the cell attachment to Vn was slightly reduced in comparison with the Fn or Col I integrins. Its influence was still remarkable ($p<0.05$), however the results suggest other integrins may have more impact on the adhesivity of the osteoblastic cells.

The morphology results confirm the previous statements.

These evaluations show that the grafting of SO_3^- groups onto Ti6Al4V substrates can favor the adhesion of cells that are capable of resisting detachment under stress conditions.

2.7 Sensors

In this segment we continue the discussion on the protein adsorption and the changes they induce in the cell behavior when protein binding domains or important integrins of the cell membrane are blocked. The QCM-D technique was applied to measure mass changes and four surfaces were tested: Ti6Al4V, poly(NaSS) physisorbed sensors, gold (standard for QCM-D testing) and poly(DTEc).

2.7.1 Cell Attachment

The attachment of MC3T3-E1 cells, after 2 h of culture, onto a poly(NaSS) coating is compared with those onto uncoated Ti6Al4V, gold, and poly(DTEc) surfaces in Figure 63A. These experiments were carried out in the presence of 10% FBS supplemented medium (MEM-α) (control) and with pre-adsorbed proteins, BSA, Fn and Col I. Here, the use of FBS containing medium during cell attachment had minimal effect in the outcome of the experiments, since the FBS proteins were blocked by 1% BSA solution as demonstrated in Figure 63B.

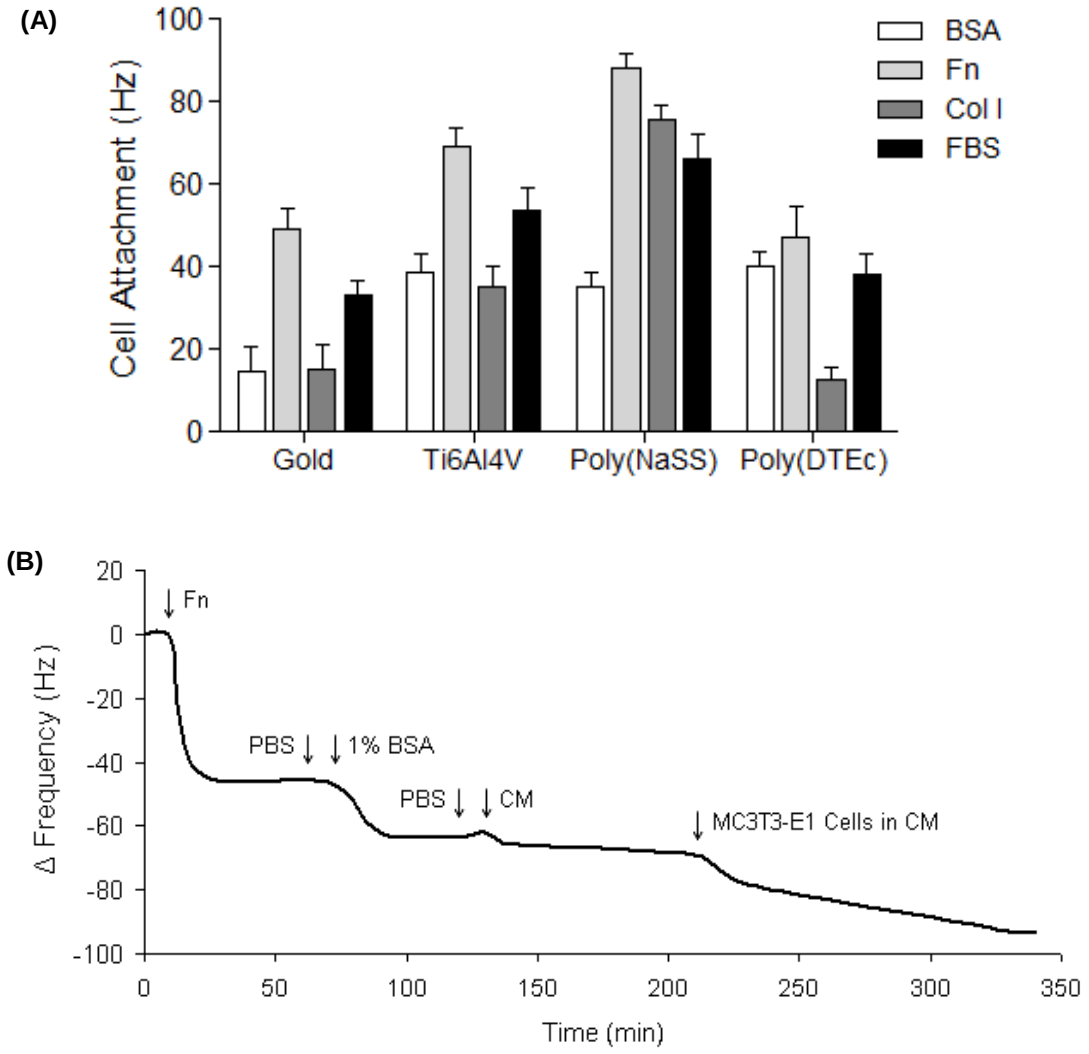

Figure 63. (A) MC3T3-E1 cells attachment (2h, 37°C) onto Ti6Al4V, Ti6Al4V physisorbed poly(NaSS), gold, and poly(DTEc) sensors pre-adsorbed with FBS, BSA, Fn and Col I, under static conditions. (B) Pattern of frequency shift during cell attachment tests in static conditions. Though the image represents the cell attachment on gold sensors pre-adsorbed with Fn, all sensors behaved similarly with the 3 proteins (CM = complete medium or MEM-α supplemented with 10%FBS).

The FBS columns in Figure 63A show that under the conditions of the experiment the cell attachment is better on poly(NaSS) coating than on uncoated Ti6Al4V and the other substrates. This result is in agreement with previous studies in which poly(NaSS) was found to promote the attachment of osteoblastic cells onto Ti based substrates [173] and with the results discussed in earlier sections. Most interestingly, the attachment of the cells onto poly(NaSS)-coated substrates remains high even when Fn and Col I are pre-adsorbed onto the substrate prior to cell exposure, while BSA inhibits the cell attachment. Interestingly, Col I pre-adsorbed surfaces displayed the lowest cell attachment rates with the exception of poly(NaSS) coated sensors. Moreover, Fn increased the cell attachment for all substrates. This is

expected, since Fn is known to promote cell attachment because of the role of its RGD sequence in the integrin-mediated recognition processes [222]. Furthermore, the RGD sequence is found in Col I as well, but not in BSA [236]. This finding was further investigated by studying the interplay of protein adsorption and the potentially RGD/integrin dependent mechanism.

2.7.2 Protein Adsorption

To better understand the cell attachment results, the adsorption of BSA, Fn and Col I onto physisorbed poly(NaSS), uncoated Ti6Al4V, gold and poly(DTEc) substrates was investigated. The hydrated surface masses of protein specific to the various substrates, calculated from QCM-D experiments, are compared in Figure 64. It should be noted that unlike surface plasmon resonance and ellipsometry, QCM-D is sensitive to the hydration state of the adsorbed layer.

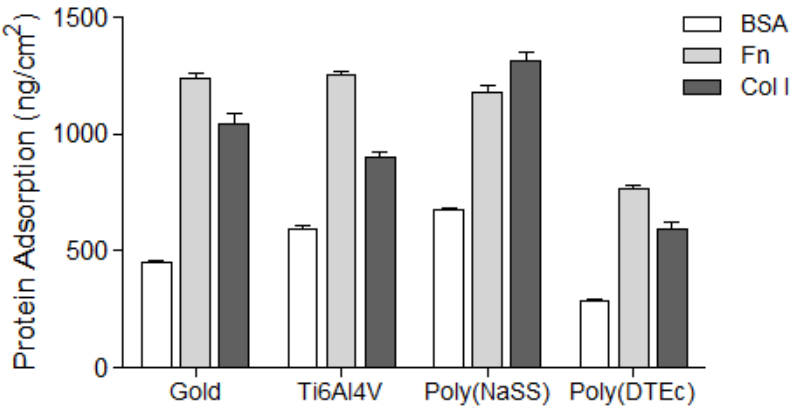

Figure 64. Adsorption of BSA, Fn and Col I onto Ti6Al4V, Ti6Al4V physisorbed poly(NaSS), gold, and poly(DTEc) at 37°C and 25 µL/min flow, until saturation.

For the majority of the cases, the poly(NaSS) coating showed the highest amounts of adsorbed protein. The only exception was Fn, however no statistical significance between surfaces was detected. This is expected since poly(NaSS) with its SO_3^- pendant chains is a polyanion, and electrostatic interactions are a main driver for protein adsorption [258]. On the other hand, adsorption to uncharged surfaces, such as gold and poly(DTEc), is dependent on weaker forces such as hydrophobic contributions or London dispersion forces. Changes in protein conformation or even denaturation along with loss of functional activity may occur when hydrophobic amino acid side chains are exposed to the interface [259,260]. Presence of poly(NaSS) may reduce these effects due to its hydrophilic character which makes proteins less

susceptible to structural changes and less tightly bound to the surface, so their original conformation can be preserved [261,262]. Moreover, previous studies have shown that poly(NaSS) grafted substrates are able to adsorb proteins until saturation. It was demonstrated, for instance, that the saturation level of BSA was three times greater on chemically grafted surfaces than on ungrafted [263].

Poly(DTEc) sensors show some interesting results. Even though adsorption was small with each of the three proteins investigated, cell attachment was high [174,264]. It could be because although electrostatic interactions are responsible for protein adsorption, on poly(DTEc) surfaces there could be a different class of specific binding interactions that promote cell attachment. It is possible that despite the low concentration of the adsorbed proteins on poly(DTEc), the conformation/orientation of the adsorbed protein, on this hydrophobic surface, is favorable for cell attachment.

2.7.3 Antibody Interference with Integrin-Mediated Adhesion

Studies were carried out to see how antibodies interfere with the cell attachment that is initiated by the interaction between the integrins on the cells membrane and the binding domains/sequences of the adsorbed proteins. Specifically, we wanted to understand how poly(NaSS) coating effects Fn and Col I adsorption and then cell attachment. Anti α_5 and anti β_1 were associated with cells to block interactions with Fn pre-adsorbed substrates, while anti α_2 and anti β_1 anti integrins were used for the Col I. These are heterodimers of two noncovalently associated transmembrane glycoproteins α and β, and are recognized preferentially by the Fn and Col I integrin binding domains in the presence of osteoblastic cells [235,236].

Figure 65A and 65B show the extent to which the attachment of MC3T3-E1 cells on the Fn and Col I pre-adsorbed surfaces, respectively, are inhibited by the presence of these antibodies. In addition to their superior cell adhesivity, the poly(NaSS) physisorbed surfaces showed higher osteoblastic attachment inhibition than the bare Ti6Al4V, in the experiments with antibodies. While the inhibition was only 40% with Fn, the inhibition with Col I, in some cases, was greater than 60%. One possible explanation for this observation is that poly(NaSS) changes the exposure of the specific protein domains to the cells, and this might lead to more integrin-mediated interactions. The main binding regions responsible for cell attachment in Fn are: the HB domains, the synergy peptide PHRSN, which stabilizes

the RGD-integrin interactions and preserves its specificity, and the central adhesive peptide RGD [237,77]; and those in Col I are: the HB domains, the RGD peptide and the von Willebrand factor A-like domain (A-domain) also known as inserted domain (I-domain) [265]. At these sites, the interactions between cells and material are mainly mediated by integrins. Biomaterial surfaces are known to induce changes in the proteins conformation during adsorption by means of intermolecular forces. Van der Waals forces, Lewis acid-base forces, electrostatic forces and hydrophobic/hydrophilic interactions are some of the many intermolecular events that affect the intrinsic structural stability of proteins [44,45]. In poly(NaSS), the SO_3^- pendant chains (polyanion) interact with Fn and Col I by means of electrostatic and hydrophilic interactions [46]. It has been shown that as a result of these interactions, regardless of their original structural arrangement, proteins unfold to a more stable conformation, thereby increasing the exposure of important active binding regions [50].

Another interesting aspect from the results is the importance of each subunit α and β to the final cell attachment. By itself, each anti-integrin may interact with other heterodimers. For instance, the anti-integrin β_1 can be recognized by more than one α subunit, i.e. $\alpha_3\beta_1$, $\alpha_4\beta_1$, $\alpha_v\beta_1$, therefore explaining the increased inhibition in cell attachment registered in Figure 65A and 65B (first two columns). Still, in combination the reaction with the respective heterodimer, $\alpha_5\beta_1$ in Fn and $\alpha_2\beta_1$ in Col I, is predominant [235,236].

In addition to mediating cell attachment, the receptors α and β also play an important role in the actin cytoskeleton organization. To assess this influence, images of individual cells stained with phalloidin (actin fibers) were taken after 2 h of culture on Fn pre-adsorbed Ti6Al4V and poly(NaSS) physisorbed sensors, both in the absence and presence of the antibodies (Figure 65C). In the absence of the antibodies (control), the focal adhesions are abundant. Integrins are the major transmembrane components present in focal adhesions. These specialized contact points provide a structural link to the actin cytoskeleton allowing the spread of the cytoplasm in all directions, developing multiple points of interaction [233]. The amount of focal adhesions detected on the Ti6Al4V was 1/6 of that on the physisorbed sensors. These results demonstrated the influence of poly(NaSS) on the interactions between MC3T3-E1 and Fn.

The use of antibodies induced a 20-50% reduction of the cells cytoplasm, size and extensions, and number of focal adhesions. However, it is remarkable to see that even when the antibodies block the $\alpha_5\beta_1$ there are still many focal adhesions detected on poly(NaSS) physisorbed sensors. We suspect that poly(NaSS) allows more than one type of integrin-mediated interactions between osteoblastic cells and the Fn binding regions, despite the clear preference for the $\alpha_5\beta_1$ combination. The $\alpha_2\beta_1$, $\alpha_3\beta_1$, $\alpha_4\beta_1$, $\alpha_v\beta_1$ and $\alpha_v\beta_3$ are possible alternatives known to support osteoblastic cells attachment in the presence of Fn [63]. Similar observations are expected on Col I pre-adsorbed substrates.

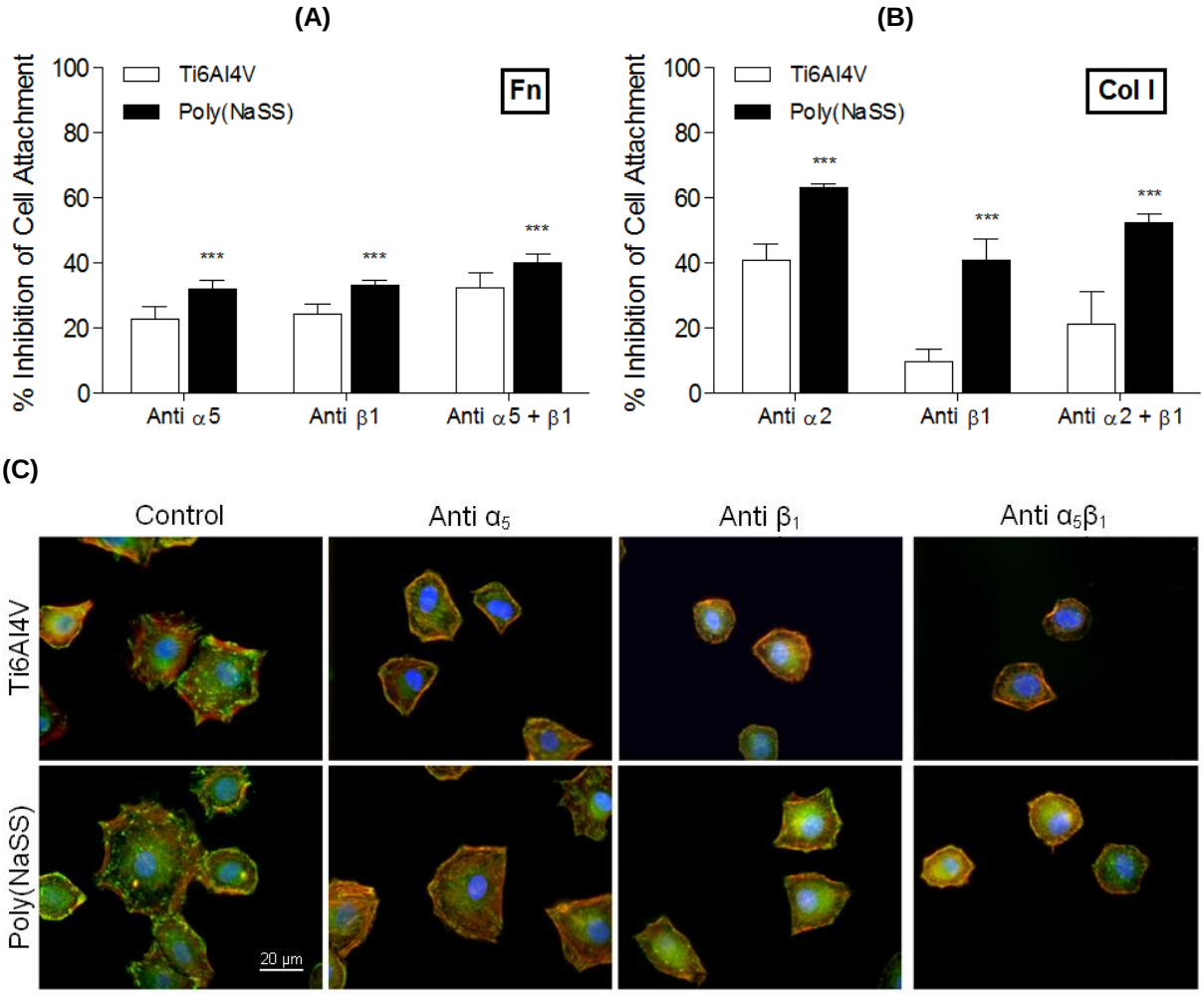

Figure 65. Percentage of cell attachment inhibition on Ti6Al4V and poly(NaSS) physisorbed sensors, pre-adsorbed with (A) Fn and (B) Col I, by the presence of anti-integrins (2 h at 37ºC and 0 µL/min). (C) Morphological characteristics of cells cultured for 2 h on Fn pre-adsorbed substrates, in the absence (control) and presence of anti-integrins (50x magnification). Significant differences between surfaces are indicated by * (* $p<0.05$, ** $p<0.001$ and *** $p<0.0001$).

2.7.4 Effect of Poly(NaSS) Coating on the Fn Conformation

While Figure 64 shows that the amount of Fn adsorbed is about the same on gold, Ti6Al4V and poly(NaSS), Figure 63A shows that the cell attachment is the highest with poly(NaSS). The hypothesis is that the orientation or the conformation of Fn, not just the amount adsorbed plays a role in cell attachment. This hypothesis that poly(NaSS) coating affects on the orientation/conformation of Fn adsorbed compared to uncoated Ti6Al4V was investigated using specific antibodies recognizing HB domains (N- and C- terminal) and the RGD sequence (Figure 66A). The data shown in Figure 66B were obtained to demonstrate the effect of poly(NaSS) on the Fn orientation at the interface. The results show that the exposure of the three sites was enhanced by the presence of the polymer, confirming that the orientation of the protein, and most likely its conformation, is different on poly(NaSS) coated Ti6Al4V relatively to uncoated.

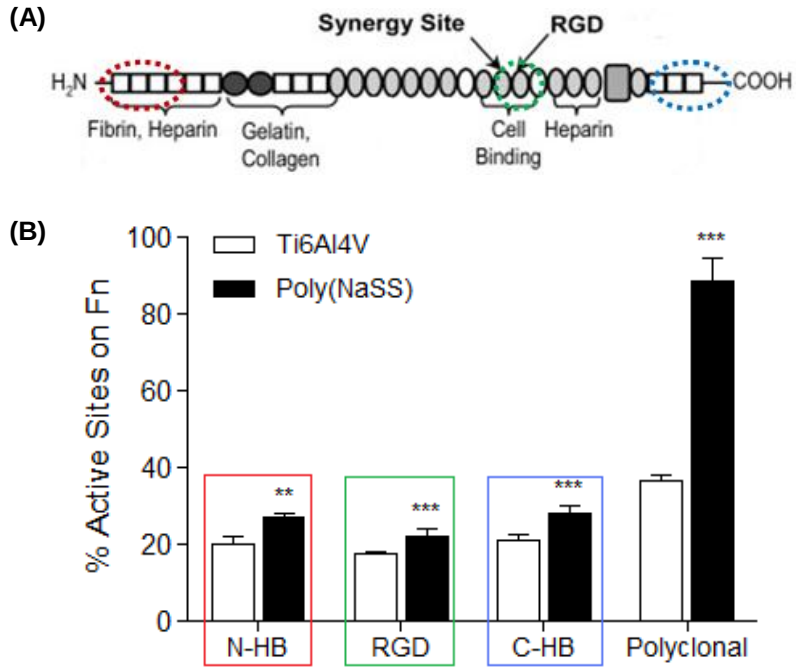

Figure 66. (A) Schematic structure of a Fn fragment, with identification of binding domains of interest [adapted from 41]. (B) Percentage of active sites, namely RGD peptide and heparin domains N-terminal (N-HB) and C-terminal (C-HB), exhibited by Fn pre-adsorbed on Ti6Al4V sensors with and without poly(NaSS) (25 µL/min). Significant differences between surfaces are indicated by * (** $p<0.001$ and *** $p<0.0001$).

The conformation and orientation of a protein adsorbed on a surface has a significant effect on the binding of cells because they determine the exposure of the cell-binding sites. It has been shown that both the RGD and the HB domains are directly involved with the attachment of osteoblastic cells to Fn [266]. These

observations were also confirmed by the use of a polyclonal antibody against the entire Fn molecule in which the exposure of the Fn active sites was found to be 2x higher on poly(NaSS) physisorbed surfaces than on uncoated Ti6Al4V. Latz et al. [218] reached similar conclusions with PMMA substrates grafted with poly(NaSS). They found enhanced expression of the C-terminal HB domain, and even by the entire molecule, and they attributed this to the conformational changes in Fn induced by the SO_3^- groups. They also found increased cellular attachment and adhesion strength stimulated by integrin activation at the RGD and HB binding regions.

These results validate our findings and support our conclusions on the integrin-mediated cell attachment, and thus demonstrating the influence of the poly(NaSS) on both protein adsorption and cell attachment.

- Adhesive Proteins in Double Depleted Medium -

In this segment we continue the investigation on the role of proteins at the interface cell-biomaterial. However, this time proteins were not left to adsorb before cell culture, they were combined with the medium. FBS depleted of Fn and Vn, hereafter referred as double depleted serum or DD medium, was used to test the role of these serum glycoproteins in the adhesion and morphology of MC3T3-E1 cells on ungrafted and grafted Ti6Al4V

DD was furnished by the laboratories of CSIRO Molecular Science in Sydney, Australia, and was prepared by following the procedure described in [267].

2.8 Cell Behavior in Double Depleted Medium

The current set of experiments were carried out to examine the role of Fn and Vn in the initial attachment and spreading of early passage MC3T3-E1 osteoblast-like cells to ungrafted and grafted Ti6Al4V surfaces. Our main goal was to understand the influence of poly(NaSS) on the adsorption of these two proteins, when in DD medium, and infer about the cell behavior as product of these settings. To set the conditions of this experiment, tests were initially conducted with FBS and SFM. Here, cells were left to interact with the surfaces in the presence of a variety of proteins and in its absence. Afterwards, three culture mediums were prepared: DD, DD + Fn and DD + Vn. Again, the cells morphology, attachment and adhesivity after 4 h and 30 min of contact were our main objects of study.

2.8.1 Spreading and Morphology

Cell morphology analyses were conducted 4 h after cell seeding, in FBS and SFM, and DD, DD + Fn and DD + Vn conditions. The results are shown on Figure 67A and 67B, respectively.

Cells seeded in FBS showed the highest overall level of cell attachment (visually) during the 4 h test period. Their organization was found consistent with the images from Figure 51. The MC3T3-E1 cells exhibited a well structured polygonal shape, with many cytoplasmic protrusions extending along the surfaces, and several bundles of actin fibers were identified. Furthermore, many focal adhesion points were detected. This was seen on both ungrafted and grafted Ti6Al4V, although cell spreading and formation of focal adhesion points was intensified by the SO_3^- groups [164,166,173,208]. On the other hand, only few cells were found spread in SFM cultures. Most of them still displayed a small round shape, with little cytoplasm extensions. The area of the spread cells was also smaller than that observed in cells cultured in FBS. The same differences in morphology were reported by Degasne et al. [249] following the Saos-2 osteoblast-like cells attachment and proliferation on acid etched and sandblasted Ti disks. This is to be expected, since in this situation proteins are not present, and the interactions between cell and biomaterial are only based in physical contacts rather than chemical. The absence of focal adhesion points on the ungrafted and small quantities on the grafted surfaces proves this statement correct. In early sections, we have shown that stronger physical bonds can be developed in the presence of SO_3^- groups, through the activation of specific cell functions [216]. For instance, we have demonstrated that the morphology of the cells can be sustained for longer on grafted materials, even in SFM (Part 2, Section 1). Poly(NaSS) has been identified as a trigger of early signaling pathways associated with important cell events, namely adhesion, migration and spreading. Knowing the ECM of osteoblastic cells to be a complex and diverse system with many different proteins and growth factors [20,217,218], it is expected, in SFM conditions, the surface properties and in particular the bioactive poly(NaSS) to stimulate the production of proteins of interest by the cells and, consequently, to activate the signal pathways necessary to extend the cell interaction with the biomaterial.

Regarding Figure 67B, cell expansion on DD cultures was very restrained compared to the rest. The majority of the cells were round with very little protrusions,

on both ungrafted and grafted Ti6Al4V. Nevertheless, evidences of small cytoplasm expansions were detected on the grafted material, supporting our initial conclusions.

Interestingly, both ungrafted and grafted substrates showed a lower cell attachment and spreading in DD serum compared to SFM. This implies that the presence of non-adhesive serum components may act to block cell attachment rather than promoting it, in this conditions. The same was reported by McFarland et al. [268] and Steele et al. [269] on various polymeric substrates.

(A)

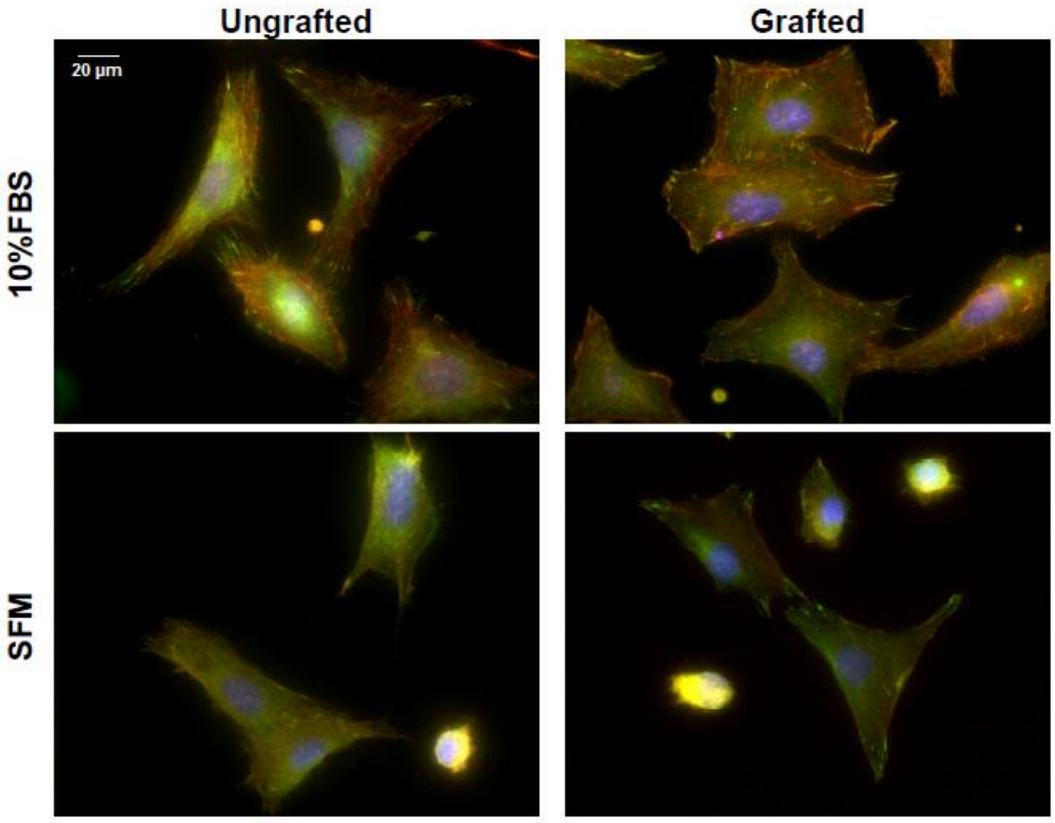

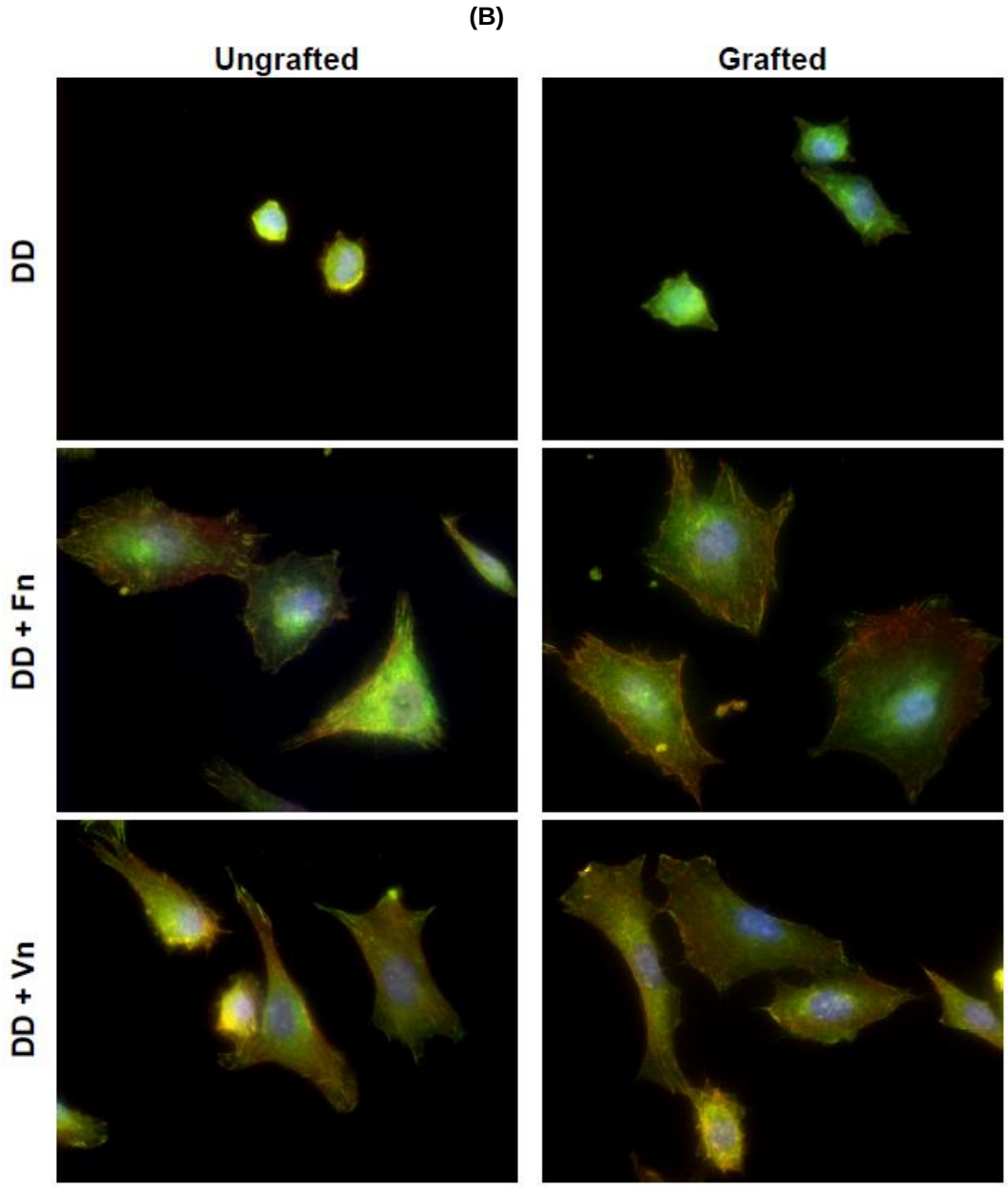

Figure 67. MC3T3-E1 cells morphology on ungrafted and grafted surfaces cultured in (A) FBS and SFM and (B) DD, DD + Fn and DD + Vn (50X magnification).

In contrary to the DD results, the MC3T3-E1 cells cultured in DD + Fn and DD + Vn conditions exhibited a spread morphology and many focal adhesion points. In Fn, the functionalized surfaces allowed for cells to express the typical osteoblastic morphology, with increased cytoplasmic extensions and well defined polygonal shape. On the other hand, in the ungrafted surfaces some cells exhibiting a more fibroblastic morphology were detected (stretched). The same was seen in the presence of Vn. In this case, however, round shaped cells were still observed, even in the grafted material. These results suggest that the contribution of Fn to cell attachment to be more significant than the contribution of Vn on Ti materials.

McFarland et al. [268] reached similar conclusions with TCPS, PHEMA/HEMA and PEMA/THFMA. In their study, they showed that cell adhesion and morphology are promoted by DD + Fn more intensively than by DD + Vn. They explained these differences by possible alterations in the Vn conformation, and by extension the ability to bind cells, during adsorption as a result of the surfaces chemistry. Here, probable conformational changes may be taking place as well. By comparing the morphology results from Figure 67 with the observations made on Figure 60A and 60C (1st two images on both), it is clear the changes in the morphology and amount of cells. It seems that cells adhere more easily onto surfaces previously coated with the protein in question than when they are combined with the protein in a serum free solution. It is conceivable that the conformation of the proteins may change as product of competitive behaviors between non-adhesive proteins and the adhesive proteins in solution. For instance, Pegueroles et al. [270] has shown that BSA can strongly bind to the Ti oxide surfaces and even displace Fn. Therefore, we can assume that Fn and Vn conditioning events may be taking place at the interface, which may account for the reduce number of focal adhesion, affecting somehow the cell behavior.

2.8.2 Attachment

The attachment of cells onto ungrafted and poly(NaSS) grafted Ti6Al4V in FBS, SFM, DD, DD + Fn and DD + Vn conditions is shown on Figure 68.

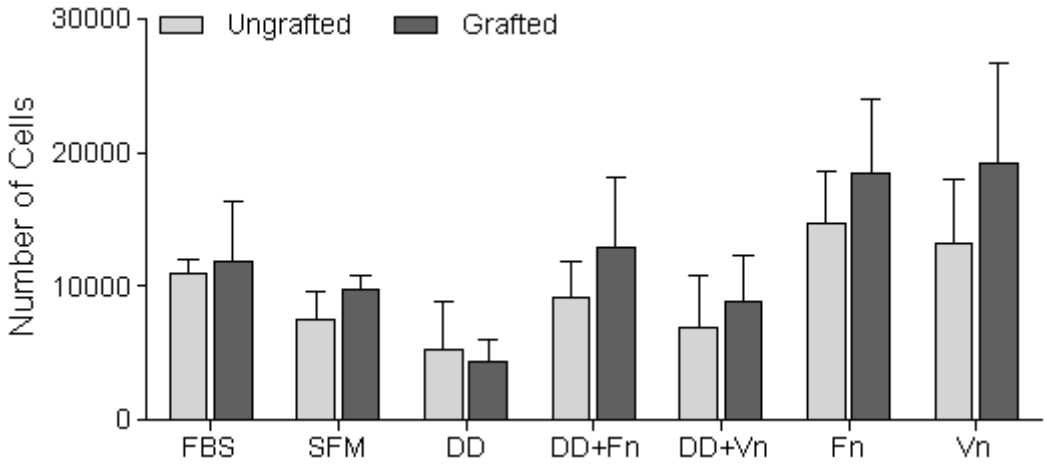

Figure 68. MC3T3-E1 cells attachment on ungrafted and grafted substrates cultured in FBS, SFM, DD, DD + Fn and DD + Vn medium conditions and Fn and Vn pre-adsorbed surfaces.

For the majority of the conditions, poly(NaSS) was found to induce a slight increase in the MC3T3-E1 numbers. However, it was not significant.

High levels of cell attachment were detected on both surfaces in the presence of FBS proteins, which has been in many cases appointed as a result of the competitive binding between Fn and Vn [267]. When by itself, Fn and Vn may compete against other molecules in the DD serum such as BSA or fibrinogen (Fg). As seen by the morphology results, the non-adhesive proteins on the DD may somehow hinder the cell spreading and attachment possibly through the alteration of the Fn and Vn conformations above the ungrafted and grafted substrates. The DD results point, once more, to possible competitive events between non-adhesive proteins that may inhibit the cell attachment, while the SFM attachment numbers may result from the production of adhesive proteins by cells.

These observations corroborate the analyses made on the cells morphology.

2.8.3 Attachment Strength

The adhesivity of the cell-biomaterial bond was tested 30 min after seeding. A shear stress of 10 dyn/cm^2 was applied to each sample for 15 min. The MC3T3-E1 osteoblast-like cells attachment strength in FBS, SFM, DD, DD + Fn and DD + Vn conditions, on ungrafted and grafted surfaces is shown by Figure 69.

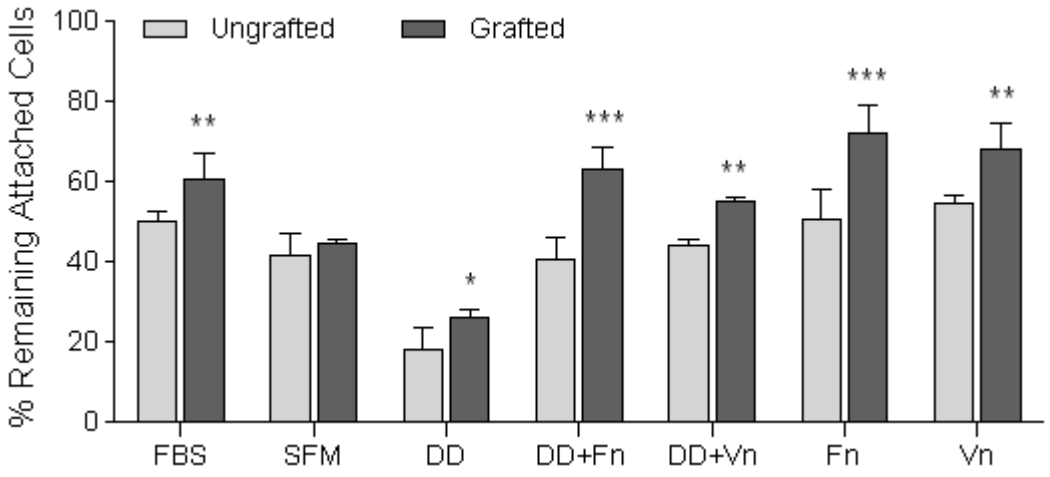

Figure 69. Percentage of cells that remained attached to the substrates after the application of a shear stress of 10 dyn/cm^2 for 15 min. MC3T3-E1 were cultured for 30 min in FBS, SFM, DD, DD + Fn and DD + Vn conditions. Significant differences between ungrafted and grafted surfaces pre-adsorbed with the same proteins are indicated by * (*p<0.05, **p<0.001 and ***p<0.0001).

The resilience of the bond cell-biomaterial was highly improved by the SO_3^- groups of the poly(NaSS), for nearly all tested conditions. The Fn proteins on DD promoted the most significant bond strength between cell and grafted material. Its resistance was slightly superior compared to the FBS but significantly enhanced over the DD + Vn ($p<0.001$), SFM and DD ($p<0.0001$). Most importantly, the poly(NaSS) improved the cells adhesivity in ≈ 36% compared to the ungrafted (DD + Fn). In regard to the other adhesive protein in study, Vn, the improvement of poly(NaSS) over the untreated materials was of ≈ 20%.

Fn and Vn possess various binding sites for cell attachment, including the HB domains and the RGD sequence [77,78,84]. These regions are known to offer strong adhesion points that support cell expansion above the surface, creating an environment compatible with osteointegration [83,222]. The results from Figure 69 suggest that the conformation of the proteins is favored by the bioactive polymer; however not as much as the surfaces coated with each one of these proteins. Almost 64% of cells cultured on grafted materials in DD + Fn conditions were capable of resisting to a shear of 10 dyn/cm^2. This percentage is smaller than that revealed by the Fn pre-coated surfaces, ≈ 75%. As explained earlier, pre-adsorption and adsorption by DD mixtures may not result in equal protein conformations [268]. Changes introduced by the competitive behavior of proteins in DD may condition integrin association, the main components of the focal adhesions known to support and strength the cell-biomaterial structural links [72,73], and therefore result in less tightly bonds. These same explanations can be applied to the differences of bond strength induced by Vn pre-coated substrates, ≈ 68%, and the DD + Vn, ≈ 55%.

The DD serum was only capable of sustaining ≈ 18% and ≈ 26% of their cells attachment to ungrafted and grafted surfaces, respectively. Garcia et al. [238] has shown that BSA (the main component of DD) does not affect significantly the cells adhesion strength, explaining that variations in non-specific interactions have little influence on cell attachment. However, this medium possesses as well Fg. Perhaps the competitive behaviors between these proteins that influenced the DD + Fn and DD + Vn results can also explain the reduced levels of attachment strength. Besides, the lack of focal adhesion points and a less advanced cytoplasmic body structure observed in these conditions (DD) could also explain the weakness of the links between the MC3T3-E1 and the surfaces.

The morphology results confirm our conclusions.

Main Conclusions

In vitro biological tests using MC3T3-E1 osteoblastic cells attested on the Ti6Al4V grafted with poly(NaSS) ability for biomedical applications. Substrates pre-adsorbed with FBS, BSA, Fn and Col I were studied. The morphological analyses showed that the presence of proteins with RGD adhesive-sequences tend to facilitate the interaction between the cells and the surfaces. Fn was found to be an instigator of MC3T3-E1 proliferation when associated with poly(NaSS), right from the initial stages of development. On the other hand, the pre-adsorption of Col I on grafted surfaces was associated with significant improvements on the osteoblastic cells matrix mineralization. BSA did not reveal any particular effect.

Cell attachment to protein adsorbed substrates was determine as highly dependent on protein active binding sites, such as the N-HB and C-HB binding domains and the RGD peptide of Fn. It was seen as well that cells interact preferentially through the integrins $\alpha_5\beta_1$ and $\alpha_2\beta_1$ on Fn and Col I pre-coated surfaces, respectively, specially on grafted materials. To the contrary, the integrin $\alpha_v\beta_1$ did not display much influence on the cell attachment to Vn, raising the possibility of other integrins to intervene more significantly in this task (i.e. $\alpha_v\beta_3$).

The effect of pre-adsorption of BSA, Fn and Col I on uncoated and poly(NaSS) physisorbed Ti6Al4V, gold and poly(DTEc) sensors on osteoblast-like cells attachment was investigated using the QCM-D technique, as well. Cell attachment was found to depend on the substrate and adsorbed protein. Poly(NaSS) exhibited the highest cell adhesivity, particularly in the presence of Fn and Col I. Integrin dependent attachment was observed between the MC3T3-E1 cells and the Fn/Col I pre-adsorbed poly(NaSS) sensors. Our findings also reveal that poly(NaSS) exerts a large influence over the Fn conformation, resulting in more available binding sites (RGD and HB domains) being exposed to cells.

The effect of Fn and Vn in DD serum conditions was promoted by poly(NaSS). The same way the SO_3^- groups allowed for more cells to spread on FBS and SFM, instigating the development of more focal adhesions. By comparing the results of Fn and Vn pre-adsorbed surfaces with the DD + Fn and DD + Vn, a small decrease in cell spreading, attachment and adhesivity was observed. Our results revealed that possible competitive behaviors may be taking place between the DD proteins, hindering the osteoblastic cells development.

3. PROTEIN COMPETITION

Once implanted, the biomaterial is quickly surrounded by proteins that adsorb onto its surface and mediate all the interactions with the biological tissue. Protein adsorption is a complex and competition based process very difficult to predict. It depends not only on the nature of the proteins in the mixture but as well on the physicochemical properties of the surface. Generally, proteins seek active sites on the surface, and compete with each other for those sites until they finally adsorb [153,261]. Their conformation, type and amount at the biomaterial surface will trigger an appropriate cell response. This is the basis for the long term compatibility of a biomaterial and its successful implantation [152,271]. In this section, the competitive behavior of three proteins, BSA, Fn and Col I, was examined on QCM-D crystals (Ti6Al4V, poly(NaSS) physisorbed sensors, gold, poly(DTEc) and PS).

As competitive adsorption behavior of proteins is complex and cannot be predicted from the adsorption behavior of individual proteins alone, data was collected in two ways (broad perspective): in one, the proteins were allowed to be adsorbed onto the substrates sequentially, so the effect of one protein on the subsequently adsorbed protein was determined; in the other, the substrate was exposed to a two-protein mixture and their mutual competition assessed.

3.1 Competitive Protein Adsorption

When a biomaterial is implanted and surrounded by tissue the surface is exposed to numerous proteins. The cellular response depends on the nature of the protein layer that is formed on the material surface out of that mixture of proteins by competitive adsorptive behavior. This process was investigated by using six pairs of three proteins, BSA, Fn and Col I. Sequential adsorption will be indicated by "+" symbol (i.e. BSA + Fn to indicate adsorption of BSA first followed by Fn), and adsorption from mixture will be indicated by "&" (i.e. BSA & Fn).

3.1.1 Sequential Adsorption

The results obtained by exposing the substrates to six pairs of proteins are presented in Figure 70. With many of these pairs, the amount of the adsorbed protein on the substrates is smaller than that observed with a single protein on the surface

[270]. This effect was more noticeable when the first protein was larger or more complex than the second (i.e. Col I + BSA; Figure 70C). Interestingly, the total amount of adsorbed protein from the combinations BSA + Fn and Fn + BSA (Figure 70A) is about the same as that of Fn by itself, particularly on the poly(NaSS) physisorbed sensors. In this instance, important protein rearrangements that are not noticeable in the QCM-D data may occur between BSA and Fn. Fn has been known to have large affinity to poly(NaSS), exhibiting a stable and favorable conformation for cell attachment [218]. It has been suggested, as well, that in hydrophilic charged surfaces Fn adapts an active conformation exposing more binding sites, including the RGD sequence, for cell attachment [91]. In contrast, BSA possesses no specificity to any substrate, sharing only weak links with the surface. Therefore, in the BSA + Fn sequence, a continuous replacement of BSA for Fn may be taking place, while in Fn + BSA sequence, the extent of BSA adsorption may be almost insignificant, probably to bound to the few non-specific binding sites. The same is seen on the Col I + BSA sequence (Figure 70C).

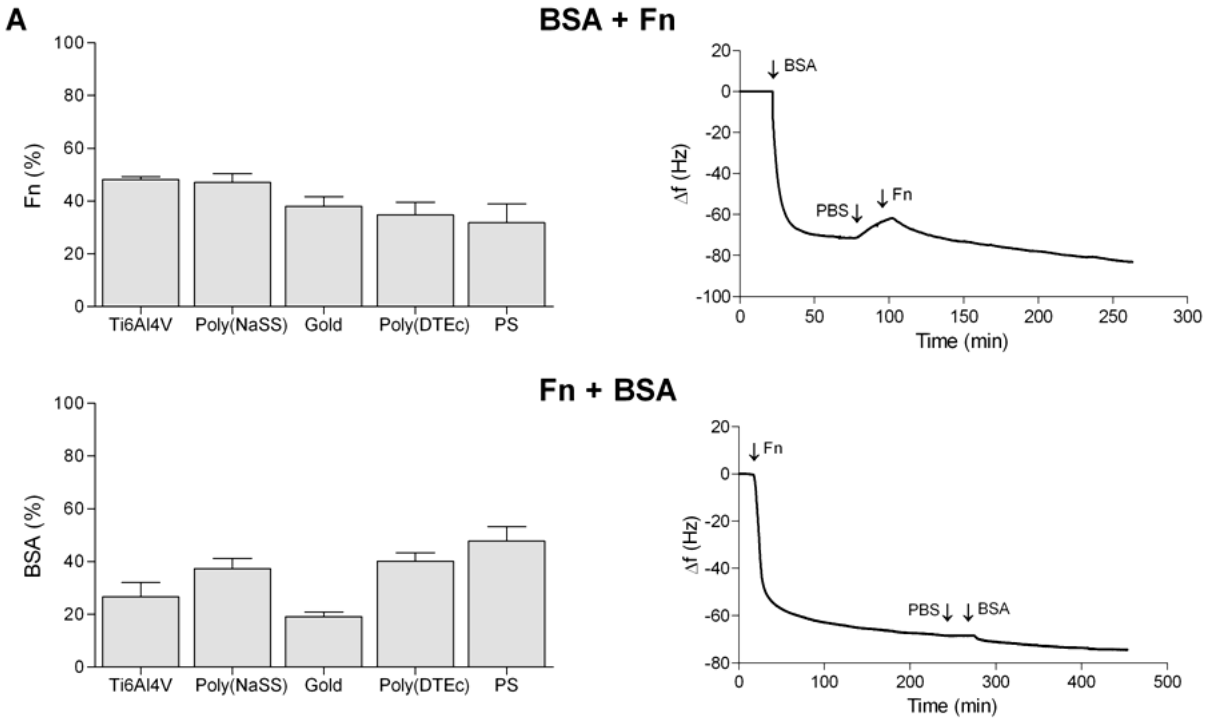

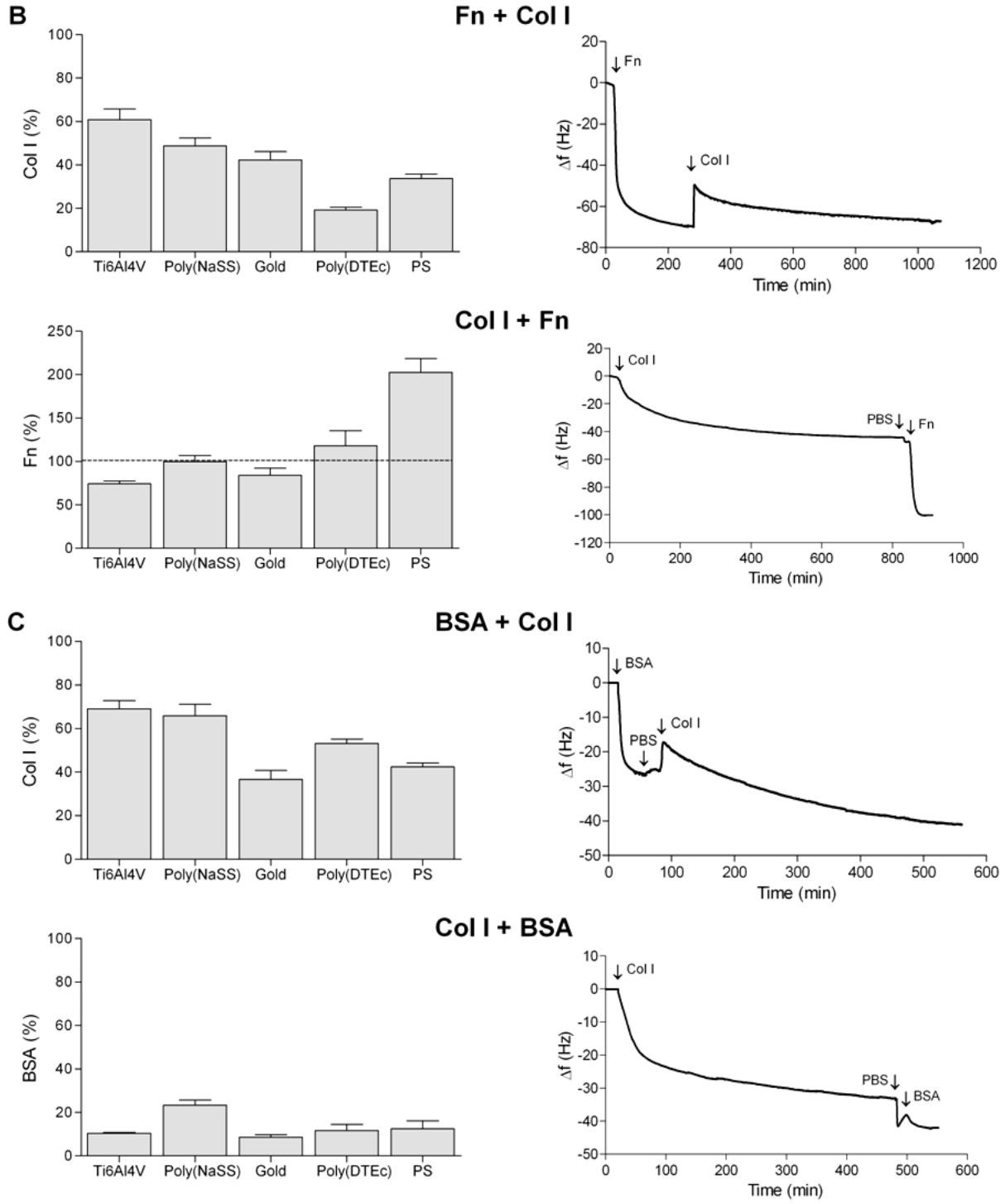

Figure 70. (Left) Percentage of a second protein adsorption onto Ti6Al4V, poly(NaSS), gold, poly(DTEc) and PS after pre-adsorption of a first until saturation (sequential tests, at 37°C and 25 µL/min). The percentage values were determined by relating the sequential adsorption rates of the second protein with its own individual values. (Right) Representation of the changes in frequency (overtone 9) registered on all surfaces in the sequential tests ((A) BSA + Fn and Fn + BSA; (B) Fn + Col I and Col I + Fn; (C) BSA + Col I and Col I + BSA).

In the two particular cases of Fn + Col I (Figure 70B) and BSA + Col I (Figure 70C), the effect of the larger protein on the smaller was more pronounced than that

registered on the BSA + Fn sequence. Here, the second protein, Col I, displaced the first, a clear example of the Vroman effect. Col I, the less motile protein with greater affinity to the substrate replaced a pre-existing protein [62]. These results were confirmed by fluorescent microscopy of FITC conjugated (Sigma) with the first protein (Fn or BSA), which was recovered from the waste fluid as it was displaced by Col I. Figure 71 shows evidences of the displacement of the protein solutions BSA and Fn, stained in yellow by the FITC conjugate, after being removed by Col I. The stained liquids started being collected from the waste 20 min after introduction of the Col I solution in the QCM-D system (time necessary to complete a cycle, in-out, in the QCM-D apparatus).

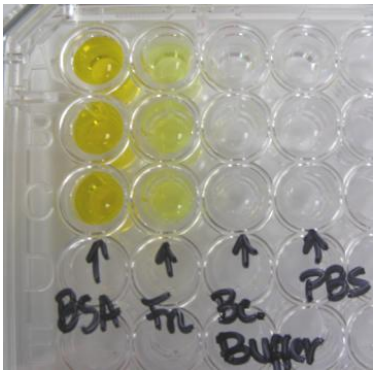

Figure 71. BSA (1st column) and Fn (2nd column) protein solutions stained in yellow by the FITC conjugate. Liquids recovered from the QCM-D apparatus waste 20 min after Col I injection.

The adsorption behavior of Col I and Fn in the sequence Col I + Fn (Figure 70B) was highly dependent on the substrate. While in the Ti6Al4V and the gold crystals the adsorption of Col I limited the adsorption of Fn, in the poly(NaSS) coated sensors the amount of Fn after Col I was similar to that of Fn by itself. It is possible that conformational rearrangements between proteins took place on this biomaterial as a result of the negatively charged sulfonate groups characteristics of the poly(NaSS), allowing interactions between Fn and Col I. Fn is thought to mediate important interactions between cells and other ECM components, namely collagen [175]. Fn possesses a collagen binding domain, which could explain the lack of restrictions for its adsorption.

The hydrophobic materials were also found to influence the proteins adsorption. Proteins typically adsorb preferentially on more hydrophobic surfaces despite the concomitant changes in their conformation [272,273]. In more hydrophilic materials, the proteins are less tightly bound to the surface so their original

conformation, which is favorable for cell development, is maintained [261]. The poly(DTEc) and the PS surfaces appear to influence the conformation of Col I in a way that facilitates its interactions with Fn.

3.1.2 Adsorption from Mixtures

Three protein mixtures, each containing two of the proteins used in this study, BSA, Fn and Col I, were used to determine the proteins competitive character for the adsorption sites on the surface. Figure 72 shows the total amount of proteins adsorbed onto the five surfaces and the corresponding kinetics.

In the BSA & Fn mixture (Figure 72A), the amount of proteins adsorbed was determined by the wettability of the surfaces. The more hydrophilic (Ti6Al4V) achieved the highest mass densities, while the more hydrophobic (PS) the least. These two proteins aside from their ability to be dissolved in PBS, when in solution achieve equilibrium at approximately the same pHs, BSA at 7.0 and Fn at 7.2; their behavior in mixture is therefore simpler to interpret. These similarities are reflected in their adsorption kinetics. Here, a sharp drop in frequency is observed with the saturation being achieved in less than 5 h.

In contrast with these results, the Fn & Col I mixture (Figure 72B) show an early drop in frequency caused by the initial adsorption of the proteins, which is then followed by a small but continuous increase in frequency. Equilibrium was only achieved 12 hours after initial protein injection. Comparing these results with the sequential adsorption kinetic curves, it appears that the increase in frequency, i.e., or the additional mass loss, could be due to a constant rearrangement of the proteins, with new interactions being formed between the Fn binding sites and the Col I, or to a possible displacement of Fn (both events observed in sequential tests). The total amount of protein adsorbed on the five substrates from the Fn & Col I mixture was about the same, the only exception being the uncharged hydrophobic poly(DTEc) substrate, which adsorbed the least amount of proteins. This same behavior was seen on the Col I & BSA mixture (Figure 72C). However, in the last case the proteins mass on the poly(DTEc) surfaces surpassed the rest of the substrates. Poly(DTEc) showed a very unusual protein adsorption pattern in the presence of Col I: in some instances the adsorption was higher whereas in others it was the lowest. We can only speculate that the proteins affinity towards this

particular material changes depending on the mixture of proteins and protein-protein and protein-surface interactions.

In spite of the extensive time consumed to reach saturation (12 h) and the important drop in frequency registered ($\Delta f \approx 200$ Hz), the kinetics of the Col I & BSA mixture (Figure 72C) was similar to that of BSA & Fn. In many of the tested mixtures, the total amount of proteins on each surface was always less than in the sequential studies. This suggests that once the finite number of adsorption sites on the surface is occupied, interaction between dissimilar proteins prevent remodeling of the adsorbed layer that could increase the amount of adsorbed protein. Such remodeling probably occurs if only one type of protein is present as in sequential adsorption. The Col I & BSA mixture is an exception to this statement, since the total amount of protein adsorbed was higher in mixture than in sequential adsorption. There are two possible explanations for this observation. The first is based on a continuous rearrangement of the proteins conformation due to the influence of one protein on the other; an optimal protein structure being eventually attained. The second possibility is the formation of multiple protein layers. The first protein layer being directly influenced by the surface properties, while the subsequent layers being dependent on the conformation of the previous protein. BSA possesses numerous binding sites for lipids and other hydrophobic molecules. It is therefore plausible to BSA to bind to Col I via these hydrophobic pockets when in a mixture.

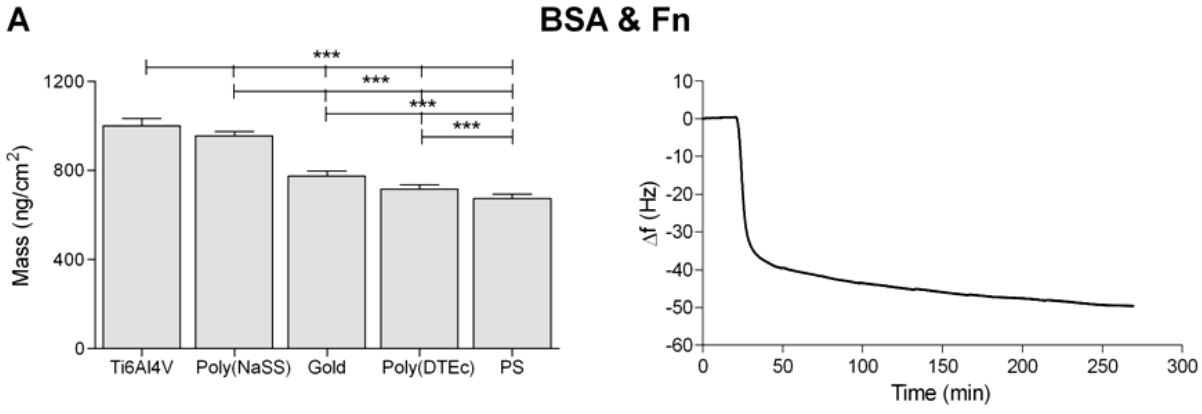

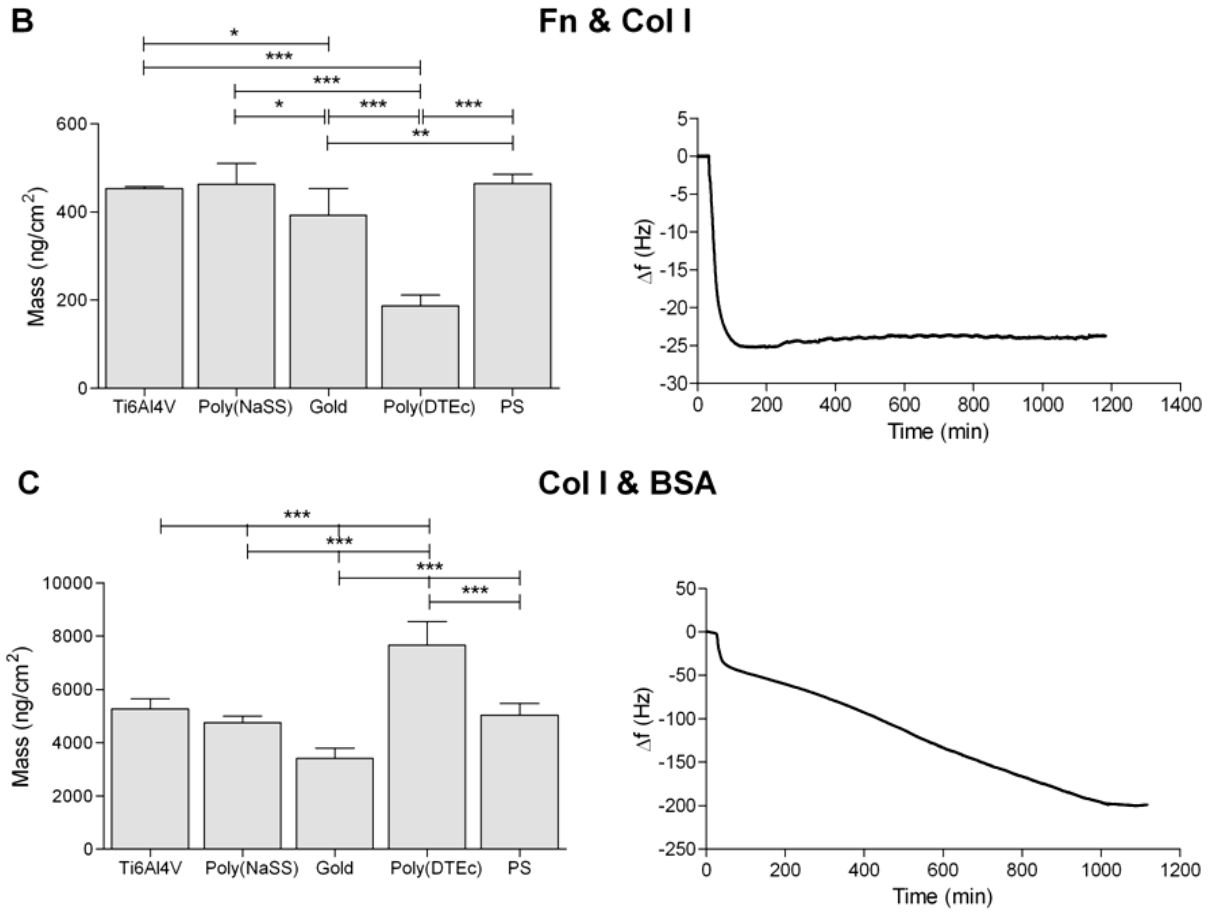

Figure 72. Mass density (left) and frequency changes (right) on Ti6Al4V, poly(NaSS), gold, poly(DTEc) and PS resultant from the adsorption of two proteins in a mixture: (A) BSA & Fn; (B) Fn & Col I; (C) Col I & BSA, at 37°C and 25 µL/min. Significant differences between surfaces pre-coated with the same protein are indicated by * (* $p<0.05$, ** $p<0.001$ and *** $p<0.0001$).

Main Conclusions

Competitive adsorption between proteins was found both in mixtures and in sequential depositions. The first protein that interacts with a biomaterial surface restricts the deposition of a second on the same material. Evidence of the Vroman effect, a very common competitive behavior of proteins, was identified in the sequential adsorption of Fn + Col I and BSA + Col I. Proteins competition is intensified in mixtures.

The Col I & BSA adsorption was substantially higher than that registered on the other mixtures and even sequential adsorptions. This was seen for the totality of the substrates. In the presence of Col I, protein adsorption on poly(DTEc) is different from other substrates.

4. ADSORPTION FROM PROTEIN MIXTURES AND CELL BEHAVIOR

The competitive adsorption of proteins regulates many interfacial phenomena, in particular the biocompatibility of biomaterials when exposed to blood and cell tissues. Body fluids contain different types of proteins that can mutually compete to adsorb to any exposed surface. As seen before, protein adsorption from these fluids may be very complex but also favorable as it enriches a biomaterial surface with proteins exhibiting the highest affinity to it [59-61].

In early experiments, we demonstrated poly(NaSS) grafted surfaces to modulate the cell response *in vitro*. Individual adsorption of adhesive proteins onto these chemically changed materials was found to stimulate the cell attachment, adhesion and even maturation. Still, when implanted in the human body a biomaterial is surrounded not by one protein type but by many. Their competition for the active sites on the surface is responsible for the host response. In order to identify the effect of selected proteins and their competition on the osteointegration process, we investigated the osteoblast response as a result of controlled mixtures of two proteins.

4.1 Viability

The viability of cells in contact with substrates treated with protein mixtures determines the validity of these mixtures to support the cells development. Cell survival rates analyses were conducted on the 3 experimental groups, Fn & BSA, BSA & Col I and Col I & Fn, after 4 h of culture. The results are given by Figure 73.

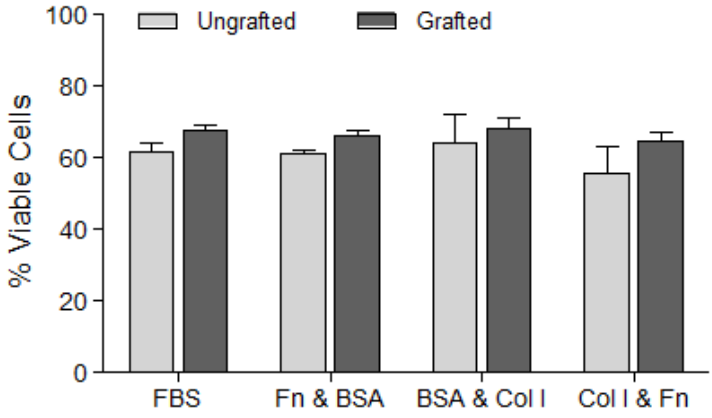

Figure 73. Percentage of viable cells attached to the ungrafted and grafted Ti6Al4V surfaces after 4 h of culture.

Data was found similar between protein combinations and between types of surface (ungrafted vs grafted). The pre-adsorption of the proteins had no effect on the MC3T3-E1 cells viability. Survival rates were found at ≈ 60% for the totality of the tested conditions. The absence of superior survival rates may be an effect of the short incubation period and/or detachment of cells during processing. Equal observations were made earlier with FBS coated substrates (2nd Part, Section 1 and Section 2).

4.2 Spreading and Morphology

The MC3T3-E1 cells morphology after 4 h of contact with ungrafted and grafted surfaces, pre-adsorbed with protein mixtures, is shown on Figure 74.

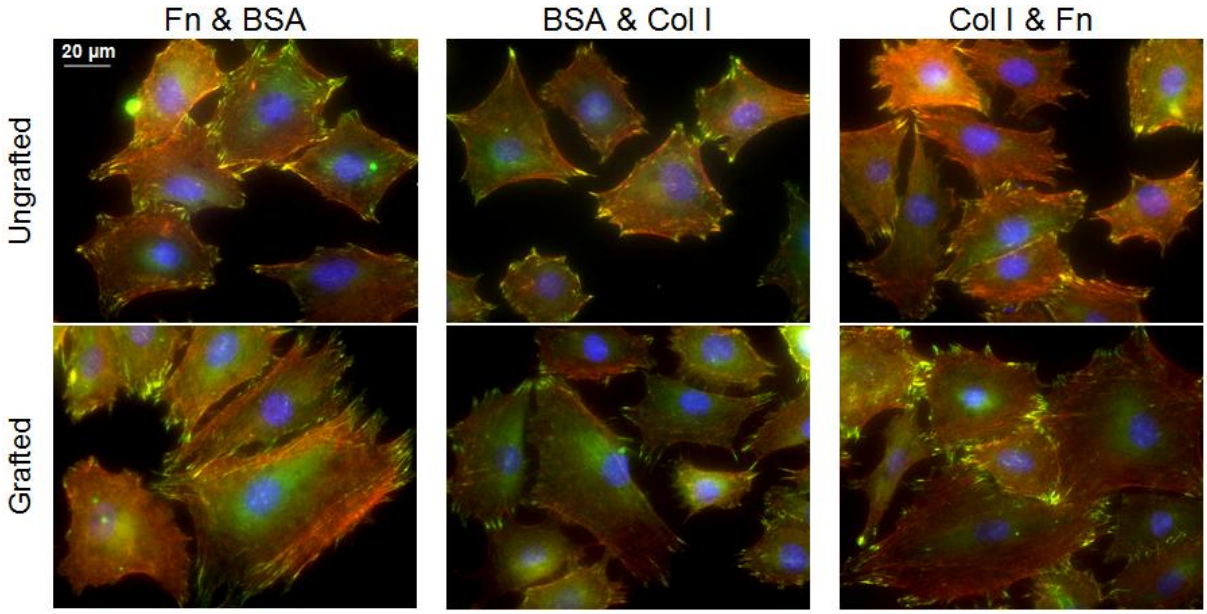

Figure 74. MC3T3-E1 cells morphology on ungrafted and grafted Ti6Al4V surfaces pre-adsorbed with protein mixtures after 4 h of culture (50x magnification).

For all the experiments, cells exhibited a well defined polygonal shape and actin cytoskeleton, with cytoplasmic protrusions extending in all directions. At this point, as a result of the surfaces roughness, the cells growth pattern possesses no organization or orientation defined. Cells cytoplasm expansion was intensified in the presence of poly(NaSS), achieving sizes two times larger than on ungrafted surfaces.

Interestingly, the existence of Fn in the mixtures enhanced the amount of focal adhesions between the osteoblastic cells and the material (both grafted and ungrafted), aside from the number of cells (visually). Focal adhesions are majorly

composed by integrins, which play a crucial role in the assembly of the actin cytoskeleton [72,73]. These specialized contact points provide a strong structural link with the substrate, essential for an optimal cell development (migration, proliferation, differentiation and mineralization). Fn is an ECM protein with several cell adhesion sites (the HB domains, the PHRSN peptide, and the RGD sequence). In case of osteoblastic cells, various cell membrane receptors, $\alpha_5\beta_1$, $\alpha_2\beta_1$, $\alpha_3\beta_1$, $\alpha_4\beta_1$, $\alpha_v\beta_1$ and $\alpha_v\beta_3$, can interact with the Fn binding regions increasing the amount of focal contacts [63,233].

The Col I & Fn mixture on grafted surfaces revealed the most important cytoplasm spreading/extension, attachment numbers and amount of focal contacts. The bioactive macromolecular chains from the poly(NaSS) can induce the creation of new active sites for protein binding. This promotes changes in the conformation of Fn and Col I and intensifies integrin mediated cell attachment [166,218]. The hydrophilicity and surface energy (57.3 mN/m) of the grafted substrates allows for electrostatic and hydrophilic interactions to be established with the proteins. This contributes significantly to the proteins unfolding to a more stable conformation, increasing the exposure of important cell binding regions [49]. Such modulation of the proteins behavior can trigger signaling pathways different from the ones registered on ungrafted surfaces and condition the totality of the cellular development. Besides, Col I possesses as Fn various binding sites for osteoblast-like cells integrin receptors, including the RGD peptide, the HB domains and the von Willebrand factor A-like domain [265], which availability may increase during unfolding of the Col I triple helix structure. Furthermore, Fn and Col I can benefit from protein-protein interactions, through collagen specialized binding regions on the Fn molecule, leading to new protein rearrangements beneficial for the cells. The evaluation of the competitive character of these two proteins, both in sequence and when in mixture, confirms this statement. Col I and Fn enroll in conformational rearrangements and can establish interactions with each other when combined.

Comparing the images from Figure 74 with the results obtained from experiments on poly(NaSS) grafted Ti6Al4V substrates individually adsorbed with Fn and Col I from Figure 51, our latest conclusions are confirmed. Fn and Col I by itself on grafted surfaces stimulate the cells attachment and expansion compared to ungrafted, however their combination is more successful. The assembly of these two

adhesive proteins with the bioactive polymer creates an environment incentive for early osteoblast-like cells attachment.

4.3 Attachment Strength

The cells adhesivity or attachment strength was evaluated 30 min after incubation. The results are given by Figure 75.

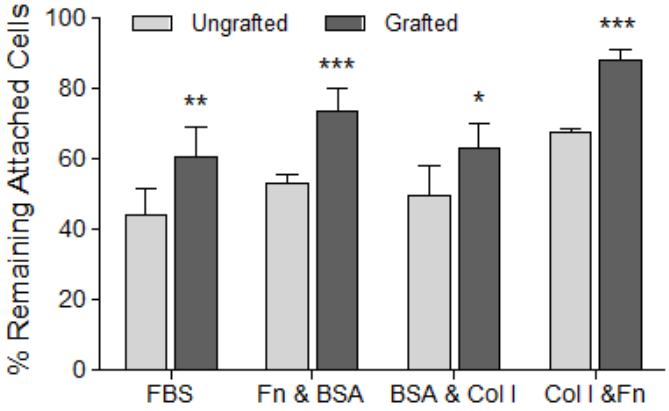

Figure 75. Percentage of cells that remained attached to the substrates after the application of a shear stress of 10 dyn/cm^2 for 15 min. MC3T3-E1 cells were cultured for 30 min. Significant differences between ungrafted and grafted surfaces pre-adsorbed with the same protein combinations are indicated by * (*p<0.05 and ***p<0.0001).

In the 3 tested groups, poly(NaSS) exerted a positive effect by increasing the cell-biomaterial bond resistance to shear stress of 10 dyn/cm^2. These results are consistent with previous investigations [164,173]. The SO_3^- groups improved significantly the MC3T3-E1 cells attachment strength, particularly when treated with Fn & BSA and Col I & Fn. In fact, a relation can be established between the cell morphology and its attachment strength. By inducing the cytoskeleton expansion, these proteins allowed stronger and more resilient interactions with the surface, translate by an increased amount of focal adhesions. Since the common element between these two mixtures is Fn and knowing that the RGD peptide is a preferable binding region for osteoblastic cells, which tend to originate strong interfaces as seen by the morphology results, we believe this to be a decisive factor in the cells attachment to the Ti6Al4V alloy [63,233]. Moreover, the BSA & Col I combination displayed the lowest percentage of remaining cells, ≈ 60%, even in the presence of poly(NaSS).

Fn possesses various regions of binding activity. Therefore, it is conceivable the presence of Fn on the protein mixtures to automatically assume a prominent position over the others, at least in the early stages of cell development.

Another interesting aspect from these results is the ability of the combination Col I & Fn to sustain almost 90% of cells on the surfaces. Again, these results are consistent with the morphological observations. Changes in protein conformation/orientation induced by the negatively charged SO_3^- groups and protein-protein interactions are responsible for this outcome [166,218]. Integrin-mediated attachment between the binding domains of Fn and Col I and specialized receptors from the MC3T3-E1 cells membrane contributed drastically to the resilience of the bond cell-biomaterial. This has been observed previously (2^{nd} Part, Section 2), and now it has been confirmed as valid.

Once more, the results sustain our innovative perspective on protein mixtures and their competitive benefits for the early cell attachment.

4.4 Proliferation

The cell proliferation curves on the differently treated substrates are shown in Figure 76. As expected, for the majority of the time points no significant differences were detected between ungrafted and grafted surfaces [240].

From the 10^{th} day to the 14^{th} a small but significant increase on the cell numbers was introduced by the poly(NaSS) on the combinations Fn & BSA (Figure 76A) and Col I & Fn (Figure 76C). Given these results to be divergent from previous studies with surfaces treated with FBS protein mixtures [172,173,240], it is conceivable poly(NaSS) to induce a new organization on the already attached cells, allowing for more to proliferate. These two combinations achieved the highest cell numbers. The results support our morphology and attachment strength analysis and provide more information about the Fn competitive character over BSA and Col I.

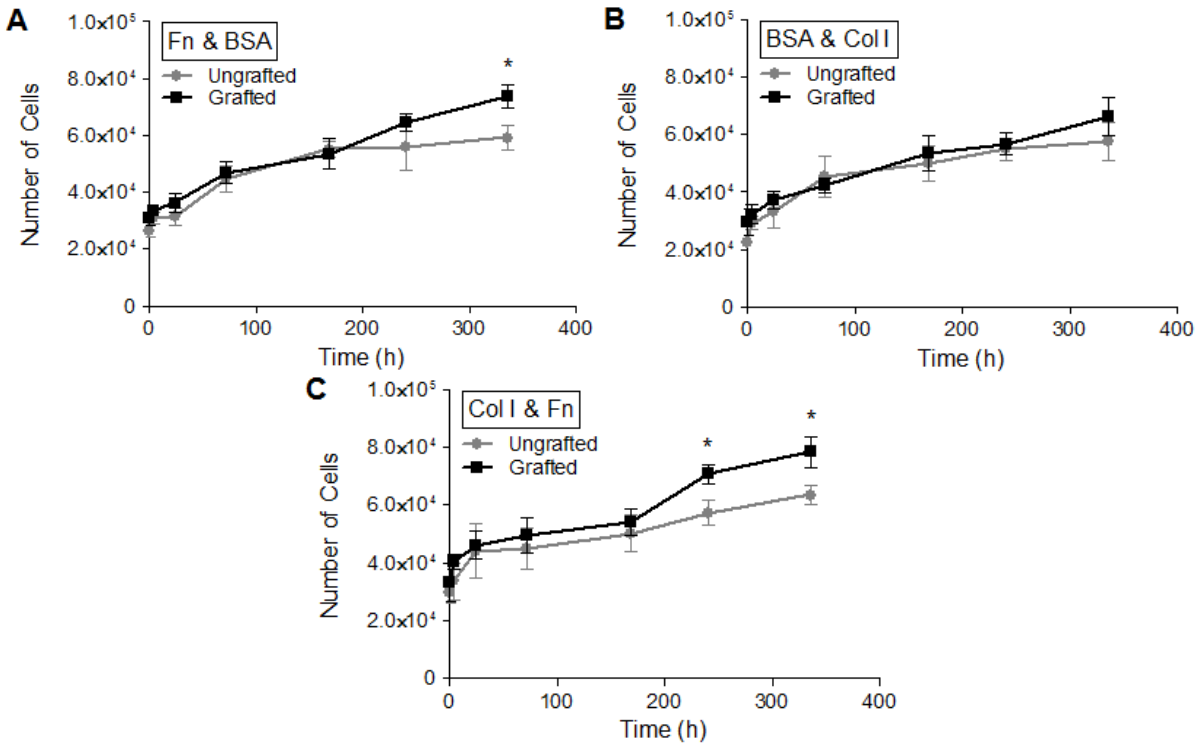

Figure 76. Proliferation curves of MC3T3-E1 cells on ungrafted and grafted surfaces, pre-adsorbed with (A) Fn & BSA, (B) BSA & Col I and (C) Col I & Fn mixtures, from 4 h to 14 days. Significant differences between ungrafted and grafted surfaces are indicated by * (*p<0.05).

4.5 Differentiation and Mineralization

The ALP activity of the osteoblastic cells was followed from 7 to 28 days. Figure 77 gives the highest ALP concentration registered during that time frame, more precisely at day 14.

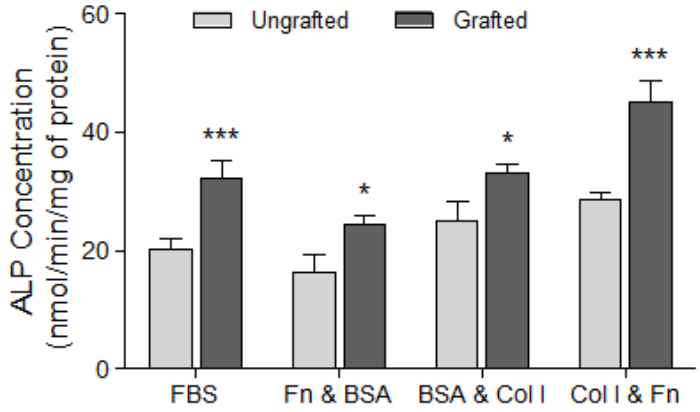

Figure 77. ALP concentration after 14 days of culture. Significant differences between ungrafted and grafted surfaces pre-adsorbed with the same protein mixtures are indicated by * (*p<0.05 and ***p<0.0001).

According to the data, poly(NaSS) has an important impact on the enzyme production in all tested groups [274]. As before, its effect was more significant for the combination Col I & Fn. The alterations in the Fn and Col I conformation and orientation appear to have a permanent impact on the cell development. Besides, as we established earlier protein-protein interactions can also occur and be determinant for the MC3T3-E1 cell growth [78-80].

Fn has been shown to enhance gene expression of ALP on MC3T3-E1 cells by accelerating their production and activity [159]. On its turn, Col I is known to activate specific signaling pathways that affect the expression of bone cell phenotypes associated to the ECM formation and maturation [244,245]. Takeuchi et al. [275] has even shown that the interaction of Col I with cell-surface $\alpha_2\beta_1$ integrin receptors on MC3T3-E1 cells is indispensable for their differentiation. By observing the ALP production induced by the BSA & Col I mixture, it is possible to infer about the contribution of Col I to the cell maturation process. As pointed in previous sections, BSA is a non-specific protein with little influence on the cells development. Hence, in this case, Col I can be assumed as the prominent protein from the group and the major responsible for the BSA & Col I and Col I & Fn ALP results. These observations reflect the competitive character of the proteins, more precisely the role they exert on the cell behavior after competing for the active sites on the surface. It is important to notice that during attachment, adhesion and proliferation (early cell development) Fn is the protein with the biggest influence, while during cell maturation Col I assumes the leadership role. The way the regions of the adsorbed proteins are exposed to the cells in slightly different conformations defines their impact on the cell functions and progress.

Besides, the supplemented medium (β-glycerophosphate and ascorbic acid addition) is considered an instigator of osteogenic markers expression, which includes Col I (≈ 80% of the organic cellular matrix). These supplements adopt an osteoblastic phenotype and secrete and organize the ECM. They trigger a series of molecular events that include the activation of signal transduction pathways very important for the osteoblast differentiation and mineralization [246,247].

The same explanations can be used for the calcium (Figure 78A) and phosphate (Figure 78B) production, which once again was instigated by the presence of Col I. It must be highlighted, though, that poly(NaSS) contributed significantly for

the calcium production on the BSA & Col I and Col I & Fn treated substrates and for the phosphate production on Col I & Fn adsorbed surfaces.

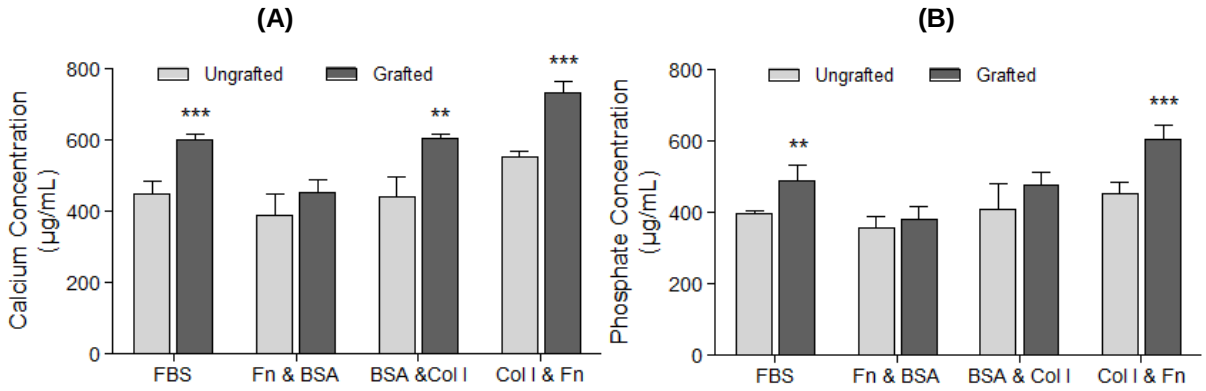

Figure 78. (A) Calcium and (B) phosphate production at 28 days of culture. Significant differences between ungrafted and grafted surfaces pre-adsorbed with the same protein mixtures are indicated by * (**p<0.001 and ***p<0.0001).

The amount of ALP, calcium and phosphate produced by the grafted surfaces adsorbed with these 3 protein mixtures was found superior than that generated by equally treated surfaces adsorbed with FBS or individual proteins (BSA, Fn and Col I), on previously shown work. This puts in evidence the meaning of the proteins competitive character to the osteointegration process.

Main Conclusions

The tests carried out in this study aimed to understand the proteins influence on the osteoblastic cells behavior when adsorbed from mixtures onto Ti6Al4V materials.

It was seen that the grafting of poly(NaSS) enhances the osteoblast-like cells attachment strength, differentiation and mineralization, particularly in the presence of Col I & Fn mixtures. While in competition, Fn and Col I prevailed over the other protein in solution, being responsible for strong early cell-biomaterial interactions, and increased production of ALP, calcium and phosphate, respectively.

V. CONCLUSIONS

The synthesis and grafting of bioactive polymers such as the poly(NaSS) onto Ti surfaces has been proposed and optimized over the years, using a grafting “from” technique that generates covalent bonds between the polymer and the implantable material.

In this work, we explored the combination of the poly(NaSS) with the Ti alloy Ti6Al4V and its influence on the osteoblast-like cells behavior. Our aim was to understand in more detail the effect poly(NaSS) exerts on the cell response, particularly in the presence of important biological molecules at the interface cell-biomaterial. The approach followed in this research consisted: first, in the establishment of the biological properties of the polymer poly(NaSS); second, stipulation of the general cell behavior on these altered surfaces; and, finally, in the comprehension of the biological molecules effect on each other and on the cells behavior at the interface.

The characterization of the ungrafted and grafted disks was our first goal. The results showed the grafting process to be successfully conducted on the Ti alloy. Poly(NaSS) was detected using the TB colorimetric method, FTIR and XPS. By measuring the surfaces wettability, we concluded that the SO_3^- groups increase the surface energy and by extension its hydrophilic character. The physisorbed QCM-D sensors were characterized as well. XPS analyses confirmed the presence of Na and S on the surface of the Ti6Al4V sensors, and TB measurements determined the quantity of poly(NaSS) coated as 1/10 of the amount on grafted disks.

In SFM conditions, we tested the single impact of poly(NaSS) on the early stages of osteoblastic cultures. The SO_3^- groups influenced positively the cells response by supporting the cell structure and morphology for longer, compared to ungrafted surfaces, and by allowing for stronger physical bonds to be generated between cell and biomaterial (superior resistance to stress). Here, it was demonstrated the capacity of poly(NaSS) to induce the production of ECM proteins by the osteoblastic cells, necessary to sustain their own viability and structure on the biomaterial surfaces. These observations were corroborated with the results from the cell cultures in DD conditions.

On the single protein adsorption experiments, it was found that the Fn protein together with poly(NaSS) can play a major role in the osteoblast-like cells early

attachment. Poly(NaSS) was seen to alter the proteins conformation by increasing the exposure of their cell binding sites, such as the RGD peptide and the HB domains in the Fn molecule. These binding regions enhanced significantly the cells morphology and adhesivity on the grafted Ti6Al4V, most likely by interacting with important integrins from the cellular membrane. On Fn and Col I pre-adsorbed substrates, the heterodimers $\alpha_5\beta_1$ and $\alpha_2\beta_1$, respectively, were found to be of extreme importance to the cell development, particularly the last.

For all tested proteins, BSA, Fn, Col I and Vn, poly(NaSS) promoted the adhesivity, morphological expansion, differentiation and mineralization of the MC3T3-E1 cells. While Fn had the most effect on the cells early attached, development of focal adhesions, and expansion above the surfaces, Col I stimulated more significantly the osteoblast-like cells matrix mineralization, by increasing the ALP activity and the calcium and phosphate productions. Vn played as well an important role on the cell early attachment, however not as relevant as the Fn or Col I. BSA, being a non-specific or non-adhesive protein, did not reveal any particular influence on the cell development. This was also detected on the experiments using DD serum. The effect of Fn and Vn in DD serum conditions was promoted by poly(NaSS). However, by comparing the results of Fn and Vn pre-adsorbed surfaces with the DD + Fn and DD + Vn, a small decrease in cell spreading, attachment and adhesivity was observed. Our findings revealed that possible competitive behaviors may be taking place between the DD proteins, hindering the osteoblastic cells development.

In regard to the BSA, Fn and Col I competitive character, it was seen that, in sequential adsorptions, the first adsorbed protein inhibit the adsorption of the second. Evidence of the Vroman effect was found only with BSA + Col I and Fn + Col I. The total amount of proteins adsorbed from a mixture was, in many instances (BSA & Fn and Fn & Col I), less than that from sequential adsorption, but not with Col I & BSA. In this case, the amount was five times higher and took four times longer to reach saturation, indicating continuous rearrangement of proteins or possible development of hydrophobic interactions between BSA and Col I. The cell behavior on surfaces pre-adsorbed with protein mixtures was positively influenced by the SO_3^- groups, in particular the cell cytoplasmic expansion, attachment strength, differentiation and mineralization, whatever the protein nature. While in competition, Fn and Col I were

capable of prevailing over the other protein in solution. The combination Fn & Col I promoted the most successful cell results.

In summary, this research project allowed for the biological influence of the poly(NaSS) on the bone cells behavior to be established. The mechanisms taking place at the interface cell-biomaterial are now clearer, and the SO_3^- groups' influence on the protein conformation and integrin-mediated cell attachment better understood.

The use of polymeric materials with bioactive functional groups, like poly(NaSS), as coatings on Ti-based implants can offer a promising solution for fast biomaterial osteointegration and enhanced bacterial inhibition, to be used in the orthopedic and dental fields.

APPENDICES

LIST OF PUBLICATIONS

- Felgueiras HP, Sommerfeld SD, Sanjeeva NS, Kohn J, Migonney V. Poly(NaSS) functionalization modulates the conformation of fibronectin and collagen type I to enhance osteoblastic cell attachment onto Ti6Al4V. Langmuir. 2014. doi/10.1021/la501862f.

- Felgueiras H, Migonney V. Sulfonate groups grafted on Ti6Al4V favor MC3T3-E1 cells performance in serum free medium conditions. Mater Sci Eng C. 2014;39:196-202.

- Felgueiras H, Migonney V. Biomimetic poly(NaSS) grafted on Ti6Al4V: effect of pre-adsorbed selected proteins on the MC3T3-E1 osteoblastic development. IFMBE Proceedings. 2014;41:1601-1604.

- Felgueiras H, Migonney V, Sommerfeld S, Sanjeeva NS, Kohn J. Competitive adsorption of albumin, fibronectin and collagen type I on different biomaterial surfaces: a QCM-D study. IFMBE Proceedings. 2014;41:1597-1600.

- Felgueiras H, Migonney V. Presence of sulfonate groups on Ti6Al4V surfaces enhances osteoblastic attachment strength at the interface. IRBM. 2013;34:371-375.

Waiting Revision:

- Felgueiras HP, Sanjeeva NS, Sommerfeld SD, Migonney V, Kohn J. Competitive adsorption of proteins studied using a quartz crystal microbalance. 2014

ORAL AND POSTER COMMUNICATIONS

- Adsorption of Col I on poly(NaSS) grafted Ti6Al4V surfaces improves MC3T3-E1 osteoblast-like cells mineralization. ESB Congress, Liverpool. 2014 (Poster Communication).

- Enhancement of integrin-mediated cell attachment by pre-adsorbed model proteins on poly(NaSS)-functionalized Ti6Al4V substrates: a QCM-D study. ESB Congress, Liverpool. 2014 (Poster Communication).

- Enhancement of integrin-mediated cell attachment by pre-adsorbed model proteins on poly(NaSS)-functionalized Ti6Al4V substrates: a QCM-D study. EORS Conference, Nantes. 2014 (Oral Communication).

- Collagen type I pre-adsorption on poly(NaSS) grafted Ti6Al4V surfaces enhances MC3T3-E1 osteoblast-like cells matrix mineralization. EORS Conference, Nantes. 2014 (Oral Communication).

- Col I pre-adsorbed on poly(NaSS) grafted Ti6Al4V surfaces induces superior matrix mineralization in MC3T3-E1 osteoblasts-like cells. Termis Conference, Genova. 2014 (Poster Communication).

- MC3T3-E1 cells attachment on poly(NaSS) grafted Ti6Al4V substrates in the presence of BSA, Fn and Col I: a QCM-D study. Termis Conference, Genova. 2014 (Poster Communication).

- MC3T3-E1 cells attachment to poly(NaSS) coated Ti6Al4V substrates in the presence of BSA, Fn and Col I. 1st Biology and Interfaces Meeting, Bobigny. 2014 (Oral Communication).

- Biomimetic poly(NaSS) grafted on Ti6Al4V: effect of pre-adsorbed selected proteins on the MC3T3-E1 osteoblastic development. GDR Congress, Marseille. 2013 (Oral Communication).

- Biomimetic poly(NaSS) grafted on Ti6Al4V: effect of pre-adsorbed selected proteins on the MC3T3-E1 osteoblastic development. Medicon Conference, Seville. 2013 (Oral Communication).

- Competitive adsorption of albumin, fibronectin and collagen type I on different biomaterial surfaces: a QCM-D study. Medicon Conference, Seville. 2013 (Oral Communication).

- Competitive adsorption of albumin, fibronectin and collagen type I on different biomaterial surfaces: a QCM-D study. ESB Congress, Madrid. 2013 (Oral Communication).

- Presence of sulfonate groups on Ti6Al4V and their impact on osteoblastic cells life expectancy. Colloque des Doctorants, Paris. 2013 (Oral Communication).

- Adsorption and competition of BSA, Fn and Col I on different biomaterial surfaces: a QCM-D study. RITS Conference, Bordeaux. 2013 (Poster Communication).

- Study of protein affinity and cellular attachment on different polymeric surfaces. LBPS seminar, Paris. 2012 (Oral Communication).

Bibliography

[1] Ross MH, Pawlina W. Bone. In: Hostology, a Text and Atlas. Lippincott Williams & Wilkins: Wolters Kluwer. 6th edition. p.202-237.

[2] Clarke B. Normal Bone Anatomy and Physiology. Clin J Am Soc Nephrol. 2008;3:131-139.

[3] Kutz, M. Bone Tissue. In: Biomedical Engineering and Design Handbook. MacGraw Hill. 2nd edition, vol.1. 2009.

[4] Shoulders MD, Raines RT. Collagen structure and stability. Annu Rev Biochem. 2009;78:929-958.

[5] Weiner S, Traub W. Bone structure: from angstroms to microns. FASEB J. 1992;6:879-885.

[6] Deng H, Liu Y, et al. Current Topics in Bone Biology. World Scientific Publishing. 2005.

[7] An YH, Draughn RA. Mechanical testing of bone and the bone-implant interface. In: CRC Press LLC, USA. 1999.

[8] Weiner S, Traub W, et al. Lamellar bone: structure-function relations. J Struct. 1999;126:241-255.

[9] Colnot C. Skeletal cell fate decisions within periosteum and bone marrow during bone regeneration. J Bone Miner Res. 2009;24:274-282.

[10] Jotereau F. Origin of osteoclasts. Ann Biol Clin. 1985;43:767-772.

[11] Solari F, Flamant F, et al. The osteoclast generation: an *in vitro* and *in vivo* study with a genetically labeled avian monocytic cell line. J Cell Sci. 1996;109:1203-1213.

[12] Boyle WJ, Simonet WS, et al. Osteoclasts differentiation and activation. Nature. 2003;423:337-342.

[13] Ross FP, Christiano AM. Nothing but skin and bone. J Clin Invest. 2006;116:1140-1149.

[14] Parfitt AM, Weinstein RS. Idiopathic osteoporosis: is the osteoclasts to blame?. J Clin Endocrinol Metab. 1998;83:716.

[15] Tate ML, Adamson JR, et al. The osteocyte. Int J Biochem Cell Biol. 2004;36:1-8.

[16] Galli C, Passeri G, et al. Osteocytes and WNT: the mechanical control of bone formation. J Den Res. 2010;89:331-343.

[17] Robey PG, Fedarko NS, et al. Structure and molecular regulation of bone matrix proteins. J Bone Miner Res. 1993;8:483-487.

[18] Arboleya L, Castaneda S. Osteoimmunology: the study of the relationship between the immune system and bone tissue. Reumatol Clin. 2013;9:303-315.

[19] Matsu K, Irie N. Osteoclast-osteoblast communication. Arch Biochem Biophis. 2008;473:201-209.

[20] Xiao G, Gopalakrishnan R, et al. Bone morphogenetic proteins, extracellular matrix, and mitogen-activated protein kinase signaling pathways are required for osteoblast-specific gene expression and differentiation in MC3T3-E1 cells. J Bone Miner Res. 2002;17:101-110.

[21] Kini U, Nandeesh BN. Physiology of bone formation, remodeling and metabolism. In: Radionuclide and Hybrid Bone Imaging. Springer-Verlag Berlin Heidelberg, Fogelman I. 2012. p.29-57.

[22] Connections: Bone. Rice University. [Online] 2013. http://cnx.org/content/m44789/latest.

[23] Hadjidakis DJ, Androulakis II. Bone remodeling. Ann NY Acad Sci. 2006;1092:385-396.

[24] Hill PA. Bone remodeling. Br J Orthod. 1998;25:101-107.

[25] Mandalunis PM. Remodelación óssea. Actualiz Osteologia. 2006;2:16-18.

[26] Bone remodeling. Michigan University [Online] 2005 http://www.ns.umich.edu/Releases/2005/Feb05/bone.html.

[27] Fujibayashi S, Neo M, et al. Osteoinduction of porous bioactive titanium metal. Biomaterials. 2004;25:443-450.

[28] Barradas AMC, Yuan H, et al. Osteoinductive biomaterials: current knowledge of properties, experimental models and biological mechanisms. Eur Cells Mater. 2011;21:407-429.

[29] Albrektsson T, Johansson C. Osteoinduction, osteoconduction and osseointegration. Eur Spine J. 2001;10:96-101.

[30] Guitierres M, Lopes MA, et al. Substitutos ósseos: conceitos gerais e estado actual. Arqui Med. 2006;19:153-162.

[31] Branemark P-I, Hansson BO, et al. Osseointegrated titanium implants in the treatment of the edentulous jaw. Scand J Plast Reconstr Surg. 1977;11:1-175.

[32] Alberktsson T, Branemark P-I, et al. Osseointegrated titanium implants. Requirements for ensuring a long-lasting, direct bone anchorage in man. Acta Orthop Scan. 1981;52:155-170.

[33] Williams DF. Osteointegration. In: The Williams Dictionary of Biomaterials. Liverpool University Pree. 1999.

[34] Alberktsson T. On long-term maintenance of the osseointegrated response. Aust Prosthodont J. 1993;7:15-24.

[35] Alberktsson T. Principles of osseointegration. In: Dental and maxillofacial implantology. Mosby-Wolfe. 1995. p.9-19.

[36] Macedo C. A cirurgia do quadril: tipos de proteses. [Online] 2014. http://www.protesedoquadril.com.br

[37] Canella RP, Cimbalista de Alencar PG, et al. Revision total hip arthroplasty using a modular cementless distal fixation prosthesis: the ZMR® hip system. Clinical and radiographic analysis of 30 cases. Rev Bras Ortop. 2010;45:279-85

[38] Dimitriou R, Babis GC. Biomaterial osseointegration – enhancement with biophysical stimulation. J Musculoskelet Neuronal Interact. 2007;7:253-265.

[39] Ratner BD, Hoffman AS, et al. Biomaterials science: an introduction to materials in medicine. In: Elsevier Academic Press. 2nd edition. 2004.

[40] Hu W-J, Eaton JW, et al. Molecular basis of biomaterial-mediated foreign body reactions. Blood. 2001;98:1231-1238.

[41] Anderson JM, Rodriguez A, et al. Foreign body reaction to biomaterials. Semin Immunol. 2007;20:86-100.

[42] Latour R A. Biomaterials: protein – surface interactions. In: Encyclopedia of Biomaterials and Biomedical Engineering. Informa Healthcare USA: Taylor & Francis. 2008. p.1-15.

[43] Anderson JM. Biological responses to materials. Annu Rev Mater Res. 2001; 31:81-110.

[44] Brash JL, Horbett TA. Proteins at Interfaces: an overview. In: Proteins at Interfaces. ACS Symposium Series, American Chemical Society. 1995. p.1-23.

[45] Gray JJ. The interactions of proteins with solid surfaces. Curr Opin Struct Biol. 2004;14:110-115.

[46] Norde W. Adsorption of proteins from solutions at the solid-liquid interface. Adv Colloid Interface Sci. 1986;25:267-340.

[47] Hlady V, Buijs J. Protein adsorption on solid surfaces. Curr Opin Biotechnol. 1996;7:72-77.

[48] Russel PJ. iGenetics: a molecular approach. Pearson Education, Inc. USA. 3rd edition. 2010.

[49] Horbett TA. The role of adsorbed proteins in tissue response to biomaterials. In: Biomaterials Science: An Introduction to Materials in Medicine. Elsevier academic Press. 2004.p.237-247.

[50] Horbett TA. Proteins: structure, properties and adsorption to surfaces. In Biomaterials Science: An Introduction to Materials in Medicine. Academic Press, Inc. 1996. p.133-141.

[51] Andrade JD, Hlady V, et al. Adsorption of complex protein at interfaces. Pure Appl Chem. 1992;64:1777-1781.

[52] Rabe M, Verdes D, et al. Understanding protein adsorption phenomena at solid surfaces. Adv Colloid Interface Sci. 2011;162:87-106.

[53] Takaaki A, Norde W. The behavior of some model proteins at solid-liquid interfaces. Colloids Surf. 1990;51:1-15.

[54] Matthews BW. Hydrophobic interactions in proteins. In: Encyclopedia of Life Sciences. Nature Publishing Group. 2001. p.1-6.

[55] Van Oss CJ. Hydrophobicity and hydrophilicity of biosurfaces. Curr Opin Colloid Interface Sci. 1997;2:503-512.

[56] Haynes CA, Sliwinsky E, et al. Structural and electrostatic properties of globular proteins at a polystyrene water interface. J Colloid Interface Sci. 1994;164:394-409.

[57] Van Tassel PR, Viot P, et al. A kinetic model of partially reversible protein adsorption. J Chem Phys. 1997;106:761-770.

[58] Alves CM, Reis RL, Hunt JA. The dynamics, kinetics and reversibility of protein adsorption onto the surface of biodegradable materials. Soft Matter. 2010;6:4135-4143.

[59] Hirsh SL, McKenzie DR, et al. The Vroman effect: competitive protein exchange with dynamic multilayer protein aggregates. Colloids Surf B. 2013;103:395-404.

[60] Gong P, Szleifer I. Competitive adsorption of model charged proteins: the effect of total charge and charge distribution. J Colloid Interface Sci. 2004;278:81-90.

[61] Michiardi A, Aparicio C, et al. The influence of surface energy on competitive protein adsorption on oxidized NiTi surfaces. Biomaterials. 2007;28:586-594.

[62] Jung S, Lim S, et al. The Vroman effect: a molecular level description of fibrinogen displacement. J Am Chem Soc. 2003;125:12782-12786.

[63] Anselme K. Osteoblast adhesion on biomaterials. Biomaterials. 2000;21:667-681.

[64] Chen H, Yuan L, et al. Biocompatible polymer materials: role of protein-surface interfaces. Prog Polym Sci. 2008;33:1059-1087.

[65] Bacáková L, Filová E, et al. Cell adhesion or artificial materials for tissue engineering. Physiol Res. 2004;53:35-45.

[66] Petit V, Thiery J-P. Focal adhesions: structure ad dynamics. Biol Cell. 2000;92:477-494.

[67] Wozniak MA, Modzelewska K, et al. Focal adhesion regulation of cell behavior. Biochim Biophys Acta. 2004;1692:103-119.

[68] Carragher NO, Frame MC. Focal adhesion and actin dynamics a place where kinases and proteases meet to promote invasion. Trends Cell Biol. 2004;14:241-249.

[69] Principles of Cell Biology. Memorial University of Newfoundland [Online] 2013. http://www.mun.ca/biology/desmid/brian/BIOL2060/BIOL2060-17/CB17.html.

[70] Bigges MJ, Dalby MJ. Focal adhesions in osteoneogenesis. Proc Inst Mech Eng. 2010;24:1441-1453.

[71] Ilic D, Futura Y, et al. Reduced cell motility and enhanced focal adhesion contact formation in cells from FAK-deficient mice. Nature. 1995;377:539-544.

[72] Sebé-Pedrós A, Ruiz-Trilho I. Integrin-mediated adhesion complex. Commun Integr Biol. 2010;3:475-477.

[73] Harburger DS, Calderwood DA. Integrin signaling at a glance. J Cell Sci. 2009;122:159-163.

[74] Huttenlocher A, Horwitz AR. Integrins in cell migration. Cold Spring Harb Perspect Biol. 2011. doi: 10.1101/cshperspect.a005074.

[75] Cary LA, Han DC, et al. Integrin-mediated signal transduction pathways. Histol Histopathol. 1999;14:1001-1009.

[76] Pankov R, Yama KM. Fibronectin at a glance. J Cell Sc. 2002;115:3861-3863.

[77] Mosher SF, Furcht LT. Fibronectin: review of its structure and possible functions. J Invest Dermatol. 1981;77:175-180.

[78] Potts JR, Campbell ID. Structure and function of fibronectin modules. Matrix Biol. 1996;15:313-320.

[79] Johansson S, Svineng G, et al. Fibronectin-integrin interactions. Front Biosci. 1997;2:126-146.

[80] Boughton BJ, Simpson AW. The biochemical and functional heterogeneity of circulating human plasma fibronectin. Biochem Biophys Res Commun A. 2004;69A:525-534.

[81] Cell biology. Shaoxing Collage of Life Sciences. [Online] 2006. http://www.zoology.ubc.ca/~alorch/ecm/gallery2.htm.

[82] Magnussom MK, Mosher DF. Fibronectin – structure, assembly, and cardiovascular implications. Arterioscler Thromb Vasc Biol. 1998;18:1363-1370.

[83] Garcia AJ, Boettiger D. Integrin-fibronectin interactions at the cell-material interface: initial integrin binding and signaling. Biomaterials. 1999;20:2427-2433.

[84] Schvartz I, Seger D, et al. Molecules in focus: Vitronectin. Int J Biochem Cell Biol. 1999;31:539-544.

[85] Zhou A. Functional structure of the somatomedin B domain of vitronectin. Protein Sci. 2007;16:1502-1508.

[86] Sa E Cunha C, Griffiths NJ, et al. Neisseria meningitidis Opc invasin binds to the sulphated tyrosines of activated vitronectin to attach to and invade human bone endothelial cells. PLoS Patholog. 2010;6:1-18.

[87] Pareti FI, Fujimura Y, et al. Isolation and characterization of a collagen binding domain in human von Willebrand factor. J Biol Chem. 1986;261:15310-15315.

[88] Buehler MJ. Nature designs tough collagen: explaining the nanostructure of collagen fibrins. Proc Natl Acad Sci. 2006;103:12285-12290.

[89] Gelse K, Poschl E, et al. Collagens – structure, functions, and biosynthesis. Adv Drug Delivery Rev. 2003;55:1531-1546.

[90] Alpin AE, Howe A, et al. Signal transduction and signal modulation by cell adhesion receptors: the role of integrins, cadherins, immunoglobulin-cell adhesion molecules, and selectins. ASPET. 1998;50:197-263.

[91] Grinnell F, Feld MK. Fibronectin adsorption on hydrophilic and hydrophobic surfaces detected by antibody binding and analyzed during cell adhesion in serum-containing medium. J Biol Chem. 1982;257:4888-4893.

[92] Koblinski JE, Wu M. Matrix cell adhesion activation by non-adhesion proteins. J Cell Sci. 2005;118:2965-2974.

[93] Carter DC, He XM, et al. Three-dimensional structure of human serum albumin. Science. 1989;244:1195-1198.

[94] Dockal M, Carter DC, et al. The three recombinant domains of human serum albumin – structural characterization and ligand binding properties. J Biol Chem. 1999;274:29303-29310.

[95] Berridge MJ. Cell signaling pathways. Cell Signal Biol. 2012. doi:10.1042/csb0001002.

[96] Kim S-H, Turnbull J, et al. Extracellular matrix and cell signaling: the dynamic cooperation of integrin, proteoglycan and growth factor receptor. J Endocrin. 2011;209:139-151.

[97] Lecanda F, Avioli LV. Regulation of bone matrix protein expression and induction of differentiation of human osteoblasts and human bone marrow stromal cells by bone morphogenetic protein-2. J Cell Biochem. 1997;67:386-398.

[98] Lai CF, Cheng SL. Avβ integrins play an essential role in BMP-2 induction of osteoblast differentiation. J Bone Miner Res. 2005;20:330-340.

[99] McCabe JF, Walls AWG. Applied dental materials. In: BalckWell Publishing, 9th edition. 2008.

[100] Wong JY, Bonzino JD. Biomaterials. In: CRC Press, USA. 2007.

[101] Enderle J, Blanchard S, et al. Introduction to biomedical engineering. In: Elsevier Academic Press, 2nd edition. 2005. p.257-312.

[102] Rack HJ, Qazi JI. Titanium alloys for biomedical applications. Mater Sci Eng C. 2006;26:1269-1277.

[103] Patel NR, Gohil PP. A review on biomaterials: scope, applications and human anatomy significance. IJETAE. 2012;2:91-101.

[104] Sumner DR, Galante JO. Determinants of stress shielding: design versus interface. Clin Orthop Relat Res. 1992;274:202-212..

[105] Davis JR. Overview of biomaterials and their use in medical devices. In: Handbook of Materials for Medical Devices. ASM International. American Technical Publishers Ltd. 2003.

[106] Von Recum AF. Handbook of biomaterials evaluation – scientific, technical, and clinical testing of implant materials. In: Taylor & Francis, 2nd edition. 2005.

[107] Wnek GE, Bowlin GL. Encyclopedia of biomaterials and biomedical engineering. In: Informa Healthcare, vol.3. 2008.

[108] Williams DF. On the mechanisms of biocompatibility. Biomaterials. 2008;29:2941-2853.

[109] Schmalz G, Arenholt-Bindslev D. Biocompatibility of dental materials. In: Springer, vol.1. 2009.

[110] Nandi SK, Roy S, et al. Orthopedic applications of bone graft & graft substitutes: a review. Indian J Med Res. 2010;132:15-30.

[111] Khan SN, Sandhu HS, et al. Bone graft substitutes in spine surgery. Bull Hosp Jt Dis. 2000;59:5-10.

[112] Sáenz A, Rivera-Muñoz E, et al. Ceramic biomaterials: an introductory overview. J Mater Educ. 1999;21:297-306.

[113] Shalaby SW, Salz U. Polymers for dental and orthopedic applications. In: CRC Press, NY, vol.1. 2007.

[114] Leyes C, Peters M. Titanium and titanium alloys – fundamentals and applications. In: Wiley – VCH, vol1. 2003.

[115] Long M, Rack HJ. Titanium alloys in total joint replacement – a materials science perspective. Biomaterials. 1998;19:1621-1639.

[116] Hanawa T. In vivo metallic biomaterials and surface modification. Mater Sci Eng A. 1999;267;260-266.

[117] Oshida Y. Bioscience and bioengineering of titanium materials. In: Elsevier, USA, vol.1. 2006.

[118] Niinomi M. Mechanical properties of biomedical titanium alloys. Mater Sci Eng A. 1998;243:231-236.

[119] Kasemo B, Lausmaa J. Metal selection and surface characteristics. In: Tissue-Integrated Prostheses: Osseointegration in Clinical Dentistry. Quintessence Publishing Co, Inc. vol.9. 1985. p.99-116.

[120] Guéhennec LL, Soueidan A, et al. Surface Treatments of titanium dental implants for rapid osseointegration. Dent Mater. 2007;23:844-854.

[121] Liu X, Chu PK, et al. Surface modification of titanium, titanium alloys, and related materials for biomedical applications. Mater Sci Eng. 2004;47:49–121.

[122] Yang Y, Kim K-H, et al. A review on calcium phosphate coatings produced using a sputtering process – an alternative to plasma spraying. Biomaterials. 2005;26:327–337.

[123] Rammelt S, Illert T, et al. Coating of titanium implants with collagen, RGD peptide and chondroitin sulfate. Biomaterials. 2006;27(32):5561–5571.

[124] Carew EO, Cooke FW, et al. Chapter1 – Properties of Materials. In: Biomaterials Science. Elsevier Academic Press, 2004. p.23-65.

[125] Fleming D, O'Neill L, et al. Wear resistance enhancement of the titanium alloy Ti–6Al–4V via a novel co-incident microblasting process. Surf Coat Tech. 2011;205:4941-4947.

[126] Kerner S, Migonney V, et al. Bone tissue response to titanium implant surfaces modified with carboxylate and sulfonate groups. J Mater Sci: Mater Med. 2010;21:707-715.

[127] Matsuaka K, Walboomers XF, et al. The attachment and growth behavior of osteoblast-like cells on microtextured surfaces. Biomaterials. 2003;24:2711-2719.

[128] Oliveira PT, Nanci A. Nanotexturing of titanium-based surfaces upregulates expression of bone sialoprotein and osteopontin by cultured osteogenic cells. Biomaterials. 2004;25:403-413.

[129] Linez-Bataillon, Monchau F, et al. In vitro MC3T3 osteoblast adhesion with respect to surface roughness of Ti6Al4V substrates. Biomol Eng. 2002;19:133-141.

[130] Anselme K, Bigerelle M. Topography effects of pure titanium substrates on human osteoblast long-term adhesion. Acta Biomater. 2005;1:211-222.

[131] Simon M, Lagneau C, et al. Corrosion resistance and biocompatibility of a new porous surface for titanium implants. Eur J Oral Sci. 2005;113:537-545.

[132] Gabbi C, Cacchioli A, et al. Osteogenesis and bone integration: the effect of new titanium surface treatments. Ann Fac Medic Vet di Parma. 2005;15:307-318.

[133] Hayakawa T, Yoshida E, et al. MC3T3-E1 cells on titanium surfaces with nanometer smoothness and fibronectin immobilization. Int J Biomate. 2012;2012:743465.

[134] Teixeira LN, Crippa GE, et al. The influence of pore size on osteoblast phenotype expression in cultures grown on porous titanium. Int J Oral Maxillofac Surg. 2012;41:1097-1101.

[135] Lange R, Luthen F, et al. Cell-extracellular matrix interaction and physic-chemical characteristics of titanium surfaces depend on the roughness of the material. Biomol Eng. 2002;19:255-261.

[136] Stanford CM, Keller JC, et al. Bone cell expression on titanium surfaces is altered by sterilization treatments. J Dent Res. 1994;73:1061-1071.

[137] Boyan BD, Hummert TW, et al. Role of material surfaces in regulating bone and cartilage cell response. Biomaterials. 1996;17:137-146.

[138] Rosa AL, Beloti MM. Effect of CP Ti surface roughness on human bone marrow cell attachment, proliferation and differentiation. Braz Dent J. 2003;14:16-21.

[139] Kasemo B. Biological surface science. Surf Sci. 2002;500:656-677.

[140] Hallab N, Bundy K, et al. Evaluation of metallic and polymeric biomaterial surface energy and surface roughness characteristics for direct cell adhesion. Tissue Eng. 2001;71:55-71.

[141] Schakenraad JM, Busscher HJ, et al. Thermodynamic aspects of cell spreading on solid substrata. J Cell Biophys. 1988;13:75-91.

[142] Ponsonnet L, Reybier K, et al. Relationship between surface properties (roughness, wettability) of titanium and titanium alloys and cell behavior. Mater Sci Eng C. 2003;23:551-560.

[143] Rupp F, Scheideler L, et al. Roughness induced dynamic changes of wettability of acid etched titanium implant modifications. Biomaterials. 2004;25:1429-1438.

[144] Zhao G, Schwartz Z, et al. High surface energy enhances cell response to titanium substrate microstructure. J Biomed Mater Res. 2005;74A:49-58.

[145] Kubies D, Himmlová L. The interaction of osteoblasts with bone-implant materials: the effect of physicochemical surface properties of implant materials. Physiol Res. 2011;60:95-111.

[146] Lee J-M, Kim C-W, et al. Surface analysis of titanium modified by anodization and nanoscaled Ca-P deposition. J Korean Acad Prosthodont. 2007;45:795-804.

[147] Novaes AB, Souza SLS, et al. Influence of implant surfaces on osseointegration. Braz Dent J. 2010 ;21 :417-481.

[148] Olivia A, Salermo A, et al. Behavior of human osteoblasts cultures on bioactive glass coatings. Biomaterials. 1998;19:1019-1025.

[149] Feng B, Weng J, et al. Characterization of titanium surfaces with calcium and phosphate and osteoblast adhesion. Biomaterials. 2004;25:3421-3428.

[150] Park K-D, Lee B-A, et al. Effect of magnesium and calcium phosphate coatings on osteoblastic responses to the titanium surface. J Adv Prosthodont. 2013;5:402-408.

[151] Uezono M, Takakuda K, et al. Hydroxyapatite/collagen nanocomposite-coated titanium rod for achieving rapid osseointegration onto bone surface. J Biomed Mater Res B Appl Biomater. 2013;101:1031-1038.

[152] Cecconi S, Mattioli-Belmonte M, et al. Bone-derived titanium coating improves in vivo implant osseointegration in an experimental animal model. J Biomed Mater Res B Appl Biomater. 2014;102:303-310.

[153] Puleo DA, Nanci A. Understanding and controlling the bone-implant interface. Biomaterials. 1999;20:2311-2321.

[154] Morra M. Biochemical modification of titanium surfaces: peptides and ECM proteins. Eur Cells Mater. 2006;12:1-15.

[155] Morra M, Cassinelli C, et al. Surface engineering of titanium by collagen immobilization. Surface characterization and in vitro and in vivo studies. Biomaterials. 2003;24:4639-4654.

[156] Van der Dolder J, Jansen JA. The response of osteoblast-like cells towards collagen type I coating immobilized by p-nitrophenylchloroformate to titanium. J Biomed Mater Res A. 2007;83:712-719.

[157] Pugdee K, Shibata Y, et al. Gene expression of MC3T3-E1 cells on fibronectin-immobilized titanium using tresyl chloride activation technique. Dent Mater J. 2007;26:647-655.

[158] Yoshida E, Yoshimura Y, et al. Influence of nanometer smoothness and fibronectin immobilization of titanium surface on MC3T3-E1 cell behavior. J Biomed Mater Res A. 2012;100:1556-1564.

[159] Rapuano BE, Hackshaw KM, et al. Effects of coating a titanium alloy with fibronectin on the expression of osteoblast gene markers in the MC3T3 osteoprogenitor cell line. Int J Oral Maxillofac Implants. 2012;27:1081-1090.

[160] Ferris DM, Moodie GD, et al. RGD-coated titanium implants stimulated increased bone formation in vivo. Biomaterials. 1999;20:2323-2331.

[161] Kroese-Deutman HC, Van Den Dolder J, et al. Influence of RGD-loaded titanium implants on bone formation *in vivo*. Tissue Eng. 2005;11:1867-1875.

[162] Secchi AG, Grigoriou V, et al. RGDS peptides immobilized on titanium alloy stimulate bone cell attachment, differentiation and confer resistance to apoptosis. J Biomed Mater Res A. 2006;83A:577-684.

[163] Muller R, Abke J, et al. Influence of surface pretreatment of titanium and cobalt based biomaterials on covalent immobilization of fibrillar collagen. Biomaterials. 2006;27:4059-4068.

[164] Hélary G, Noirclere F, et al. A new approach to graft bioactive polymer on titanium implants: improvement of MG63 cell differentiation onto this coating. Acta Biomater. 2009;5:124-133.

[165] Kerner S, Migonney V, et al. Bone tissue response to titanium implants surfaces modified with carboxylate and sulphonate groups. J Mater Sci Mater Med. 2010;21:707-715.

[166] El Khadali F, Hélary G, et al. Modulating fibroblasts cell proliferation with functionalized poly(methyl methacrylate) based copolymers: chemical composition and monomer distribution effect. Biomacromolecules. 2002;3:51-56.

[167] Anagnostou F, Debet A, et al. Osteoblasts functions on functionalized PMMA-based polymers exhibiting *Staphylococcus aureus* adhesion inhibition. Biomaterials. 2006;27:3912-3919.

[168] Tengvall P, Elwing H, et al. Interaction between hydrogen peroxide and titanium: a possible role in the biocompatibility of titanium. Biomaterials. 1989;10:118-120.

[169] Takemoto S, Tsuru K, et al. Highly blood compatible titania gels. J Sol-Gel Sci Technol. 2001;21:97-104.

[170] Takemoto S, Yamamoto T, et al. Platelet adhesion on titanium oxide gels: effect of surface oxidation. Biomaterials. 2004;25:3485-3492.

[171] Noirclere F. Functionalization of titanium surfaces through oxidation and grafting of bioactive polymers. Surface characterization and evaluation of the osteoblasts response. In: Institut Galilée, Université Paris 13. 2005.

[172] Mayingi J, Hélary G, et al. Grafting of bioactive polymers onto titanium surfaces and human osteoblasts response. IRBM. 2008;29:1-6.

[173] Michiardi A, Hélary G, et al. Bioactive polymer grafting onto titanium alloy surfaces. Acta Biomater. 2010;6:667-675.

[174] James K, Levene H, et al. Small changes in polymer chemistry have a large effect on the bone-implant interface: evaluation of a series of degradable tyrosine-derived polycarbonates in bone defects. Biomaterials. 1999;20:2203-2212.

[175] Bourke SL, Kohn J, et al. Preliminary development of a novel resorbable synthetic polymer fiber scaffold for anterior cruciate ligament reconstruction. Tissue Eng. 2004;10:43-52.

[176] Phyalto T, Lapinsuo M, et al. Fixation of distal femoral osteotomies with self-reinforced polymer/bioactive glass rods: an experimental study on rabbits. Biomaterials. 2005;26:645-654.

[177] Choueka J, Charvet JL, et al. Canine bone response to tyrosine-derived polycarbonates and poly(L-lactic acid). J Biomed Mater Res. 1996;31:35-41.

[178] Lock EH, Petrovykh DY, et al. Surface composition, chemistry, and structure of polystyrene modified by electron-beam-generated plasma. Langmuir. 2010;26:8857-8868.

[179] Choi L, Park H-K, et al. Collagen modified polystyrene for enhanced cell cultivation. Tissue Eng Regen Med. 2009;6:432-437.

[180] Mecea VM. Is quartz crystal microbalance really a mass sensor? Sensor Actuat A. 2006;128:270-277.

[181] Nixon WC. The general principles of scanning electron microscopy. Phil Trans Ray Soc Lond B. 1971;261:45-50.

[182] Herguth WR. Applications of scanning electron microscopy and energy dispersive spectroscopy (SEM/EDS) to practical tribology problems. In: Herguth Laboratories, Inc. 2011.

[183] Goldstein J, Newbury D, et al. Scanning Electron Microscopy and X-Ray Microanalysis. In: Kluwer Academic/Plenum Publishers, 3rd ed, NY. 2003.

[184] Wall SD, Measurement of surface microtopography. Photogramm Eng Remote Sens. 1991;57:1075-1078.

[185] Smith GT. Industrial metrology: surfaces and roughness. In: Springer. 2002. ISBN 1-85233-507-6.

[186] Quinsat Y, Tournier C. In-situ non contact measurements of surface roughness. Prec Eng. 2012;36:97-103.

[187] Olympus: Roughness 2D parameters. Olympus Corporation. [Online] 2013. http://www.olympusims.com/pt/knowledge/metrology/roughness.

[188] Fadley CS. X-ray photoelectron spectroscopy: progress and perspectives. J Electron Spectrosc. 2010;178-179:2-32.

[189] Turner NH, Colton RJ. Surface analysis: x-ray photoelectron spectroscopy, auger electron spectroscopy, and secondary ion mass spectroscopy. Anal Chem. 1982;54:293-322.

[190] Microstructure Research. Belgian Nuclear Research Center. [Online] 2012. http://www.sckcen.be/microstructure/Infrastructure/XPS.htm.

[191] SURF – Research group electrochemical and surface engineering. Vrije University of Brussels. [Online] 2012. http://surfgroup.be/semedx.

[192] Kato k, Ikata Y. Selective adsorption of proteins to their ligands covalently immobilized onto microfibers. Biotechnol Bioeng. 2004;47:556-566.

[193] Sano S, Kato K, et al. Introduction of functional groups onto the surface of polyethylene for protein immobilization. Biomaterials. 1993;14:817-822.

[194] Ramé-Hart. Contact angle goniometers and tensiometers. [Online] 2013. http://www.ramehart.com/contactangle.htm.

[195] Van Oss CJ, Ju L, et al. Estimation of the polar parameters of the surface tension of liquids by contact angle measurements on gels. J Colloid Interface Sci. 1989;128:313-319.

[196] Duygu DY, Baykal T. Fourier transformed infrared (FTIR) spectroscopy for biological studies. GU J Sci. 2009;22:117-121.

[197] Kong J, Yu S. Fourier transformed infrared spectroscopy analysis of protein secondary structures. Acta Biochim Biophysis Sin. 2007;39:549-559.

[198] Tadano S, Giri B. X-ray diffraction as a promising tool to characterize bone nanocomposites. Sci Technol Adv Mater. 2011;12:1-11.

[199] Ballaran TB, Kurnosov A, et al. Single-crystal x-ray diffraction at extreme conditions: a review. High Pressure Res: Int J. 2013;33:453-465.

[200] O'Brien J, Wilson I, et al. Investigation of the alamar blue (rezazurin) fluorescent dye for the assessment of mammalian cell cytotoxicity. Eur J Biochem. 2000;267:5421-5426

[201] Garcia AJ, Ducheyne P, et al. Quantification of cell adhesion using a spinning disk device and application to surface-relative materials. Biomaterials. 1997;18:1091-1098.

[202] Ramirez I, Guastaldi AC. Study of the Ti6Al4V biomaterial using electrochemistry and XPS techniques. Quim Nova. 2002;25:10-14.

[203] Mayingi J. Covalent grafting of bioactive polymers on titanium surface to improve the osteoblast-like cells response. In: Institut Galilée, Université Paris 13. 2008.

[204] Minko S, Gafijchuk G, et al. Radical polymerization initiated from a solid substrate. 1. Theoretical background. Macromolecules. 1999;32:4525-4531.

[205] Minko S, Sidorenko A, et al. Radical polymerization initiated from a solid substrate. 2. Study of the grafting growth on the silica surface by in situ ellipsometry. Macromolecules. 1999;32:4532-4538.

[206] Ko YC, Ratner BD, et al. Characterization of hydrophilic-hydrophobic polymer surfaces by contact angle measurements. J Colloid Interface Sci. 1981;82:25-37.

[207] Horbett TA, Waldurger JJ, et al. Cell adhesion to a series of hydrophilic-hydrophobic copolymers studied with a spinning disc apparatus. J Biomed Mater Res. 1988;22:383-404.

[208] Hélary G, Noirclere F, et al. A bioactive polymer grafted on titanium oxide layer obtained by electrochemical oxidation. Improvement of cell response. J Mater Sci: Mater Med. 2010;21:655-663.

[209] Kasemo B, Lausma J. Biomaterial and implant surface: a surface science approach. Int J Oral Maxilloface Implant. 1988;3:247-259.

[210] Paital SR, Dahotre NB. Calcium phosphate coatings for bio-implant applications: materials, performance factors, and methodologies. Mater Sci Eng R. 2009;66:1-70.

[211] Donachie MJ. Titanium a technical guide. In: USA, ASM International Technical Books Committee. 2000. ISBN 0-87170-686-5.

[212] Roberge PR. Handbook of corrosion engineering. McGraw-Hill Publishing Group. 2000. ISBN 978-1-59124-435-6.

[213] Castner DG, Ratner BD. Biomedical surface science: foundations to frontiers. Surf Sci. 2002;500:28-60.

[214] Zhou J, Ciobanu M, et al. Morphology and adhesion of human fibroblastic cells on bioactive polymer grafted ligament prosthesis. 29th International Conference of the IEEE. EMBS. 2007:5115-5118.

[215] Pavon-Djavid G, Gamble LJ, et al. Bioactive poly(ethylene terephthalate) fibers and fabrics: grafting, chemical characterization, and biological assessment. Biomacromolecules. 2007;8:3317-3325.

[216] Zreiqat H, Valenzuela SM, et al. The effect of surface chemistry modification of titanium alloy on signaling pathways in human osteoblasts. Biomaterials. 2005;26:7579-7586.

[217] Ponsonneta L, Reybier K, et al. Relationship between surface properties (roughness, wettability) of titanium alloys and cell behavior. Mater Sci Eng C. 2003;23:551-560.

[218] Latz C, Pavon-Djavid G, et al. Alternative intracellular signaling mechanism involved in the inhibitory biological response of functionalized PMMA-based termopolymers. Biomacromolecules. 2003;4:766-771.

[219] Huot S, Rohman G, et al. Increasing the bioactivity of elastomeric poly(ε-caprolactone) scaffolds for use in tissue engineering. Biomed Mater Eng. 2013;23:281-288.

[220] Le Guillou-Buffello D, Hélary F, et al. Estimation de l'inhibition de l'adhésion cellulaire sur des films de polymère par la technique du résonateur à quartz. IRBM. 2004 ;25 :34-39.

[221] Le Guillou-Buffello D, Hélary F, et al. Monitoring cell adhesion processes on bioactive polymers with the quartz crystal resonator technique. Biomaterials. 2005;26:4197-4205.

[222] Petrie TA, Raynor JE, et al. The effect of integrin-specific bioactive coatings on tissue healing and implant osseointegration. Biomaterials. 2008;29:2849-2857.

[223] Viateau V, Zhou J, et al. Ligart: Synthetic “bioactive” and “biointegrable” ligament allowing a rapid recovery of patients: chemical grafting, *in vitro* and *in vivo* biological evaluation, animal experiments, preclinical study. IRBM. 2011;32:118-122.

[224] Hu X, Neoh K-G, et al. An *in vitro* assessment of titanium functionalized with polysaccharides conjugated with vascular endothelial growth factor for enhanced osseointegration and inhibition of bacterial adhesion. Biomaterials. 2010;31:8854-8863.

[225] Li B; Liu X, et al. Biocompatibility of plasma sprayed titania coating grafting collagen and gentamicin. J Biomed Mater Res A. 2007;83A:923-930.

[226] Popat KC, Eltgroth M, et al. Decreased *Staphylococcus epidermis* adhesion and increased osteoblast functionality on antibiotic-loaded titania nanotubes. Biomaterials. 2007;28:4880-4888.

[227] Darouiche RO. Treatment of infections associated with surgical implants. N Engl J Med. 2004;350:1422-1429.

[228] Sia IG, Berbari EF, et al. Prosthetic joint infections. Infect Dis Clin North Am. 2005;19:885-914.

[229] Harris LG, Tosatti S, et al. *Staphylococcus aureus* adhesion to titanium oxide surfaces coated with non-functionalized and peptide-functionalized poly(L-lysine)-grafted-poly(ethylene glycol) copolymers. Biomaterials. 2004;25:4135-4148.

[230] Ben Aissa I, Hélary G, et al. Bioactive polymer grafting onto titanium in order to prevent hip prosthesis infection. IRBM. 2011;32::322-325.

[231] Tagaya M, Ikoma T, et al. Detection of interfacial phenomena with osteoblast-like cell adhesion on hydroxyapatite and oxidized polystyrene by the quartz crystal microbalance with dissipation. Langmuir. 2011;27:7635-7644.

[232] Molino PJ, Higgins MJ, et al. Fibronectin and bovine serum albumin adsorption and conformational dynamics on inherently conducting polymers: a QCM-D study. Langmuir. 2012;28:8433-8445.

[233] Krammer A, Craig D, et al. A structural model for force regulated integrin binding to fibronectin’s RGD-synergy site. Matrix Biol. 2002;21:139-147.

[234] Lecomte M. Influence de la microtopographie du titane sur l’adhesion et l’etalement des cellules osteoblastiques et fibroblastiques. In: Institut Galilée, Université Paris 13. 2011.

[235] De Angelis E, Ravanetti F, et al. Attachment, proliferation and osteogenic response of osteoblast-like cells cultured on titanium treated by a novel multiphase anodic spark deposition process. J Biomed Mater Res B Appl Biomater. 2009;88:280-289.

[236] Vogler EA. Structure and reactivity of water at biomaterial surfaces. Adv Coloid Interface Sci. 1998;74:69-117.

[237] Ochsenbein A, Chai F, et al. Osteoblast response to different oxide coatings produced by sol-gel process on titanium substrates. Acta Biomater. 2008;4:1506-1517.

[238] Garcia AJ, Ducheyne P, et al. Effect of surface reaction stage on fibronectin-mediated adhesion of osteoblast-like cells to bioactive glass. J Biomed Mater Res. 1998;40:48-56.

[239] Garcia AJ, Ducheyne P, et al. Cell adhesion strength increases linearly with adsorbed fibronectin surface density. Tissue Eng. 1997;3:197-206.

[240] Oughlis S, Lessim S, et al. The osteogenic differentiation improvement of human mesenchymal stem cells on titanium grafted with poly(NaSS) bioactive polymer. J Biomed Mater Res A. 2012;101A:582-589.

[241] Martin JY, Dean DD, et al. Proliferation, differentiation, and protein synthesis of human osteoblast-like cells (MG63) cultured on previously used titanium surfaces. Clin Oral Implant Res. 1996;7:27-37.

[242] Franco RL, Chiesa R, et al. Human osteoblastic cell response to Ca- and P- enriched titanium surface obtained by anodization. J Biomed Mater res A. 2009;88:841-848.

[243] Riley RH, Lane JM, et al. Bone morphogenetic protein-2: biology and applications. Clin Orthop. 1996;324:39-46.

[244] Mizuno M, Fujisawa R, et al. Type I collagen-induced osteoblastic differentiation of bone-marrow cells mediated by collagen α2β1 integrin interaction. J Cell Physiol. 2000;184:207-213.

[245] Lynch M, Stein JL, et al. The influence of type I collagen on the development and maintenance of the osteoblastic phenotype in primary and passaged rat calvaria osteoblasts: modification of expression of genes supporting gene growth, adhesion and extracellular matrix mineralization. Exp Cell Res.1995;216:35-45.

[246] Salasznyk RM, Williams WA, et al. Adhesion to vitronectin and collagent I promotes ostegenic differentiation of human mesenchymal stem cells. J Biome Biotechnol. 2004;2004:24-34.

[247] Higuchi C, Myoui A, et al. Continuous inhibition of MAPK signaling promotes the early osteoblastic differentiation and mineralization of the ECM. J Bone Miner Res. 2002;17:1785-1794.

[248] Rezania A, Healy KE. Biomimetic peptide surfaces that regulate adhesion, spreading, cytoskeletal organization, and mineralization of the matrix deposited by osteoblast-like cells. Biotechnol Prog. 1999;15:19-32.

[249] Degasne I, Baslé MF, et al. Effects of roughness, fibronectin and vitronectin on attachment, spreading, and proliferation of human osteoblast-like cells (Saos-2) on titanium surfaces. Calcif Tissue Int. 1999;64:499-507.

[250] Steele JG, MsFarland C, et al. Attachment of human bone cells to tissue culture polystyrene and to unmodified polystyrene: the effect of surface chemistry upon initial cell attachment. J Biomater Sci Polym Ed. 1993;5:245.

[251] Howlett CE, Evans MD, et al. Mechanism of initial attachment of cells derived from human bone to commonly used prosthetic materials during cell culture. Biomaterials. 1994;15:213.

[252] Yamada KM. In: Fibronectin. Moscher DF. Academic Press, San Diego, CA, USA. 1998. p.51.

[253] Smith JW, Ruggeri ZM, et al. Interaction of integrins αvβ3 and glycoprotein IIb-IIIa with fibrinogen. Differential peptide recognition accounts for distinct binding sites. J Biol Chem. 1990;265:12267-12271.

[254] Koiyunen E, Gay DA, et al. Selection of peptides binding to the α5β1 integrin from phage display. J Biol Chem. 1993;268:20205-20210.

[255] Akiyama S, Yamada KM. Synthetic peptides competitively inhibit both direct binding to fibroblasts and functional biological assays for the purified cell-binding domain of fibronectin. J Biol Chem. 1985;260:10402-10405.

[256] Johansson S, Forsberg E, et al. Comparison of fibronectin receptors from rat hepatocytes and fibroblasts. J Biol Chem. 1987;262:7819-7824.

[257] Aota S, Nagai T, et al. Characterization of regions of fibronectin besides the arginine-glycine-aspartic acid sequence required for adhesive function of the cell-binding domain using site-directed mutagenesis. J Biol Chem. 1991;266:15938-15943.

[258] Shirahama H, Lyklema J, et al. Comparative protein adsorption in model systems. J Colloid Interface Sci. 1999;139:177-187.

[259] Zoungrana T, Findenegg GH, eta. Structure, stability and activity of adsorbed enzymes. J Colloid Interface Sci. 1997;190:437-448.

[260] Barrias CC, Martins CL, et al. Adsorption of a therapeutic enzyme to self-assembled monolayers: effect of surface chemistry and solution pH on the amount and activity of adsorbed enzyme. Biomaterials. 2005;26:2695-2704.

[261] Wilson CJ, Clegg RE, et al. Mediation of biomaterial-cell interactions by adsorbed proteins : a review. Tissue Eng. 2005;11:1-18.

[262] Haynes CA, Norde W. Globular protein at solid/liquid interfaces. Colloid Surf B. 1994;2:517-566.

[263] Pavon-Djavid G, Hélary G, et al. Inhibiting bacterial adhesion and proliferation: a challenge to prevent infection of prosthetic materials. IRBM. 2005;26:183.

[264] Bae YH, Johnson PA, et al. Minute changes in composition of polymer substrates produce amplified differences in cell adhesion and motility via optimal ligand conditioning. Acta Biomater. 2006;2:437-482.

[265] Xu Y, Gurusiddappa S, et al. Multiple binding sites in collagen type I for the integrins α1β1 and α2β1. J Biol Chem. 2000;275:35-40.

[266] Dalton BA, McFarland CD, et al. Role of the heparin binding domain of fibronectin in attachment and spreading of human bone-derived cells. J Cell Sci. 1995;198:2083-2092.

[267] Evans MDM, Pavon-Djavid G, et al. Vitronectin is significant in the adhesion of lens epithelial cells to PMMA polymers. J Biomed Mater Res A. 2004;69:469-476.

[268] McFarland CD, Mayer S, et al. Attachment of cultured human bone cells to novel polymers. J Biomed Mater Res. 1999;44:1-11.

[269] Steele JG, Johnson G, et al. Role of serum vitronectin and fibronectin in adhesion of fibroblasts following seeding onto tissue culture polystyrene. J Biomed Mater Res. 1993;26:861-884.

[270] Pegueroles M, Toda-Turo C, et al. Adsorption of fibronectin, fibrinogen and albumin on TiO2: time-resolved kinetics, structural changes and competition study. Biointerphases. 2012;7:1-13.

[271] Servoli E, Maniglio D et al. Quantitative analysis of protein adsorption via atomic force microscopy and surface plasma on resonance. Macromol Biosci. 2008;8:1126-1134.

[272] Malmsten M, Lassen B. Competitive adsorption at hydrophobic surfaces from binary protein systems. J Colloid Interface Sci. 1994;166:490-498.

[273] Tremsina YS, Sevastianov VI, et al. Competitive adsorption of human serum albumin and gamma-globulin from a binary protein mixture onto hexadecyltrichlorosilane coated glass. J Biomater Sci. 1998;9:151-161.

[274] Angwarawong T, Dubas ST, et al. Differentiation of MC3T3-E1 on poly(4-styrenesulfonitacid-co-maleic acid) sodium salt-coated films. Dent Mater J. 2011;30:158-169.

[275] Takeuchi Y, Nakayama K, et al. Differentiation and cell surface expression of transforming growth factor-eta receptors are regulated by interaction with matrix collagen in murine osteoblastic cycles. J Biol Chem. 1996;271:3938-3944.

Synthesis and Grafting of Bioactive Polymers to Create Biomimetic Surfaces Capable of Controlling the Host Response

Abstract

In this investigation, we combined the good mechanical properties of the titanium (Ti) alloy Ti6Al4V with the biological properties, namely bioactivity, of the polymer poly(sodium styrene sulfonate) (poly(NaSS)). By chemically grafting the poly(NaSS) on the surface of the Ti alloy we generated biofunctionalized biomaterials. On these substrates, the MC3T3-E1 osteoblast-like cells response was followed in the presence and absence of individual proteins and important information about the competitive behavior of proteins and their effect on the cell development was uncovered.

In serum free medium conditions, poly(NaSS) influenced positively the cells response, by enhancing their attachment strength and by extending their viability and inherent morphology. Fn together with poly(NaSS) was found to play a major role in the cell early attachment, even when in double depleted medium. It was also seen, that poly(NaSS) alters the proteins conformation by increasing the exposure of active binding sites, such as the RGD peptide in the Fn molecule, and this way promoting integrin-mediated cell attachment. Between all proteins, Col I was found to stimulate more significantly the osteoblast-like cells matrix mineralization, by increasing the alkaline phosphatase activity and the calcium and phosphate productions. Grafted surfaces pre-adsorbed with Fn & Col I mixtures promoted the cell cytoplasmatic expansion, attachment strength, differentiation and mineralization. The competitive behavior of Fn and Col I was seen to prevail over BSA.

In summary, the poly(NaSS) together with the Ti6Al4V material offers a promising solution for fast biomaterial osteointegration to be used in the orthopedic and dental fields.

Key Words: TI6Al4V, poly(NaSS), grafting, osteoblast response, protein, fibronectin, collagen type I, binding domains, integrins, osteointegration.

Synthèse et greffage de polymères bioactifs pour créer des surfaces biomimétiques capables de contrôler la réponse de l'hôte

Résumé

Dans cette étude, nous avons combiné les bonnes propriétés mécaniques de l'alliage de titane Ti6Al4V avec les excellentes propriétés biologiques apportées par le greffage d'un polymère « bioactif » le poly(styrène sulfonate de sodium) (poly(NaSS)). Le greffage chimique du poly(NaSS) réalisé à partir de la surface de l'alliage a permis de générer des biomatériaux « fonctionnalisés » et « bioactifs ». Sur ces substrats, la réponse de cellules ostéoblastiques de la lignée MC3T3-E1 a été étudiée en présence et en absence de protéines d'intérêt (seules ou en mélange). Nous avons pu mettre en évidence l'effet de ces protéines, de leur conformation et de leur compétitivité sur la réponse cellulaire (adhésion, étalement, différenciation).

Dans des conditions de culture sans sérum, la seule présence du poly(NaSS) améliore la réponse cellulaire en augmentant l'adhérence, l'étalement et en prolongeant la viabilité cellulaires. Nous avons montré qu'en présence du poly(NaSS) la Fn joue un rôle majeur dans l'attachement précoce des cellules quel que soit le milieu de culture même « déplété » en certaines protéines. D'autre part nous avons également montré que le poly(NaSS) modifie la conformation des protéines adsorbées en augmentant l'exposition de leurs sites de liaison « actifs », tels que le peptide RGD dans la molécule Fn favorisanr ainsi l'adhésion et la fixation cellulaires par le biais des intégrines. Entre toutes les protéines étudiées, Col I a été identifiée comme la protéine qui stimule de manière la plus significative la minéralisation de la matrice ostéoblastique, en augmentant l'activité de la phosphatase alcaline et la production de phosphate et de calcium. Les surfaces greffées de poly(NaSS) pré-adsorbées du mélange protéique Fn & Col I favorisent l'expansion cytoplasmique des ostéoblastes, leur force d'attachement, leur différenciation et leur minéralisation. La compétitivité des protéines Fn, Col I et BSA protéine a également été étudiée.

En résumé, le poly(NaSS) greffé sur des surfaces de Ti6Al4V propose une solution prometteuse pour l'ostéointégration rapide des biomatériaux, avec des applications possibles dans les domaines orthopédiques et dentaires.

Mots-clés: TI6Al4V, poly(NaSS), greffage, réponse ostéoblastique, protéine, fibronectine, collagène type I, sites de liaison, intégrines, ostéointégration.